DEVELOPMENT OF ALTERNATIVE DIELECTRIC FLUID FOR POWER AND DISTRIBUTION TRANSFORMER

A Thesis
Submitted in Partial Fulfillment of the Requirements for the Award of the Degree of

Doctor of Philosophy (PhD)

By

Mrutyunjay Maharana

Centre for Energy
Indian Institute of Technology Guwahati
Guwahati, Assam-781039 India
April, 2019

Dedicated

To

My Grandfather

Late Bidyadhar Maharana,

my Supervisor

Dr. Sisir Kumar Nayak

and ***Family Members*** *for their Support and Love*

Declaration

I hereby certify that the work presented in this thesis entitled '**DEVELOPMENT OF ALTERNATIVE DIELECTRIC FLUID FOR POWER AND DISTRIBUTION TRANSFORMER**' is entirely my own account of research performed under the guidance of Dr. Sisir Kumar Nayak and Professor Niranjan Sahoo. Any part of this work has not earlier been submitted for the award of any degree, diploma, associate-ship, fellowship or its equivalent to any University or Institution.

Date:

(Mrutyunjay Maharana)
Registration No. 146151009
Centre for Energy
Indian Institute of Technology Guwahati
Guwahati – 781039, India

Centre for Energy
Indian Institute of Technology Guwahati
Guwahati – 781039, India

Certificate

This is to certify that the thesis entitled "***Development of alternative dielectric fluid for power and distribution transformer***", submitted by ***Mrutyunjay Maharana*** (146151009), a research scholar in the Centre for Energy, Indian Institute of Technology Guwahati, for the award of the degree of Doctor of Philosophy, is a record of an original research work carried out by him under our supervision and guidance. The thesis has fulfilled all the requirements as per the regulations of the institute and in my opinion has reached the standard needed for submission. The results embodied in this thesis have not been submitted to any other University or Institute for the award of any degree or diploma.

Date:

Place:

Dr. Sisir Kumar Nayak
Associate Professor
Dept. of EEE
IIT Guwahati
Guwahati - 781 039,
Assam, India.

Prof. Niranjan Sahoo
Professor
Dept. of Mechanical Engineering
IIT Guwahati
Guwahati - 781 039,
Assam, India.

Acknowledgements

The first and foremost gratitude goes to my supervisor **Dr. Sisir Kumar Nayak and Prof. Niranjan Sahoo** for their valuable guidance throughout the research work. I thank them for their encouragement, patience towards research and support, which enabled me to develop a better understanding of the subject leading to the present this thesis. I would like to thank them for spending their precious time to discuss thoroughly on the topic and make me what I am today. I would also like to acknowledge my sincere gratitude to my doctoral committee members, **Prof. Santosha K. Dwivedy, Prof. Sashindra K. Kakoti** and **Prof. Harshal B. Nemade,** for their advice and suggestions throughout my research work.

My sincere thanks to Prof. S. Kanagaraj, Dept. of Mechanical Engineering and Dr. S R Kannan former Vice President Crompton Greaves limited for their valuable advice during my research work. I also like to extend my gratitude towards the members of by the Regional Testing Laboratory (RTL), Central Power Research Institute (CPRI) Guwahati especially Mr. Manas Chakraborty for the support in availing the testing facility. I also like to acknowledge Mr. Das and the members of Power Maker, EPIP, Amingaon, Guwahati Assam for providing us the raw material for the experiments failing which the experimental analysis couldn't be performed. The facility provided by the insulating oil testing laboratory (IOTL), Nagaon and the support provided by Mr. K C Barik, and Mr. P Srinivas are highly acknowledged.

I am grateful to my research group members Ms. Niharika Baruah, Ms. Moon Moon Bordeori, Mr. Alakesh Nanda, Ms. Sujita S. Dey for their co-operative assistance and suggestions in performing experiments.

I am thankful to the most important support system during my research was my friends and it feels me immense pleasure to thank Mr. Uttam Kumar Tarai, Dr. Purushottam Gangsar, Mr. Sibabrata Pradhan, Mr. Ravi Valecha, Mr. Himanshu Charurvedi, Mr. Samir Kumar Panda, Mr. Subodh Diwan, Mr. Abhay Kr. Pradhan, Dr. Sanjay Kr. Tudu, Mr. Avinash Yadav, Ms. S. Sahu, Mr. Sunil Kumar Singh, Dr. Besufekad, Dr. Manas Deka, Mr. Durgaprasad, Kelli, Mr. Rajendra Soni, Ms. Bhabani Panda, Mr. Shatrughan Jaiswal, Mr. Ankan Misra, Mr. Vaibhav Jaiswal, Mr Sharaban Kumar for their encouragement.

I would like to thank all the faculty members, and staffs of Centre for Energy and Mechanical Engineering Department for rendering their whole hearted cooperation and support in the entire course of work. A word of appreciation goes to the senior technician and technical

support staff of Mechanical Engineering Department Mr. Saiffuddin Ahmed. I am thankful to Scientific Officers, Mr. Debarshi Baruah, Dr. Lepakshi Barbora, Mr. Dhiren Huzuri, Ms. Rashmi Baruah and Junior Assistant Mr. Paragjyoti Sharma, Centre for Energy for enthusiastic support for various apparatus.

I am grateful to MHRD, Govt. of India, for providing me financial support through DST and STAF, IIT Guwahati to attend and present a technical paper in 8th International Symposium on Electrical Insulating Materials (ISEIM), held at Toyohashi City, Japan during September 12-15, 2017 and Conference on Electrical Insulation and Dielectric Phenomena (CEIDP) held at Cancun, Mexico during October 21-25 2018. I am also thankful to SERB, DST for fund my research.

I also thank the present lab members Mr. Sounak Bera, Mr. Sanjeev Mishra, Mr. Philip Bernstein Sainik, Mr. Chitta Ranjan Barik, Dr. Madhusmita Dash, Ms. Sumitha Banu J, Ms. Dipti Yadav, Mr. Mohd Ghulam Abdul Quadir, Mr. Prabin Kumar Sharma, Mr. Sumit Agarwal, Dr. Parakash Sahu, Mr. Soumya Nanda, Dr. Ch Venkatanarasimha Rao, Mr. Naik, Bukke Kiran, Niranjan Meher for their enthusiastic support for various apparatus during various experimental activities.

I would like to thank my parents, Mrs. Saraswati Maharana and Mr. Gourhari Maharana for all their love and encouragement. I feel proud for them for their patience in times when I was unable to spend even a single week at a stretch with them during the last four years. Special thanks go to my sister Mrs. Manjulata Maharana, my brother-in-law Mr. Biswamber Nayak, my uncle Manoranjan Moharana and aunty Manjulata Maharana and my brother Mr. Prakash Ranjan Maharana for their continual support and love. I would like to express appreciation to my beloved fiance Miss. Subhalagna Nayak for her constant support in the moments when there was no one to answer my queries and encouraged me throughout this endeavor.

Lastly, I am and always be thankful to God for guiding me through this testing period of my life. I will be grateful to Him who has destined my life to be a part of Indian Institute of Technology Guwahati.

(Mrutyunjay Maharana)
Registration No. 146151009
Centre for Energy
Indian Institute of Technology Guwahati
Guwahati – 781039, India

Abstract

The thesis presents development of alternative dielectric fluid for power and distribution transformer. It addresses the nanofluid (NF) development and modification in the transformer oil (TO). It also addresses the development of vegetable oil (VO) based TO is a potential insulating liquid dielectric for the transformer.

In the present study deals with the development of stable mineral oil (MO) based nanofluid (NF) for transformer application. Due to an extraordinary thermal and insulating properties of the hexagonal boron nitride (h-BN) nanoparticle (NP), it is selected as a material to be dispersed in MO to prepare the NF. Bulk h-BN NP of size 1 μm is exfoliated into 2-D nanosheets of size 150-200 nm subsequently enhancing the surface area of exfoliated h-BN (Eh-BN). Eh-BN nanosheets are homogeneously dispersed in MO at 30^{o}C using probe sonication for an hour. Two batches of NF (h-BN/MO and Eh-BN/MO) at five different filler concentration in the range of 0.01-0.1wt% are prepared. However, enhanced dispersion stability of 0.01wt.% Eh-BN/MO NP in MO is observed, which is chosen for further analysis. Thermophysical properties such as viscosity, thermal conductivity, interfacial tension (IFT), flash point, fire point and pour point, and electrical properties such as AC breakdown voltage (ACBDV), dielectric dissipation factor (DDF), dielectric constant (DC) of Eh-BN/MO NF compared to MO and observed to superior. The enhancement in thermal conductivity and ACBDV of Eh-BN/MO-NF are studied by F-K model and analysis of charge dynamics respectively. Therefore, 0.01 wt.% Eh-BN NF is explored more for transformer application because of its enhanced dispersion stability, thermophysical and electrical properties.

TO suffers sever oxidation during the full loading operation of the transformer. Therefore, in this work a comparative assessment of physicochemical thermal and electrical properties are studied at fresh and aged environment for MO and NFs. An open beaker, single temperature oxidative thermal ageing experiment is performed at 115^{o}C for different ageing times, i.e. 164, 328, 492 hours. A concentration of 0.01wt% of NP for both titanium oxide (TiO_2) and Eh-BN/MO are selected to prepare the NFs for ageing. The superiority in physicochemical and insulation performance of Eh-BN/MO-NF are observed compared to TiO_2 NF and MO at post ageing condition. Higher thermal conductivity, insulation Eh-BN NPs on dispersion with MO provide better cooling and insulation even after an ageing.

The prediction of the breakdown probability for a new batch of Eh-BN/MO-NF is performed. Weibull 2-parameter model distribution function has been used to predict the

ACBDV probability percentage at 5, 10, 50 and 63.2% of failure. To verify the effect of ageing on the other allied properties like DDF, resistivity, IFT, acid number and thermal conductivity of the insulating NF, sealed beaker oxidative ageing test has been performed at three different ageing duration such as 164, 328, 492 hours and compared with the MO. The probability of ACBDV failure are analyzed using Weibull 2-parameter model and it is observed that at a distinct failure percentage, lowest failure probability is observed for Eh-BN/MO-NF. The enhancement in ACBDV of NF is due to the stimulated charge accumulation on the surface of the NP of the NF. The high aspect ratio of the exfoliated NP surface enhances the heat transfer capabilities in the NF.

A comparative accelerated thermal ageing study of the kraft paper is carried out to study the electrical breakdown, tensile strength and the degree of polymerization of the oil impregnated paper (OIP). To understand the degradation of the aforementioned properties of the OIP, accelerated thermal ageing study has been performed. An ageing study of both MO impregnated kraft paper (MOIKP) and NF impregnated kraft paper (NFIKP) is performed in two different ageing vessels at 160^{o}C for different aging durations such as 100, 500, 1000 and 2000 hours respectively. It is observed from the experimental results that both modulus and tensile strength of NFIKP are superior than that of MOIKP. Early polymerization in MOIKP is the reason for drastic degradation of its mechanical strength. Eh-BN/MO-NF reduces the effect of early polymerization and minimum affinity towards polar contamination during thermal ageing and hence provides better electro-mechanical stability to the insulating NFIKP. Therefore, the Eh-BN/MO-NF filled TO could be a potential alternative for transformer application.

This work presents a vegetable oil (VO) specifically crude karanji oil (CKO) based TO as an alternative liquid dielectric. The nature of biodegradability, environment friendly and easy availability makes this oil a suitable candidate for liquid insulation. The CKO is not at all suitable for the transformer use because of the higher acid number and viscosity, it will affect negatively on the heat transfer and flowability of liquid inside the transformer. therefore, two step transesterification process has been followed for the extraction of karanji oil methyl ester (KOME) from CKO. Characterizations like Fourier transform infrared spectroscopy (FTIR), proton nuclear magnetic resonance (^{1}H-NMR) and gas chromatography-mass spectroscopy (GCMS) of the KOME are carried out to ascertain the formation of methyl ester oil. Thermophysical properties such as thermal conductivity, viscosity, density, IFT, colour, flash point, pour point, chemical properties such as acid and iodine number, moisture and electrical

properties such as dielectric strength, DDF, and DC are measured as per standard and compared with MO. ACBDV of the KOME is studied and the Weibull statistical analysis is carried out at 95% confidence interval to evaluate breakdown probability. Oxidative ageing of MO and KOME are performed and the effect of thermal conductivity and ACBDV with ageing are studied. It is observed from the results that the performance of the KOME is superior then MO for transformer application.

Ester oil is emerged as a strong alternative TO worldwide. The study investigates the effect of oxidative ageing on the thermal, physicochemical and electrical characteristics of the nonedible ester oil (NEO) compared to NF and MO. The developed NEO is required to analyze its thermal, physicochemical and electrical characteristics to ascertain its usability in transformer. Hence, insulating oil such as NEO, MO and NF are undergone a 164 hours of oxidative ageing. The comparative analysis of the thermal conductivity, physicochemical and electrical characteristics such as, colour, moisture content, acidity, IFT, kinematic viscosity, DC, DDF and breakdown strength of the aged samples are carried out. To study the withstand voltage level of the liquids at the fresh and ageing condition, Weibull statistical analysis of ACBDV have been carried out for a range of distributed data. The ACBDV of the insulating oils at risk levels of 1, 5, 10, 50 and 63.5% are studied. Oxidative ageing result in formation of carbonaceous particles in the oil which is fluorescent in nature therefore, a fluorescence based analysis has been carried out to understand and monitor the oil degradation.

The dispersion of nanofillers into the VO is expected to improve the physicochemical and electrical performance. Surface modified insulating NP is dispersed into the VO to prepare the VO based NF. An open beaker oxidative ageing study is carried out at 115ºC for VO and NF at three distinct ageing duration such as 100, 300 and 500 hours. Alterations in the molecular level of aged VO and NF are studied through various spectroscopic and physicochemical analyses such as NMR, FTIR, UV-Vis absorbance, fluorescence, colour, acid number, IFT and flash point. The fluorescence-based analysis is carried out for VO and NF at fresh and aged condition to monitor the comparative ageing degradation. Oxidative ageing of VO and NF results in the formation of flammable and harmful gasses, which are analyzed using dissolve gas analysis technique. A comparative analysis of the electrical properties such as ACBDV, DC and DDF for fresh and aged sample of VO and NF are studied.

Table of Contents

List of Figures

List of Tables

List of Acronyms

ACBDV	AC breakdown voltage
AN	Acid number
BTH	Butylated hydroxy toluene
CKO	Crude karanji oil
DBPC	Ditertiary-butyl para-cresol
DC	Dielectric constant
DDF	Dielectric dissipation factor
DGA	Dissolve gas analysis
EEM	Excitation emission matrix
Eh-BN	Exfoliated Hexagonal Boron Nitride
Em	Emission
Ex	Excitation
FAME	Fatty acid methyl ester
FESEM	Field emission scanning electron microscopy
FFA	Free fatty acid
FTIR	Fourier transform infrared spectroscopy
FWHM	Full width half maximum
GA	Gallic acid
GCMS	Gas chromatography and mass spectrometry
h-BN	Hexagonal Boron nitride
IFT	Interfacial tension
IPA	Isopropyl alcohol

KFT	Karl Fischer titration
KOME	Karanji oil methyl ester
kV	Kilovolts
MO	Mineral oil
MOIKP	Mineral oil impregnated kraft paper
NEO	Non-edible ester oil
NF	Nanofluid
NFIKP	Nanofluid impregnated kraft paper
NMR	Nuclear magnetic resonance
NP	Nanoparticle
PPD	Pour point depressant
Ppm	Parts per million
RBDFVD	Refined, bleached, deodorized, filtration and vacuum drying
TEM	Transmission electron microscopy
TGA	Thermogravimetric analysis
TO	Transformer oil
UV-vis	Ultra violate visible infrared spectroscopy
VO	Vegetable oil
VO-NF	Vegetable oil nanofluid
XRD	X-ray powder diffraction

List of Symbols

φ	*Volume fraction of the dispersed nanoparticles*
μ_{bf}	*Coefficient of viscosity of the base fluid*
ρ_e	*Electron density*
ε_r	*Relative permittivity*
$\bar{T}$	*Average temperature of the nanofluid*
C_ε	*Equivalent permittivity*
C_p	*Specific heat at constant pressure*
C_σ	*Equivalent conductivity*
d_p	*Diameter of the nanoparticles*
E_0	*Electric field*
K_{bf}	*Thermal conductivity of the base fluid*
K_{eff}	*Effective thermal conductivity*
K_{nf}	*Thermal conductivity of the nanofluid*
K_p	*Thermal conductivity of the particles*
L_C	*Average thickness of one multilayer*
mV	*Millivolt*
N_e	*Numbers of electrons*
Nm	*Nanometer*
N_{np}	*Total number of nanoparticles*
Q_s	*Saturation charge*
Q_t	*Charge accumulation*
R	*Average radius of the nanoparticles*
s^{-1}	*Second inverse*
β	*Full width at half maximum*
ε_0	*Permittivity of the free space*
ε_1	*Permittivity for the first particle*
ε_2	*Permittivity for the second particle*
Λ	*Wavelength*

Σ	*Conductivity of the nanoparticles*
τ_{pc}	*Charging time constant*
τ_r	*Relaxation time*
T_1	*The measured temperatures by the transient hot wire with the time* t_1
T_2	*The measured temperatures by the transient hot wire with the time* t_2
K	*Thermal conductivity*
q	*The measure of dissipation of heat flux by the wire*
α	*The scale parameter Weibull distribution*
β	*The shape parameters in Weibull distribution*
^1H	*Proton*

1

Introduction

Contents

1.1 Introduction to the oil filled transformer

The transformer is a critical link in a power system and its reliability is crucial to the continuity of power supply. It is subjected to multiple stresses such as electrical, mechanical, chemical and thermal simultaneously. Among all the functional systems in a transformer, comprising mainly of oil and cellulose, kraft paper is the weakest element and susceptible to degradation. While oil can be replaced without opening up the transformer, any damage to cellulose requires the transformer to be opened up for repair or replacement, a long drawn out process. Transformer shutdown causes major disruption to the power supply and should be minimized. Hence, efforts are taken to control the factors that cause ageing of solid insulation.

Cellulose ages fast in the presence of heat and moisture. Being next to the heat generating conductor, it is always subjected to high temperature and care is taken by design to limit this well below the withstand level. Oil, used as coolant and insulant plays a crucial role. Higher the thermal conductivity of oil, lower will be the temperature rise on cellulose. Cellulose is hygroscopic and holds much more water than oil. If the moisture equilibrium between oil and cellulose can be altered such that oil can take away more water from cellulose during temperature rise, cellulose ageing will be lower [1].

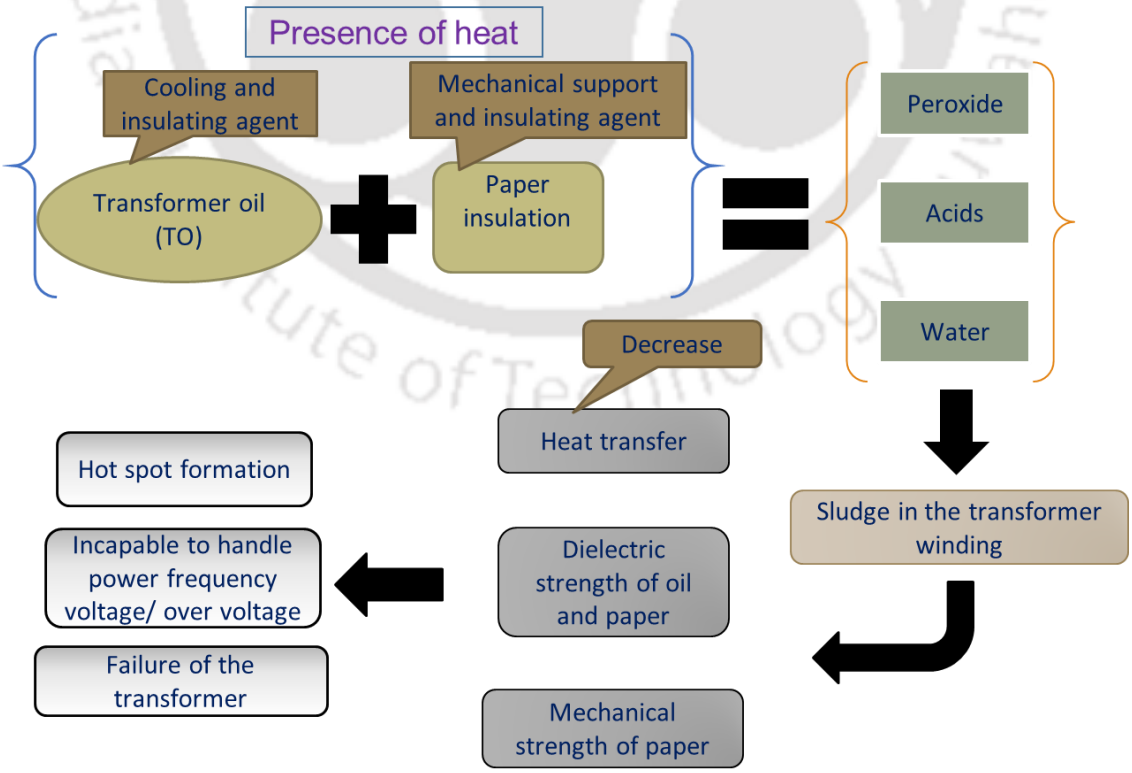

Figure 1.1: Flowchart of the motivation.

Further, degradation of the oil will not only affect its own insulation strength but also the heat transfers from cellulose. Transformer oil impregnated cellulosic kraft paper in the presence of heat for a certain period of time generates aged byproducts such as dangerous acids, oxides, and peroxide in the oil. The generated solids and gaseous byproducts in the oil is the key link in creating hotspots in the transformer winding which further leads to failure in insulation and uneven thermophysical performances in the insulating liquid. Moreover, the ageing byproducts actively take part in the formation of sludge and solid wax which deposits in the winding and bottoms of the transformer tank as seen in Figure 1.1.

Dielectric constant of the insulating liquid is a key parameter of any dielectric medium. The degradation in this property makes the oil inappropriate to be used as an insulating liquid. With the increase of dielectric constant, the electric flux density increases, and this enables materials to hold their electric charge of larger values for longer periods of time. An optimum value of dielectric constant is desirable for better functioning of the transformer oil as an insulating liquid. With the addition of nanoparticles (NPs) there is an increase in dielectric constant of the nanofluids (NFs). This is due to the polarization of the NPs in the oil under the effect of an external electric field.

Partial discharge (PD) is one of the main fault and ageing mechanism in an insulation system. The PD includes internal discharges, surface discharges and corona discharges. Two important criteria must be fulfilled in order to develop PD in cavities, first there must be sufficient free electrons to initiate an electron avalanche and a sufficiently high electric field to support the avalanche and create a breakdown path. The study of PD will give an indication of the state of insulation and its impacts on the lifespan of the oil.

To summarize, there be an excellent motivation to develop an alternative to transformer oil (TO) with improved thermal conductivity, moisture absorption from cellulose, high dielectric constant and flash point. The observed thermal, physicochemical and electrical properties of the mineral oil (MO) based TO is inferior to expected [2, 3]. Hence, an oil with high flash point is required to design to avoid accidental fire breakdown.

In order to improve the performance in the existing TO, in 1994 T. J. Lewis introduced the concept of nanofluid (NF) with enhanced thermal and dielectric properties. Since then various research has been carried out for the application of NF in thermal management and superior thermal performances for transformer application [4-6]. However, very few researches have been carried out on the dielectric and electrical performance enhancement of the NF [7]. Therefore, studies have been conducted here on the MO and vegetable oil (VO) based nanofluid (NF) for TO application.

1.2 Literature survey

It is observed that the use of nanoparticles (NPs) in fluids such as ethylene glycol, ester oil and MO increase the heat transfer properties. Since there is a fundamental lack of understanding about the physical mechanisms involved in their improved performance compared to the host fluid, its application as dielectric liquid is yet to be fully explored area in nanotechnology research. This motivates the researchers to explore the possibilities to develop the NF based TO to increase the cooling and other effects which will enhance the life of the transformer. Increasing research can be judged by increasing in the publication from 2007 to 2017 [8].

The studies are aimed to investigate the cooling effect of the transformer using various MO-NF based TO. Though different types of NPs have been used to prepare the MO-NFs for thermal management, very few of them has the ability to provide electrical insulation [9-12]. In order to enhance the life of a transformer at the higher loading condition, the requirement of providing sufficient cooling effect and dielectric strength of the TO are the major challenges [13]. To prepare a stable MO-NF based TO that can be used as a transformer coolant with many superior thermophysical and electrical properties compared to the conventional TO have been studied. Due to unique properties like high thermal conductivity, low thermal expansion, high electrical resistance and higher breakdown strength, of specific NPs are selected as a material to be used with MO as host fluid.

MO-NF studied in the context of real-time transformer application, therefore the actual transformer environment is created for the NF to study its ageing characteristics. The ageing in the solid and liquid dielectric is a natural phenomenon [14]. With the passage of time, the insulating oil and cellulosic kraft paper degrade but the rate of ageing in the sold liquid insulation system determines the remaining useful life of the transformer [15, 16]. Hence, care is taken while developing the MO-NF in terms of its response to the ageing. To investigate the physicochemical and electrical performance of the MO-NF at an accelerated oxidative environment, oxidative ageing techniques are executed [17]. Since temperature is an influential parameter for the ageing, with the rise in temperature, ageing rate increases [18, 19]. Therefore, the accelerated thermal ageing study is performed for the developed NF and the thermophysical and electrical performances of the aged sample are compared with the existing MO-based TO at fixed and varying ageing durations.

With the ageing of the solid-liquid insulation system, not only the oil performance deteriorates but also there is a notable degradation in solid insulation system. A major

percentage of winding failure and initiation of partial discharge in the winding is because of the generated hotspot. Superior chemical, insulation, and mechanical strength of the solid insulation prevent an early hotspot generation [20]. Solid insulation such as kraft paper and pressboard is immersed in the oil for a longer period of time at varying heat inside the transformer tank. So an investigation is also carried out to understand the electrical, mechanical and chemical degradation of the oil impregnated paper (OIP) at certain ageing duration. Since paper is hygroscopic in nature, the presence of moisture in the oil is absorbed by the cellulosic kraft paper and pressboard which then actively take part in accelerating the ageing [21]. To study the effect of ageing on the degradation of the OIP, MO impregnated kraft paper (MOIKP) and NF impregnate kraft paper (NFIKP) is aged for similar ageing condition and compared. Analysis of the tensile strength of the OIP provides information about the sustainability of mechanical strength to withstand the dynamic thermo-mechanical stress [22, 23]. Moreover, the chemical structure of the TO and the OIP both alter with the period of ageing. The alteration in chemical properties of the TO is evaluated by various spectroscopic analysis to ascertain the degradation. However, remaining useful life of the OIP is studied by analyzing the alteration in its chemical structure [24-26]. The investigation of the OIP is carried out by studying the degree of polymerization (DP) at different ageing durations.

1.3 NF based TO

The research is focused on the development of a new liquid dielectric alternative to MO with enhanced thermophysical and electrical performances [27-31]. Therefore, researchers have found out that the thermal performances of the fluid can be enhanced with the implementation of nanotechnology [8]. New nanotechnology-based materials with superior properties have been developed and are already used in many everyday products and processes. These are some particular applications of NF in industrial, commercial, residential, medical and transportation sectors [32-38].

Since the study involved here in the investigation of NFs for transformer application, an extensive review of literature is carried out in this topic to evaluate its potential usability in the transformer.

In the advancement of nanotechnology, research has got the attention of the development of nanodielectrics materials. Development, characterization and implementation of the nanodielectrics in the field of electrical insulation is the major thrust of the dielectric material

research [39]. There is an investigation by Lewis [40] in 1994 which suggests that the implementation of the nano-size particles in the base fluid has a significant effect on the dielectric properties.

The nanoparticle with an enhanced aspect ratio at nanometric thickness ratio arises certainly at the interface, plays a crucial role in altering the physical phenomena of the nanodielectrics [41]. Initially, the term "nanodielectric" was coined by Frechette [42], he defined nanodielectrics as "A nanodielectric is a dielectric exhibiting behaviour in one of its properties that is different than expected due to an alteration on a nanoscale".

MO and VO are the suitable base fluid to prepare the NFs for transformer application [38, 43-45]. NF is the colloidal suspension of two phases; liquid phase considered as matrix or base fluid and solid phase are the NPs which dispersed into the base fluid. [6, 46, 47]. Initially, the NF is developed aiming at enhancing the heat transfer characteristics which can be treated as a suitable coolant for industrial applications. Research also reports that the dispersion of high thermally conducting NPs into the low thermally conducting base fluid enhances the heat transfer characteristics of the NFs. From the available literature, the rise in thermal conductivity of the NF for different NPs and base fluid are presented in Table 1.1.

Table 1.1: Comparison of thermal conductivity (K) of different nanoparticle based NFs

Ref.	NPs	Base fluid	Size of NPs	(Vol. %)	%Rise of K	Observation
Masuda *et. al.*, 1996. Eastman *et. al., 1997*	Al_2O_3	H_2O	13	4.3	30	The smaller size of nanoparticles requires less concentration for the same enhancement.
			33	5	30	
Xie *et. al.*, 2002, Yu *et. al., 2011,* Shukla and Aiyer *2015*	Al_2O_3	H_2O (0.61 W/mK)	60	5	20	The % enhancement of thermal conductivity of nanofluid was observed inversely proportional to their thermal conductivity of base fluid
		EG (0.25W /mK)	60	5	30	
		PO (0.14 W/mK)	60	5	40	
		H_2O (0.61 W/mK)	10	0.5	100	Due to the small size of nanoparticles, high enhancement was observed even at less concentration
		H_2O	18.6	4.3	10	More % enhancement of thermal conductivity was

Nnanna A *2007*	CuO	EG	18.6	4	20	observed for lower thermal conductivity of base fluid
		EG	23	10	35	More enhancements were observed due to the higher concentration of nanoparticles.
		H_2O	23	15	55	
Murshed *et. al., 2005*	TiO_2	H_2O	15	5	33	More enhancement was observed due to the small size of nanoparticles
		H_2O	27	4.35	10.7	
Lee *et. al., 2008*, Liu *et. al.,2016*	AlN	TO	50	0.5	8	High thermal conductivity and oleophilic nature of h-BN was observed to be responsible for high enhancement.
Tijerina *et. al.2012*	h-BN	TO	600	0.1	80	

Due to unique properties of NPs such as high thermal conductivity, low thermal expansion, high electrical resistance and higher breakdown strength, their dispersion in MO and VO is expected to improve their dielectric and cooling performance. NF for transformer application was initially suggested by Segal *et al*. in 1998. He and the group of researchers have studied the implementation of magnetic NP to improves the dielectrics performance of the NF [57].

The NF in the dielectric application is moderately researched. However, it is observed that the insulating and cooling performance of some specific NFs has high performance compared to the base fluid [8, 45, 46, 50-53].

1.3.1 Synthesis and preparation of NF

As the NF related research is limited in the laboratory scale, manufacturing of NFs in industrial scale is not undertaken at current stage. The dielectric and thermal performance of the NF reported by several scientists are obtained by fabricating NF in the research laboratory. There are three different kinds of NPs such as conductive, semi-conductive and insulating are used to prepare the NF. The example of conductive NPs are Fe_3O_4 or ZnO, semi-conductive are TiO_2, Fe_2O_3, CuO, or CuO_2, and insulating are Al_2O_3, SiO_2, SiO, h-BN. The range of the aforementioned NPs diameter is in the range of 10-70 nm [58-61]. Most of the reported research work presented in the literature in the context of NF based TO are developed by taking MO as the base fluid. Moreover, a very few pieces of literature have

reported taking natural ester-based VO and synthetic ester-based oil as the base fluid for preparation of NF in transformer application [62–67].

The uniform distribution of solid NPs of an adequate wt.% into the base fluid is required to prepare a stable NF. Since NF is a colloidal solution of base fluid and nanoscale size solid particles, getting a stable compound of the physical mixture is challenging. However, the two-step dispersion method has employed in the preparation of NF considering MO and VO as a base fluid. Many researchers have successfully implemented the two-step method for the preparation of NF because it involves very generic equipment, simple steps and low cost. The addition of NP directly into the base fluid will cause agglomeration and sedimentation restricting the enhancement in the dielectric performance of the NF [64]. Two-step method prevents the agitation of the NP in the base fluid by the process of ultra-sonication. To maintain the stability and uniformity of the NP distribution in the base fluid, the addition of a surfactant is preferred. The addition of surfactant in the NF reduces the repulsive force among the NP and the base fluid that results in a stable colloidal mixture and hence the stability is maintained for a longer period by avoiding the agglomeration. There is no fixed surfactant which can be used for the stability of the NF. Moreover, different surfactants for different NPs are reported by several researchers which can be used accordingly to obtain stability in the NF [68-72].

1.3.2 Cooling effect of the NFs

NPs have been used for increasing the thermal conductivity of the transformer oil for enhancing the cooling effect without disturbing the electrical insulation property, which can give longer life to a transformer [38]. Different NFs have been prepared for thermal management of the system, but very few of them are applicable in electrical devices, where the NF is expected to provide both thermal and electrical management of the system. In the case of oil-filled power and distribution transformer, NF will provide enough cooling due to its high thermal conductivity. Therefore, various NPs are used in TO for providing enough cooling and electrical insulating strength even at high load condition [73, 74]. So, study of electrical properties of the NFs for the transformer application is very much necessary before drawing any specific conclusion about the insulation performance.

1.3.3 Electrical properties of the NFs

Addressing the electrical properties of the NF initially, the research has focused on the development of NF by the dispersion of magnetic NPs into the MO. The AC and impulse breakdown voltage (BDV) is measured in which, the NF shows significant improvement in

the properties compared to base fluid. The effect of moisture on the BDV is studied and it is observed that, with the rise in moisture content, BDV value decreases for NF and base fluid as well. Moreover, the study is extended for the partial discharge inception voltage (PDIV) of the NF compared to MO. As expected, The PDIV of the NF is superior to the MO [75]. The improvement in AC breakdown voltage (ACBDV) of the magnetic NF is explained through streamer analysis using needle sphere electrode. The charge dynamics of the NP during the applied voltage to the NF are studied to understand the enhancement in the ACBDV [58, 76, 77].

Many researchers investigated that the dispersion of semi-conductive NP such as TiO_2 into the MO improves the thermal and electrical performances of the NF. The ACBDV and the thermal conductivity of TiO_2/MO-NF have enhanced at a certain vol. % of NP dispersion. The PD analysis of this batch of NF results in the delay of PD propagation and affirming the superior liquid dielectric fluid [78-80]. Though surfactant addition has improved the stability of the semi-conductive NF, long-term stability in real time application is a challenge.

It is observed that the thermal and insulation performance of conducting NF is superior to the existing MO-based TO. Since the magnetic field already exists in the transformer, the presence of magnetic NP varies the field distribution and hence performance likely to be affected. However, maintaining the stability of the magnetic NF for a longer period to obtain the repeatability in its performance is a big challenge. Due to the lack of proper technological advancement, NFs are not prepared commercially for specific usages.

The NFs prepared by the dispersion of the conducting and semiconducting nanofillers upon exposed to the electric field, likely to align in the direction of electric field to form the conducting channels in NFs. Hence, an early breakdown may take place for the NF based TO. Since the transformer is a long run device, the reliability of high dielectric strength is essential. Therefore, the research is focused on an alternative nanofillers, dispersion of which the electric breakdown strength and thermal performance can be enhanced in the NF.

An investigation is carried out on the insulating NP-based dielectric fluid in which various insulating NPs such as Al_2O_3, ZnO, SiO_2, and BN etc. are dispersed as the potential nanofillers in the MO. The study shows that the dielectric strength of the insulating BN NF enhances compare to the base fluid at the same time the thermal performance either enhances or unaffected. The mean ACBDV of the insulating NF is superior to that of the MO. Therefore, the failure analysis using Weibull statistical analysis is carried out to evaluate the percentage of probability failure in ACBDV [81-84].

Though very few studies have been reported that the insulating NF results in enhancement of the electric strength, yet stability of the NF is not focused for transformer application [46,47]. Unlike MO based TO ages with the passage of service time, ageing of the insulating NF is not given attention. Studies have not been reported on the effect of ageing on the physicochemical and electrical performance of the NF at real time transformer environment.

Seeking the aforementioned literature of NFs and its application in liquid dielectric for transformer it is observed that, the thermophysical and electrical performance of the insulating NF is improved compared to the base fluid. However, in practical application of insulating NF based TO is a challenge. Studies on NF have not revealed about the effect of ageing on the NF based TO and the experimental validation of the NF application with specific ageing techniques is not given enough attention. Moreover, because of the complications in the stability, biodegradability and insignificant fire resistance capability of MO and MO based NF, VO based liquid dielectric is given importance for the research.

1.4 Sustainable VO

Since the ever-growing alertness on environmental safety and biodegradability, it has become necessary to afford a sustainable and environment-friendly dielectric fluid with higher heat transfer, fire resistance and insulating characteristics. Low biodegradability, low fire resistance the limited available resources of petroleum crude have motivated to explore a sustainable alternative TO with modified characteristics. Therefore, the study has moved into the next level to replace the non-renewable petroleum resources based TO and NF with renewable and naturally occurring VO as a liquid dielectric for transformer application.

The VO sources being a potential liquid dielectric for the transformer is an emerging research topic. Therefore, the researchers are keenly focusing the VO for transformer application. Moreover, the transformer industries like ABB and Siemens have already implemented the VO based liquid dielectric for transformer application [27-29]. The VO such as BIOTEMP from sunflower and ENVIROTEMP from soybean are extensively used as TO [30]. The ACBDV and fire resistance properties is the main thrust of their study. However, all the physicochemical and thermal conductivity of the VO is not investigated [85-90]. Therefore, the physicochemical and heat transfer performance of the VO is required special attention.

There are many sources are available for the production of VO in India e.g. rapeseed, palm kernel, colona, sunflower, soybean etc. The careful processing of the crude VO yields

the suitable natural ester oil; it is the potential candidate being TO. Since the oil requirement for the transformers is huge, to meet the requirement of ester oil, edible food crops are to be used to extract the oil for the transformer which is likely to cause the food crises in the future [31]. Commercially available rapeseed and canola-based dielectric fluid have raised the question of its functionality in oxidation related issue and insulating capabilities. Seeking the aforementioned drawbacks related to the thermal stability, oxidation stability, nature of unsaturation and importantly affecting the food requirement, hinders its commercial applications. Therefore, an investigation is also needed to be carried out to evaluate the possible implementation of a non-food crop oil as a dielectric fluid for the transformer. Hence, it is required to study the option left with the nonedible VO and its application as TO in the context of thermophysical and electrical characteristics. A very few research has been carried out in the field of thermophysical and electrical properties of the VO based TO for the replacement of MO [90-94]. But enough attention is not given on the applicability of nonedible VO as an insulant and coolant.

1.4.1 Nonedible VO

Very few non-food seeds such as Jatropha curcas, neem, mahua, karanji etc. are available for the extraction of nonedible VO. However, a limited study on AC, DC and impulse BDV are carried out on the Jatropha curcas oil. The streamer propagation is also studied for the Jatropha curcas methyl ester [31]. But the research did not reveal the response of heat transfer and other allied physicochemical and electrical properties of the nonedible VO. Hence, in this research work, the development of a new nonedible VO, named karanji oil methyl ester (KOME), as a novel TO is presented. The KOME is derived by the process of two-step transesterification from the crude karanji oil (CKO) extracted for the karanji fruit seeds. The Karanji fruits are drought resistant, semi-deciduous and nitrogen-fixing leguminous tree. It grows about 15-20 meters in height with a large canopy which spreads equally wide [95]. We collected the ripened karanji fruits from the karanji tree available in the IIT Guwahati premises followed by removal of karanji seeds and drying. Then the CKO is extracted from the dried karanji seeds using mechanical expeller. Two-step transesterification process has been carried out to prepare the KOME. The thermophysical (thermal conductivity, viscosity, interfacial tension, flash point, pour point and colour), chemical (moisture content, acid number, iodine number) and electrical (ac breakdown voltage, resistivity, dielectric constant, dielectric loss) properties of KOME are studied and compared with MO. Finally, with the ageing and statistical analysis of ACBDV compared to MO ascertain the chemical and dielectric integrity of the KOME.

Karanji tree is a deciduous medicinal plant, which found in the region of northeastern part of India, Indian subcontinent, south-east Asia to north-eastern region of Australia, Fiji and Japan. Karanji belongs to the family of pea and it has many common names such as Indian beech, Pongam oil-tree, Karanji tree, and Pongamia pinnata tree. It grows in the tropical and subtropical region, which does not require a fertile land. The seeds of the karanji tree are now a day widely used for the biodiesel production as shown in Figure 1.2 [96]. The production of the biodiesel from the karanji seeds is a solution for the energy crises and environmental safety.

Many applications of the karanji trees have been explained in several literatures, for example, conservation of soil water, reclamation of the soil, control of soil erosion, major feedstock for pharmaceutical and cosmetic industries. The production of biodiesel from the seeds of the karanji fruits is the key application involved in the recent past of the research. The karanji seeds are processed into a suitable biodiesel, which acts as a less polluting fuel compared to petroleum-based oil [97]. The byproduct of the karanji oil cake is treated as a suitable organic fertilizer for organic farming. The implementation of the aforementioned application will strengthen the economy of rural people.

Figure 1.2: Nonedible VO based TO [96].

CKO can be obtained from the extraction process of solar dried karanji seeds. Mechanical expeller is being used for oil extraction. The CKO is further processed into the two-step transesterification process to obtain KOME as an insulating oil for the electrical transformer.

The karanji oil can also be extracted using the soxhlet, cold percolation and Solvent extraction process by taking karanji seeds powder as an input. But in these chemical extraction process, the oil percentage is more compared to mechanical extraction [98]. However, the chemical extraction involves a lot of hazardous chemical treatments, so mechanical expeller is more suitably preferred for the extraction of CKO.

1.5 Motivation

In the above literature, the importance of an alternative and environment-friendly liquid dielectric for the power and distribution transformer are studied. The NF and nonedible VO based liquid dielectric for the transformer is studied. Many researchers have put their effort to study the thermal performances of the NF but very few research has been reported on the dielectric characteristic of the NF. In addition to that considering the application of nonedible VO in the transformer as a dielectric insulant, very few works have been reported. From the above survey, there is no clear summary of the nonedible VO properties and its application for power and distribution transformer. The technical gaps which are big hurdles for using NF and nonedible VO based liquid dielectric with improved insulation and heat transformer applications are as follows:

- The studies have been conducted extensively on the enhancement of thermal conductivity of NF, but other important characteristics of NF for transformer application such as electrical conductivity, partial discharge, moisture absorbent, flash point, viscosity, pH value and pressure drop of the NF are not discussed in detail.
- The theoretical reason behind the enhancement of thermal conductivity and stability of NF is not discussed and available formulae for calculating the enhancement in thermal conductivity of NF does not satisfy the actual value of enhancement of experimentally obtained thermal conductivity.
- Feasibility study and real-time study on the MO-NF, VO and VO-NF based dielectric fluid is very much necessary.
- There are very few studies reported related to charge accumulation of the NF based TO.
- No specific attempts are made to implement the nonedible VO to the power/distribution transformer.
- High viscosity and density of the crude nonedible VO limits its use in the transformer application. Thus it is important to find out the way by which the thermophysical and electrical specification of the developed oil meet the standard TO.

- The theoretical reason behind the enhancement of AC breakdown voltage of VO is not addressed.
- Moisture content in the VO and NF and its harmful effect is not discussed. The moisture exclusion from the VO and NF based TO is a major challenge for the researchers.
- Not enough literature is published on the study of partial discharge phenomena in the VO and NF based TO.
- Not enough studies are reported on the analysis of thermo-mechanical and electrical properties of the VO and NF based TO and oil impregnated solid insulation.

1.6 Objective of the thesis

The study has been performed to introduce an alternative liquid dielectric for power and distribution transformer. The following objectives are mentioned for the successful implementation of the novel and an alternative liquid dielectric for the transformer.

- To examine the dielectric strength and heat transfer capacity of MO-based NF by dispersing a suitable concentration of highly insulating and thermally conducting nanofillers with MO.
- To study the stability of the MO-NF and VO-NF by dispersing the NPs initially in MO and then in VO.
- To investigate the physicochemical properties such as thermal conductivity, viscosity, density, water content, colour, acid number, flash point, pour point, IFT and electrical properties such as ACBDV, dielectric strength, DC, DDF and specific resistance of the NF and VO and compared with the existing MO based TO as per ASTM/IEC standard.
- To analyze the effect of ageing on thermal, physicochemical and electrical characteristics of the MO, VO and NF by oxidative and accelerated thermal ageing method.
- To study the dielectric breakdown probability of the fresh and aged TO such as MO, MO-NF and VO.
- To study the DP characteristics of the NF and nonedible VO impregnated solid cellulosic insulation such as kraft paper and pressboard.
- To analysis the degree of degradation of the fresh and aged TO by spectroscopic study.

1.7 Main contribution

The main contribution of the thesis is as follows:

- A thermally conducting, electrically insulating hexagonal boron nitride (h-BN) is dispersed with MO to prepare the stable MO-NF. The thermophysical and electrical characteristics of the NF is analyzed in the context of efficient cooling and insulation in the transformer.
- The design and development of open beaker oxidative apparatus and sealed beaker accelerated thermal ageing setup are developed.
- An open beaker oxidative ageing study is performed for the developed insulating NF and the effect of ageing on the thermal, electrical and physicochemical properties are analyzed and compared with the fresh and aged MO.
- Thermophysical and electrical properties with statistical analysis of the ACBDV failure are studied for the sample sealed beaker oxidative aged NF and MO.
- The electromechanical, DP and ACBDV characteristics of the thermally aged oil impregnated kraft paper such as MOIKP and NFIKP are studied.
- A nonedible VO based liquid dielectric is studied for transformer application. Extraction, chemical processing, and characterization of the nonedible ester oil (NEO) are performed. Thermal, chemical and electrical properties of the developed oil are studied for fresh and aged oil. Moreover, the percentage of dielectric failure is also evaluated using Weibull statistical analysis.
- A comparative study of the oxidative ageing degradation of NEO and its NF is carried out. The thermal, physicochemical, electrical and the fluorescence-based analysis are performed for the different ageing degradation of the oil.
- The spectroscopic analysis of the fresh and accelerated aged ester oil based NF is carried out. The chemical stability and oil degradation with ageing are studied using fluorescence spectra analysis. The electrical properties of the aged oil are also verified.

1.8 Organization of the thesis

This thesis is organized in nine chapters as follows:

In Chapter 2, the characterization including morphological studied of the suitable NPs is performed. The exfoliation process for the surface modification of the pure hexagonal boron nitride (h-BN) NP of 3D structure to 2-D nanosheets is carried out. Considering the stability of the Eh-BN based NF, 0.01wt% concertation of nanofiller is used to prepare the stable NF.

Thermophysical and electrical properties of the Eh-BN/MO-NF is investigated and compared with the base fluid i.e. MO. The charging dynamics study is performed to understand the enhancement in ACBDV of the NF compared to MO.

In Chapter 3, the design and development of open beaker oxidative ageing apparatus as per ASTM 1934 standard are presented. An open beaker single temperature oxidative ageing study of the liquid dielectrics is performed. The effect of ageing on the thermal, electrical and physicochemical properties of the MO and NF are studied.

Chapter 4, describes the sealed beaker oxidation stability analysis for liquid insulation. A sealed beaker with oxidation stability analysis for MO and NF is performed at a fixed temperature as per ASTM-D2440 standard. The prediction of the breakdown probability of aged NF is performed by Weibull 2- parameter model distribution function. This distribution function is used to predict the ACBDV probability percentage at 5, 10, 50 and 63.2% of failure. The effect of oxidative ageing on the other allied properties like dielectric dissipation factor, resistivity, interfacial tension, acid number and thermal conductivity of the insulating NF, are studied for three different ageing duration and the results are compared with the existing MO.

A natural and forced convection imposed accelerated thermal ageing simulator is carried out in Chapter 5. The effect of oxidation and elevated temperature on the TO is studied by the developed simulators. The electro-mechanical characteristic such as tensile strength, ACBDV analysis and chemical characteristics such as colour and degree of polymerization (DP) of the aged oil impregnated kraft paper (OIKP) are studied for different ageing durations. The comparative analysis of the thermally aged NFIKP and MOIKP are studied for distinct ageing durations.

Chapter 6 presents the novel VO based liquid dielectric an alternative oil for the transformer. Two-step transesterification process has been followed for the extraction of KOME from CKO. Thermophysical and electrical properties are measured as per ASTM D117 standard and compared with MO. The ACBDV of the KOME is studied and the Weibull statistical analysis is carried out at 95% confidence interval to evaluate the breakdown probability. Oxidative ageing of MO and KOME are performed and the effect of thermal conductivity and ACBDV with ageing are studied.

Chapter 7 investigates the effect of oxidative ageing on the thermal, physicochemical and electrical characteristics of the nonedible ester oil (NEO) compared to NF and MO. The

analysis of thermal, physicochemical and electrical characteristics is carried out for developed NEO to ascertain its usability in the transformer. Insulating oil such as NEO, MO and NF are undergone 164 hours of oxidative ageing. The comparative analysis of the thermal conductivity, physicochemical and electrical characteristics such as colour, moisture content, acidity, interfacial tension, kinematic viscosity, dielectric constant, dissipation factor and breakdown strength of the aged samples are carried out. Weibull statistical analysis of AC breakdown voltage and a fluorescence-based analysis has been carried out to understand and monitor the oil degradation of NEO compare to MO.

In Chapter 8, the alterations in the molecular level of aged VO and NF are studied through various spectroscopic and physicochemical analyses such as NMR, FT-IR, UV-Vis absorbance, fluorescence, colour, acid number, interfacial tension and flash point. The fluorescence-based analysis is carried out for VO and NF at the fresh and aged condition to monitor the comparative ageing degradation. Oxidative ageing of VO and NF results in the formation of flammable and harmful gasses, which are analyzed using dissolved gas analysis (DGA) technique. Comparative electrical properties such as ACBDV, dielectric constant, dielectric DDF are studied for the fresh and aged sample of VO and VO-NF.

Chapter 9 presents the conclusion of the thesis and the suggestions for the extension of this research work in future.

2

Thermophysical and electrical properties of the MO based NF

Contents

2.1 Introduction

Transformer is a critical link in a power system and its reliability is crucial to the reliability of power supply. It is subjected to multiple stresses such as electrical, mechanical, chemical and thermal simultaneously. Mostly insulation system of the transformer comprising of oil and cellulosic kraft paper, which is the weakest element. While oil can be replaced without opening up the transformer, any damage to cellulose requires the transformer to be opened up for repair or replacement, a long drawn out process. Transformer shutdown causes major disruption to power supply and should be minimized. Hence, efforts are being taken at both design and operations stage to arrest the rate of ageing of cellulose.

Cellulose ages fast in the presence of heat and moisture. Being next to the heat generating conductor, it is subjected to high temperature and care is taken by design to limit this well below withstand level. Oil used as coolant and insulant in the transformer plays a crucial role. Higher the thermal conductivity of oil, lower will be the temperature rise on cellulose. Cellulose is hygroscopic and holds much more water than oil. If the moisture equilibrium between oil and cellulose can be altered such that oil can take away more water from cellulose when hot, cellulose ageing will be lower [1].

In recent past, dielectric nanofluids (NFs) have been developed by dispersing nanoparticles (NPs) in the mineral oil (MO) which exhibits superior insulating and cooling properties [33, 76, 99, 100]. Using various NFs, the thermal properties of base fluids could be improved choosing suitable volume fractions of desired NPs [32, 101-107]. In addition to thermal conductivity and moisture holding ability, another desirable property would be a higher dielectric constant [14, 40, 71, 108]. With normal MO having a dielectric constant almost a third of cellulose, oil takes more electrical stress than cellulose. With oil having lower dielectric strength, this leads to a higher oil duct and size and hence cost of transformer. Hence any increase in the dielectric constant and/or dielectric strength of oil would help to reduce the size of transformer [34, 109, 110]. To provide an efficient cooling in power/distribution transformer, a novel NP has to disperse in the heat-transfer fluid to exhibit very high thermal conductivity in combination with excellent electrical properties [111, 112]. Among the various types of NPs, it is observed that the titanium oxide (TiO_2) enhances the AC Breakdown voltage (ACBDV) of the MO. Whereas early sedimentation and hydrophilic surface of TiO_2 NP is restricting its application in the transformer [34, 111, 112]. It is studied from the literature that due to strong Van der Waals force of attraction between the bulk h-BN powders early sedimentation is experienced in the NF.

Considering the parameters such as ACBDV, thermal conductivity and stability of the NFs, an exfoliation process of hexagonal boron nitride (h-BN) is performed. This process converts 1 µm size nanopowder to 2D nanosheets of 150-300 nm [46, 47]. It is observed that exfoliated h-BN (Eh-BN) is a new batch of insulating NP which can improve the thermal conductivity of the NF. High value of thermal conductivity and well suited particle surface for exfoliation, is used for the application in heat transfer. By seeking the heat-transfer and insulation properties of Eh-BN 2D nanofiller, 0.01-0.1 wt.% of particle are dispersed into MO and necessary thermophysical and electrical properties of Eh-BN/MO NF are studied. Electrical strength and dielectric dissipation factor have also been studied after 164 hrs closed beaker oxidative test method.

The thermophysical and chemical characteristics of NF based TO have been studied initially at pre ageing condition. In order to provide a real-time environment for oxidation of these insulating NF, an open beaker oxidative thermal ageing test apparatus has been developed as per ASTM D1934 [113]. This apparatus consists of four beakers based ageing facility with an advanced attachment to provide oxygen, air, and heat in the presence of the copper catalyst. Single temperature oxidative ageing study has been performed at three different ageing durations, such as 164, 328 and 492 hours. Before performing the oxidative ageing for the NFs and MO, the stability of the NF has been verified through zeta potential analysis. The dispersion of 0.01wt% of each of the nanofiller with MO is suitable for the preparation of NF for oxidative ageing analysis.

2.2 Experimental process

2.2.1 Characterization of NPs and MO

As the primary particles size of the nanopowder are approximately in the form of large spherical agglomerates so the surface modifications of the NPs are very much necessary to get enhanced dispersion behavior in the base fluid. The specification of the h-BN NP is presented in Table. 2.1. The surface of h-BN particle is modified into 2D nanosheets by exfoliation process [23, 24]. In this process, the pure 5gm h-BN powder is mixed with isopropyl alcohol (IPA) of 300 ml and then extensively sonicated for 3 hours using the probe sonicator. To maintain the solution at room temperature, ice cubes are kept around the beaker so to avoid rise in temperature of the semi prepared sample. The solution is then centrifuged at 1500 RPM for 30 minutes after sonication, and the collected sample is vacuum filtered and dried to get the Eh-BN particles. The IPA is observed to be a better polar solvent to peel off the pure h-BN powder [24]. The process flow diagram is shown in Figure 2.1.

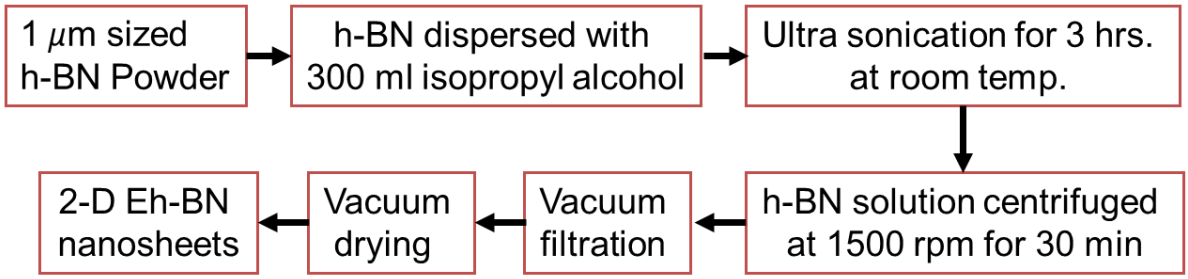

Figure 2.1: Exfoliation process of the h-BN power.

Table 2.1: Specifications of h-BN NP and MO

Characteristics	Specification
Purity	98 %
Distribution size of NPs	1 μm
Density	2.29 g/cm³
Dielectric Constant	3-4
Thermal Conductivity	300 W/m-K at 25°C
Electrical Resistivity	10^{15} Ω-cm
Thermal expansion coefficient	4×10^{-6}/°C
Chemical composition of MO	C_nH_{2n+2}
Paraffinic structure MO	Straight and branched chain

The pure and Eh-BN powders are characterized by X-ray diffraction (XRD), transmission electron microscopy (TEM) and field emission scanning electron microscopy (FESEM). The XRD pattern of a material is like a unique identification of that material. The powder diffraction method is thus suitable for characterizing and identifying the polycrystalline phases. In this study, XRD apparatus (Model-Rigaku, TTRAX III diffractometer, supply: 55 kV, 250 mA) is used for confirming the reduction of the size of pure h-BN by using the Scherrer equation. It is confirmed from Figure. 2.2 that the size of Eh-BN particle is decreased. The size of the particle calculated from the Scherrer equation (2.1) is as follows:

$$L_c = \frac{0.89\lambda}{\beta \cos\theta} \tag{2.1}$$

Where λ (=1.5406Å) is the wavelength of the X-rays, L_C is the average thickness of one multilayer, β is the full width at half maximum (FWHM) of the peak in radians and θ is the

Bragg angle. As the FWHM value of Eh-BN is 0.0034 radian which is more than that of h-BN powder i.e. 0.0028, which suggests that the size of bulk h-BN is reduced after exfoliation. The peaks observed for Eh-BN is matching with JCPDS data (JCPDS No: 34-0421) [23].

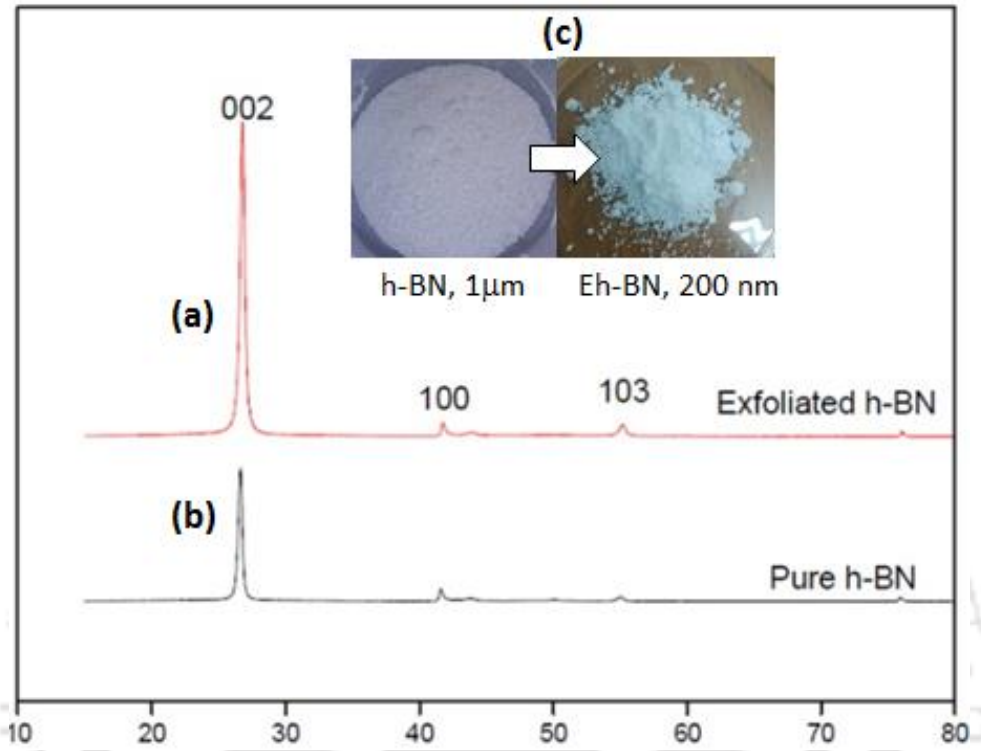

Figure 2.2: XRD pattern of (a) bulk h-BN, (b) exfoliated h-BN powders, and (c) is the image of Eh-BN powder.

It is observed from the studies that the Eh-BN powder show the maximum exposure at (002) planes [25-27]. FESEM image of bulk h-BN and Eh-BN are shown in Figure. 2.3 (a) and (b), where the particle size is reduced from 1 µm to the range of 150-300 nm due to an exfoliation process. This reduction of particle size is also supported by the results obtained from the XRD pattern in Figure. 2.2. The average size of the Eh-BN powder is observed to be 50-100 nm as per TEM analysis. It is observed from Figure. 2.4 (b) that around 10 to 12 layers of h-BN nanosheets are present in Eh-BN. Only 5gm of Eh-BN nanosheets are obtained that for the 8 gm of pure h-BN powder. It confirms that the size of the particles is reduced from 1 µm to 200-300 nm as shown in in Figure. 2.4. Enhancement of surface area to volume ratio occurs is because of exfoliation of the h-BN-NPs.

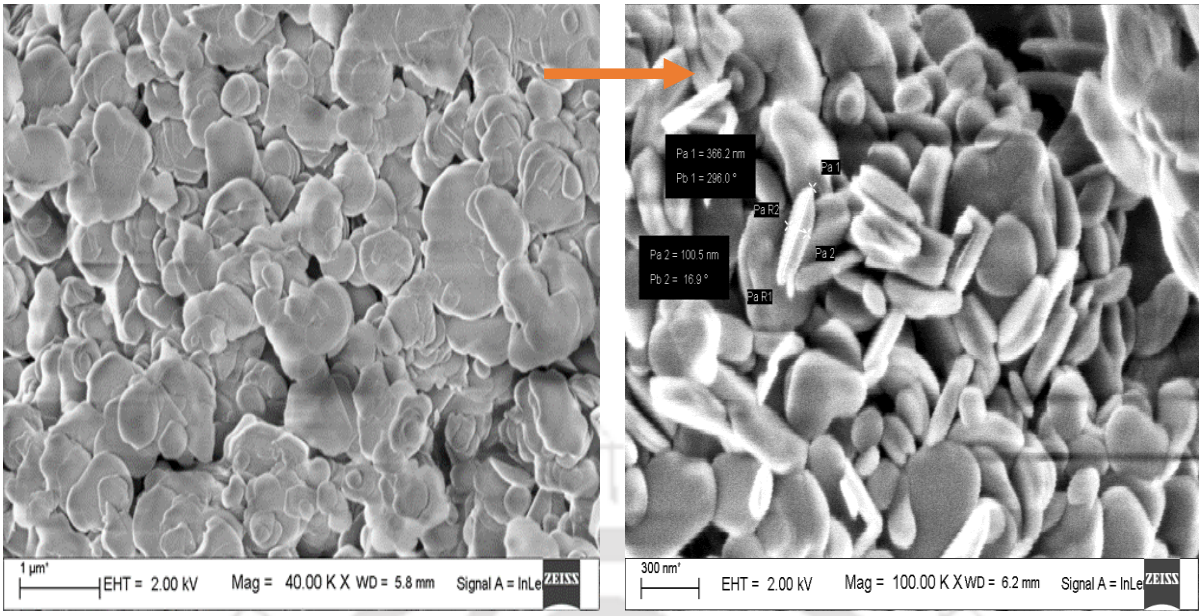

(a) (b)

Figure 2.3: FESEM images of (a) procured pure h-BN from Sigma-Aldrich, of average particle size of 1µm and (b) Exfoliated h-BN nanosheets average particle size of 300nm.

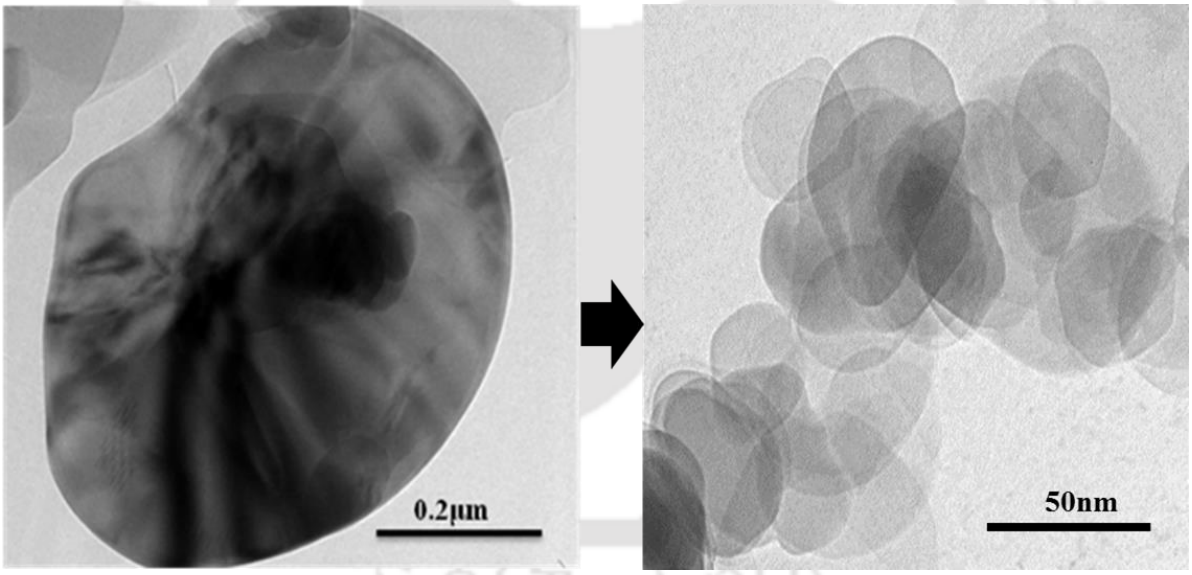

(a) (b)

Figure 2.4: TEM images of (a) a pure h-BN of single particle size of 0.2 µm and (b) an exfoliated h-BN nanosheets of average of 10 to 12 2D sheets having average diameter of 50 nm.

2.2.2 Preparation of NF

The NF samples are prepared by taking MO as a base fluid with the dispersion of Eh-BN NPs. Bulk h-BN powder of size 1 µm procured from Sigma-Aldrich is exfoliated into 2-D nanosheets for the enhancement of its aspect ratio and high surface area for better heat transfer capabilities. The exfoliation process of 1µm size h-BN (shown in Figure 2.1) has been carried

out and the hexagonal structure of h-BN particle is modified to 2D nanosheets with the particles size of 150-300 nm.

Figure. 2.5: preparation of NF as per two step method.

The selection of the NP concertation is based on the investigation of the dispersion stability of the NF. Figure. 2.5 shows the two-step method to prepare the Eh-BN/MO NFs at five different nanofiller concentrations from 0.01-0.1wt.%. For fully dispersed NF, the mixture NP and MO are sonicated for an hour using probe Sonicator. The dispersed NF are kept in a shaking incubator at a temperature of 60^{o} C and 120 RPM to avoid moisture and sedimentation of the NP in the liquid. Again the prepared NF is kept in the vacuum oven for one day at room temperature and high pressure for further moisture evaporation. The moisture measurement for the NF is performed using Karl Fischer titration (KFT) method. Upon confirming the moisture limit of the prepared samples meeting the specified limit of insulating oil standard, further experimental analysis has been performed.

2.3 Results and discussion

The thermophysical properties such as thermal conductivity, viscosity, flash point, pour point, stability, moisture content, acidity etc. and electrical properties such as dielectric strength, permittivity, and dielectric dissipation factor are presented in this present research work.

2.3.1 Stability analysis by zeta potential

Stability of the NF is one of the most important factors for practical application. Due to insufficient stability, it leads to settlement of NPs in the NF which results in clogging of microchannels and decrease of the thermophysical and electrical properties of NF. An adequate stability can be obtained at a zeta potential range of 40-60 mV, beyond 60 mV zeta potential value a permanent stability can be achieved.

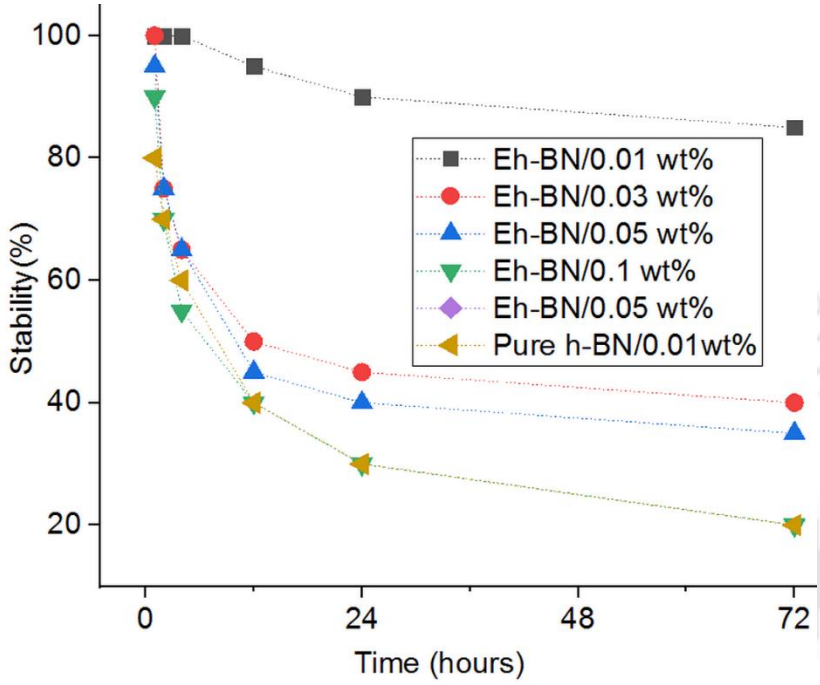

Figure 2.6: Stability analysis of the NF of different nanofiller concertation using zeta potential analysis.

The variation of the NPs concentration in the supernatant of NF is measured using the absorbance of UV-vis spectrophotometer with sedimentation time. Zeta potential is measured from the electrical double layer repulsion of the NPs during the uniform dispersion. High value of zeta potential indicates the greater repulsive force between the particles and hence, signifies the dispersion stability of the NP in the fluid. In the NF, the supernatant NPs concentration directly influences absorbance of the suspended particles. It is observed from the Figure.2.6 that the stability of the Eh-BN/MO NF decreases rapidly with an increase of concentration of the Eh-BN particle. It is also observed that there is no sedimentation of 0.01wt% of Eh-BN NFs up to 72 hrs but after that negligible sedimentation is observed. This is because of the weak van der Waals force of attraction and strong electrical double layer repulsion among the NP interface. The dispersion of 0.01wt.% of Eh-BN nanoparticle into the MO is the most stable dispersion. Upon dispersion of multilayer Eh-BN NP in the matrix (i.e. MO), residual

aggregation is avoided for longer stability. Considering suitable electrothermal properties and maximum dispersion stability, 0.01wt.% concertation of Eh-BN nanofiller is dispersed into the MO for the preparation of NF. The thermophysical and electrical properties of the MO and NF are studied further.

2.3.2 Moisture analysis of the NF

Figure. 2.7: Karl Fischer Titration method for moisture analysis.

In the insulating oil, the moisture content can be originated externally from the atmosphere or produced during oxidation process. The moisture content of MO and NF is determined by Karl Fischer Titration method shown in Figure 2.7 as per ASTM-D1533 [114]. As per this standard, the maximum moisture content is limited to 30 ppm for better dielectric performance of the oil. Usually moisture in microscopic amounts can reduce the electrical breakdown strength of the oil than any other impurities. Therefore, the prepared NF for transformer application has been filtered and dried prior to performing any other test. In this work the dielectric performances of the NF are studied at a moisture content of 18 and 24 ppm.

2.3.3 Viscosity

Rheological parameters of NFs and MO are measured by a Rheometer (Model-Physica MCR 101, Anton Paar) as shown in Figure 2.8.

Figure 2.8: Rheometer to analyse the rheological parameters.

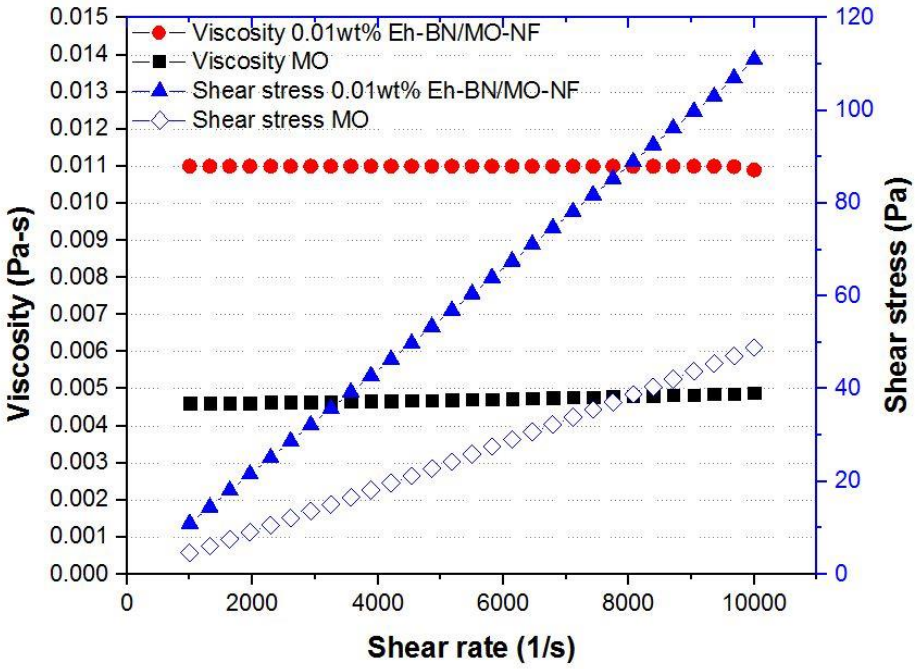

Figure 2.9: Rheological behavior of 0.01 wt. % NF.

In this work, a cone plate (CP50-1) is used for the measurement of all prepared samples because the angle provided in the cone plate helps the liquid to stay in between the fixed and measuring plate. For the NFs and MO, the shear rate is selected in the range of 10^3-$10^4 s^{-1}$ and the corresponding values of dynamic viscosity in the temperature range of 25-60^oC are measured. A low shear rate (10 s^{-1}) is selected to study the pour point of the test sample. Shear stress is directly proportional to shear rate and the viscosity remains constant with the increased shear rate as shown in Figure. 2.9. It shows that the fluid is having Newtonian behavior which gives the information about the interaction between the NPs in the base fluid. It also indicates that the dispersion of NP is not affecting the NF behavior physically.

2.3.4 Viscosity with temperature

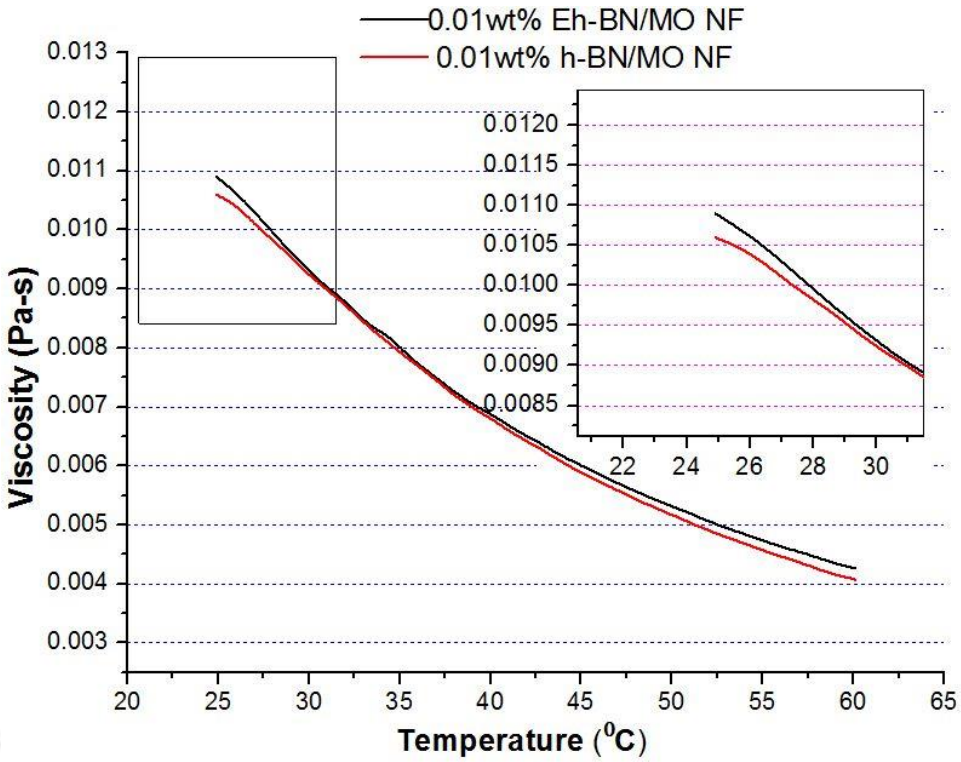

Figure 2.10: Dynamic viscosity of 0.01 wt.% NFs at varying temperature.

It is observed from the Figure.2.10 that the change of viscosity due to the exfoliation of h-BN NPs is negligible above 35°C. This indicates that the effect of 0.01wt % Eh-BN particle on the ACBDV of the MO is purely not due to change of viscosity. It is also observed that the viscosity of NF decreases with increasing temperature, which is desirable for getting more enhancement in heat transfer at higher temperature [110].

2.3.5 Thermal conductivity analysis

Thermal conductivity of MO and NFs is measured using a KD2 probe (Decagon Device Inc., model KD2 Probe) shown in Figure 2.11. It follows the mechanism of transient hot-wire method. In this process a definite extent of probe is fully dipped in a fixed liquid medium and the probe is being excited electrically for heat transmission. With the help of Wheatstone bridge circuit, the change in resistance due to the change in temperature is measured as a function of time. The effects of temperature, time, particle size and particle concentrations on the thermal conductivity of MO based NFs are examined by transient hot wire method. The slope of heating power and the change in temperature with logarithmic time scale is the measure of thermal conductivity.

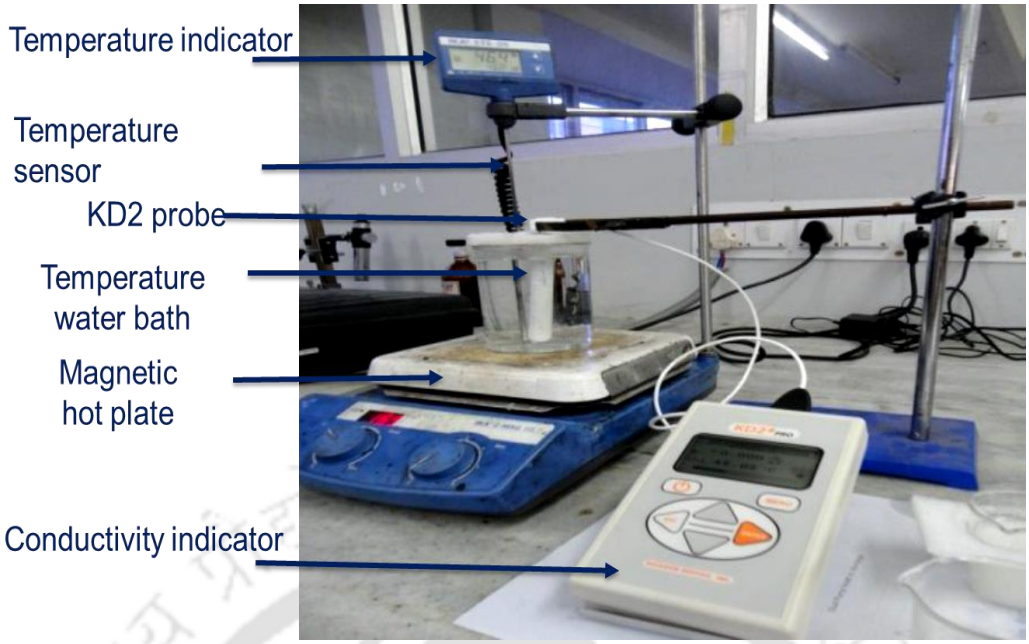

Figure 2.11: Thermal conductivity measurement using a KD2 probe.

The effective thermal conductivity of the NF can be achieved by using Feng-Kleinstreuer (F-K) analytical expression as given in (2.2). The percentage enhancements of the thermal conductivity of pure h-BN/MO and Eh-BN/MO NFs for five different wt% from 0.01 to 0.1 at room temperature are presented in Table 2.2 and Figure. 2.12. The addition of minute nanofiller concentration results appreciable increment in thermal conductivity because of large surface area of Eh-BN sheets. At higher concentration of the nanofiller, the enhancement of thermal conductivity drops violating Maxwell's classical theory.

$$k_{eff} = \left(1 + \frac{3\left(\frac{k_p}{k_{bf}} - 1\right)\phi}{\left(\frac{k_p}{k_{bf}} + 2\right) - \left(\frac{k_p}{k_{bf}} - 1\right)\phi}\right) k_{nf} + \frac{8250 k_B}{\pi \mu_{bf} d_p} \left(\rho c_p\right)_{nf} \phi^2 T \ln T - T \quad (2.2)$$

Where k_p, k_{bf} and k_{nf} are the thermal conductivity of the particles, base fluid and NF respectively. ϕ, μ_{bf}, c_p and ρ are the volume fraction of dispersed NPs, coefficient of viscosity of the base fluid, specific heat and density of the fluid respectively. The diameter of the NP and the average temperature of the NF are d_p and $\overline{T}$ respectively.

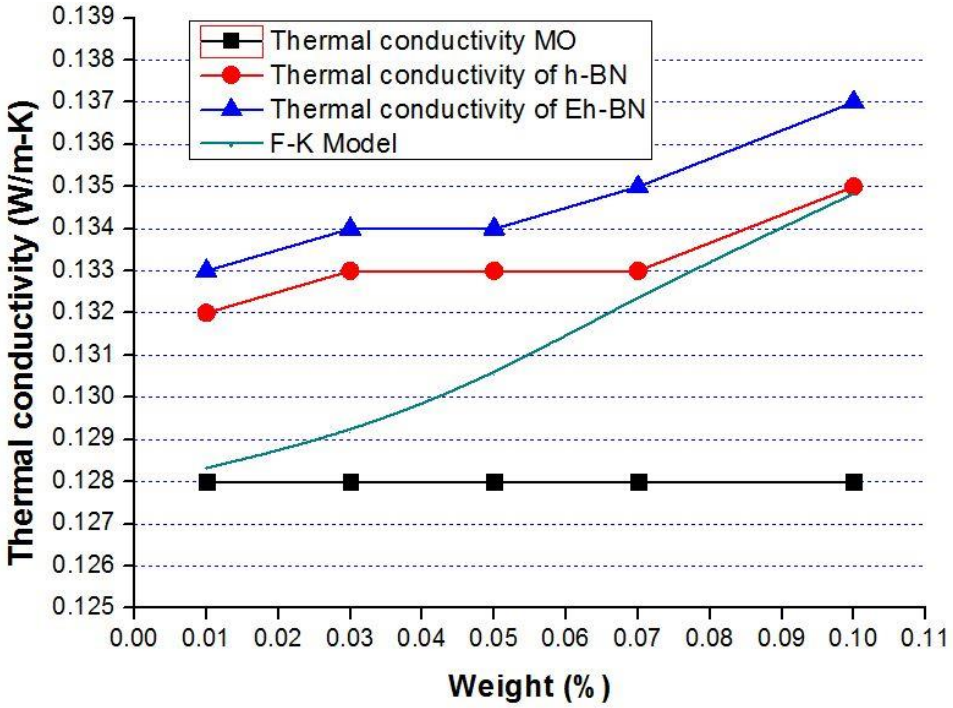

Figure 2.12: Thermal conductivity of NFs with wt.% of the NPs.

Heat transfer characteristic of the NFs and MO at elevated temperature are studied for stable concertation of 0.01 wt% of NP. NF is heated to six different stages of temperature from 298 to 323 K and the thermal conductivity is measured using KD2 probe (KS-1) with the help of temperature sensor to detect the oil temperature.

Table 2.2: Thermal conductivity of the NF compared to MO at room temperature

Wt. %	Thermal conductivity of NF (W/m-K) at 25°C			
	Pure h-BN/MO		Eh-BN/MO	
	Absolute	% Rise	Absolute	% Rise
0.00	0.128	0.0	0.128	0.0
0.01	0.132	3.12	0.133	3.90
0.03	0.133	3.90	0.134	4.68
0.05	0.133	3.90	0.134	4.68
0.07	0.133	3.90	0.135	5.46
0.1	0.135	5.46	0.137	7.03

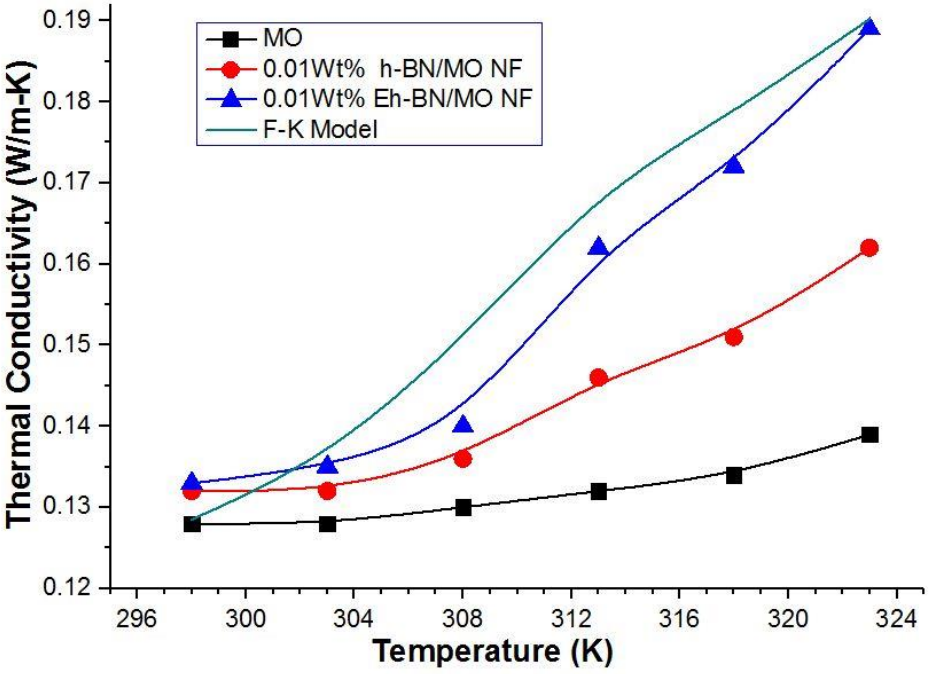

Figure 2.13: Thermal conductivity of NFs with temperature.

Thermal conductivity of MO and 0.01wt % NF at different temperature are studied and compared analytically with F-K analytical model as shown in Figure. 2.13. Thermal conductivity of the MO, 0.01wt.% of h-BN/MO and 0.01wt.% Eh-BN/MO NF increase from 0.128 to 0.139 W/m-K, 0.132 to 0.162 W/m-K and 0.133 to 0.189 W/m-K respectively with increase in temperature from 298 to 323 K. The thermal conductivity of the NF obtained by F-K model increases from 0.128 to 0.190 W/m-K with the increase of temperature as mentioned in Figure 2.13. There is a significant enhancement in thermal conductivity of Eh-BN based NF compared to MO and h-BN/MO NF. The enhancement in the thermal conductivity is due to the increase in Brownian motion of the NPs. The liquid layering at the particle liquid interface also plays an important role for the enhancement in thermal conductivity of the NF [102].

It is seen from the figure that the exfoliation of bulk h-BN powder to 2D nanosheets enhances thermal conductivity of the Eh-BN/MO NF from 4 to 36% with the increase in temperature whereas, the enhancement in thermal conductivity are 3 to 16% for h-BN/MO NF. Since, the enhancement in thermal conductivity of the Eh-BN based NF is superior to MO, it has the potential to replace MO in the transformer as a better heat transfer fluid.

2.3.6 Pour and flash point study

Figure 2.14: Pensky-Martens cup apparatus for flash point, (RTL, CPRI, Guwahati).

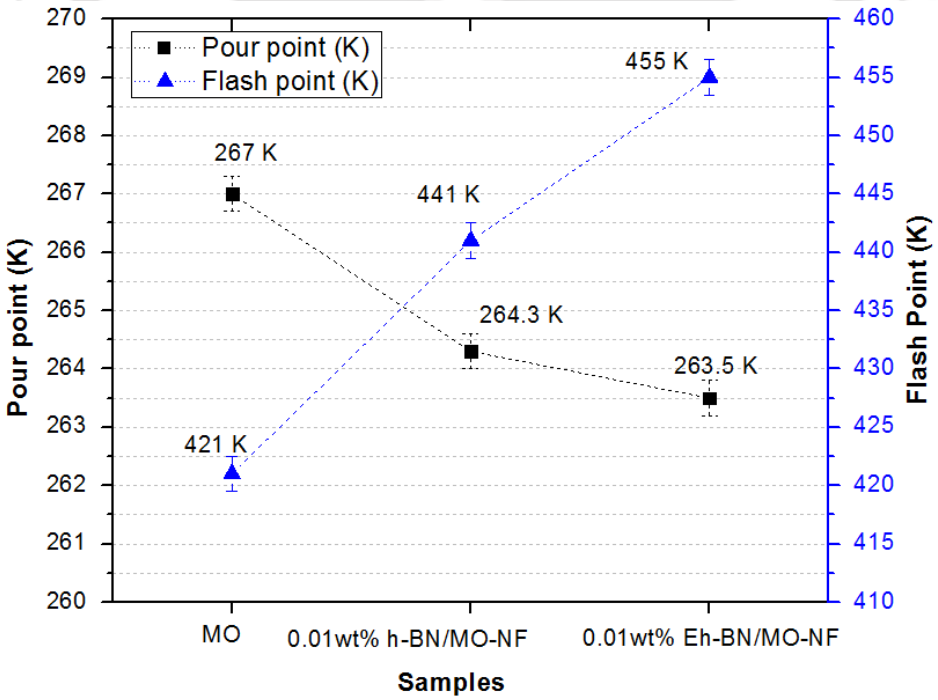

Figure 2.15: Pour and flash point of MO and NF at 0.01wt.% of NPs.

Pour point of a liquid is defined as the minimum temperature at which it can flow. In general, it should be minimum in order to use the NF at very low temperature. The flash point of oil is the minimum temperature at which oil must be heated, so that it gives enough vapor which can

generate a flammable mixture with the air under the prescribed conditions of the test. This is determined by employing a Pensky-Martens closed cup apparatus as per ASTM D93 [115] shown in Figure 2.14. Degradation of oil and topping-up with oil having volatile combustible lower molecular hydrocarbons can cause lowering of flash point. A minimum value of flash point is specified in order to prevent the risk of fire that might result by accidental ignition.

It is seen from Figure 2.15 that the NF having 0.01 wt.% of Eh-BN has lower pour point temperature than the MO, which shows the promising molecular interaction between Eh-BN and MO. It is observed that the pour point temperature of NF is influenced by the nature of NPs. The pour point temperature is getting reduced for Eh-BN/MO–NF. The reason behind lowering the pour point temperature of NF is associated with nanoscale dimension of Eh-BN, high intermolecular interaction and liquid layering with Eh-BN NPs. The NF having 0.01wt.% Eh-BN has highest flash point temperature than MO and 0.01wt.% h-BN NF as seen in the Figure 2.15. The enhancement in flash point in the NFs directly indicates that the dispersed NP arrests the generation of vapor pressure which is a function of temperature. Since NF has superior thermal conductivity, the vapor pressure will be minimized to attain an enhanced flash point.

2.3.7 Interfacial tension (IFT)

Figure 2.16: Tensiometer for IFT (RTL, CPRI, Guwahati).

The interlayer molecular force of attraction between the oil and water is measured in terms of IFT. The interfacial tension is determined using suitable tensiometer (Torsion

balance), in which the force required to lift a planar ring of platinum from the oil/water interface into the oil is measured The role of polar contamination which is measured as IFT determines the oil property. Higher the value of IFT lesser is the polar contamination in the NF and hence better serviceability of the oil is expected. To measure the IFT of the MO and Eh-BN/MO-NF, a torsion balance tensiometer shown in Figure 2.16 is used and the test has been performed as per ASTM-D971 [116].

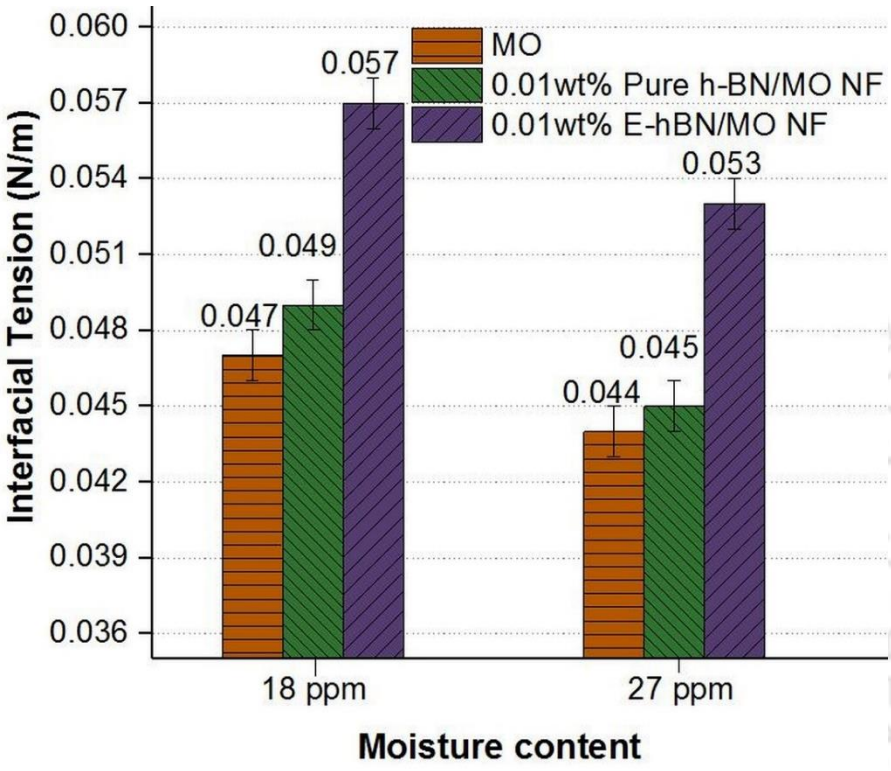

Figure 2.17: IFT of the MO, h-BN and Eh-BN NFs at different moisture level.

The IFT value for insulating oil provides sensitive information for detection of polar contaminants in the oil. Inadequate value of the IFT is the main cause of deterioration of the oil which may leads to generation of oxides and peroxide in the insulating oil during service. IFT is determined by means of suitable tensiometer (Torsion balance, Model: SEO-DST30M), as shown in Figure 2.16 in which the force required to lift a planar ring of platinum from the oil/water interface into the oil. This test has been performed as per ASTM-D971 [116]. It is observed from the Figure 2.17 that IFT of Eh-BN/MO NF is higher than that of h-BN/MO NF and MO. Decreasing value of IFT indicates an increase in contaminants and/or oxidation byproducts within the oil. IFT is determined by the difference of the interactions between the molecule of the material (fluid) themselves and interaction of these molecules with molecules

of contacted material (air or solid or another fluid). So, the well dispersed 0.01wt% of Eh-BN-NP concentration enhances IFT of NFs more than the MO.

To study the electrical performance of the developed NF, various electrical properties such as AC breakdown voltage (ACBDV), dielectric losses (Tan δ), dielectric dissipation factor and resistivity are analyzed and explained below.

2.3.8 AC breakdown voltage (ACBDV)

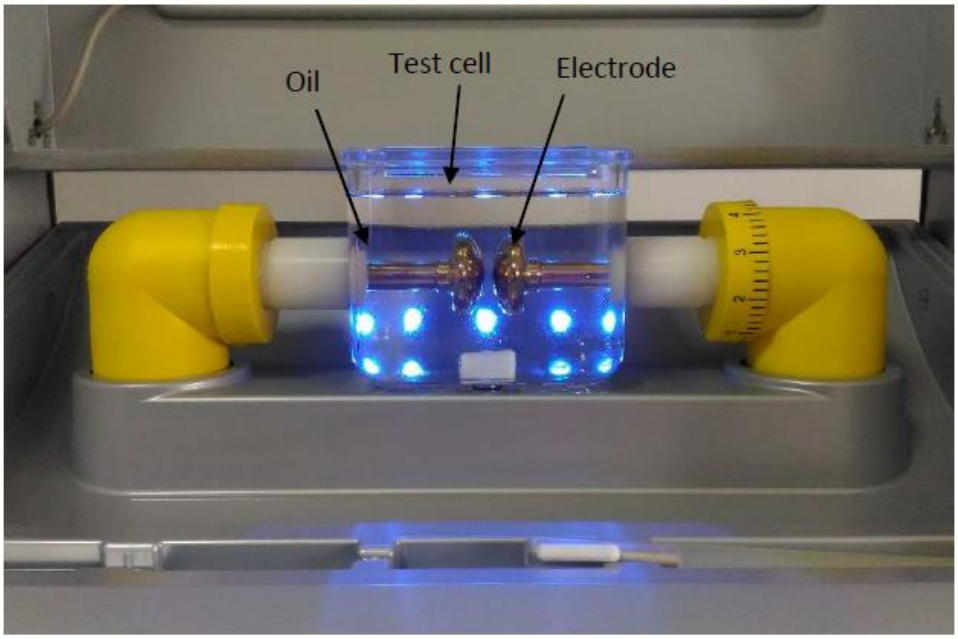

Figure 2.18: Baur ACBDV Setup, PGCIL, Nagaon, Guwahati.

The electric strength (or BDV) is the measure of the ability of the oil to withstand electric stress. The BAUR DTA 100 C, oil tester is used to perform the ACBDV voltages test as per ASTM D1816 [117] using brass mushroom-capped electrodes set at 2.50 mm gap as shown in Figure 2.18. The ACBDV test of MO and NFs are carried out in Insulating Oil Testing Laboratory (IOTL) at PGCIL, Nagaon, Assam, India. The gradual applied voltage is selected at a rate of 2 kV/s. Initially, the standing time is set for 10 minutes before the application of voltage. After each breakdown, the time interval of 1-minute for stirring is fixed. In one set of experiments, six breakdown voltages data are measured and the mean BDV has been reported.

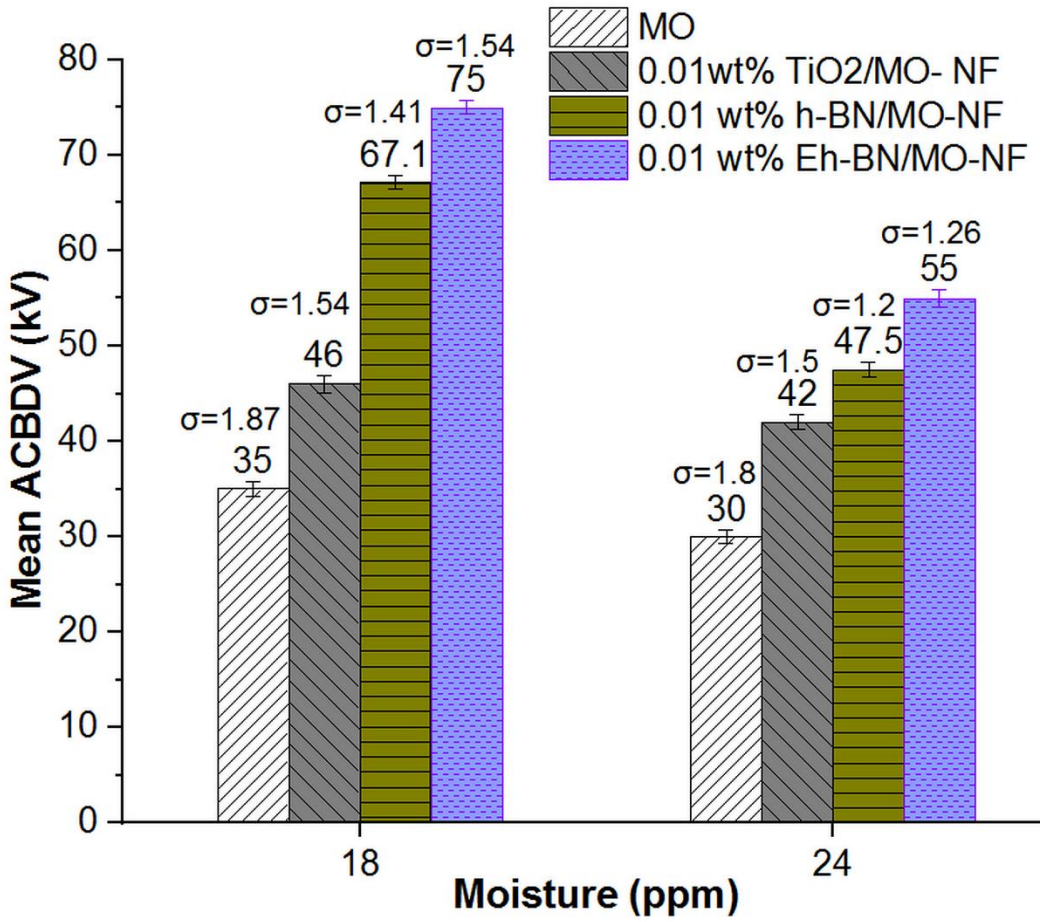

Figure 2.19. ACBDV of MO and NFs at 18 and 24 ppm moisture content.

To study the ACBDV of the NFs, 0.01wt.% of TiO_2, h-BN and Eh-BN NPs are dispersed in MO. The moisture content has a sufficient influence on the ACBDV of MO and NFs. Pure h-BN and TiO_2 NPs have hydrophilic surface, which has the potential to bind the water at their interface. In practice, due to pass of time and ageing, the moisture content of the oil in transformer can rise more than 30 ppm. Hence in the present study, the ACBDV of the oil are measured at moisture content of 18 and 24 ppm. The mean value of the measured breakdown strengths of the NFs compared to that of MO at different moisture contents such as 18 and 24 ppm are presented in Figure 2.19 It is seen from the figure that the ACBDV of Eh-BN/MO, h-BN/MO, TiO_2/MO NFs and MO at 18 ppm moisture content are 75, 67.1, 46 and 35 kV respectively. Whereas, at 24 ppm, ACBDV of the aforementioned NFs and MO are 55.5, 47.5, 42 and 30 kV respectively. The enhancement in ACBDV of TiO_2 based NF compared to MO is 31.4 and 26.7% at 18 and 24 ppm respectively. Whereas, the enhancement in ACBDV of Eh-BN based NFs compared to MO is 114.2 and 85% for the moisture content of 18 and 24 ppm respectively.

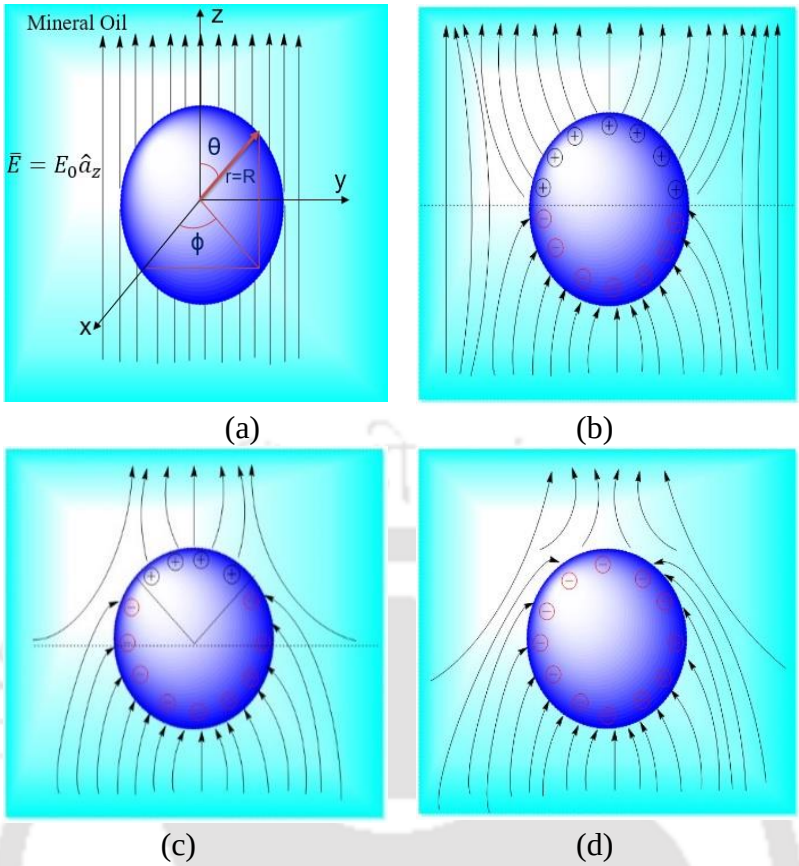

Figure 2.20: Charging of the NP (a) particle exposed to an external field, (b) ionization or polarization of the NP, (c) depletion of the positive ions and (d) complete depletion of the positive ions.

In order to understand the enhancement in the ACBDV, the charge dynamics analysis of the NPs in the liquid dielectric is studied considering the spherical Eh-BN dielectric and TiO_2 semiconducting NPs having average radius R (=75 nm and 12.5 nm for Eh-BN and TiO_2 respectively), permittivity ε_2 (= $4\varepsilon_0$ and $31\varepsilon_0$ F/m for Eh-BN and TiO_2, respectively) and conductivity σ_2 (= 10^{-13} and 10^{-6} S/m for Eh-BN and TiO_2, respectively) and surrounded by MO with permittivity ε_1(= $2.2\varepsilon_0$ F/m) and conductivity σ_1 (= 10^{-12} S/m) are considered as shown in Figure 2.20 a. The time-varying radial component of the electric field in the MO outside the NP due to the excitation, E_0 is [76],

$$\vec{E}_r(r \geq R^+, \theta) = \hat{a}_r E_0 \left[1 + \frac{2R^3}{r^3} C_\epsilon exp\left(-\frac{t}{\tau_r}\right) + \frac{2R^3}{r^3} C_\sigma \left(1 - exp\left(-\frac{t}{\tau_r}\right)\right)\right] \cos\theta \quad (2.3)$$

Where $C_\varepsilon = \frac{\varepsilon_2 - \varepsilon_1}{2\varepsilon_1 + \varepsilon_2}$, $C_\sigma = \frac{\sigma_2 - \sigma_1}{2\sigma_1 + \sigma_2}$ and the relaxation time $\tau_r = \frac{2\varepsilon_1 + \varepsilon_2}{2\sigma_1 + \sigma_2}$

Since, the NP has finite conductivity, it takes finite time to place the charges on the surface of the NPs depending on the particle and oil conductivities and permittivities. It is observed from the Figure 2.20 b that when the NP is exposed to an external electric field, the positive and negative ions are generated in the upper half ($0 < \theta \leq \frac{\pi}{2}$) and lower half ($\frac{\pi}{2} < \theta \leq \pi$) of the particles without any space charge in the bulk. As time progress, the electrons originated from ionization or polarization, deposit on the particle and curtail the positive ions, so positive ions are confined in $0 < \theta < \theta_c$ and the negative ions in $\theta_c < \theta < \pi$ as shown in Figure 2.20 c**.** In this situation, the modified expression of the electric field in the MO on the surface of the NP in the presence of deposited electron charge *Q(t)* is,

$$E_r(r \geq R, \theta) = E_0 \left[1 + \frac{2R^3}{r^3} C_\epsilon exp\left(-\frac{t}{\tau_r}\right) + \frac{2R^3}{r^3} C_\sigma \left(1 - exp\left(-\frac{t}{\tau_r}\right)\right)\right] cos\theta + \frac{Q(t)}{4\pi\varepsilon_1 r^2} \quad (2.4)$$

As the deposition of the electrons on the nanoparticle continues, the positive charge diminishes to zero ($i.e., E_r(r = R, \theta) \geq 0$) and the particle is fully charged by a saturation charge Q_s as shown in Figure 2.20 d. The saturation charge Q_s for the NP derived from $E_r(r = R, \theta) = 0$ is,

$$Q_s = -12\pi\varepsilon_1 R^2 E_0 \frac{\varepsilon_2}{2\varepsilon_1 + \varepsilon_2} \quad (2.5)$$

The charging rate of the NP derived from equation (2.4) is given as:

$$\frac{dQ(t)}{dt} = \frac{3Q_s}{\tau_{pc} C(t)} \left[\frac{Q(t)}{\frac{Q_s}{\frac{\varepsilon_2}{2\varepsilon_1 + \varepsilon_2}}} - \frac{C(t)\cos\theta}{3}\right]^2 \quad (2.6)$$

Where the charging time constant of the NP is expressed as:

$$\tau_{pc} = \frac{4\varepsilon_1}{|-\rho_e|\mu_e} \quad (2.7)$$

and

$$C(t) = 1 + 2C_\epsilon exp\left(-\frac{t}{\tau_r}\right) + 2C_\sigma \left(1 - exp\left(-\frac{t}{\tau_r}\right)\right) \quad (2.8)$$

Solving (2.6), using MATHEMATICA, the expression of the charge accumulation *Q(t)* on the Eh-BN and TiO_2 NP are presented in (2.9) and (2.10**)** respectively.

$$Q(t) = \frac{\left(6.11165\times10^{8}e^{-0.0564717t}\left(733.935e^{-0.0282358t}+81.8484e^{-0.0564717t}+9e^{-0.0282358t}t+e^{-0.0564717t}t-318.744e^{-0.0282358t}Log\left[9e^{-0.0282358t}+e^{-0.0564717t}\right]-35.416e^{-0.0564717t}Log\left[9e^{-0.0282358t}+e^{-0.0564717t}\right]\right)\right)}{\left(-8.44609\times10^{27}-1.03572\times10^{26}t+3.66809\times10^{27}Log\left[9e^{-0.0282358t}+e^{-0.0564717t}\right]\right)} \quad (2.9)$$

$$Q(t) = \frac{\left(\left(-5.70125\times10^{100}-9.17391\times10^{100}i\right)e^{3190.5t}+\left(9.17401\times10^{101}+1.47619\times10^{102}i\right)e^{6380.99t}-\left(3.69051\times10^{102}+5.93838\times10^{102}i\right)e^{9571.49t}-2.79501\times10^{104}e^{3190.5t}t+4.49749\times10^{104}e^{6380.99t}t-1.80924\times10^{106}e^{9571.49t}t+2.92014\times10^{100}e^{3190.5t}log\left[e^{9571.49t}-8.04557e^{12762.0t}\right]-4.69884\times10^{101}e^{6380.99t}log\left[e^{9571.49t}-8.04557e^{12762.0t}\right]+1.80924\times10^{102}e^{9571.49t}log\left[e^{9571.49t}-8.04557e^{12762.0t}\right]-e^{6380.99t}\left(0.5e^{6380.99t}\left(\left(-6.66934\times10^{95}+5.36586\times10^{96}e^{3190.5t}\right)^2-4\left(\left(-2.22098\times10^{119}-3.57377\times10^{119}i\right)+\left(1.7869\times10^{120}+2.8753\times10^{120}i\right)e^{3190.5t}-1.08882\times10^{123}t+8.76016\times10^{123}e^{3190.5t}+1.13756\times10^{119}log\left[e^{9571.49t}-8.04557e^{12762.0t}\right]-9.15235\times10^{119}e^{3190.5t}log\left[e^{9571.49t}-8.04557e^{12762.0t}\right]\right)\left(3.05227\times10^{65}e^{3190.5t}t-2.49092\times10^{62}log\left[e^{9571.49t}-8.04557e^{12762.0t}\right]+1.81361\times10^{63}e^{3190.5t}log\left[e^{9571.49t}-8.04557e^{12762.0t}\right]\right)\right)\right)}{\left(\left(-2.22098\times10^{119}-3.57377\times10^{119}i\right)+\left(1.7869\times10^{120}+2.8753\times10^{120}i\right)e^{3190.5t}-1.08882\times10^{123}t+8.76016\times10^{123}e^{3190.5t}+1.13756\times10^{119}log\left[e^{9571.49t}-8.04557e^{12762.0t}\right]-9.15235\times10^{119}e^{3190.5t}log\left[e^{9571.49t}-8.04557e^{12762.0t}\right]\right)} \quad (2.10)$$

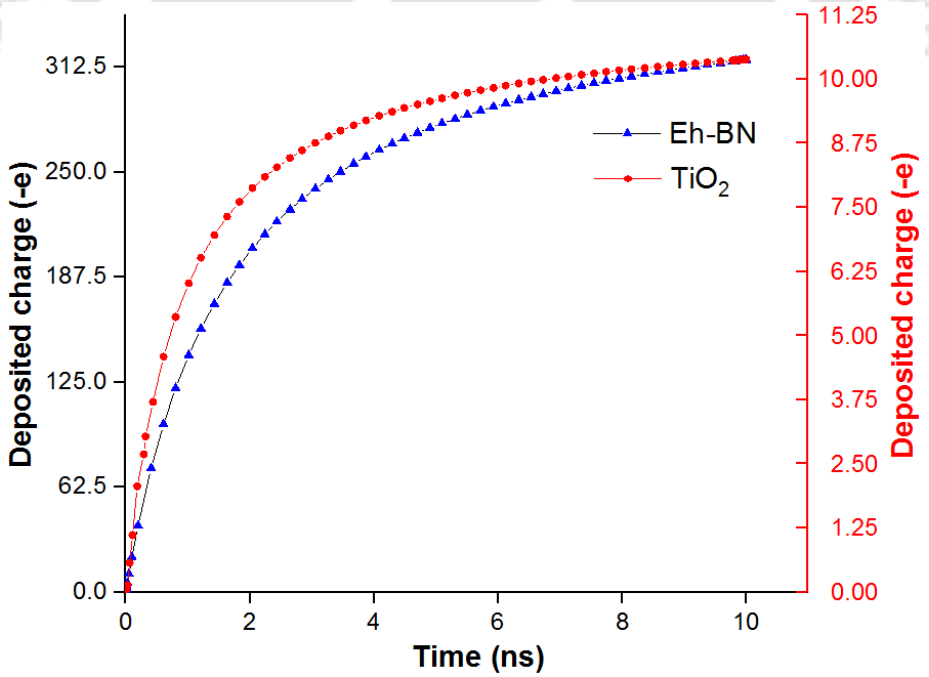

Figure 2.21: Charging characteristics of Eh-BN and TiO_2 in MO.

The number of electrons absorbed on the surface of the Eh-BN and TiO_2 NP are 369 and 11 respectively as shown in Figure 2.21 and Table 2. 3. The total number of particles in 0.01wt% of Eh-BN and TiO_2 are calculated as 2.43×10^{20} and 7.54×10^{19} respectively. This decelerates the ionization process in Eh-BN/MO-NF and hence BDV increases.

TABLE 2.3: Electron captures by the NPs

NPs	Q_s per NP $\times10^{-18}$ (C)	N_e per NP	N_{np} in 100 gm of MO $\times10^{19}$	Total N_e $\times10^{19}$
TiO_2	-1.81	11.3	7.54	85.2
Eh-BN	-59.01	368.8	24.63	9073

Note: N_e and N_{np} are the number of electron and total number of NPs.

From Table 2.3, it is observed that the captured saturation electrons for the Eh-BN/MO-NF is higher than that of TiO_2/MO-NF. Since, more number of electrons are captured by the Eh-BN NPs in the NF the ionization process hinders and hence the BDV increases compared to TiO_2/MO-NF and MO.

2.3.9 Dielectric constant and dissipation factor

A multipurpose Tan Delta-DTR-3K measuring equipment as shown in Figure 2.22 is used to study the dielectric dissipation factor (tan δ) and dielectric constant at 90°C at a constant frequency of 50 Hz. The test was conducted as per the ASTM-D924 [118] standard. In order to realize any possible impact of ageing on the dielectric properties of the liquid under study, the closed beaker oxidative test of the liquid has been performed according to the ASTM-D2440 [119] standard for 164 hrs at 110°C, 50 Hz. It is seen from the Figure. 2.23 that the dielectric constant of the insulating liquid such as MO, h-BN, and Eh-BN based NF before oxidative ageing were 2.03, 2.04 and 2.06 respectively. However, the dielectric constant of the aforementioned fluids after oxidative ageing decreases to 2.01, 2.03 and 2.04 respectively.

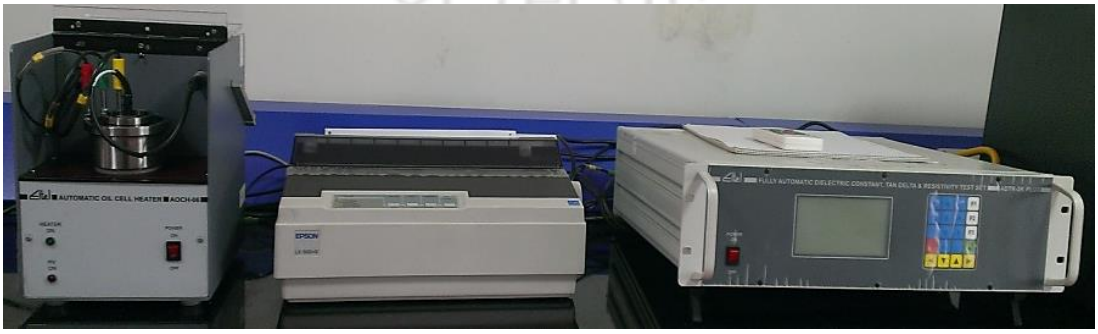

Figure 2.22: Tan Delta-DTR-3K Measuring setup (RTL, CPRI, Guwahati).

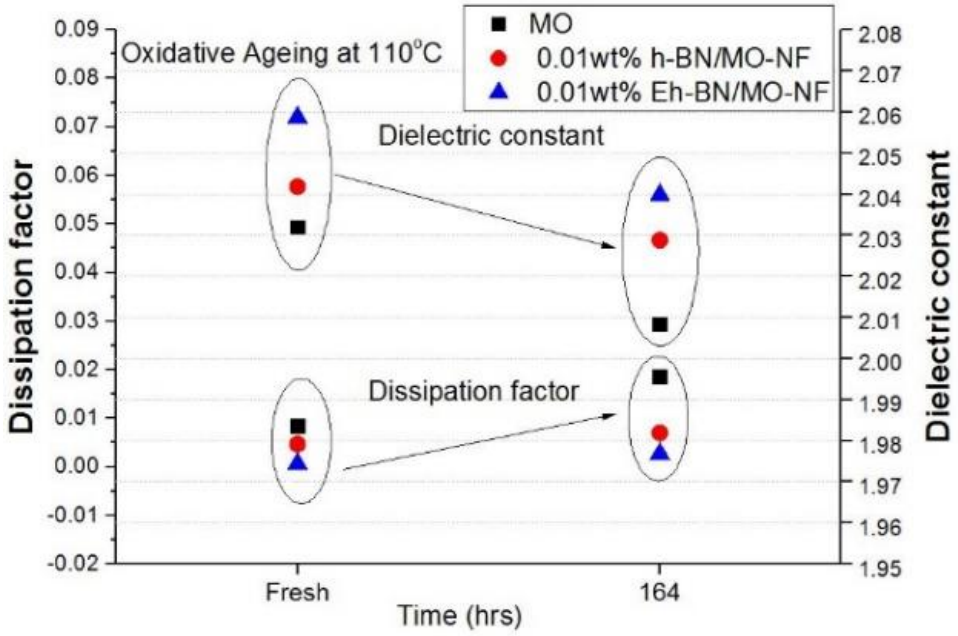

Figure 2.23: Dissipation factor (tan δ) and dielectric constant of the fluids before and after the oxidative ageing.

The above results indicate that the dielectric constant of the Eh-BN NF is higher than that the MO and the ageing period leads to a minor decrement in the dielectric constant. The dissipation factor of the fluids increases with increasing the aging period as shown in Figure 2.23 Formation of sludge and water during oxidative ageing increase the tanδ value hence dielectric properties decays. Since, the dielectric constant and dissipation factor of the Eh-BN/MO NF are always better than MO, using Eh-BN NPs, ageing of the transformer oil can be minimized, which in turn improves the life of the transformer.

2.4 Summary of the chapter

In this work, the experimental and analytical analysis of the thermophysical and electrical properties of the Eh-BN/MO-NF are presented. The important conclusion of this work are as follows:

- The dispersion stability of 0.01wt% of Eh-BN NP is observed to be stable due to exfoliation and weak van der Waals force of attraction and strong electrical double layer repulsion.
- The higher aspect ratio of Eh-BN NP dispersion leads to improve the thermal conductivity of the NF significantly.
- Uniform dispersion of Eh-BN NP in MO does not hampers the Newtonian behavior of the NF even at elevated temperature. However, flash and pour point temperature is significantly improved for Eh-BN/MO-NF.

- Moisture and polar contaminations in the MO and NFs affect negatively for IFT, acidity, ACBDV, dielectric constant and DDF. However, hydrophobic nature of the Eh-BN NP has less affinity towards polar contamination.
- Least affinity of the Eh-BN NP towards polar contamination shows minute degradation in its insulating properties even after the oxidative ageing.
- Since, the Eh-BN NP scavenges the free electrons available in the MO under excitation, the initiation of the streamer is arrested and hence, there is an enhancement in the ACBDV for Eh-BN/MO-NF compared to MO.

Considering the aforementioned advantages of the Eh-BN NF over existing MO based transform oil, it will be the alternate insulating and coolant for distribution/power transformer.

To verify the usability and feasibility from the practical aspect of implementing NF based TO, an oxidative thermal ageing study has been performed to understand the degradation behavior of MO and insulating NF at three different ageing periods in the next chapter.

3

Open beaker oxidative ageing analysis of MO and NF

Contents

3.1 Introduction

An effective power transmission has only been possible with the minor power drop inside the transformer. TO, apart from providing electrical insulation, also serves the vital function of conducting heat away from the solid insulation and lowers its operating temperature. The design of superior insulating oil and maintenance of adequate cooling is a direct mode of energy saving process for the power and distribution transformers. A major portion of energy drops in the transformer is due to the ineffective heat transfer inside the transformer. Any improvement in thermal conductivity of the transformer oil without adversely affecting insulation properties, will enhance the life of the cellulose and hence that of the transformer. Alternately, it will permit the operation of the transformer at higher loads without the reduction in life and energy, thus increasing the capital utilisation [89]. Several reasons are identified for an energy deficient transformer performance, in which substandard insulating mineral oil (MO) is the front runner [33]. Efficient insulating oil in the transformer is a key medium to maintain the effective insulation and cooling, which further is responsible for the energy saving. The insulation capability of the oil degrades due to oxidation and the combination of thermal, chemical, mechanical and electrical stresses inside the transformer [1, 33, 68]. Development of an energy efficient NF with enhanced electrical, mechanical and thermal characteristics is expected to lead to a power transformer with a much lower life-cycle cost [34, 120]. The efficacy and superior performance of the NF based TO add more life to the transformer by enhancing the insulation, dropping the heat loss and hence preventing power wastage. MO is being widely used in the transformer as an insulating and cooling agent, but inferior thermophysical and chemical characteristics of the MO-based TO motivates to develop NF based TO The NF in dielectric applications is being heavily researched to improve the understanding of the physical mechanisms involved in their improved performance compared with the base fluid [35-37].

To verify the usability and feasibility from the practical aspect of implementing NF based TO, an oxidative thermal ageing study has been performed to understand the degradation behaviour of MO and insulating NF at three different ageing periods. It has been observed that the use of nanoparticles (NPs) in dielectric liquids such as ethylene glycol, vegetable oil and MO increases the thermophysical and electrical properties, but these properties of NFs in the oxidative environment of the transformer are still an important parameter to study [94, 121-124]. This is a key motivation for this investigation to explore the possible impact of ageing on the MO and NF Based TO and its degradation characteristics.

3. Open beaker oxidative ageing analysis of MO and NF

In this study, two different batches of NF namely, Titanium Oxide (TiO_2) and Eh-BN based insulating NF has been prepared by taking MO as the base fluid. The basic properties of the MO are depicted in the Table 3.1. Properties of the MO have been verified from Table 1 before the dispersion of TiO_2 and Eh-BN nanofillers into it. The thermophysical and chemical characteristics of NF based TO have been studied initially at pre ageing condition. In order to provide a real-time environment for oxidation of these insulating NF, an open beaker oxidative thermal ageing test apparatus has been developed as per ASTM D1934 [113].

This apparatus consists of four beakers based ageing facility with an advanced attachment to provide oxygen, air, and heat in the presence of the copper catalyst. Single temperature oxidative ageing study has been performed at three different ageing durations, such as 164, 328 and 492 hours. Before performing the oxidative ageing for the NFs and MO, the stability of the NF has been verified through zeta potential analysis. The dispersion of 0.01wt% of each of the nanofiller with MO is suitable for the preparation of NF for oxidative ageing analysis. To evaluate the critical changes in the characteristics [125] of the prepared insulating oil samples at the post ageing condition, the standard procedures as given in Table 3.2 is followed.

Table 3.1: Properties of MO

Properties	MO
Viscosity at 40°C (ASTM D445), cSt	11.25
Density (ASTM D1298)	0.825
Interfacial tension, dynes/cm (ASTM D971)	47
Acid number, mg KOH/g (ASTM D974)	<0.01
Flash point (ASTM D92), °C	164
Dielectric dissipation factor (Tan Delta) at 90^{o} C (Max).	0.00041
AC Breakdown Voltage (ASTM 1816) kV @ 24 ppm	30

Table 3.2: Parameters for aged oil analysis

Properties	Experimental standards
Viscosity at 40°C, cSt	ASTM D445
Thermal conductivity	Transient hot wire method
Moisture in oil, ppm	ASTM D1533
Colour	ASTM D1500
Acid number, mg KOH/g	ASTM D974
Interfacial tension (IFT)	ASTM D971
Dielectric constant and dissipation factor at 90°C	ASTM-D-924
AC Breakdown Voltage	ASTM D1816

3.2 Design and development of oxidative ageing simulator

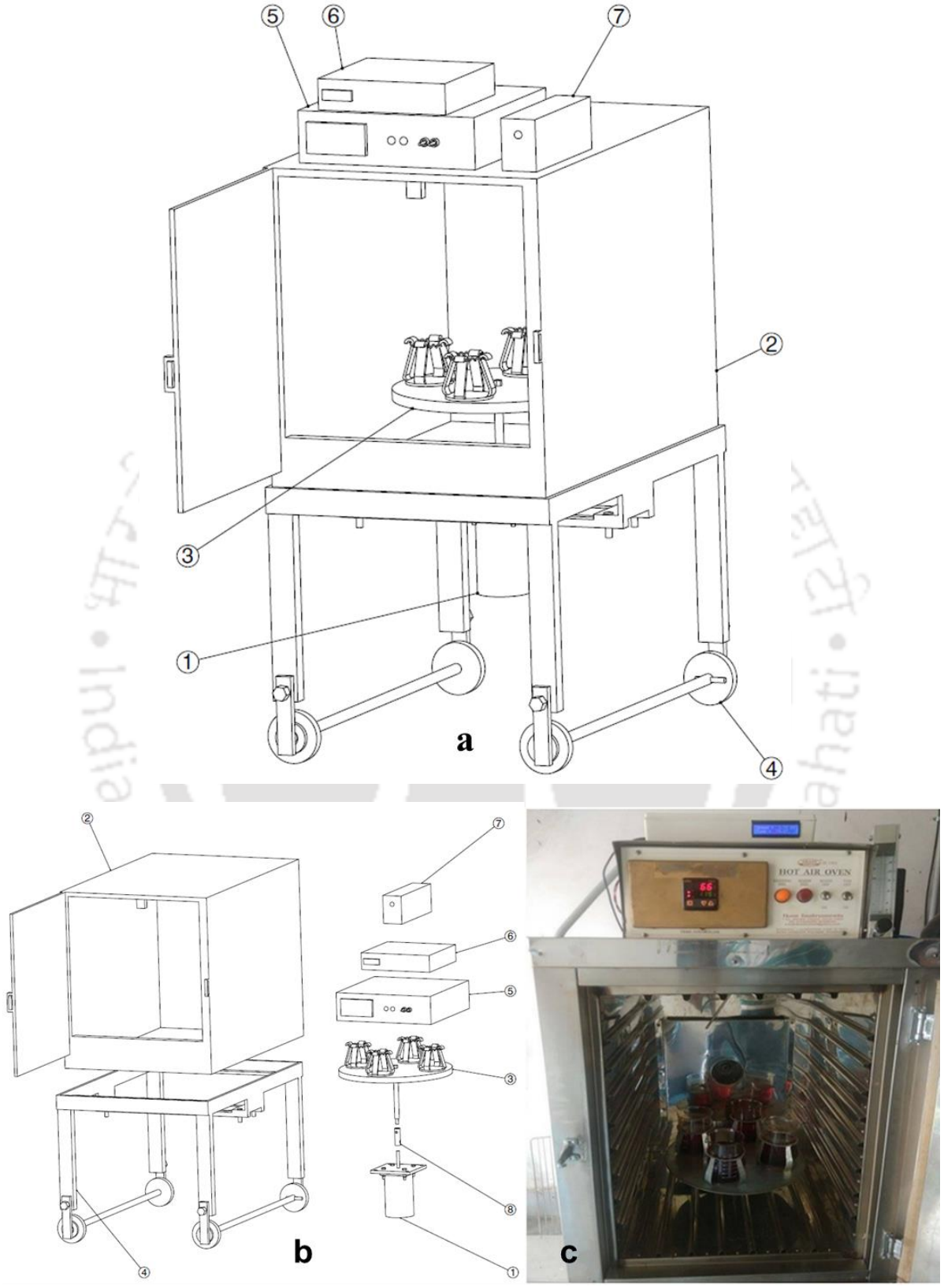

Figure 3.1: Oxidative ageing (a) schematic diagram of complete setup, (b) exploded view of each parts and (c) fabricated setup oxidative ageing setup.

The parts of the oxidative ageing setup are described in the Table 3.3

Table 3.3: Different functional parts of the oxidative ageing

Parts of the oxidative ageing	Description
1	DC motor attachment with driven shaft
2	Hot air oven with temperature sensor, where the samples are kept for testing
3	The beaker stand to hold the sample for testing, which is placed inside the oven
4	The oven stand which is drafted in such a way, that it can hold the motor
5	Temperature controller and indicator
6	Speed and a time control unit containing relay module, DC driver and Arduino boards.
7	The UPS for power backup to the Arduino UNO boards and DC driver.
8	The coupler link fitted with the beaker stand with driver shaft

Figure 3.1 (a) shows the assembly view of the developed open beaker oxidative ageing test setup with multiple attached components. Various parts including driver shaft, driven shaft, connecting rod, beaker holder, oven, temperature controller, speed and time display controller, UPS are present in it. Figure 3.1 (b) shows the exploded view of the assembly the position of different parts of open beaker oxidative ageing test setup is mentioned in order to have a detailed understanding about every attachment. The Figure 3.1 (c) shows the fabricated oxidative ageing test setup with ageing sample in it.

3.3 Ageing degradation

The operating conditions of the transformer is responsible for the ageing of the TO. During the transformer operation, TO experience a thermal, chemical and electrical stress causing a permanent change in the properties of the TO [126]. The extrinsic ageing stress on the TO and the presence of polar contaminants in the oil accelerates the ageing degradation in the oil [127]. Due to unavoidable circumstances such as lightning, short-circuit faults etc., enhance mechanical ageing stress is being developed in the oil. The severity of ageing in the TO mostly depends on the ageing stress and temperature in it. In the presence of moisture at an elevated temperature, oxygen start dissolving in the TO leads to chemical degradation. Ageing by-products such as acids, oxides, peroxide, sludge, saturated esters, hydrocarbons and water are

generated which again comes in contact with the metal catalyst to further accelerates the ageing of oil and hence service life of the transformer decreases. The ageing stresses such as mechanical vibration, short circuit forces, transient over voltage, thermal stress, thermal faults, arc and spark, partial discharge, polar contaminations, metallic particles and fibers inclusion, chemical stresses, including acids, oxides and peroxide are involved in the transformer and the possible for ageing degradation.

The severity of these stresses are even more if the load on the transformer increases. Irrespective of the nature of the TO due to these stresses, ageing in the oil occurs inside the transformer. thermal, physicochemical and electrical properties TO degrades because of ageing. Generally, serviceability of the used TO is verified by measuring its thermal, physicochemical and electrical properties. However, the comparative degradation in the above performance of the TO due to ageing of the developed NFs need to be evaluated before implementing it into the real transformer. In the present study, a comparative analysis of oxidative aged sample of MO and 0.01wt% Eh-BN/MO-NF are performed for different ageing duration. The nature of the degradation of the insulating oil are as follows:

Thermal degradation: Temperature is the most influential parameter for TO ageing. With the rise in temperature of 5-10^{o}C oil decomposes generating oxidative by-product which further take part in degradation of solid insulation.

Oxidative degradation: In the presence of heat, the oxidation degradation compounds occurs due to the breaking of chemical bond and initiation of chain reaction. Polar contaminations of oxide, peroxide, acids, waters, sludge and impurities generates, causing early failure to the liquid insulation.

Hydrolytic degradation: Ageing of the oil-paper insulation in the transformer resulting significant amount of moisture content in the transformer. Hydrophilic nature of the paper traps the moisture in it and causing damage to both solid and liquid insulation by taking part chemical reaction and hence degradation.

Insulation degradation: Due to the aforementioned degradation, dielectric integrity of the insulating oil gets affected. Both electrical and dielectric strength of the TO get affected negatively in the presence polar contaminations and sludge in it. Dissolve moisture and impurities causes local hotspots and partial discharges initiates causing insulation degradation.

3.3.1 Oxidative ageing of MO and NFs

In this study, two different batches of NF namely, Titanium Oxide (TiO_2) and Eh-BN based insulating NF has been prepared by taking MO as the base fluid (as per Chapter 2). The basic properties of the MO are depicted in the Table 3.1. Characteristics of the MO have been verified from Table 1 before the dispersion of TiO_2 and Eh-BN nanofillers into it. Bothe the NFs are prepared as per two-step dispersion method and vacuum dried to remove moisture to meet the desired moisture limits.

3.3.2 Open beaker oxidative ageing

The oxidative thermal ageing study has been performed to investigate the thermal and insulating capabilities of the insulating oils for transformer application. In this study, an open beaker oxidative ageing set up (as shown in Figure 3.1) is used to age an insulating oil at a uniform temperature for various ageing duration [126] such as 164, 328, and 492 hours. This ageing test results provide an information about the probable effect of the polar contaminants on the ageing of liquid insulation in the presence of the copper catalyst.

The oxidative ageing simulator has an arrangement to accommodate four ageing beaker each containing of 300 ml of oil sample. Equivalent amount of thermally treated solid insulation such as kraft paper and press board are put in to the MO and NFs (0.01wt% Eh-BN/MO and 0.01wt % TiO_2/MO) sample in the presence of copper catalyst in the ageing beaker. The operating temperature in this ageing study is mentioned at 115±1^oC with accelerated ageing duration of from 0 to nearly 500 hours. A uniform ageing environment is mentioned for MO and NFs samples by simultaneous air blowing and continuous rotation of the oil sample base at 2±0.1 rpm in the ageing chamber. After completion of ageing of MO and NFs for the ageing duration of 164, 328 and 492 hours, physicochemical and electrical characteristics are analyzed and compared with the fresh oil.

3.4 Experimental (physicochemical and electrical) properties analysis

The preparation of NFs and its various thermophysical and electrical properties (Chapter 2) of the fresh and aged sample are studied as mentioned in the Chapter 2, section 2.3 and 2.4 respectively. A comparative oxidative ageing analysis is carried out for MO and NFs and the observed results are mentioned below.

3.4.1 Zeta Potential Analysis

It is the analysis of any colloidal dispersion which measures the stability of the solution. The value of the zeta potential provides an information of the uniformity of NP dispersion in the base fluid. A colloidal solution with a high value of zeta potential (negative or positive) is

electrically stable, whereas colloids with lower zeta potential leads to agglomeration and instability. Transformer filled with stable insulating oil ensures its better performance and hence improves its life. Thus, a measure of the stability of the insulating oil is important to analyse for the selection of the stable NF before ageing.

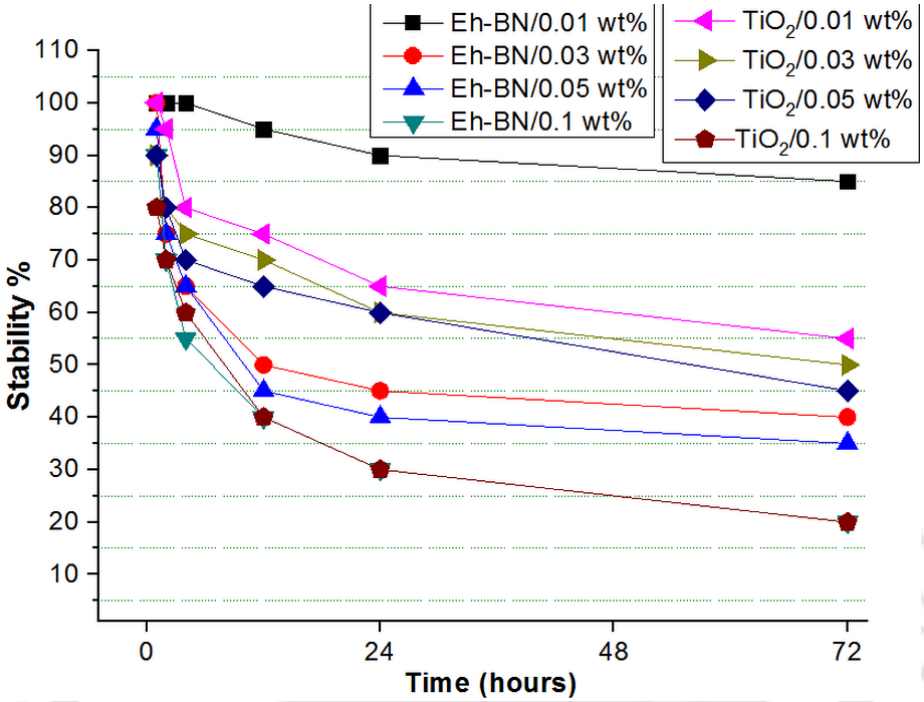

Figure 3.2: Measurement of stability by analysing the zeta potential for NFs.

To verify the stability of two batches of NF, zeta potential analysis has been carried out at room temperature for 72 hours. It is observed from Figure 3.2 that the stability of NFs decreases rapidly with an increase in concentration which suggests that the rate of agglomeration of the NPs is higher, and the agglomerated particles settle down due to gravity. The stability of Eh-BN/MO-NF with 0.01 wt. % of NPs is observed to be maintained even after 72 hours and there is a minimum settlement of NPs in the NF. At all the concentrations of TiO_2/ MO-NF, less than 55% of stability is observed in the same time period, whereas 0.01 wt.% of TiO_2 NP shows better stability among all the TiO_2/MO-NF. Hence, the oxidative thermal ageing study has been performed to evaluate all the necessary parameters for thermophysical and chemical characteristics, by seeking the optimum stabilised NP concentration of 0.01 wt.% for both Eh-BN and TiO_2.

3.4.2 Colour

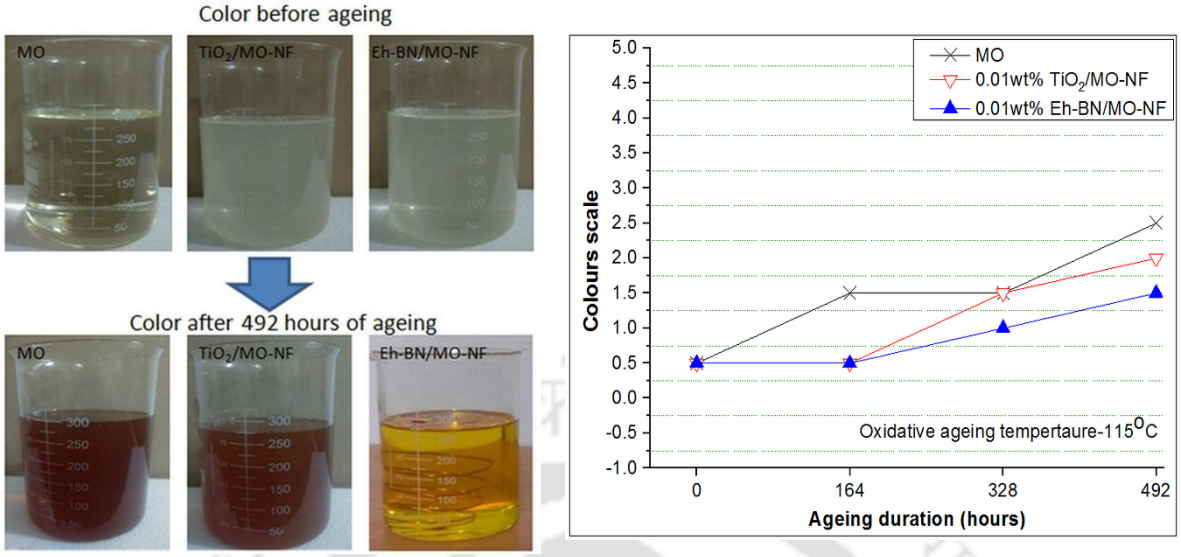

a b

Figure 3.3: Change of colours (a) appearance of fresh and aged oil (b) Colour scale of MO and NFs versus ageing duration.

The colour of the insulating oil is one of the signatures for the degradation or probable contamination in the sample during the ageing process. But the change in colour does not always indicate the deterioration of the oil sample as it is not very accurate to draw the critical conclusion. Several other thermophysical and chemical properties are studied in support to the colour characteristics. Furthermore, nature and character of the colour have been analysed in a single number colour scale as per ASTM D1500 [128]. The detailed changes in colour of these three samples, namely, MO, TiO_2/MO-NF and Eh-BN/MO-NF are clearly visualised in Figure 3.3.

In the present study, Figure 3.3 (b) reveals the colour scale for both fresh and aged samples of three insulating oils. It is clearly seen from the graph that the colour of MO changes from light to dark with ageing durations. In case of TiO_2/MO-NF and Eh-BN/MO-NF, negligible changes in colour are observed up to 164 hours of ageing. Upon completion of 328 hours of ageing, all the three insulating oils have changed their colour to marginally darker shade, but it is very difficult to compare a colour scale between TiO_2/MO-NF and MO as both approaches same point. However, after completion of 492 hours of ageing, MO and TiO_2/MO-NF forms a darker colour as compared to Eh-BN/MO-NF. The colour of the insulating oils is an indication of possible degradation or contamination in the oil. Thus, it is observed that ageing has

maximum effect on the degradation of MO, TiO_2/MO-NF and minimum effect on Eh-BN/MO-NF restricting its affinity for polar contaminations.

3.4.3 Viscosity

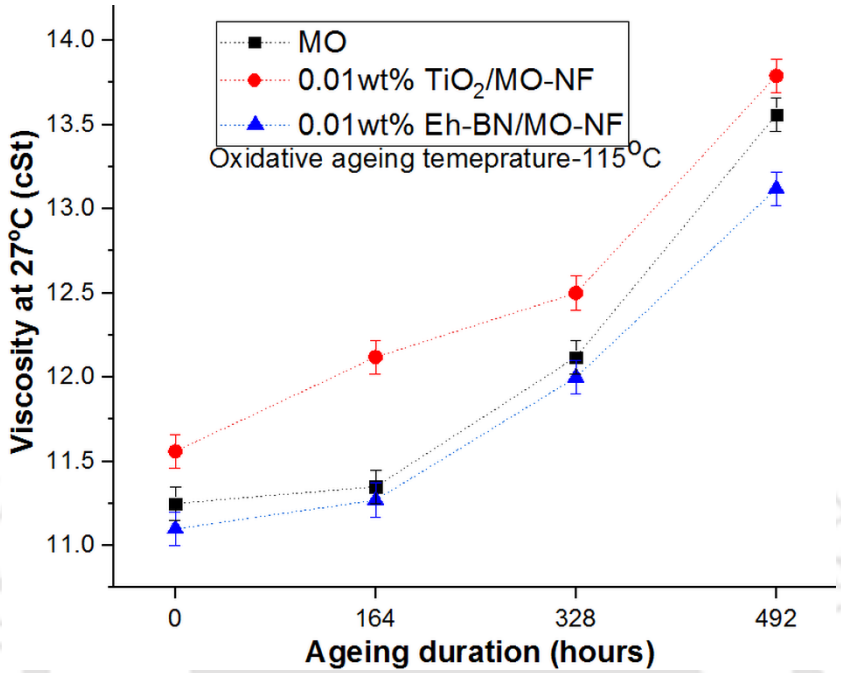

Figure 3.4: Viscosity of the MO and NFs versus ageing duration.

For an insulating oil, viscosity is a key parameter to understand the heat transfer characteristics. The rise in viscosity of the insulating oil, restricts its property of flowability inside the transformer which affects negatively on the heat transfer characteristics. In the process of ageing, an extensive rate of oxidation degradation takes place in the oil. Furthermore, in the presence of oxygen, air and copper catalyst in the course of ageing, an oxidation process accelerates which may affect the viscosity of the insulating oils. In order to understand the effect of ageing on the viscosity of the oil, its analysis is carried out as per ASTM D445 [129] and the results are verified.

Since the cooling of the power/distribution transformer is related to the viscosity of the insulating oil, the measurement of viscosity is essential to analyse the aged oil. Due to oxidation in MO as well as NFs, the degradation process starts leading to increase in viscosity.

3.4.4 Thermal conductivity

It is an important parameter to analyse the heat transfer performance of the transformer oil. High values of thermal conductivity in the insulating oil treated as a better cooling oil medium for the transformer. Insulating oil with superior thermal conductivity absorbs more heat inside the transformer which minimises the heat loss and improves an efficiency of the system. A

KD2 Pro-Decagon device (Figure 2.11) in chapter 2 which follows the principle of transient hot wire method is used to measure the thermal conductivity of the liquids accurately and precisely for the temperature range of 25-45°C. In this method, a fixed extent of the probe is fully dipped in a finite fluid medium and the wire is electrically heated. Using Wheatstone bridge circuit, the change in resistance with the change in temperature is measured as a function of time. The thermal conductivity value is determined from the heating power and the slope of the temperature change with logarithmic time scale as mentioned in in (1).

$$k = \left[\frac{q}{4\pi(T_2 - T_1)}\right] \ln\left(\frac{t_2}{t_1}\right) \tag{3.1}$$

Where T_1 and T_2 are the measured temperatures by the transient hot wire with the time t_1 and t_2, q is the measure of dissipation of heat flux by the wire.

Thermal conductivity is measured for fresh MO, TiO_2/MO-NF and Eh-BN/MO-NF and to evaluate the effect of oxidative ageing on the heat transfer characteristics of the above-mentioned oils, thermal conductivity studies have been repeated for the aged oils at different ageing duration. Considering the temperature inside the transformer, thermal conductivities are evaluated for fresh and aged insulating oils at five different temperatures starting from room temperature to a maximum of 45°C at an interval of 5°C. The mean thermal conductivity has been reported by taking five readings per sample and the errors for each reading are shown in Table 3.4.

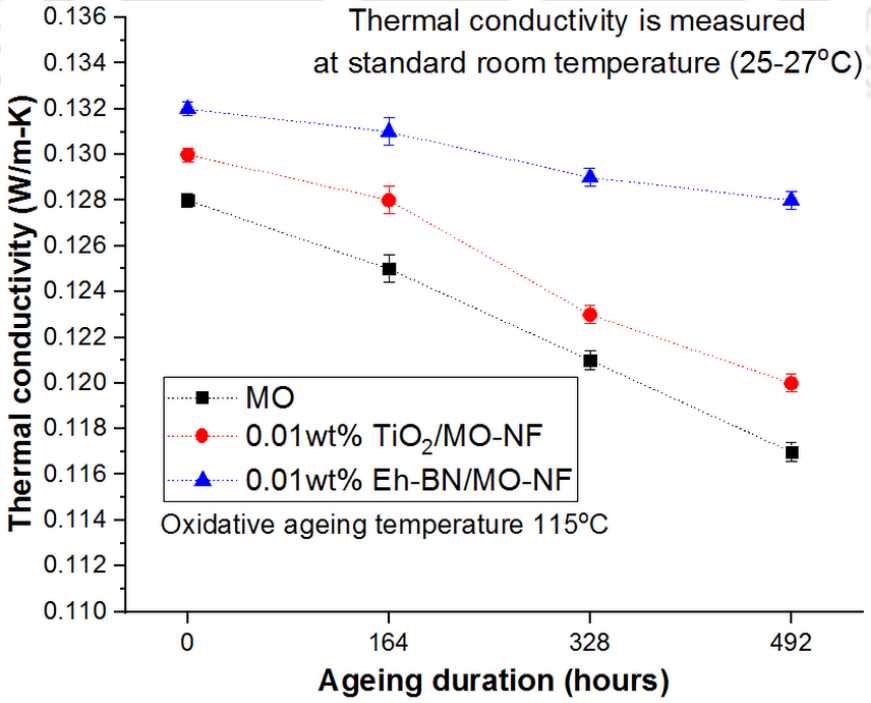

Figure 3.5: Thermal conductivity of the MO and NFs versus ageing duration.

Table 3.4: Measurement of thermal conductivity

Samples	Ageing in hrs	Thermal conductivity at varying temperature (°C)				
		25	30	35	40	45
MO	0	0.128±0.0006	0.128±0.0004	0.130 ±0.0006	0.133±0.0004	0.135±0.0006
	164	0.125±0.0006	0.125±0.0003	0.126±0.0006	0.127±0.0006	0.129±0.003
	328	0.121±0.0002	0.122±0.0006	0.124±0.0006	0.126±0.0006	0.128±0.0006
	492	0.117±0.0006	0.119±0.005	0.122±0.0002	0.124±0.0005	0.125±0.0006
TiO_2/ MO-NF	0	0.13±0.0004	0.132±0.0006	0.134±0.0006	0.131±0.0006	0.13±0.0006
	164	0.128±0.0006	0.129±0.002	0.131±0.005	0.130±0.0004	0.130±0.003
	328	0.123±0.0003	0.124±0.0006	0.127±0.0006	0.126±0.002	0.126±0.0006
	492	0.12±0.0006	0.122±0.0006	0.124±0.003	0.122±0.0006	0.123±0.002
Eh-BN/ MO-NF	0	0.132±0.0002	0.137±0.0006	0.141±0.0006	0.161±0.0006	0.182±0.0004
	164	0.131±0.002	0.133±0.002	0.137±0.003	0.142±0.0006	0.150±0.005
	328	0.129±0.0004	0.130±0.0006	0.134±0.0006	0.137±0.0006	0.143±0.0006
	492	0.128±0.0006	0.129±0.005	0.131±0.0006	0.133±0.0006	0.140±0.002

The mean value of thermal conductivity of all the three samples are measured in the present study. Figure 3.5 and Table 3.4 show the comparative analysis of thermal conductivity at pre and post ageing conditions. Three different ageing durations have been considered to analyse the effect of ageing on thermal conductivity. The addition of NPs into base fluid enhance its thermal conductivity [130-132], which is observed in case of fresh and aged samples. The 0.01wt.% Eh-BN provides better thermal conductivity than MO and TiO_2 at the same concentration. As the ageing periods of the fluids increases, the thermal conductivity of all the three samples goes on decreasing, but a marginal decrement of thermal conductivity is observed for 0.01wt.% Eh-BN/MO-NF.

The superior thermal conductivity of Eh-BN NP is the reason for the rise in thermal conductivity of NF. The higher oxidation affinity of MO and TiO_2/MO-NF degrade the oil during ageing, hence there is a declination in thermal conductivity. To study the effect of temperature on thermal conductivity for all the three insulating oil samples, varying temperature, thermal conductivity is measured for both fresh and aged samples. Considering the maximum working temperature inside the transformer, the upper bound temperature to measure the thermal conductivity is limited to 45°C as depicted in Table 3.4. For the fresh samples of MO and Eh-BN/MO-NF, thermal conductivity goes on increasing with increase in temperature, whereas the increase in thermal conductivity of TiO_2/MO-NF is observed till 35°C and thereafter it starts decreasing till 45°C. This may be due to the presence of some impurity

which acts negatively on the TiO_2/MO-NF. Eh-BN/MO-NF has a significant percentage enhancement in thermal conductivity of 37.87% at 45°C compared to room temperature. In the case of MO and TiO_2/MO-NF, the enhancement is 5.4 and 3.07% respectively. For all samples of insulating oils, thermal conductivity decreases with ageing duration. But the Eh-BN/MO-NF at 492 hours of ageing has higher thermal conductivity than that of fresh samples of MO and TiO_2/MO-NF. This superior thermal performance of Eh-BN/MO-NF could be a suitable candidate for heat transfer in power/distribution transformer.

3.4.5 Moisture analysis

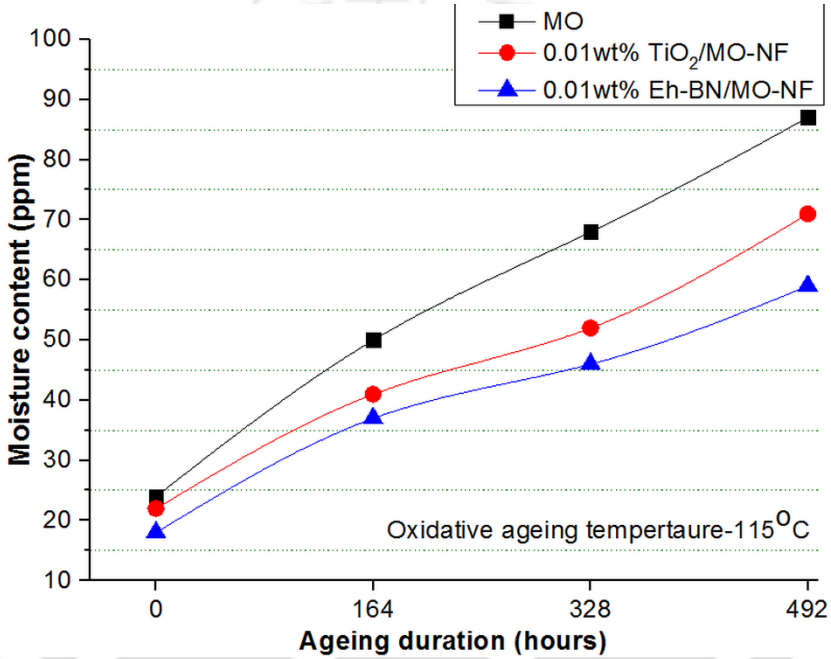

Figure 3.6: Moisture content of MO and NFs versus ageing duration.

Moisture or water contamination in liquid insulation is an important parameter to analyse. It not only affects the thermophysical and chemical characteristics, but also it has a significant influence on the dielectric integrity. In this study, moisture absorbance in all three insulating oils is monitored for pre and post ageing conditions to verify the oil quality. Figure 3.6 provides the variety of the moisture contamination of the three samples at three different ageing times. With the increase in ageing time, moisture contamination goes on increasing linearly. During the ageing process, the presence of oxygen, air, copper catalyst and heat leads to the formation of polar contaminants and moisture in the oil. Since fresh oils have minimum exposure to oxidative agents, lesser moisture content is present in the oil. The freshly prepared Eh-BN/MO-NF has the least affinity to bind the moisture and hence at same drying conditions, it contains lesser moisture than TiO_2/MO-NF. Whereas, strong affinity towards polar contamination of

MO binds the moisture in it results in higher moisture content. It is observed from the figure that after completion of 492 hours of ageing the amount of moisture present in Eh-BN/MO-NF is very much lesser than TiO_2/MO-NF and MO. It is observed that even after ageing, Eh-BN/MO-NF has minimum polar contamination confirming its safe use in the transformer to avoid the formation of oxidative by-products like sludge and impurities in the TO.

3.4.6 Acid number

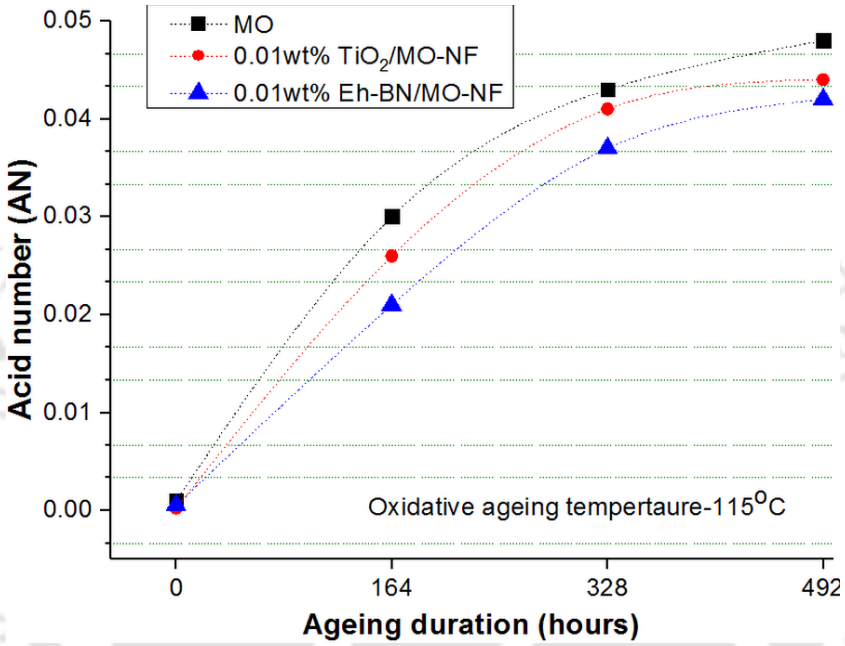

Figure 3.7: Acid number versus ageing duration.

Figure 3.7 shows the variation of acidity of fresh and aged insulating oil samples at different ageing durations. Acidity is enhanced with the increase in ageing time. It is observed that fresh insulating oil samples have nearly zero acidity, but at the end of 164 hours of ageing, the acid number goes on increasing linearly. Thereafter the acid number increases, but beyond 328 hours of ageing, the acidity of the oil approaches towards saturation. At 492 hours of ageing, it is observed that all three insulating oils have a saturation acid number. As moisture content is directly proportional to acidity during ageing, so higher moisture in MO and TiO_2/MO-NF leads to the formation of a greater acid number than Eh-BN/MO-NF. Lesser the affinity towards the acid generation better is the performance of the insulating oil. Negligible moisture content in Eh-BN/MO-NF has the ability to provide superior performance as an insulating and heat transfer fluid.

3.4.7 Interfacial Tension

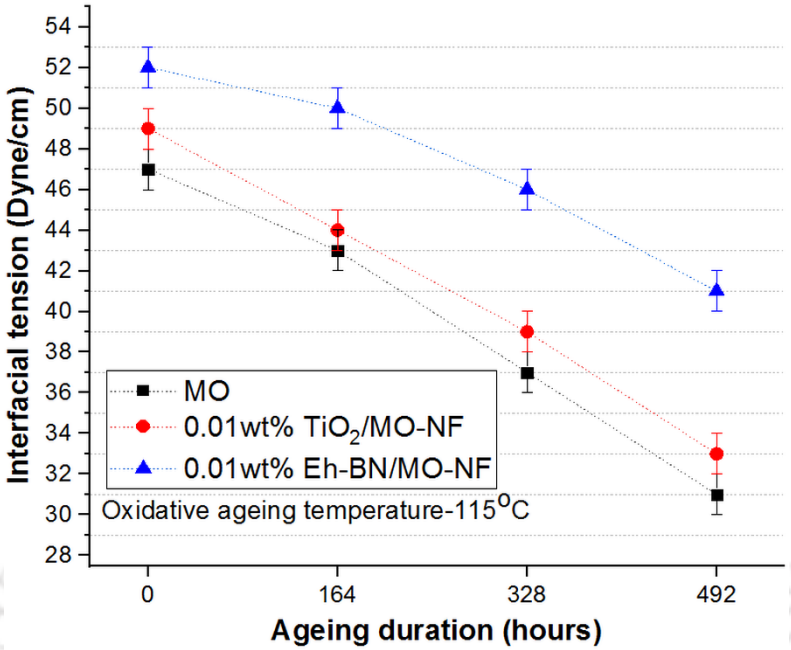

Figure 3.8: Interfacial tension versus ageing duration.

It is observed from the Figure 3.8 that with the rise in ageing duration, IFT value decreases. Since the ageing studies of the three sample of the insulating oils are performed in the presence of oxygen, it may lead to the formation of sludge and impurities in the oil. The IFT value of Eh-BN/MO-NF is far more superior then the TiO_2/MO-NF and MO before ageing; this indicates the excellent dispersion of Eh-BN NPs to the base fluid. A gradual increase in oxidative ageing period leads to decay in IFT for both MO and NFs, but in all the cases the NFs have a superior IFT compared to MO. It is observed from the Figure 3.7 and Figure 3.8 that IFT and acid number are inversely proportional to each other i.e. lower the IFT, higher the acid number. The reason of formation of sludge/impurities in the MO is due to the amalgamation of oil, moisture and copper catalyst in the presence of heat. The insulating nature of Eh-BN NP has the least affinity towards the moisture and polar contamination, which may restrict the formation of the higher acid number and lower IFT, whereas, strong affinity towards polar contamination of MO and TiO_2/MO-NF forms higher acid number, which decays its IFT significantly.

3.4.8 AC breakdown voltage

To analyse the dielectric integrity of the insulating oil for the transformer, an ACBDV study has been performed. A BAUR DTA 100 C, oil tester is used to perform the ACBDV test as per ASTM D1816 [117] using brass mushroom-capped electrodes set at a gap length of 2.50 mm.

The gradual applied voltage is selected at a rate of 2 kV/s. Initially, the standing time is set for 10 minutes before the application of voltage. After each breakdown, the time interval for stirring is fixed for one minute. All experiments are carried out at a frequency of 50 Hz and at room temperature. In one set of experiments, six breakdown voltages data are measured and the mean BDV has been reported in Figure 3.9.

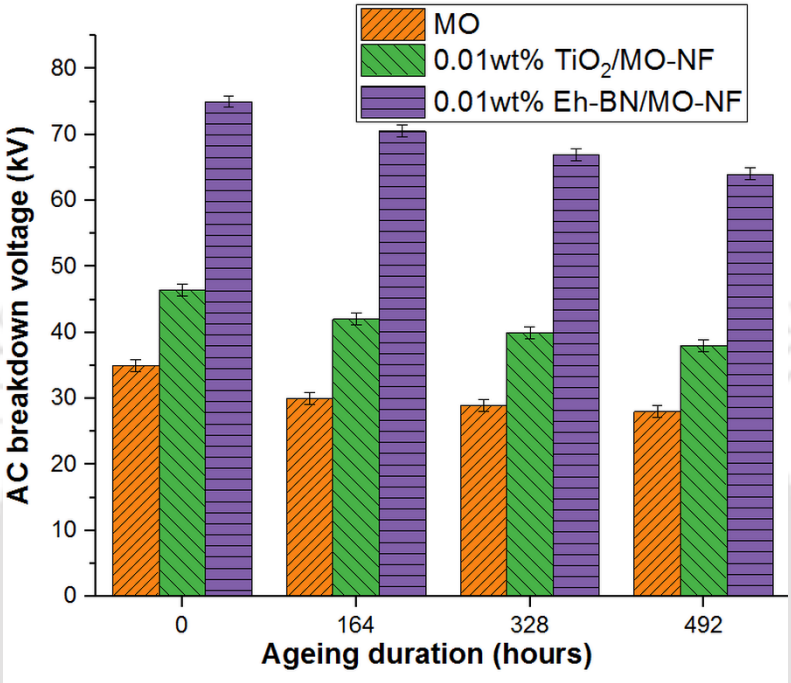

Figure 3.9: ABCDV measurement of MO and NFs versus ageing duration.

The comparative analysis of ACBDV for fresh and aged insulating oil are studied. It is observed that the BDV value of E-BN/MO-NF is far more superior than the MO and TiO_2/MO-NF. Highly insulating Eh-BN NP plays an important role in enhancing the BDV of the Eh-BN/MO-NF. When the insulating Eh-BN NP are dispersed in to the MO, because of its enhanced particle aspect ratio, large surface energy is created. Since the dispersed NPs are capable of scavenging the stimulated electrons in the NFs during the applied voltage, trapping of total number of electrons by the NP is studied in chapter 2, section 2.6. More number of electrons scavenged by the NPs and its dispersion is expected to improve the ACBDV of the Eh-BN/MO-NF.

3.4.9 Dielectric constant

The dielectric constant of any insulating oil is the major parameter to analyses for pre and post ageing conditions. To verify any probable influence of ageing on the dielectric constant of the insulating oil, oil permittivities is measured and the results are depicted in the Figure

3.10. It is clearly seen from the figure that the dielectric constant of the three insulating oil goes on decreasing with the rise of ageing time. Out of these three oils, MO has the highest declination in dielectric constant compared to the NFs. The decline values of dielectric constant for the insulating oils because of its ageing are not at all preferred for transformer application, as it disturbs the electric field distribution. In the course of ageing, Eh-BN/MO-NF has negligible decrement and superior stability in the dielectric constant compared to TiO_2/MO-NF and MO.

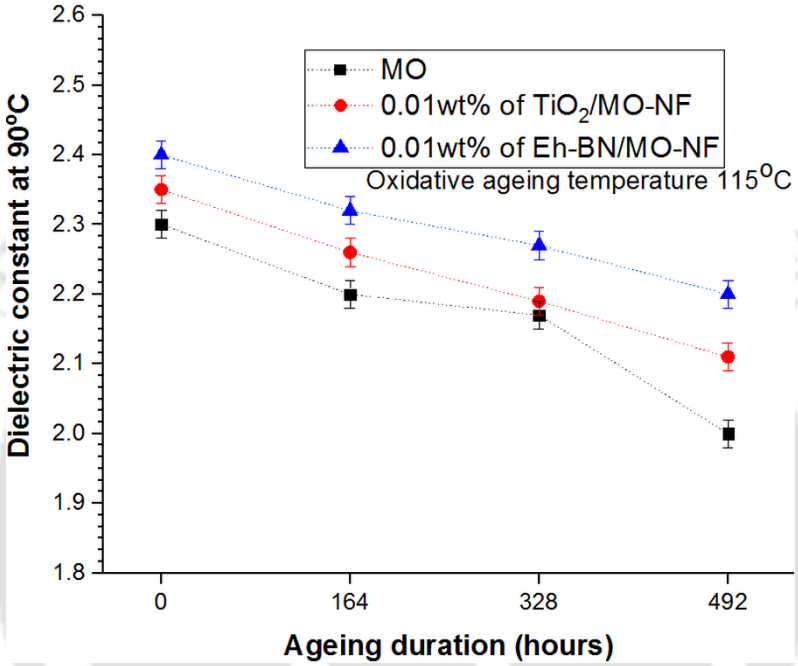

Figure 3.10: Dielectric constant versus ageing duration.

3.4.10 Dielectric dissipation factor (DDF)

DDF of any insulating liquid is a critical parameter to measure. It measures the degradation in dielectric losses in the insulating oil. The effect of DDF of MO, TiO_2/MO-NF and Eh-BN/MO-NF are evaluated for fresh and aged oil of three different ageing duration such as 164, 328 and 492 hours. It is observed from the Figure 3.11 that with an increase in ageing duration the DDF increases indicating the decay in dielectric properties. It is observed that MO at all stages of ageing has higher DDF than that of NFs, which shows the weak dielectric strength of MO. The DDF of a freshly prepared sample of MO is greater than that of the NFs, which informs that the NFs is better dielectric fluid to minimize the discharge. Since the highly insulating Eh-BN NP have a hydrophobic surface which restricts the early contamination of developed moisture during ageing, the DDF of Eh-BN/MO-NF is observed to be less compared to Mo and TiO_2/MO-NF. It is also observed from the figure that even after 492 hours of

oxidative ageing, the DDF of Eh-BN/MO-NF is less affected compared to MO. Therefore, Eh-BN/MO-NF is a better insulating liquid for the transformer application.

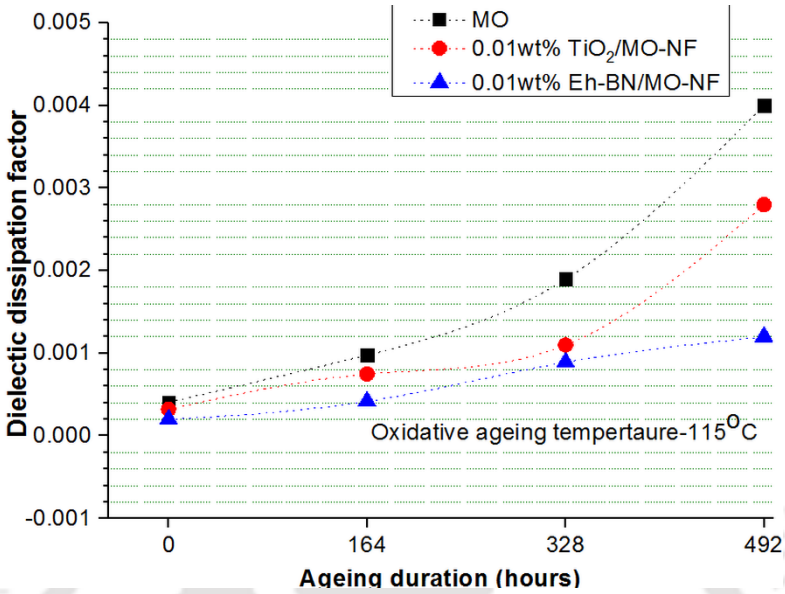

Figure 3.11: Dielectric dissipation factor versus ageing duration

3.5 Uncertainty analysis

3.5.1 Uncertainty in thermal conductivity

Table 3.5: Uncertainty of thermal conductivity using KD2 probe

Uncertainty error	± Error (%)
Repeatability (U_1)	1.0
Instrument accuracy(U_2)	0.50
Electrical probe(U_3)	0.2
Measurement (U_4)	0.1
Cumulative uncertainty (U_c)	1.140

$$U_c = \sqrt[2]{U_1 + U_2 + U_3 + U_4} = 1.140 \quad (3.2)$$

The uncertainty calculation is critical to ascertain the accuracy of the obtained measured results from the instrument. The thermal conductivity measurement is performed using KD2 probe decagon device. The uncertainty for the thermal conductivity measurement is calculated by taking different parameters as mentioned in the Table 3.5. Uncertainty in thermal conductivity of MO and NFs measured using KD2 probe is 1.14%.

3.5.2 Uncertainty in ACBDV

The ACBDV measurement is performed using BAUR DTA 100 C BDV tester as per standardize gap length. The uncertainty is calculated by taking the parameter mentioned in the

Table 3.6 and 3.7.

Table 3.6: ACBDV measurement with standard deviation

	Eh-BN/MO (n=6)		h-BN/MO (n=6)		MO (n=6)		TiO_2/MO (n=6)	
ppm	18	24	18	24	18	24	18	24
BDV (x)	75	55	67.1	47.6	35	30	46	42
S.D (s)	1.54	1.26	1.41	1.76	1.87	1.8	1.54	1.5
U_1	0.62	0.51	0.57	0.71	0.76	0.73	0.62	0.61
U_1%	0.838	0.93	0.85	1.50	2.18	2.44	1.36	1.45
Uc	1.327	1.410	1.335	1.819	2.411	2.648	1.705	1.780

$$U_1 = s/\sqrt{n} \tag{3.3}$$

$$U_1\% = 100 \times u/x \tag{3.4}$$

Table 3.7: Uncertainty of ACBDV measurement

Uncertainty error	± Error (%)
Repeatability (U_1)	0.85 to 2.45
Instrument accuracy(U_2)	0.916
Gap gauge (U_3)	0.44
Electrode(U_4)	0.168
Cumulative uncertainty (U_c)	1.31 to 2.64

There are three batches of the sample such as MO, TiO_2/MO-NF and Eh-BN/MO-NF. Each one having different standard deviation and moisture content. Hence, with the help of (3.2), (3.3), and (3.4) during calculation of uncertainty of ACBDV, the obtained range is in between 1.31 to 2.64% for MO and NFs.

3.6 Summary of the chapter

During the oxidative ageing study, two different batches of NF namely Eh-BN/MO and TiO_2/MO-NF are prepared by dispersing 0.01 to 0.1 wt.% of nanofillers with MO as the base fluid. Out of eight different nanofiller concentrations, zeta potential confirms 0.01wt.% of Eh-BN/MO-NF to be the most stable. Comparative experimental analysis has been carried out to understand the possible mechanism of the degradation behaviour in the insulating oil for specified ageing durations. In order to evaluate the effect of thermophysical ageing parameters such as thermal conductivity, viscosity, interfacial tension and their correlation to the heat transfer properties over the ageing period has been studied. Similarly, the effect of ageing on the dielectric performance and their possible interaction with insulation mechanism is verified. Many observations are made from this study, which will further provide necessary information

about the effectiveness of the insulating NF and its stable performance with ageing. The various important observations from the aforementioned study are reported below:

- The minimum increment in viscosity of Eh-BN/MO-NF is observed compared to other two insulating oil samples at the post ageing period, hence provides its effectiveness for better heat transfer capability.
- The dispersion of Eh-BN and TiO_2 NPs into the MO enhances the thermal conductivity for the NF as compared to the conventional MO. In the course of ageing, the thermal conductivity of the NF gradually declines, but Eh-BN/MO-NF even after 492 hours of ageing shows minimal decay in thermal conductivity. The variation of thermal conductivity with the rise in temperature is studied. It is observed that TiO_2/MO-NF shows the unpredictable nature of thermal performance, whereas minimum thermal conductivity enhancement for MO and the highest thermal conductivity for Eh-BN/MO-NF is reported at 45^oC. The higher thermal conductivity of Eh-BN NP may be a reason for superior heat transfer performance.
- Hydrophobic nature of Eh-BN NP restricts the polar contamination and shows the lesser affinity towards the moisture. As a result, minimal changes in colour scale, the formation of acidity, absorbent of moisture and values of interfacial tension are observed for Eh-BN/MO-NF even after 492 hours of ageing. The hydrophilic nature of TiO_2/MO-NF and MO has a larger affinity towards polar contamination and hence severe degradation of the aforementioned parameters during ageing is observed.
- The Eh-BN/MO-NF provides superior insulation properties by possessing higher dielectric constant value and lesser DDF during ageing. The degradation value of dielectric constant and DDF of TiO_2/MO-NF and MO may affect the field distribution which may lead to ineffective insulation performance.

Hence, analysing all the aforementioned experimental results and the performance characteristics of all the three insulating oils, before and after ageing, Eh-BN/MO-NF is a potential energy efficient insulating NF for transformer application.

For the detailed understanding of the degradation in thermophysical and electrical properties of the MO and MO-NF in the oxidative environment, the sealed beaker oxidative ageing analysis of the TO is carried out in the next chapter.

Note: This work, "Nanofluid based transformer oil: effect of aging on thermal, electrical and physio-chemical properties" has been published in IET Science, Measurement & Technology.

4

Sealed beaker oxidative ageing analysis of MO and NF

Contents

4.1 Introduction

Insulating oil in power/distribution transformer acts as an important medium for insulation and cooling. Consistency in the dielectric and thermal performance of the oil is required for the longevity of the transformer operation. Various insulating oil is being used with suitable electrothermal characteristics inside the transformer, but in the long run process, repeatability of the same properties is not observed. Hence, an alternative form of fluid should be developed to meet the growing requirement of an efficient oil in the transformer industry. In recent scenario, NF based transformer oil is a promising material as an insulant and coolant in power/distribution transformer. In order to analyse the effect of insulating capability of this NF based transformer oil, ACBDV study is required. Various experimental analyses have been conducted considering different types of nanoparticles (NPs) which are dispersed with MO to form NF for transformer application [82, 83].

Various research groups have studied the electrothermal behaviour of the NFs. It is observed that though NF plays a significant role in enhancing the thermophysical properties of the transformer oil, dielectric properties of the NF in the transformer is the key parameter to analyse [133]. Various studies are conducted for the NF considering three different kinds of NPs namely conductive, semi-conductive and insulating [58, 65, 135, 136]. Seeking the physical significance of the NF in the real time application in the power and distribution transformer, the saturation charge on the surface of the conducting and semiconducting NPs in the MO alien the NPs along the direction of the applied field forming a conducting channel which may create accidental breakdown in the transformer. Moreover, the leakage current in the insulating NPs based NF is less than the conducting and semiconducting based NF. Therefore, the insulating NP is a suitable candidate for electrically insulating NF. Since the breakdown voltage is the key parameter to decide the dielectric integrity of the insulating fluid, the study of the statistical breakdown voltage is the major information for the prediction of the lowest breakdown probability and average dielectric strength of the NF for long run [134, 135]. This paper reveals the major findings of statistical ACBDV of insulating NF and it also reports about the effect of necessary thermophysical, electrical and chemical properties of the NF based transformer oil at different oxidative ageing periods. Various insulating NPs and its properties on dispersion with MO are studied, out of which h-BN has all the dominant properties to be dispersed with base fluid i.e. MO for preparation of NF. Bulk h-BN NPs are large spherical agglomerates restricting its effective utilization for NF, so exfoliation techniques are implemented to modify the surface and convert into 2-D nanosheets of the NP [46]. Superior thermal conductivity,

large surface area, highly insulating and corrosion resistance nature of the Eh-BN NP motivates the researcher for its implementation in the NF. 0.01 wt.% of Eh-BN NP is chosen for its dispersion into the MO to prepare the NF to study further [47].

The prepared NF (0.01 wt.% Eh-BN/MO) samples are dried and vacuum filtered to minimize its moisture content resulting in better dielectric performance. The ACBDV tests of this particular NFs sample are carried out to understand the dielectric strength as per ASTM D1816 [117]. Maximum percentages of transformer oil are used as an insulating and cooling agent for any transformer, whereas the average dielectric insulation of the same oil is a concern. Hence, minimum ACBDV can be obtained by the help of statistical analysis method. The margin of safety may vary when Eh-BN/MO is used in place of MO if the dispersion behaviour of BDV is different. This makes it essential to carry out the statistical analysis of both the fluids to gauge their similarities with regards to breakdown strength.

A comparative study of statistical ACBDV of MO and NF having different moisture levels such as 18 and 24ppm are investigated. ACBDV tests of MO and NF (0.01wt.% Eh-BN/MO-NF) are carried out for 9 samples with each of 10 instants making a whole of 90 tests. To estimate the withstand voltage, necessary probability distribution of dielectric failure has been considered. The probable failure in the dielectric property of the NFs, at 5, 10, 50 and 63.2% are analysed from the statistical analysis of BDV by Weibull probability distribution technique [90, 136].

Apart from breakdown probabilities, other thermoelectrical properties such as IFT, acid AN, DDF, resistivity and thermal conductivity are very much essential to evaluate. Interpretation of the thermoelectrical properties of the insulating oil has the direct influence on the dielectric performance of it. Hence, a sealed beaker oxidative ageing apparatus is used to study the thermophysical and electrical properties of the aged sample both MO and Eh-BN/MO-NF. Sealed beaker oxidative test has been carried out at 3 ageing durations (164, 328 and 492 hrs.) as per ASTM D 2440 [119]. Ageing characteristic and thermoelectrical properties of the Eh-BN/MO-NF are compared with the MO at distinct ageing duration. The qualitative degradation percentage of the aforementioned insulation oil in response to oxidative ageing are studied. The degradation rate of thermoelectrical properties with respect to ageing time are also evaluated [137-139]. Specified and standard properties of the MO are shown in Table 3.1 in Chapter 3.

4.2 Sealed beaker ageing and its analysis

In this study, sealed beaker oxidation stability test has been performed for the different ageing duration up to 492 hours as per ASTM-D2440 using the sealed beaker oxidation stability testing facility shown in Figure 4.1 available in Insulating Oil Testing Laboratory (IOTL), Power Grid Corporation of India Limited, Nagaon, Assam. During the period of ageing, MO and Eh-BN/MO NF are exposed to oxygen and heated in the presence of the copper catalyst in a sealed beaker. As per the standard, the ageing temperature is maintained at 110 ± 0.5°C and the testing is carried out without the inclusion of the pressboard in the oil sample. The copper catalyst of diameter 1.01 mm and length of 300 mm shaped as a helical coil (shown in Figure 4.2 of outer diameter of 16 mm and a height of 50 mm approximately is used per batch of ageing sample. However, the copper quantity is around 1.4 ± 0.2 gm per 25 gm of oil sample.

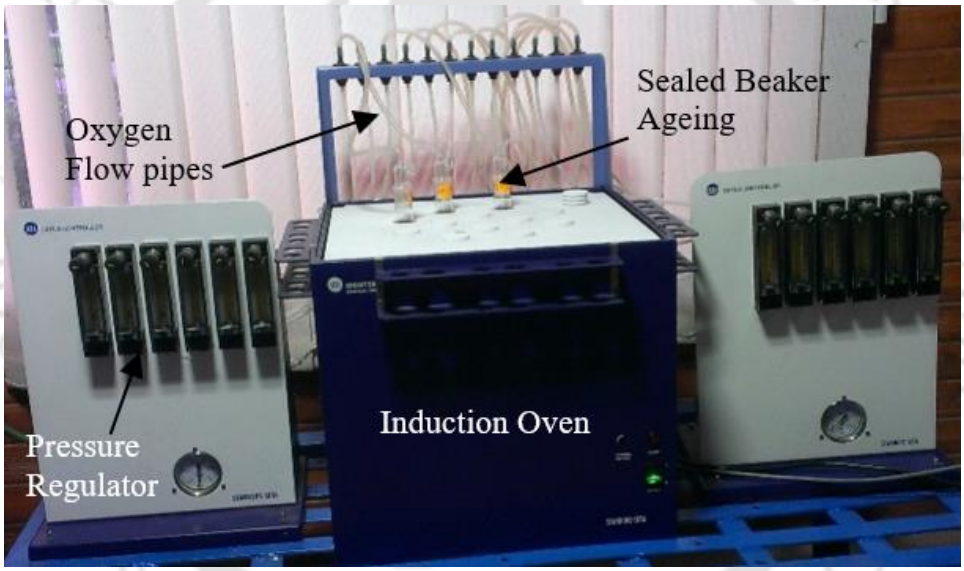

Figure 4.1: Sealed beaker oxidative ageing setup.

4.3 Results and discussion

4.3.1 Colour characteristics

The change in colour of MO and Eh-BN/MO-NF for different ageing duration are present in Figure 4.2. In order to verify and confirm the probable ageing effect of the insulating oil inside the transformer, various properties such as DDF, AN, IFT, resistivity and thermal conductivity are analyzed taking 0.01 wt.% of Eh-BN NF based transformer oil into consideration.

4. Sealed beaker oxidative ageing analysis of MO and NF

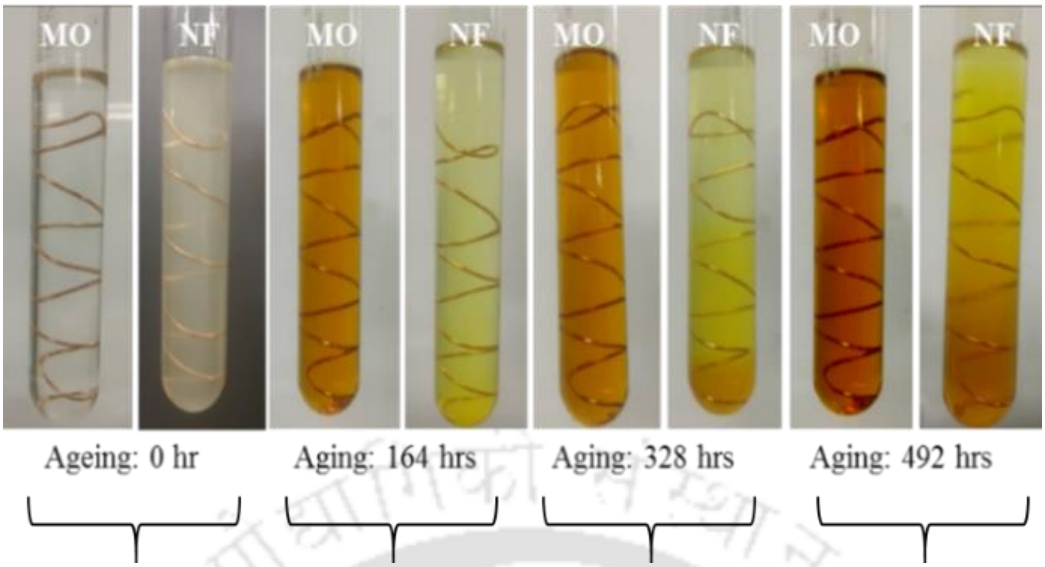

Figure 4.2: Colours of MO and Eh-BN/MO-NF before and after the oxidative ageing.

The colour of insulating oil provides a firsthand information for the degradation or probable of the sample during the ageing process. The change in colour does not always indicate the deterioration of the oil sample as it is not very accurate to draw the exact impression of degradation. Several other physio-mechanical and chemical characteristics are studied in support of the colour characteristics. Furthermore, nature and character of the colour have been analyzed in a single number colour scale as per ASTM D1500 [128]. The detailed change in colour of these two samples namely, MO and Eh-BN/MO-NF is clearly seen from the Figure 4.2.

In the present study, Figure 4.3 reveals the colour scale for both fresh and aged samples of two insulating oils. It is clearly observed from the graph that the colour of MO changes from light to dark with ageing duration from 0 to 492 hrs. In case of Eh-BN/MO-NF, negligible changes in colour is observed up to 164 hours of ageing. Upon completion of 328 hours of ageing, all these samples of two insulating oils have changed their colour to marginally darker shade but it is very easy to compare a colour scale between MO and Eh-BN/MONF as both approaches different point. However, after completion of 492 hours of ageing, MO forms a darker colour compared to Eh-BN/MO NF. Thus it is observed that ageing has the maximum effect of degradation on MO compared to Eh-BN/MO-NF, restricting its affinity for polar contaminations.

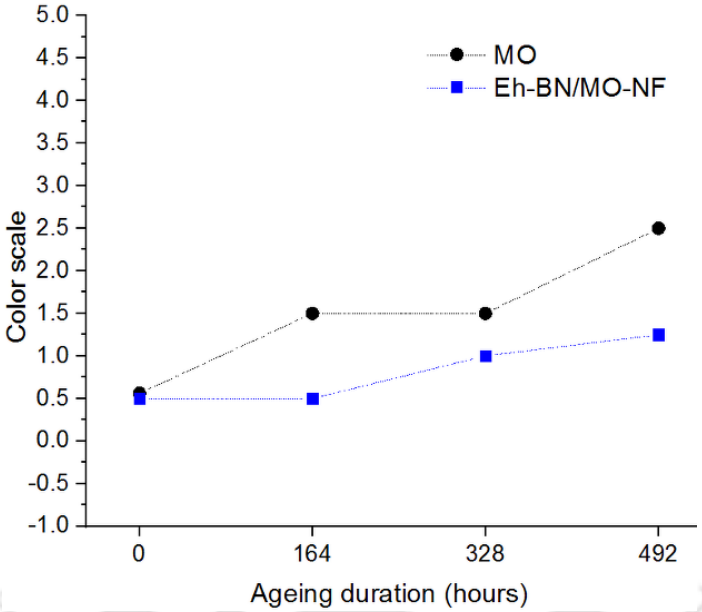

Figure 4.3: Colour of aged oil as per ASTM D1500 colour scale.

4.3.2 Acid number (AN) and interfacial tension (IFT)

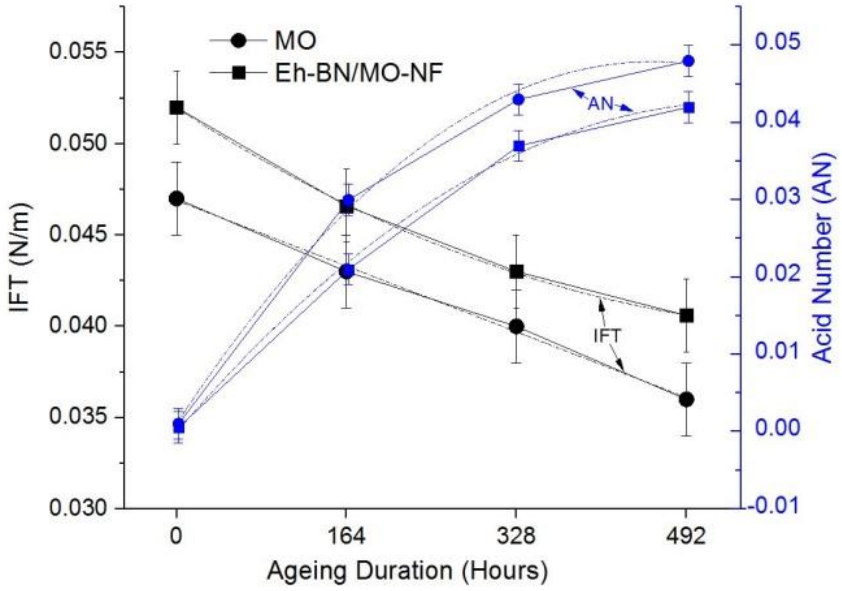

Figure 4.4: IFT and AN with ageing time in hours.

$$\begin{bmatrix} IFT_{MO} \\ IFT_{NF} \end{bmatrix} = \begin{bmatrix} -2.23 \times 10^{-7} \\ -1.49 \times 10^{-7} \end{bmatrix} t^2 + \begin{bmatrix} 2.04 \times 10^{-4} \\ 1.56 \times 10^{-4} \end{bmatrix} t + \begin{bmatrix} 1.4 \times 10^{-3} \\ 2.04 \times 10^{-4} \end{bmatrix} \quad (4.1)$$

$$\begin{bmatrix} AN_{MO} \\ AN_{NF} \end{bmatrix} = \begin{bmatrix} 5.01 \times 10^{-23} \\ 2.79 \times 10^{-8} \end{bmatrix} t^2 + \begin{bmatrix} -2.2 \times 10^{-5} \\ -3.68 \times 10^{-5} \end{bmatrix} t + \begin{bmatrix} 4.69 \times 10^{-2} \\ 5.1 \times 10^{-2} \end{bmatrix} \quad (4.2)$$

The AN is the quantity of acid concentration in a new and aged oil and the standard unit of measurement is mg KOH/g (the amount of potassium hydroxide (KOH) base required to

neutralize the acid per gram of a sample). The concentration of polar compounds increases with the increase of oxidation level in the oil and hence acid forms. A comparative study of AN has been performed taking MO and Eh-BN/MO NF into consideration. The presence of total acidity of these two fluids at certain ageing period has been studied and reported as per ASTM-D974 [140].

To measure the IFT of the MO and Eh-BN/MO-NF, a torsion balance tensiometer is used and the test has been performed as per ASTM-D971 [116]. The IFT values of two different samples such as MO and Eh-BN/MO-NF after different ageing duration have been measured and compared. Figure 4.4 shows the relation of AN and IFT with ageing duration of the MO and Eh-BN/MO NF. It is observed that the rise in ageing duration IFT value decreases and AN increase simultaneously. Since the ageing studies of both the insulating oils are performed in the presence of oxygen it leads to the formation of sludge and impurities in it. The empirical expression of the IFT and AN with ageing duration obtained from the curve fitting with R^2 of 0.999 and 0.992 are presented in (4.1) and (4.2) respectively. IFT value of NF is far more superior than MO before ageing; which shows the excellent dispersion of NP in MO and hydrophobicity of the NF. A gradual increase in ageing period leads to decay in IFT for both MO and NF, but in all the cases the NF has a superior IFT than that of MO. It is observed that IFT and ANs are inversely proportional to each other i.e. lower the IFT higher the AN. The insulating nature of Eh-BN NP has a lesser affinity towards the moisture and polar contamination, which is restricting the formation of higher AN and lower IFT. However, strong affinity towards polar contamination of MO forms higher AN, which decay its IFT appreciably.

4.3.3 Dielectric dissipation factor (DDF) and resistivity

The DDF of an oil sample is a critical parameter which provides the sensitive information about the polar contamination which may lead to dielectric losses. It is generally related to the resistivity of the oil and is affected by the contaminants present in the oil. The resistivity of the insulating oil indicates the ability of the oil to prevent the formation of conducting channel in the liquid avoiding local breakdown. Various aged Eh-BN/MO-NF samples are tested for DDF and resistivity using a multipurpose Tan Delta-DTR-3K measuring setup at a frequency of 50Hz as per the ASTM-D-924 [118]. Test results of Eh-BN/MO-NF are compared with MO under same ageing condition.

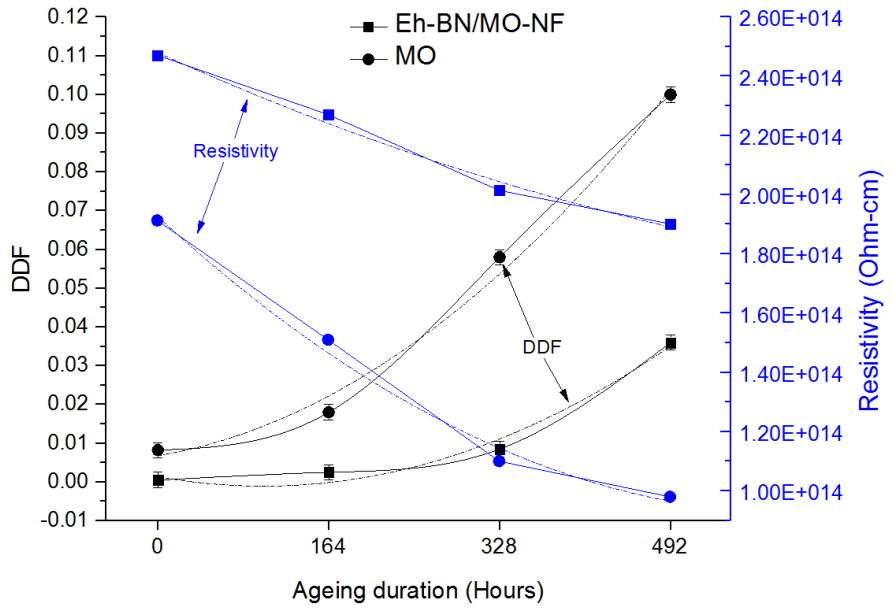

Figure 4.5: DDF and resistivity with ageing at a temperature of 90°C.

$$\begin{bmatrix} DDF_{MO} \\ DDF_{NF} \end{bmatrix} = \begin{bmatrix} 2.99 \times 10^{-7} \\ 2.37 \times 10^{-7} \end{bmatrix} t^2 + \begin{bmatrix} 4.5 \times 10^{-5} \\ -4.8 \times 10^{-5} \end{bmatrix} t + \begin{bmatrix} 6.79 \times 10^{-3} \\ 1.37 \times 10^{-3} \end{bmatrix} \tag{4.3}$$

$$\begin{bmatrix} \text{Resistivity}_{\text{MO}} \\ \text{Resistivity}_{\text{NF}} \end{bmatrix} = \begin{bmatrix} 2.63 \times 10^{8} \\ 8.09 \times 10^{7} \end{bmatrix} \text{t}^2 + \begin{bmatrix} -3.25 \times 10^{11} \\ -1.59 \times 10^{11} \end{bmatrix} + \begin{bmatrix} 1.93 \times 10^{14} \\ 2.48 \times 10^{14} \end{bmatrix} \tag{4.4}$$

The effect of DDF of MO and Eh-BN/MO-NF are studied at three different ageing periods such as 164, 328 and 492 hours. It is observed from the Figure 4.5 that with the increase in ageing duration, the DDF increases indicating the decay in dielectric properties. A comparative analysis of DDF for MO and NF are reported to analyze the performance characteristics of NF. It is seen that the MO at all stage of ageing has higher DDF then that of NF signifying the weak dielectric strength of MO. The DDF for a freshly prepared sample of MO is greater than that of the NF, which indicates that the NF is a better dielectric fluid having minimum the discharge affinity. Highly insulating Eh-BN NP has a hydrophobic surface restricting the early contamination of developed moisture during ageing of the NF, in different ageing duration such as 164, 328 and 492 hrs. The moisture content of the MO and NF at different ageing duration are measured and it is observed that the moisture content in the MO are 50, 68, 86 ppm and in the NF are 36, 45, 60 ppm at 164, 328 and 492 hours of ageing respectively. The DDF of MO are observed to be 94.73, 84.74 and 65% higher than that of NF showing the poor dielectric nature of the MO in the oxidative environment.

The resistivity of the MO and Eh-BN/MO NF for aforementioned ageing duration are studied. Superior resistivity is observed for the NF even at a higher oxidative ageing period. Dispersion of the Eh-BN NP makes the NF more resistant towards the polar contamination providing an affinity of lesser discharge and hence excellent insulation is achieved. MO largely consist nonpolar alkane which does not absorb the moisture. However, there are few polar compounds still exist in the freshly manufactured MO used as transformer oil which absorbs the moisture. During ageing, MO in the presence of heat, copper catalyst and oxygen there is an alteration in the chemical chain which accelerates the absorption of moisture. Hydrophilic nature of MO allows the moisture to be absorbed by it resulting inferior resistivity and insulation. The empirical expression of the DDF and resistivity with ageing duration obtained from the curve fitting with R^2 of 0.977 and 0.975 are presented in (4.3) and (4.4) respectively. Using these two expressions, the DDF and resistivity can be predicted at any ageing duration.

4.3.4 Thermal conductivity

In order to study the cooling properties of the transformer oil at different ageing duration, thermal conductivities of MO and NF are measured using KD2 probe Decagon Device Inc. at room temperature following single probe transient hot-wire method as per ASTM D5334 [141] discussed in Chapter 2. The results of thermal conductivity of the MO and Eh-BN/MO NF for different oxidative ageing duration are studied and presented in Figure 4.6.

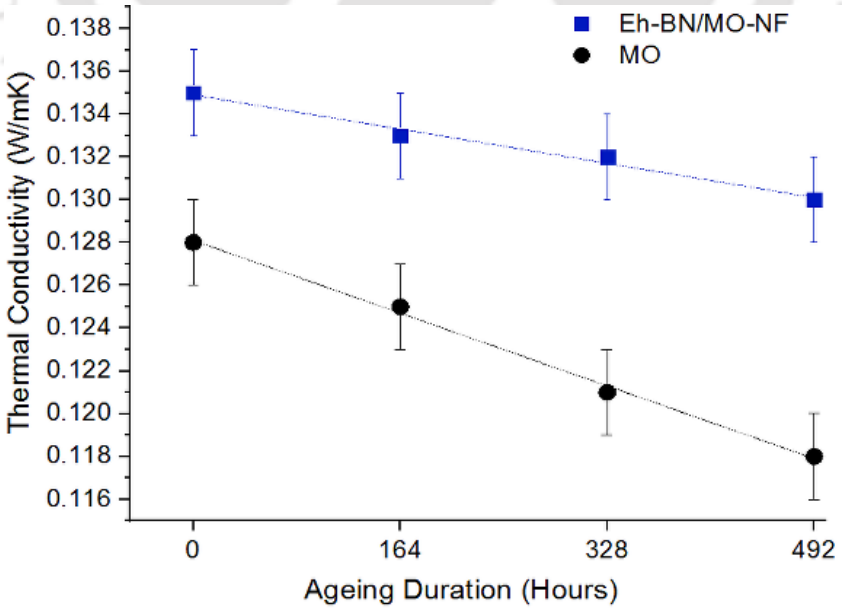

Figure 4.6: Thermal conductivity w.r.t. ageing time.

$$\begin{bmatrix} Thermal\ Conductivity_{MO} \\ Thermal\ Conductivity_{NF} \end{bmatrix} = \begin{bmatrix} 0.1349 \\ 0.1281 \end{bmatrix} t + \begin{bmatrix} -9.756 \times 10^{-6} \\ -2.073 \times 10^{-5} \end{bmatrix} \quad (4.5)$$

It is observed from the figure that the heat transfer capabilities of both the sample degrade gradually in the course of ageing period. However, the rate of degradation of thermal conductivity of the MO is fast compared to NF. It is also observed that the thermal conductivity of the NF is superior to MO in all stages of ageing and even before ageing. To analyze the rate of degradation of the thermal conductivity of the MO and NF, an empirical expression as presented in (4.5) of thermal conductivity with ageing duration are obtained from curve fitting with correlation factor R^2 of 0.986. The superior thermal conductivity of the Eh-BN/MO NF before and after ageing is due to the stable dispersion of highly thermally conducting Eh-BN NP into the MO. High surface area Eh-BN NP has the ability to absorb heat and enhance the heat transfer capabilities in the NF for superior thermal conductivity. Higher sludge/impurities formed in the MO due to ageing may be the potential obstruction for improper heat transport in the oil. Hence, there is a reduction in thermal conductivity of MO compared to NF at any ageing period.

4.3.5 ACBDV

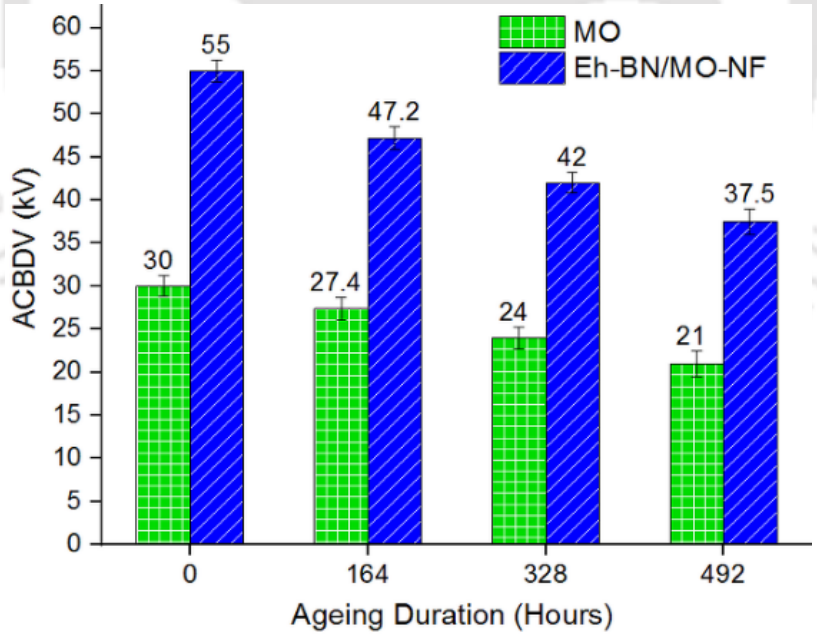

Figure 4.7: Mean ACBDV with ageing period.

Degradation in the dielectric properties of the fluids before and after oxidative ageing are studied and analyzed. A comparative study of the mean value of the measured ACBDV of NF and MO are presented in Figure 4.7. It is observed from the figure that with the increase in ageing duration, ACBDV value of MO and NF decreases. The percentage enhancement of

ACBDV of NF compared to MO are 83.3, 72.6, 75 and 76.19 % at 0, 164, 328 and 492 ageing hours, respectively. At pre-ageing condition, NF has superior BDV value compared to MO.

4.4 ACBDV statistical analysis

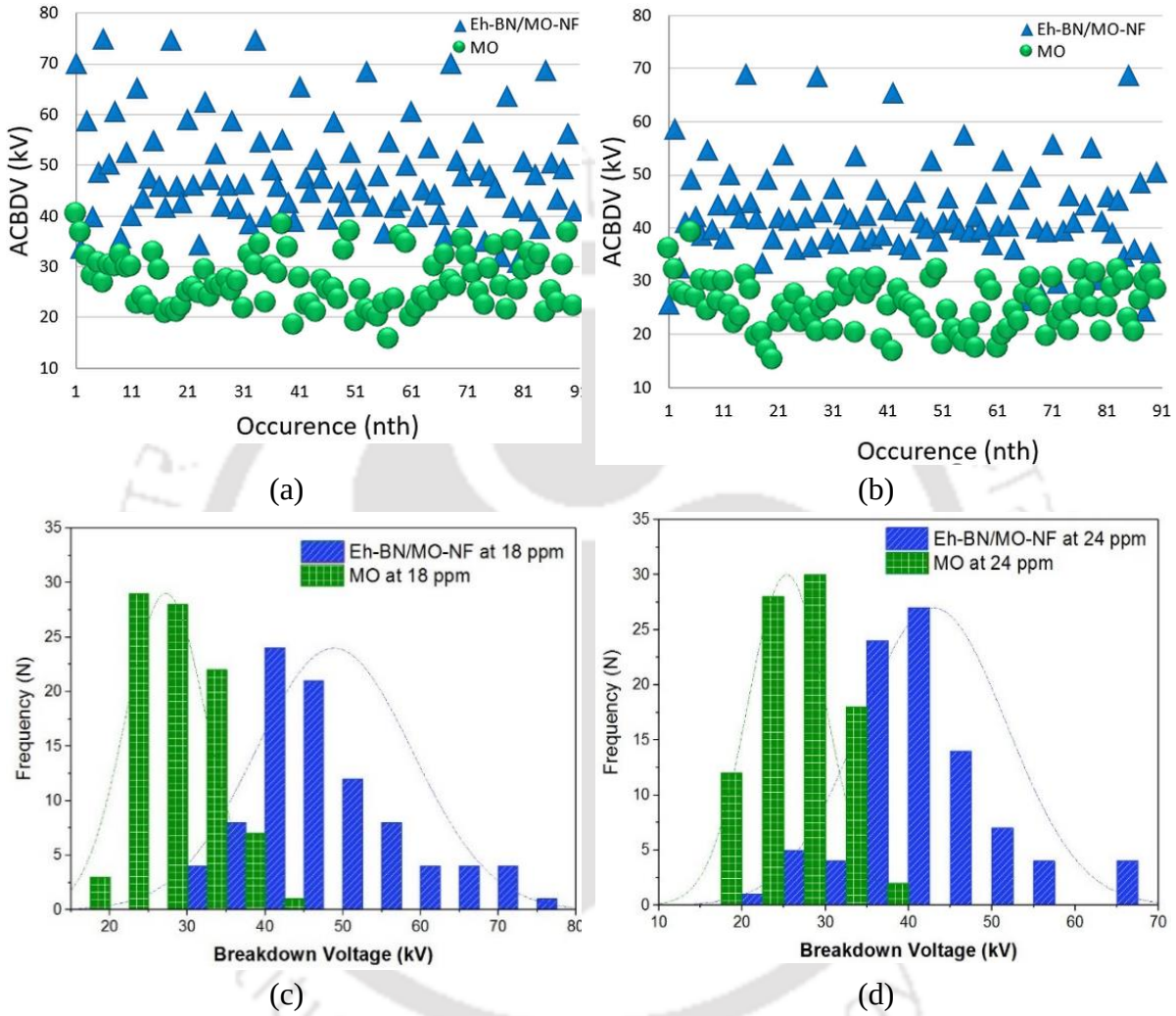

Figure 4.8: Frequency and distribution of ACBDV (a) BDV levels of MO and Eh-BN/MO NF at 18 ppm, (b) BDV levels of MO and Eh-BN/MO NF at 24 ppm, (c) Probability density of MO and Eh-BN/MO NF at 18 ppm, (d) Probability density of MO and Eh-BN/MO NF at 24 ppm.

The key objectives of these experiments are to determine the range of breakdown test voltages in a fixed sample of tests. The AC breakdown voltage (ACBDV) data is obtained for MO and Eh-BN/MO-NFs at 18 and 24 ppm moisture levels using a Baur DPA100 Oil breakdown tester, as per ASTM D1816. The breakdown level of oil is an important aspect when transformer oil is taken into account for insulation purpose. So, a closer look at its range will provide a better idea to ascertain the lowest level at which the oil will exhibit breakdown properties. The

occurrence ACBDV, the frequency of distribution of MO and NFs at 90 different instant of tests at 18 and 24 ppm moisture level are presented in Figure 4.8. It is observed from the Figure 4.8 (c) and 4.8 (d) that the frequency of maximum breakdown occurs in the range of 23-30 kV for MO and 40-48 kV for NF at 18 ppm. Whereas, at 24 ppm, the frequency of maximum breakdown is observed to be 22-29 kV for MO and 36-42kV for NF.

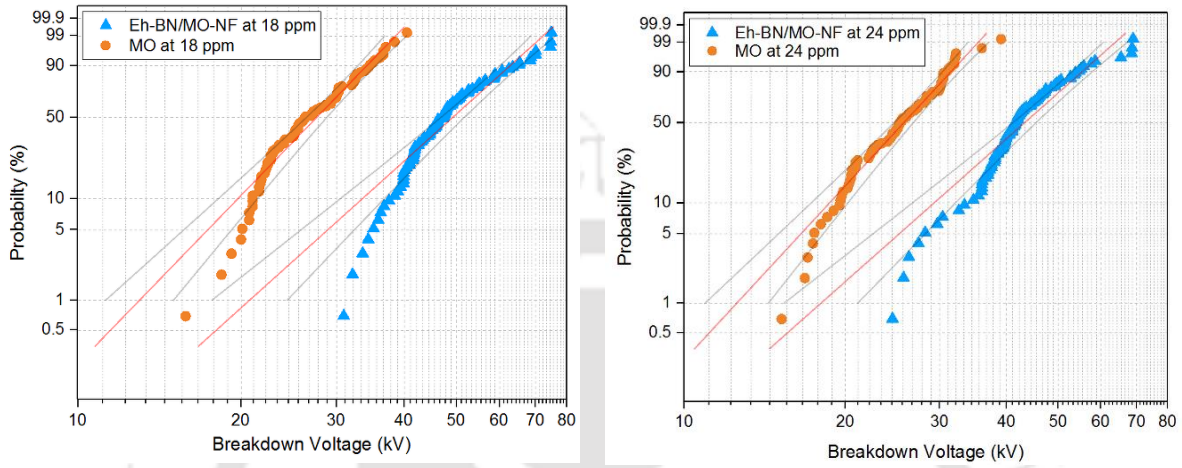

(a) (b)

Figure 4.9: Weibull 2 parameter analysis of ACBDV dielectric strength at (a) 18 ppm, (b) 24 ppm.

Table 4.1: Weibull distribution parameters.

Parameters	Liquid dielectrics			
	18 ppm		24 ppm	
	MO	NF	MO	NF
α	29.38	53.02	27.31	46.58
β	5.62	4.90	5.89	4.83
ρ	95%	95%	95%	95%

There are many statistical methods to analyze the given set of data, out of which Weibull distribution is a preferred method for the ACBDV analysis in liquid dielectric. In this study, the distribution of ACBDV data for MO and Eh-BN/MO NF at 0.01wt% of NP concentration for 18 and 24 ppm moisture content are plotted in Figure 4.9(a) and 4.9(b) using 2 parameter model Weibull plot. The Weibull distribution of cumulative density function ($F(x)$) expressed in (4.6) is plotted with a correlation factor of ρ (=95%) which indicates the closeness of the probability line with the experimental data.

Table 4.2: Comparison of withstand voltage of MO and Eh-BN NF at 18 and 24 ppm.

Oil Sample		Probability (%)			
		63.2%	50%	10%	5%
18 ppm	MO	29.3 kV	26.3kV	21 kV	20.1 kV
	Eh-BN/MO-NF	49.8 kV	47.3 kV	38 kV	35 kV
24 ppm	MO	27.4 kV	25.3 kV	19.6kV	17.5 kV
	Eh-BN/MO-NF	44 kV	41.6 kV	34 kV	28 kV

Two-parameter Weibull distribution of cumulative density function used for the present analysis is given as follows:

$$F(x:\alpha,\beta)=1-\exp(-(x/\alpha))^{\beta};\quad x>0 \tag{4.6}$$

Where x is the ACBDV; α and β are the scale and shape parameters respectively. The distribution parameters are presented in Table 4.1.

The probabilities of failure in breakdown voltages are noted at 5, 10, 50, 63.2% of failure instance in Table 4.2. It is observed from the figure and table that there is an enhancement of 74.12 and 60% in ACBDV of the Eh-BN/MO NF compared to MO at 18 and 24 ppm moisture content for 5% probability of failure. Whereas, the enhancement in the ACBDV for NF compared to MO at 63.2% failure probability for 18 and 24 ppm moisture level are 69.96 and 60.49% respectively.

4.5 Summary of the chapter

In this study, the thermophysical, electrical and ageing characteristics of MO and 0.01 wt.% of Eh-BN NP dispersed NF are studied. A sealed beaker oxidative ageing study has been performed for MO and NF for the three distinct ageing durations such as 164, 328 and 492 hrs and the electrothermal and chemical characteristic of the aged oil samples are analyzed experimentally. ACBDV of the MO and NF is studied as per ASTM D1816. Weibull 2-parameter model is used to study the breakdown probability of the MO and NF at 18 and 24 ppm respectively. The mechanism of enhancement in the thermal conductivity and ACBDV of the NF has been introduced. The important outcomes of the present study are as follows:

- Dispersion of 0.01wt% Eh-BN NP into MO, an average size of 100-200 nm enhances the electrothermal properties and hinders the early oxidation of the NF.

- During the progression of the ageing duration, there is a degradation of the thermophysical and electrical properties of both the oils. However, higher hydrophobicity and aspect ratio of the insulating Eh-BN NP has minimum affinity towards oxidation hindering early degradation of electrothermal properties of the NF.
- Breakdown probability of the MO and NF at five instances such as 5, 10, 50, 63.5% has been studied and it is observed that in each instance the NF has lower breakdown probability than MO.

As the thermophysical and electrical properties of the NF is superior than the MO, NF based transformer will increase the power transmission efficiency, reliability and reduce the cost of transmission.

Since the properties of the kraft paper degrades in the presence of moisture and temperature under the transformer operation, the mechanical, electrical and chemical properties of the aged oil impregnated kraft paper are studied with the help of accelerated thermal ageing simulator which is described in the next chapter.

Note: This work, "Effect of oxidative ageing on the thermophysical and electrical properties of the nanofluid with statistical analysis of AC breakdown voltage" has been published in IET Science, Measurement & Technology.

5

Thermal ageing analysis of MO and NF impregnated solid insulation

Contents

5.1 Introduction

The solid insulating material is the key constituent in the oil filled power and distribution transformers. For the safe operation in the functional parts of the transformer, appropriate insulation is very much essential. An adequate insulation isolates the coil from one another and at the same time safely prevents the accidental over voltage. Since the solid insulations such as kraft paper and press board come in contact with TO, both the TO and paper experiences the electrical, mechanical, thermal and chemical stresses during the transformer operation. That results an ageing and permanent degradation in the insulating system either externally or internally over the period of time [1]. Temperature in the solid-liquid insulation system plays a key role in stimulating the degradation in the electro-mechanical and chemical strength of the oil impregnated paper [19, 20]. Since oxygen dissolves in the oil at an elevated operating temperature, ageing rate of the solid insulation accelerates.

Thermal ageing is the major phenomena of the transformer to study the degree of degradation of the insulation system. Therefore, thermal ageing study of MO and NF impregnated kraft paper are studied at a temperature of 160 ^{o}C. The Eh-BN/MO-NF has superior thermo-electrical properties than MO. Therefore, NF impregnated kraft paper (NFIKP) is expected to experience a low rate of ageing degradation. A comparative thermal ageing study on the MO impregnated kraft paper (MOIKP) and NFIKP are carried out for different ageing duration such 100, 500, 1000 and 2000 hours. The ageing degradation characteristics of the impregnated paper such as colour, ACBDV, tensile strength and degree of polymerization (DP) are studied and compared with fresh kraft paper.

5.2 Design of thermal ageing simulator

Natural and force convection imposed accelerated thermal ageing apparatus is designed with temperature controlled and motorize stirring mechanism along with real time ageing environment. It incorporates natural and force convective flow of the insulating oil in the ageing vessels through the coil holding bar. The flow of the oil inside the vessels is controlled through the DC motor and controller. The ageing vessel is provided with functional transformer circumstance with elevated temperature to accelerate the ageing process. The parts of the ageing simulator are made up of a mild steel and the copper coil, which provides the real transformer environment during the ageing. The setup has the advantages of easy machining, light weight, portable and automatic temperature controlled.

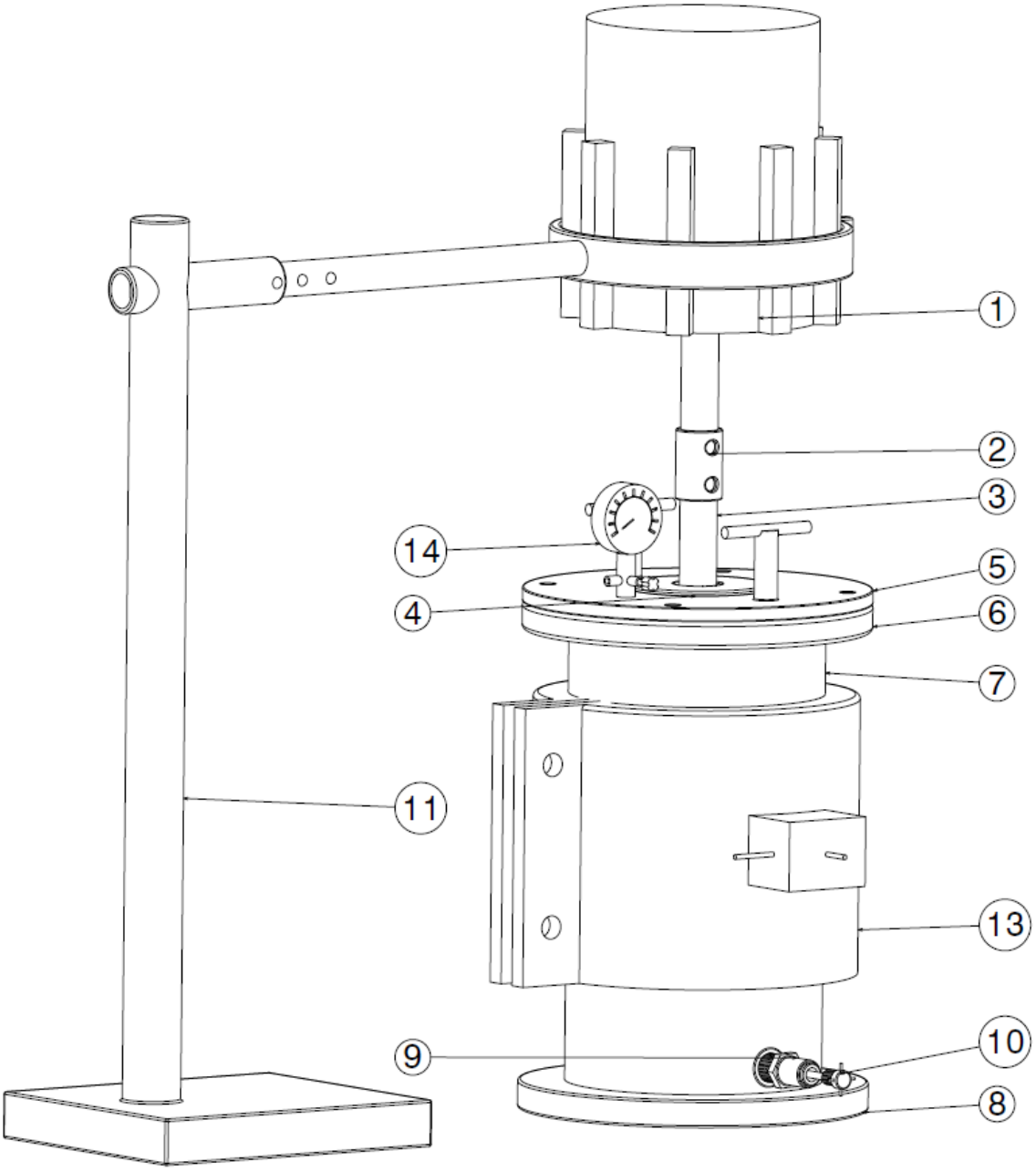

Figure 5.1: Schematic diagram of accelerated thermal ageing setup.

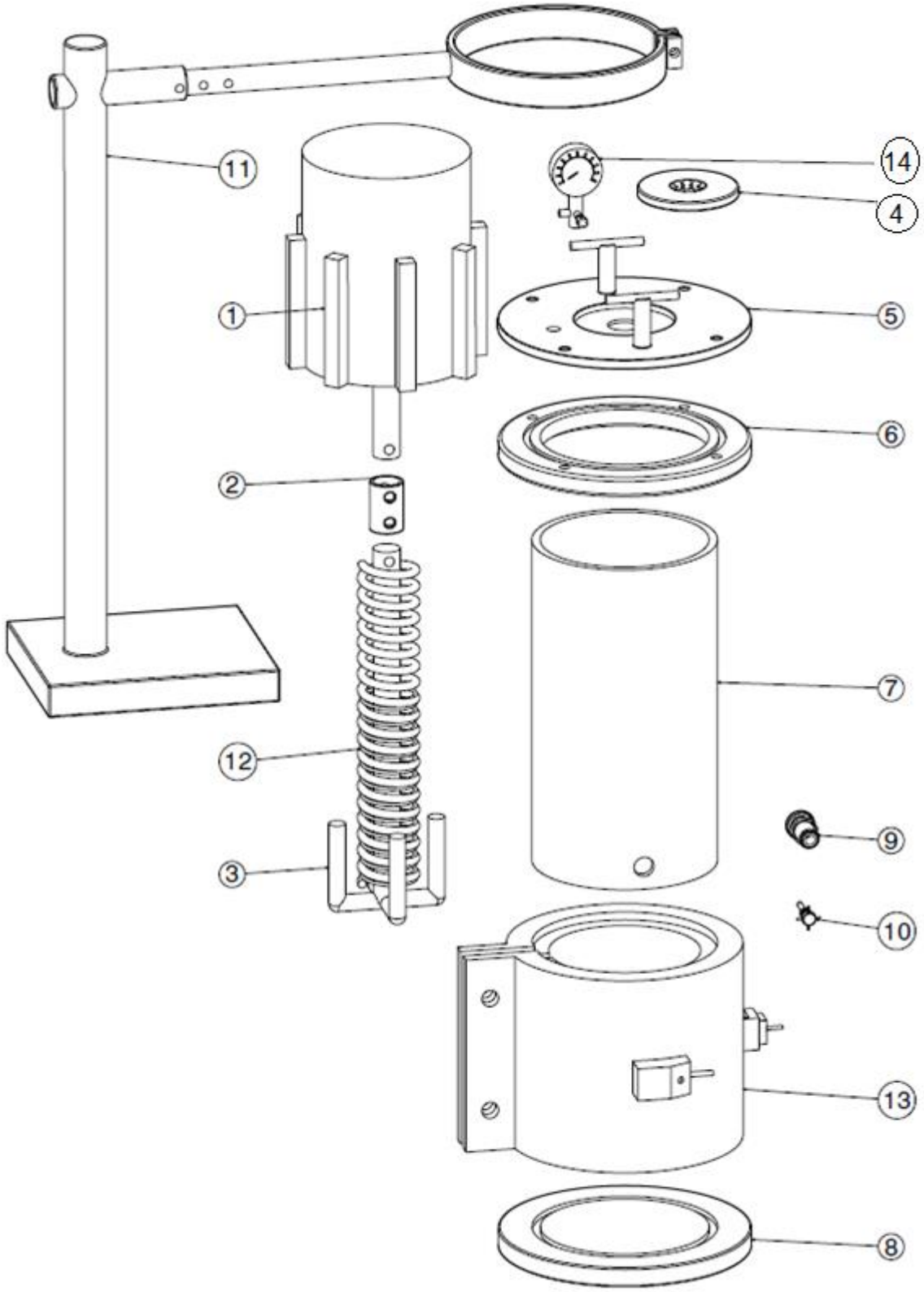

Figure 5.2: Schematic diagram of exploded view of each parts of the accelerated thermal ageing setup.

Table 5.1: Different functional parts of the thermal ageing simulator

Parts of the simulator	Description
1	DC motor with a driven shaft used in setup.
2	Coupler to accommodate the driver shaft of the DC motor to the driven coil holder rod.
3	Coil holding bar which has the provision for the placement of copper coil in it
4	Sealed bearing, which is placed on the top of the cover plate to support coil holding bar and to make it rotate smoothly
5	Top cover part of the ageing setup, which is used to keep the ageing vessel airtight and have the provision to open the ageing vessel until the ageing process get completed.
6	Top and bottom part of the top flange used to support the top cover. It has the provision to place the O-Ring for complete sealed.
7	Cylindrical shell which contains the insulating oil for the accelerated thermal ageing
8	The bottom flange which act as base for the cylindrical container
9	The oil opening valve mechanism from the ageing setup
10	The closing pin of the oil opening valve of the convection imposed accelerated thermal ageing setup
11	The adjustable stand to hold the DC motor to ascertain the convection inside the ageing container
12	The oil opening valve mechanism from the ageing setup
13	The cylindrical band heater to provide uniform heating to the ageing container
14	The pressure regulator cum releasing valve

Figure 5.1 shows the assembly of the convection imposed accelerated thermal ageing setup along with various functional components like DC motor, coupler, bearing, cover plate, top and bottom part of the flange, oil output valve closing pin, adjustable stand holder for the DC motor and band heater for the ageing performance. Figure 5.2 shows the exploded view of the assembly of the convection imposed accelerated thermal ageing setup along with the hidden parts like coil and coil holder that is present inside the cylindrical container which

are invisible in the assembly view Figure 5.1.

Force convective flow of the insulating oil inside the ageing vessel is achieved by DC motor controlled stirring mechanism. Variable velocity of the convective flow during ageing of the insulating oil inside the ageing vessel is achieved. Airtight sealing of the vessels is done by providing O-ring on the top flange and sealed bearing on the top cover plate, top plate and top cover is bolted tightly to avoid moisture contamination into the oil during ageing. The arrangement of aged oil evacuation is provided at the bottom of the ageing vessel by the help of opening valve. Ageing process is carried out for different ageing duration in terms of hour and the sampling and testing of the insulating oil is performed as per ASTM D117-10 [142]. The description of the simulator and each parts of the accelerated thermal ageing simulator are described in the Table 5.1. The real transformer environment is achieved by keeping the copper coil, kraft paper and press board at an adequate aspect to the insulating oil inside the ageing vessel as shown in Figure 5.3.

Figure 5.3: Fabricated setup of natural convection imposed accelerated thermal ageing simulator.

5.3 Accelerated thermal ageing of solid insulation

A sealed thermal ageing test vessel of capacity two-litter as shown in Figure 5.3 is used for the ageing of the MOIKP and NFIKP. In order to make kraft paper moisture free, it is dried and heat treated before putting into the ageing vessel. As per the ASTM D117-10, an equivalent amount of ageing reinforcement such as kraft paper of 15 gms and copper catalyst of 430 gms are kept inside the insulation oil enclosed in the ageing vessel. The temperature of the ageing is set at 160 ^{o}C and the ageing of the solid as well as liquid insulation is carried out for four different ageing durations such as 100, 500, 1000 and 2000 hours. The effect of ageing on electro-mechanical and chemical properties of the solid insulation is studied. The solid insulation is nothing but the cellulosic compound whose chemical structure is presented in the Figure 5.4. The properties of the insulating kraft paper are presented in the Table 5.2.

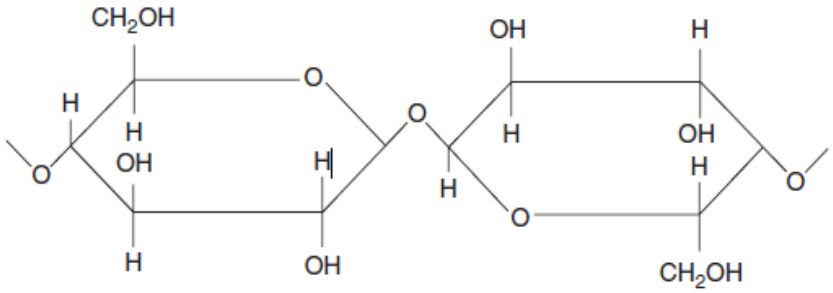

Figure 5.4: Chemical structure of cellulose (polymer chains of glucose) [19].

Table 5.2 Insulating kraft paper

Characteristics	Specifications
Thickness (mm)	0.5-1
Width (mm)	12
Density (g/cc)	0.75-0.85
Moisture Content (ppm)	6-8

5.4 Results and discussion

Ageing degradation of the insulating kraft paper are studied in different phases such as physical appearance, mechanical strength, chemical and electrical strength. Deterioration of these properties severely affect the performance of its insulation properties [16]. Therefore, post ageing analysis of the insulating kraft paper are carried out and are explained below.

5.4.1 Colour of the fresh and aged kraft paper

Physical appearance such as colour of the kraft paper is an indicator of the ageing degradation of the solid insulation. The colour of the fresh and aged kraft paper samples are shown in the Figure 5.5. It is observed from the figure that colour of the both MOIKP and NFIKF changes from clear to darker with the rise in ageing duration upto 2000 hrs of ageing. Negligible changes in the colour is observed upto 500 hrs of ageing for the kraft paper. As ageing accelerates from 500 to 1000 and then 2000 hours, there are noticeable changes in the colour of the kraft paper from clear to dark and darker correspondingly. It is observed that the rate of ageing degradation of the NFIKP is slower than the MOIKP at any particular ageing duration. Superior thermal conductivity of the NF deaccelerates the thermal ageing of the NF. Therefore, NFIKP experience lesser thermal and physical degradation showing slight darker colour even after 2000 hours of ageing.

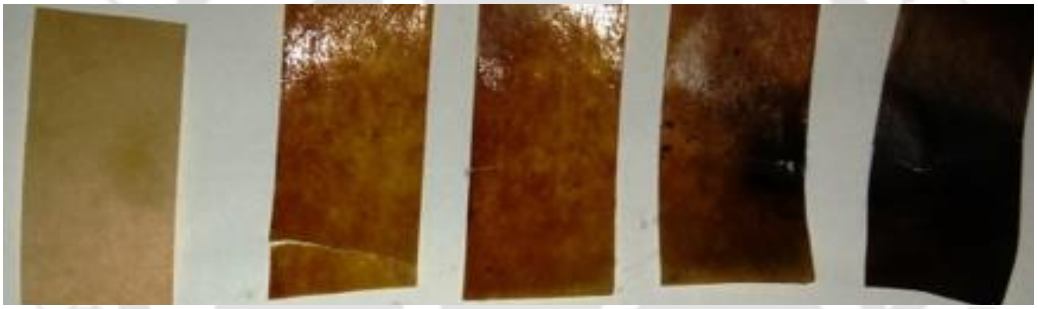

Fresh 100 hrs 500 hrs 1000 hrs 2000 hrs

(a)

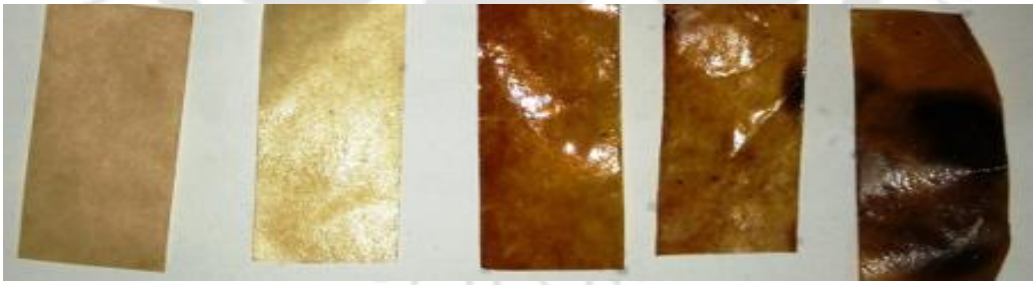

Fresh 100 hrs 500 hrs 1000 hrs 2000 hrs

(b)

Figure 5.5: Colour of the accelerated thermally aged kraft papers at different ageing instant for (a) MOIKP and (b) Eh-BN/MO NFIKP.

5.4.2 ACBDV of aged kraft paper

Analysis of ACBDV of the insulating kraft paper provides an information about its dielectric integrity. Higher ACBDV value ascertain the superior dielectric integrity in the

paper. In this study, ACBDV analysis is carried out for thermally aged kraft paper at different ageing periods. ACBDV of MOIKP and NFIKP at different ageing duration such as 100, 500, 1000 and 2000 hours are studied and compared with fresh kraft paper. Figure 5.6 shows the schematic arrangement of the ACBDV analysis of the kraft paper as per ASTM D149 standard. Since fresh kraft paper are moisture hungry, vacuum drying process is followed to avoid the moisture contamination before ACBDV study. The aged kraft paper sample are collected from the ageing vessel and stored in vacuum desiccator before performing the test. A total of ten measurements of each sample are carried out and the Weibull study of ACBDV is reported. The BDV measurement is carried out at a power frequency of 50 Hz and at room temperature of 27 ^{o}C.

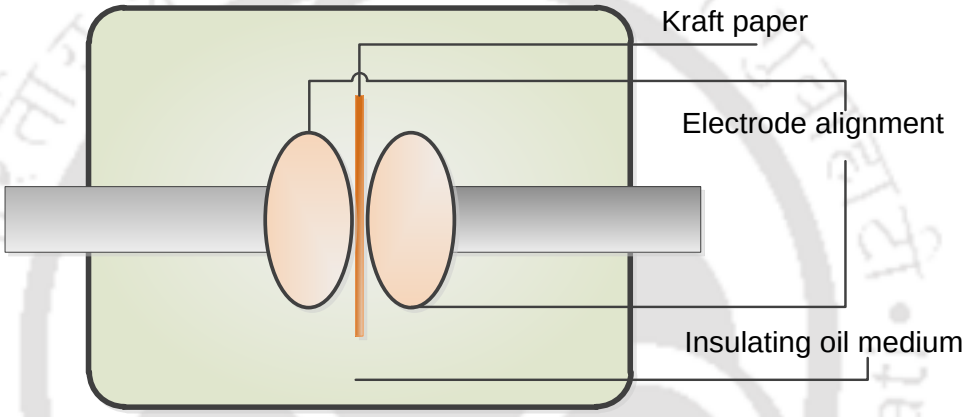

Figure 5.6: Schematic diagram of ACBDV test of the kraft paper.

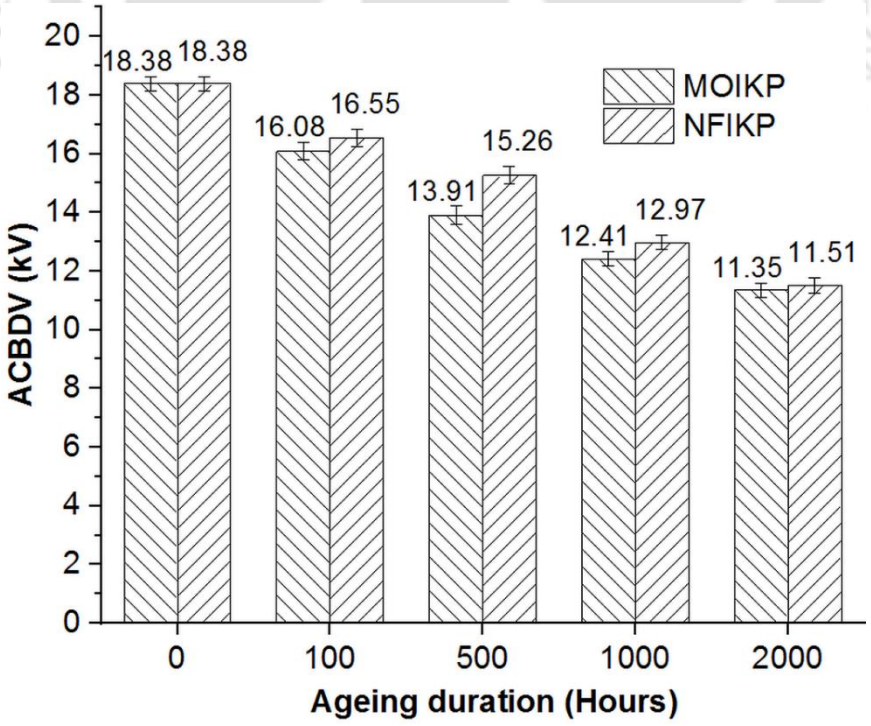

Figure 5.7: Mean ACBDV of the MO and NF impregnated kraft papers.

Table 5.3: Percentage enhancement of ACBDV in the kraft paper

Ageing duration (hours)	MOIKP	NFIKP	% degradation
0	18.38	18.38	0
100	16.08	16.55	2.92
500	13.91	15.26	9.70
1000	12.41	12.97	4.51
2000	11.35	11.51	1.45

Figure 5.7 shows the comparative ACBDV data analysis of the MOIKP and NFIKP for different ageing duration. It is observed from the Figure 5.7 and Table 5.3, the mean ACBDV value of MOIKP and NFIKP degrades with increase in ageing period. The effect of NF with the impregnation to the kraft paper during ageing minimizes its dielectric degradation. It is seen from the table that the ACBDV of NFIKP is 2.92, 9.70, 4.51 and 1.45 % higher compare to the ACBDV of MOIKP at 100, 500, 1000 and 2000 hours of ageing respectively.

For transformer insulation, the minimum withstand voltage is important rather than the mean voltage. The two popular statistical analysis to understand the probability distribution of breakdown failure are normal distribution and Weibull distribution. Weibull distribution shows better accuracy with failure analysis by referring to extremely small amount of samples. Hence, Weibull distribution is used in this study. The breakdown probabilities for the 2-parameter Weibull are calculated using (5.1).

$$F(t:\alpha,\beta) = 1 - e^{-\left(\frac{t}{\alpha}\right)^{\beta}}, \quad t \geq 0$$
$$= 0, \quad t < 0 \tag{5.1}$$

where α is the scale parameter, β is the shape parameter, and t is the time to breakdown.

The breakdown voltage (kV) and cumulative probability $F(t)$ at the confidence bound of 95% is plotted along x- axis and y-axis respectively in the Figure 5.8. In this figure, BDV probability density plot for MOIKP and NFIKP are studied and compared with fresh kraft paper for the Weibull distribution [90]. The various shape and scale parameters along with the ACBDV failure at different failure percentage of MOIKP and NFIKP are given in Table 5.4. and 5.5 respectively.

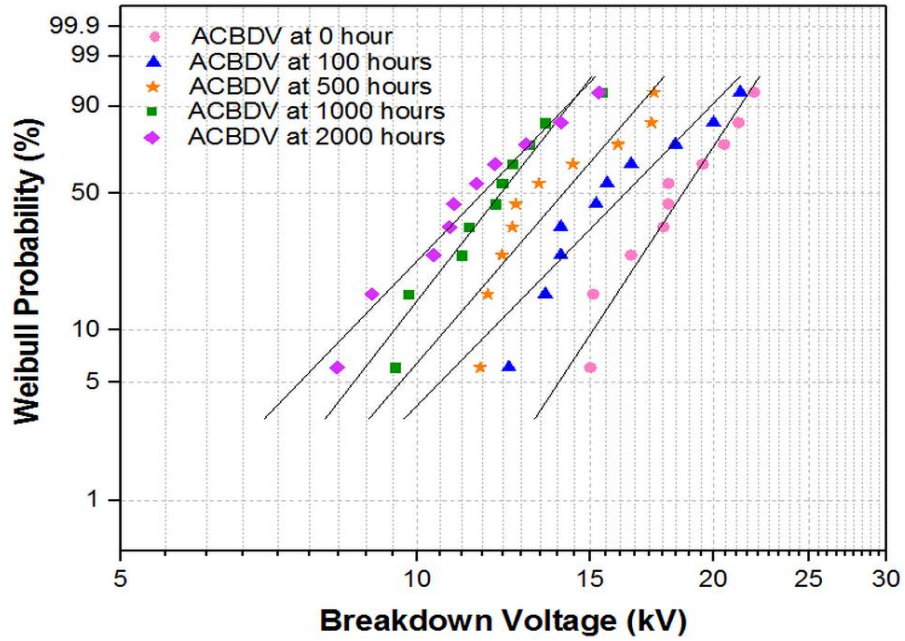

(a)

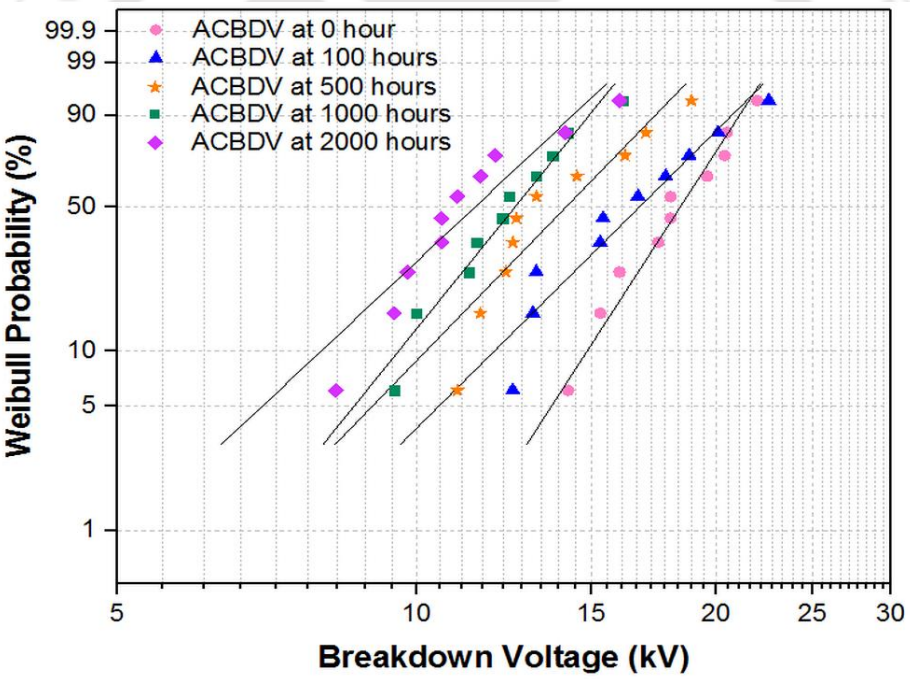

(b)

Figure 5.8: Weibull plot of the (a) fresh and aged MOIKP (b) fresh and aged NFIKP at different ageing duration

It is observed from the Figure 5.8 and Table 5.5 that the probability of failure in ACBDV for NFIKP and MOIKP is more or less similar for the probability range of 5, 10, 50 and 63.2 % at fresh and aged condition.

Table 5.4: Weibull ageing duration parameter of

	MOIKP				
Weibull parameters	0 h	100 h	500 h	1000 h	2000 h
Shape (β)	8.99	6.017	6.839	7.578	6.098
Scale (α)	14.384	17.288	14.856	12.764	12.375
	NFIKP				
Shape (β)	8.764	5.619	5.824	7.009	5.305
Scale (α)	19.19	17.874	15.047	13.231	12.264

Table 5.5: ACBDV at different failure percentages

	MOIKP			
Ageing duration (hours)	5%	10%	50%	63.2%
0	14.89	14.29	18.50	19.44
100	11.89	12.22	15.41	16.8
500	10.58	10.71	12.80	14.2
1000	8.66	9.30	11.19	12.4
2000	7.52	8.29	11.02	11.8
	NFIKP			
0	13.69	14.54	18.32	19.80
100	12.04	12.67	16.30	17.92
500	10.64	11.51	13.09	14.61
1000	9.17	9.84	12.68	13.15
2000	8.21	8.86	11.44	12.21

5.4.3 Mechanical strength analysis

Mechanical strength of the kraft paper is measured by its tensile strength analysis. With passage of time, the cellulosic kraft paper present in the transformer is weakened by losing its mechanical strength due to which the local hot spots are formed. That leads to the initiation of partial discharges and dielectric losses in the oil and paper as well. Therefore, an investigation of tensile strength of the MOIKP and NFIKP at different ageing duration is carried out. The tensile strength of fresh and oil impregnated kraft paper is studied using a BISS universal testing machine (UTM) as shown in Figure 5.9 as per ASTM D828-97 [144].

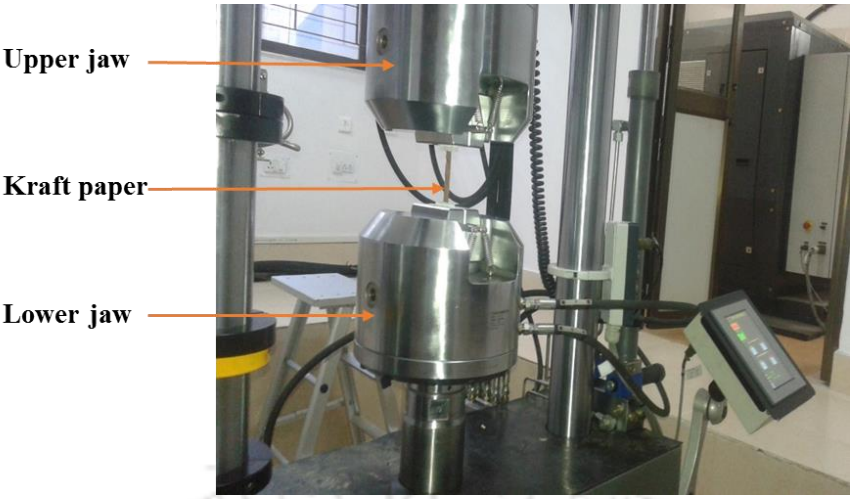

Figure 5.9: UTM used to measure the tensile strength of aged kraft paper.

The tensile strength and modulus of the oil impregnated kraft paper degrades at initial stage of thermal ageing and the degradation is observed to be severe at an elevated ageing period. Ageing temperature plays a crucial role in accelerating the mechanical degradation by altering and weakening the chemical structure of the cellulosic molecule in the kraft paper.

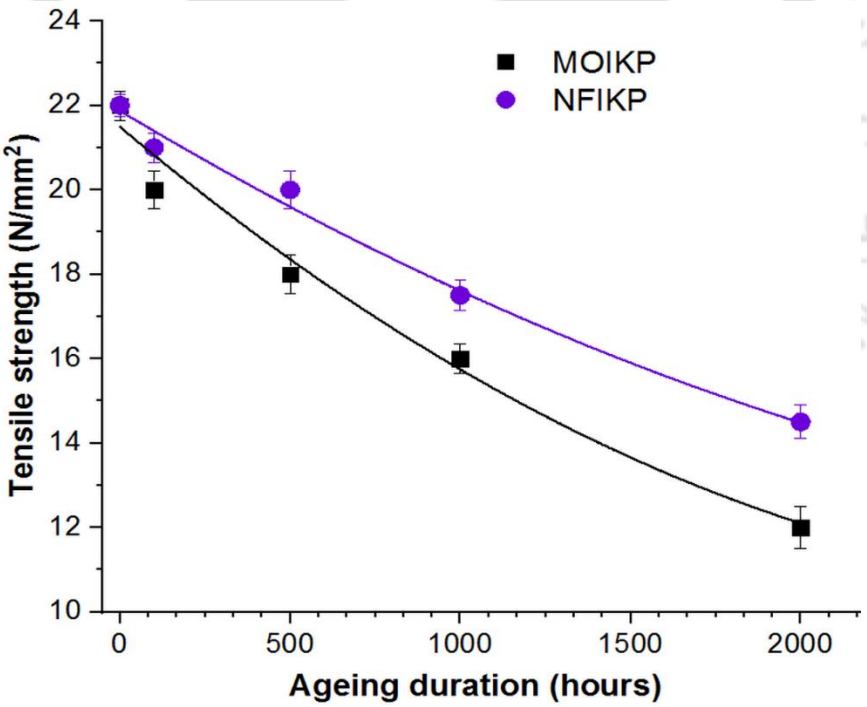

Figure 5.10: Tensile strength degradation of MOIKP and NFIKP.

The tensile strength and comparative percentage degradation with ageing hour is presented in the Figure 5.10 and Table 5.6. It is observed that the rate of tensile degradation percentage of NFIKP is slower than the MOIKP. The superior thermal conductivity of Eh-BN/MO NF conducts the heat away from the NFIKP during the ageing and the cellulose molecules in the

kraft paper are less harmed. Since MO is having inferior thermal conductivity, the MOIKP are greatly affected by the temperature stress and hence suffers high rate mechanical degradation.

$$\begin{bmatrix} Tensile\ Strength_{MOIKP} \\ Tensile\ Strength_{NFIKP} \end{bmatrix} = \begin{bmatrix} 21.493 \\ 21.873 \end{bmatrix} t^2 - \begin{bmatrix} 0.0068 \\ 0.0048 \end{bmatrix} t + \begin{bmatrix} 1.0529\times10^{-7} \\ 5.7141\times10^{-7} \end{bmatrix} \quad (5.2)$$

The empirical expression of the tensile strength of MOIKP and NFIKP with ageing duration obtained from the curve fitting with R^2 of 0.979 and 0.992 are presented in equation (5.2) respectively.

Table 5.6: Percentage degradation of the tensile strength

Paper	(%) Decay in tensile strength				
Ageing duration	0 hr	100 hr	500 hr	1000 hr	2000 hr
MOIKP	0	10	18	25	45
NFIKP	0	5	10	20	32

5.4.4 Degree of polymerization (DP)

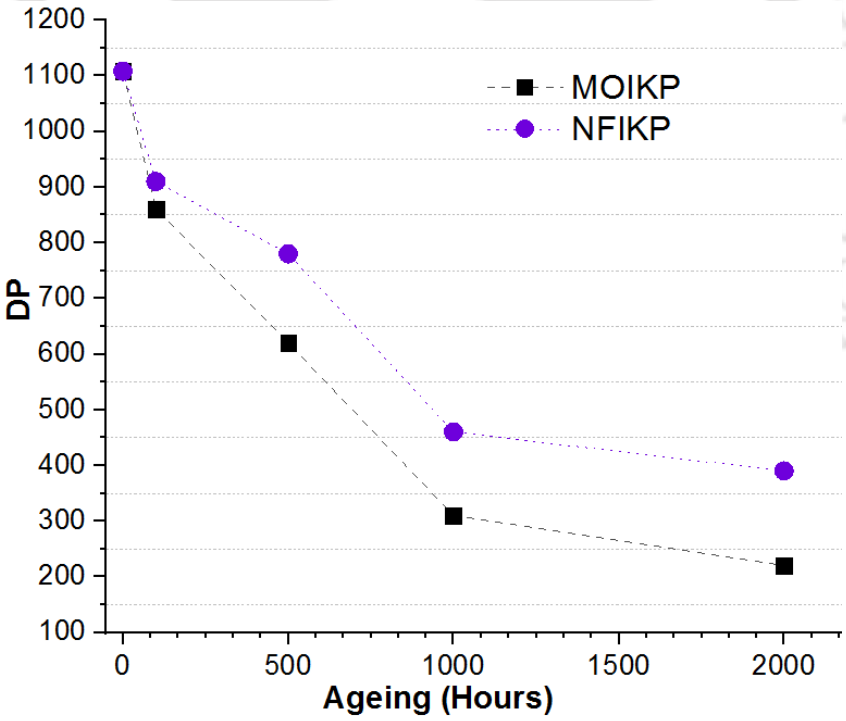

Figure 5.11: DP of MOIKP and NFIKP at different ageing duration.

The intensity of chemical degradation is measured by DP, which defines the existing average number of monomers in a cellulose molecule. In this study, the DP test is carried out for fresh and aged sample of MOIKP and NFIKP at reported ageing duration. The DP test of the insulating kraft paper is carried out as per ASTM D4243-16 standard [145]. The molecular

integrity of the cellulosic kraft paper degrades in the due course of time. The DP value decreases with increase in the ageing time as seen in Figure 5.11. Superior thermal conductivity of the NF takes away the heat generated by the conductor and allows uniform distribution of the heat stress keeping the paper away from the direct influence of thermal ageing. However, MO suffers an uneven thermal stress distribution in the oil resulting in early and abrupt chemical degradation, which leads to decay in DP value of MOIKP.

5.5 Summary of the chapter

Thermal ageing analysis of the MOIKP and NFIKP is carried out for four different ageing durations. A comparative analysis of the electro-mechanical and chemical strength degradation of the MO and NF impregnated kraft paper are studied. It is observed that temperature in the thermal ageing is the cause of degradation by altering and weakening the molecular structure of the cellulosic kraft paper resulting in changes of the physical properties. The DP and the mechanical strength of the oil impregnated kraft paper are proportional to each other. Superior thermal conductivity of the liquid insulating medium uniformly transfers the heat and hence, NFIKP experiences minimum ageing degradation compared to MOIKP.

An ever growing demand of efficient TO is a challenge for today's researchers. Since the resources of fossil fuel are decreasing day by day, VO based TO seems to be an ideal solution to the ever increasing demand of the efficient and durable TO in future. Therefore, the vegetable oil based transformer oil is discussed in the next chapter.

Note: This work, "Electro-mechanical and chemical strength analysis of thermally aged nanofluid impregnated kraft paper" has been published in IEEE Conference on Electrical Insulation and Dielectric Phenomenon (CEIDP), 21-24 Oct., Cancun, Mexico 2018.

6

Vegetable oil based liquid dielectric for transformer

Contents

6.1 Introduction

Transformer oil and its effectiveness in terms of providing enhanced insulation and thermal performance compared to MO is a challenge for high voltage and insulating material scientist. The research in the field of a novel insulating oil for transformer, many research and development has been carried out, yet an absolute substitute to the MO is still a challenge. An ever growing demand of efficient TO has been a challenge for today's researchers. The resources of fossil fuel are decreasing day by day. Vegetable oil (VO) based TO seems to be an ideal solution to the ever increasing demand of the efficient and durable TO in future. The VO is an environment sustainable liquid for transformer. The VOs are potential candidate for transformer because of their significant fire safety characteristic, sustainability, non-hazardous and biodegradable nature [27, 86-88]. Beyond the aforementioned characteristics, the superior thermo-physical and enhance dielectric properties prologue its use as a TO.

Many researchers put their effort to use the VO and their esters as a liquid dielectric in transformer [15, 86-89]. The demand of the insulating oil is huge and the requirement of the transformer is growing exponentially. Therefore, the use of edible VOs (rape-seeds, sunflower, corn, soybeans, grape-seeds, sesame, etc.) in transformer surely affects the food economy. Hence, it is required to study about the option left with the nonedible VO and its application as TO in the context of thermophysical and electrical characteristics. A very few research has been carried in the field of nonedible VO as a TO for the replacement of MO [90-94].

The present paper deals with the development of a new nonedible VO, named karanji oil methyl ester (KOME), as a novel TO. The KOME is derived by the process of two step transesterification from the crude karanji oil (CKO) extracted for the karanji fruit seeds. Karanji fruits is drought resistant, semi-deciduous, nitrogen fixing leguminous tree. It grows about 15-20 meters in height with a large canopy which spreads equally wide [95]. We collected the ripened karanji fruits from the karanji tree available in the IIT Guwahati premises followed by removal of karanji seeds and drying. Then the CKO is extracted from the dried karanji seeds using mechanical expeller. Two step transesterification process has been carried out to prepare the KOME. The thermophysical (thermal conductivity, viscosity, interfacial tension, flash point, pour point and colour), chemical (moisture content, acid number, iodine number) and electrical (ac breakdown voltage, resistivity, dielectric constant, dielectric loss) properties of KOME are studied and compared with MO. Finally, with the ageing and statistical analysis of ACBDV compared to MO ascertain the chemical and dielectric integrity of the KOME.

6.2 Nonedible karanji oil as VO

Karanji tree is a deciduous medicinal plant, which found in the region of north eastern part of India, Indian subcontinent, south-east Asia to north-eastern region of Australia, Fiji and Japan. Karanji belongs to the family of pea and it has many common names such as Indian beech, Pongam oil-tree, Karanji tree, and Pongamia pinnata tree. It grows in the tropical and subtropical region, which does not require a fertile land. The seeds of the karanji tree are now a day widely used for the biodiesel production [96]. The production of the biodiesel from the karanji seeds is a solution for the energy crises and environmental safety. Moreover, the cultivation and production of the karanji seeds and its oil generates income in the rural areas of the developing countries.

Karanji oil being a biodiesel is considered as a green fuel by minimizing the greenhouse gas emission. In engine of the vehicle, it acts as an efficient lubricant and minimizes the engine wear being natural ester. The plant need very less fertile land and rainfall, it can be grow in tropical and subtropical regions where minimum rainfall is considerably lower than that of all other edible crops. Many applications of the karanji trees has been explained in several literatures for example, conservation of soil water, reclamation of the soil, control of soil erosion, major feedstock for pharmaceutical, cosmetic industries. Production of biodiesel from the seeds of the karanji fruits is the key application involve in the recent past of the research. Karanji seeds can be processed into a suitable biodiesel, which can be act as a less polluting fuel compared to petroleum based oil [97]. The byproduct of the karanji oil cake is treated as a suitable organic fertilizer for organic farming. The implementation of the aforementioned application will strengthen the economy of the rural people.

CKO can be obtained from extraction process of solar dried karanji seeds. Mechanical expeller is being used for the oil extraction. The CKO is further processed into the two step transesterification process to obtain KOME as an insulating oil for electrical transformer. The karanji oil can also be extracted using the soxhlet, cold percolation and Solvent extraction process by taking karanji seeds powder as an input. But in these chemical extraction process, the oil percentage is more compared to mechanical extraction [98]. However, the chemical extraction involves lot of the hazardous chemical treatments, so mechanical expeller is more suitably preferred for the extraction of CKO.

6.2.1 Extraction of oil

The ripened karanji fruits are collected from the karanji tree available in IIT Guwahati campus. The buds of the karanji fruits are removed manually and the seeds are exposed to sun for surface moisture evaporation. On an average of 30% of CKO is obtained from the dried seeds of karanji through mechanical extraction.

The major component in the CKO are triglycerides and triacylglycerol. Figure 6.1 shows the molecular composition of the karanji oil. The triglycerides are esters which consist of three molecules of fatty acids, one glycol and substantial quantity of oxygen in CKO chemical structure. The present fatty acid varies in the length of their carbon chain and double bonds [146]. The composition of the CKO are shown in the Table 6.1 [147].

Table 6.1: Fatty acid compositions (area %) of CKO

Fatty acid	Formula	Common name	Structure	Wt. %
Palmitic	$C_{16}H_{32}O_2$	Hexadecanoic acid	C16:0	3.7% – 7.9%
Stearic	$C_{18}H_{36}O_2$	Octadecanoic acid	C18:0	2.4% – 8.9%
Oleic	$C_{18}H_{34}O_2$	cis-9-Octadecenoic acid	C18:1	44.5% -71.3%
Linoleic	$C_{18}H_{32}O_2$	(9Z,12Z)-octadeca-9,12-dienoic acid	C18:2	10.8% – 18.3%
Linolenic	$C_{18}H_{30}O_2$	15-trienoic acid	C18:3	2.6%
Arachidic	$C_{20}H_{40}O_2$	Docosanoic acid	C20:0	2.2% – 4.7%
Eicosenoic	$C_{20}H_{38}O_2$	Trans-11-eicosenoic acid	C20:1	9.5% – 12.4%
Behenic	$C_{22}H_{44}O_2$	Docosanoic acid	C22:0	4.2% – 5.3%
Lignoceric	$C_{24}H_{48}O_2$	Tetracosanoic acid	C24:0	1.1% – 3.5%

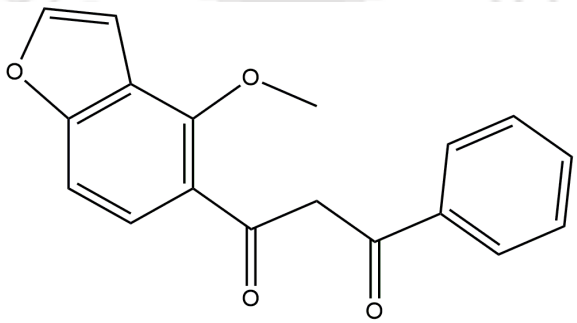

Figure 6.1: Structure of CKO.

The molecular weight of the VO is in the range of 550-900 g/mol. Iodine value of 0-200 g/100g for VO indicates the unsaturated degree of CKO. Viscosity of the CKO is more due to its high molecular weight and it is in the range of 25-64 cSt. Flash point is observed to be more than 250^{o}C. The detail thermophysical, electrical and chemical properties of CKO measured are as shown in Table 6.2.

Table 6.2: Thermophysical and electrical properties of CKO

Properties	Values
Relative Density at 15^{o}C (g/cm)	0.90– 0.95
Kinematic Viscosity at 40^{o}C (mm^{2}/s or cSt)	30.00-32.44
Thermal conductivity (W/m-k)	0.160
Water content (ppm or mg/kg)	1000 – 2000
Total acid number (mg KOH/g)	0.90 – 1.50
Flash point (^{o}C)	250
Pour point (^{o}C)	4
Breakdown voltage (kV) before filtration	89
Breakdown voltage (kV) after filtration	82

6.2.2 Chemical processing and esterification

Many literatures describe that ester oil is a suitable replacement for the MO in transformer. In the present work, the KOME is prepared from the CKO. The detail processing of the CKO to KOME is mentioned in Figure 6.2. Initially, crude oil is heated at temperature of 110-130^{o}C for 30 minutes for evaporation of contaminated moisture from the oil. Since the free fatty acid (FFA) in CKO is about is about 7.5% which is more than 1%, two step transesterification (including acid and base) process is required to form KOME.

From the IEEE C.57.147 and ASTM D6871 [148, 149] standards for VO, it is observed that the CKO does not satisfy the criteria being an insulating oil for transformer. The major fluid properties of the CKO specified in Table 6.2 are deviating from the above mentioned standards. To prepare an insulating VO of required standard for its universal acceptability, properties of fluidity need to be enhanced for CKO. So the improve properties of flowability and removal of unnecessary FFA of CKO, chemical processing is thus required by following the two step esterification process [150].

The transesterification process is a most common and popular method is widely used for the conversion of fatty acid methyl ester (FAME) from the triglycerides. In this process,

exchanging of the organic group R″ is occurred with an ester R′ of an alcohol. In the process of transesterification, the viscosity and acid level of the KOME is reduced drastically ascertaining its usability as an insulating oil for transformer. The generalized reaction of the esterification process is presented in (6.1). The reaction of methanol with triglyceride in the presence of catalyst, FAME is produced along with glycerol as expressed in (6.2).

$$RCOOR' + R''OH \underset{}{\overset{Catalyst}{\rightleftharpoons}} RCOOR'' + R'OH \tag{6.1}$$

Ester Alcohol Ester Alcohol

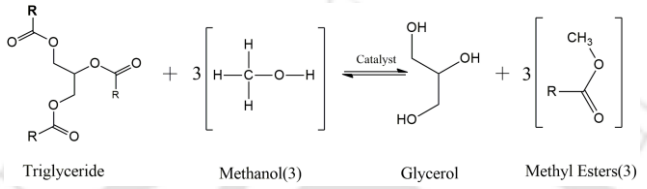

Triglyceride Methanol(3) Glycerol Methyl Esters(3) (6.2)

Acid esterification process is being followed primarily for the reduction of predominant FFA value in CKO lesser than 1% using sulfuric acid (H_2SO_4) as catalyst. The acid esterification of CKO is shown in the Figure 6.2 flow diagram and the detail experimental process is presented in Figure 6.3. The reaction unit as shown in Figure 6.3, consisting of round bottom flask, reflux condenser (the function of this type of condenser to avoid the losses of methanol from evaporation), magnetic stirring hotplate having temperature control unit and a unit of separating funnel with a drain valve arrangement. Various important key parameters such as reaction temperature, reaction time, molar ratio of methanol to crude oil and the required amount of catalyst are suitably chosen. Seeing the higher yielding percentage of the FAME, methanol to CKO molar ratio of 6:1 and 1 vol% of H_2SO_4 as catalyst are poured in to the round bottom flask when it attains the temperature of 60^oC using hotplate. The solution is constantly stirred using magnetic stirrer at 600 RPM for a period of 2 hours (reaction time). The prepared sample of mixture is then allowed to transfer into the separating funnel for the acid separation. The mixture is then kept for 24 hours in the separating funnel for the settlement. Due to the variation in densities of the oil and water, the water is precipitated in the down region, middle region consisting of lower fatty acid based oil and the mixture of sulfuric acid and methanol lies upper part of the separating funnel. Using drain tap, the settled water is taken out from the separating funnel and subsequently lower FFA oil is collected by dumping the mixture of oil and methanol. The measurement of FFA value has been carried out to ascertaining the decrement of acidity percentage of the CKO. It is observed that the acid value is 1.47 mg KOH/g which is nearly 0.72% of FFA level. It is confirmed that during acid

treatment the FFA level is below 1% so, the base transesterification is the next process to follow.

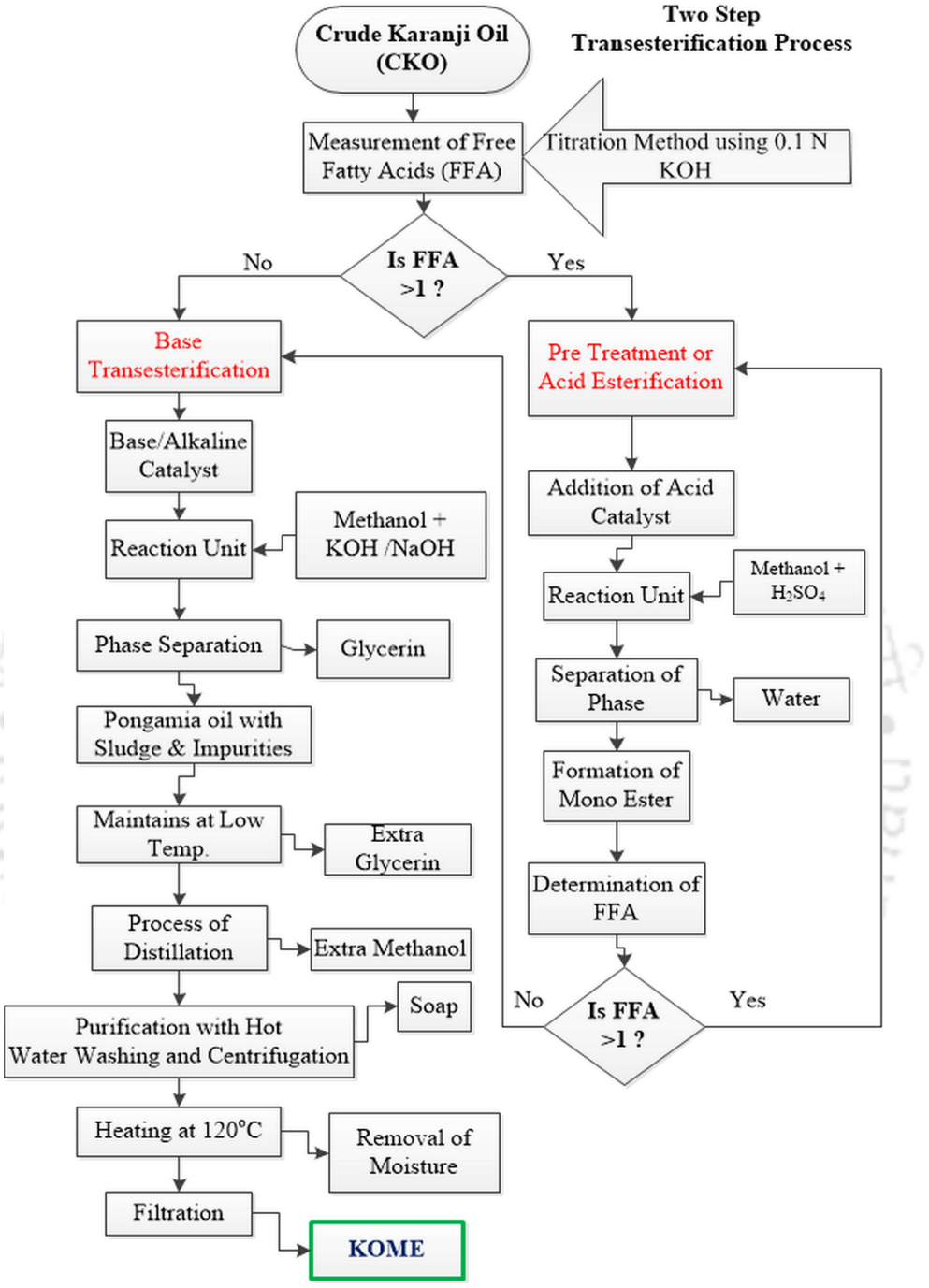

Figure 6.2: Flow chart of production process of the KOME.

In case of base transesterification, acid treated oil is collected in a clean round bottom flask and the oil is heated upto a temperature of 60^0C using temperature regulated magnetic hotplate. An adequate amount of base catalyst potassium hydroxide (KOH, 1% by wt.) and methanol to oil molar ratio of 6:1 is poured in to the mixture. The solution is heated and stirred for 3 hours.

The solution is then collected and kept in separating funnel for 24 hours for the higher density glycerol to settle down. Out of the two layers in the separating funnel, upper layer is FAME and bottom layer is glycerol. Continuous distillation and washing of the solution using hot water removes unwanted impurities form the solution. For pure yielding of FAME from the solution, it undergoes a centrifugation process at 6000 rpm for 10 minutes. Due to the alteration in density, the KOME having lower density floated on the top of the centrifuge tube while the unwanted glycerol is settled down due to more density as shown in Figure 6.3.

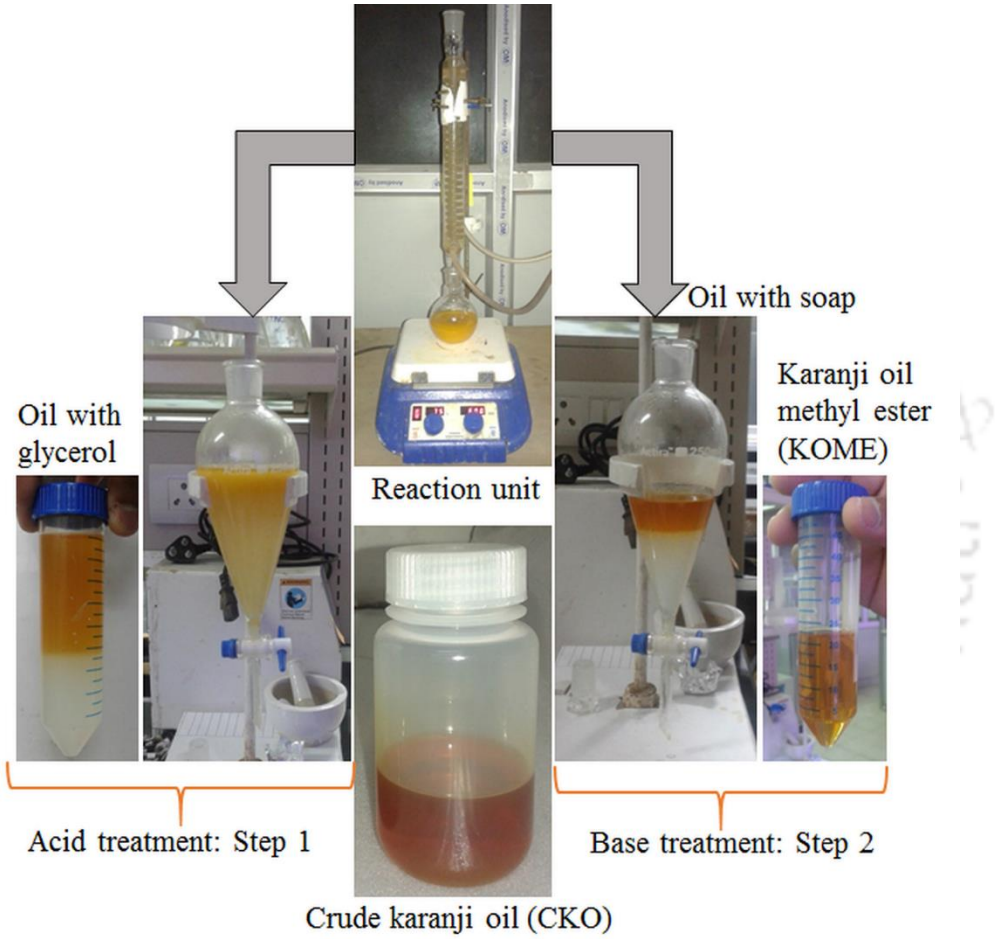

Figure 6.3: Laboratory scale two step transesterification setup.

The left part of the reaction unit is for the acid treatment and the right part is for the base treatment. After successfully completion of two step transesterification, KOME has been collected in the centrifuge tube shown in the step 2 of Figure 6.3. The collected KOME contains dissolve moisture whose ppm level is not as per ASTM D3487 [151]. Hence, to make the moisture level of the KOME as per IEEE C.57.147 guide, simultaneous shacking with water absorption technique is carried out. In this process silica molecular sieve are kept around the KOME for moisture absorption for 12 hours and then the solution is kept in the shacking

incubator at 60°C and 150 RPM.

The conversion of CKO to KOME are studied with characterization of KOME. The characterization process includes, Fourier Transform Infrared Spectroscopy (FTIR), Proton Nuclear Magnetic Resonance (^{1}H-NMR) Spectroscopy and Gas Chromatography and Mass Spectrometry (GCMS).

6.3 Chemical characterization

6.3.1 FTIR analysis

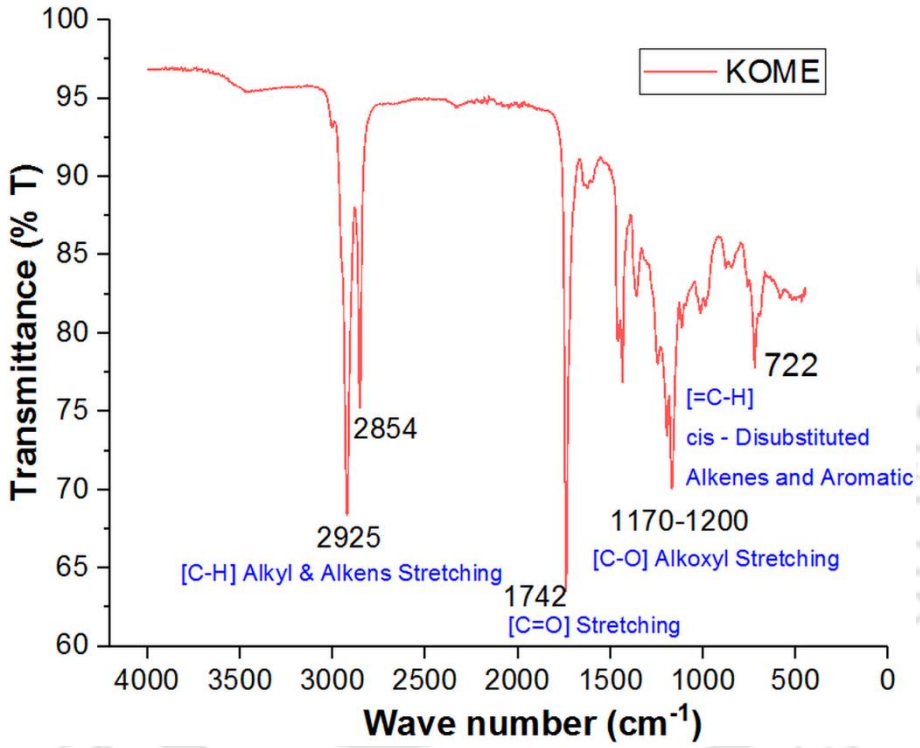

Figure 6.4: FTIR spectrum of KOME.

Formation of KOME is confirmed through the Fourier Transform Infrared Spectroscopy (FTIR) by analyzing the probable functional groups and the bands corresponding to various stretching and bending vibrations in the KOME samples using a Perkin-Elmer Spectrum Analyzer (Nicolet iS10, Thermo Scientific, USA: with solid and liquid sampling assembly) that was equipped with the detector and set in the range of 4000–400cm^{-1} as shown in Figure 6.4. In this Figure 4, x- axis represents the wave number (cm^{-1}) and the transmittance (%T) has been mentioned with a scan of 4 at a resolution of 4cm^{-1} in y-axis. The wave numbers (2850-3000) represents both KOME and CKO; its C-H alkyl stretching. At a transmittance wave number 1742 cm^{-1}, a long sharp peak is observed for KOME; represents C=O stretching

confirming the formation of ester. Again, the peak in the wave number range of 1170-1200 cm^{-1}, represents the single bond stretching of C-O confirming ester.

6.3.2 NMR analysis

NMR analysis: Proton Nuclear Magnetic Resonance (^{1}H-NMR) Spectroscopy is a powerful technique that is being used in the determination of the chemical structure of organic compounds. The quality of the VO is analyzed using the ^{1}H-NMR Spectroscopy analyzer (BRUKER, Switzerland, model: Advance 400MHz) with deuterated chloroform ($CDCl_3$) as a solvent.

The conversion of CKO (Figure 6.5(a)) to KOME (Figure 6.5(b)) are verified by methyl ester content. The observed peaks from the ^{1}H-NMR (400 MHz, $CDCl_3$) δ (ppm) for CKO: 5.34 (m, 5H), 4.310 (m, 1H), 4.169 (m, 1H), 2.71 (m, 1H), 2.335 (m, 4H), 2.040 (m, 6H), 1.610 (m, 5H), 1.256 (m, 52H), 0.883 (m, 9H) and for KOME: 5.343 (m, 1H), 3.631(s, 2H), 2.304 (m,1H), 2.002 (m, 2H), 1.637 (m, 2H), 1.258 (m, 18H), 0.896 (b, 2H). The peaks at 0 and 7.26 ppm, represents tetramethylsilane ($Si(CH_3)_4$) and deuterated chloroform ($CDCL_3$) respectively for both CKO and KOME which is a reference peak. In ^{1}H-NMR above notations s, m and b stands for singlet, multiple and broad peaks, respectively. In Figure 6.5(b), the strong singlet peak at 3.631 ppm confirms the presence of methyl ester (CH_3OCOR) group in KOME and the peaks at 2.335 ppm indicates the presence of α-carbonyl methylenes. At 1.25 ppm, the number of protons is observed to be 52 for CKO whereas, for KOME at 1.25 ppm the number of protons is reduced by 3 times i.e. 18. The reduction in proton counts implies the conversion of triglycerides content in CKO to KOME. The conversion percentage of KOME is predicted using the (6.3) [152]. The yielding of KOME is around 85.71%.

$$C_{MEster}(\%) = \frac{2A}{3B} \times 100 \tag{6.3}$$

Where A (=0.09) and B (=0.07) are an integral of methoxy methyl ester peak at 3.6 ppm and α-methylene peak at 2.3 ppm, respectively.

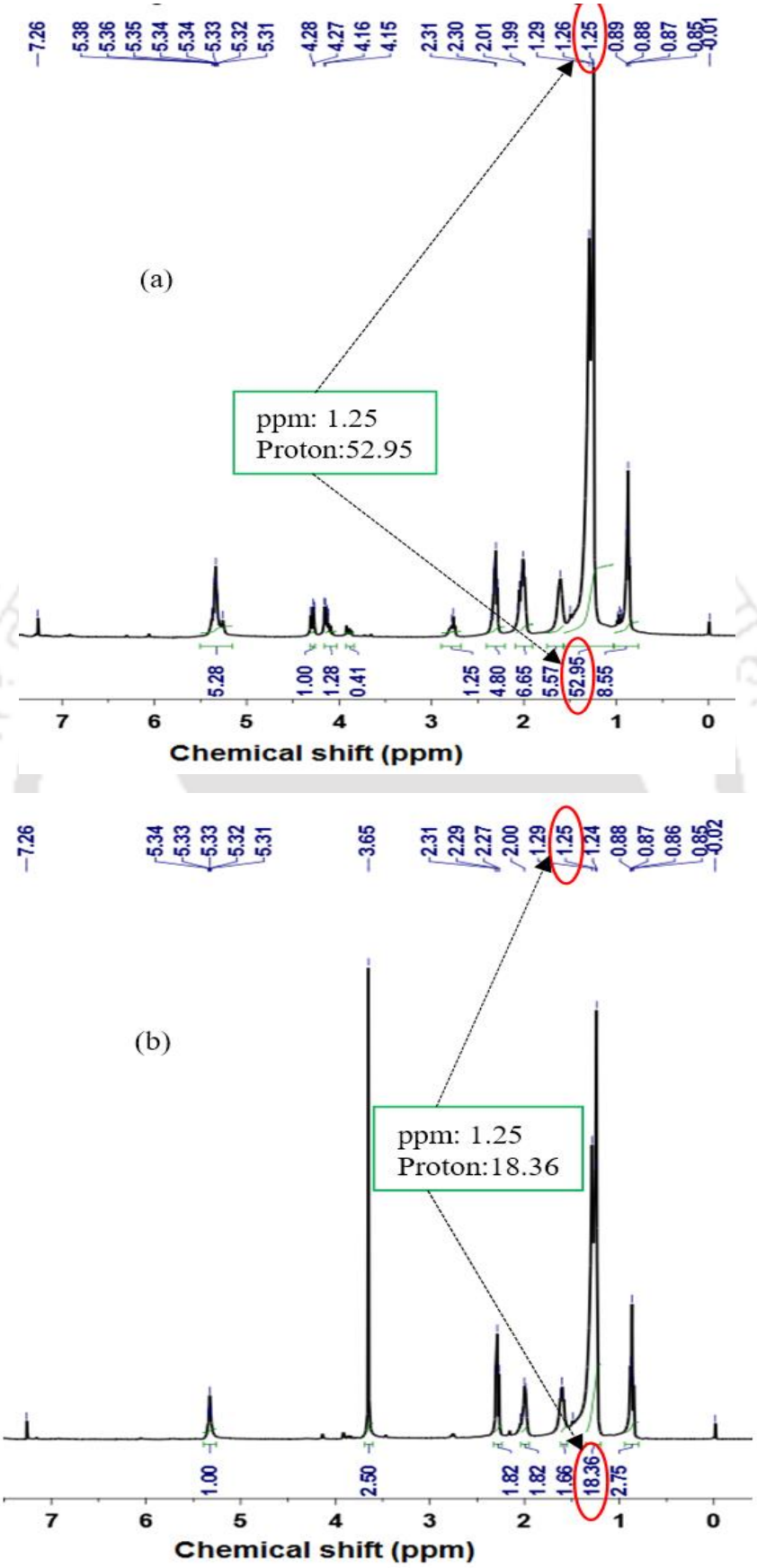

Figure 6.5: Proton NMR study of (a) CKO and (b) KOME.

6.3.3 GCMS analysis

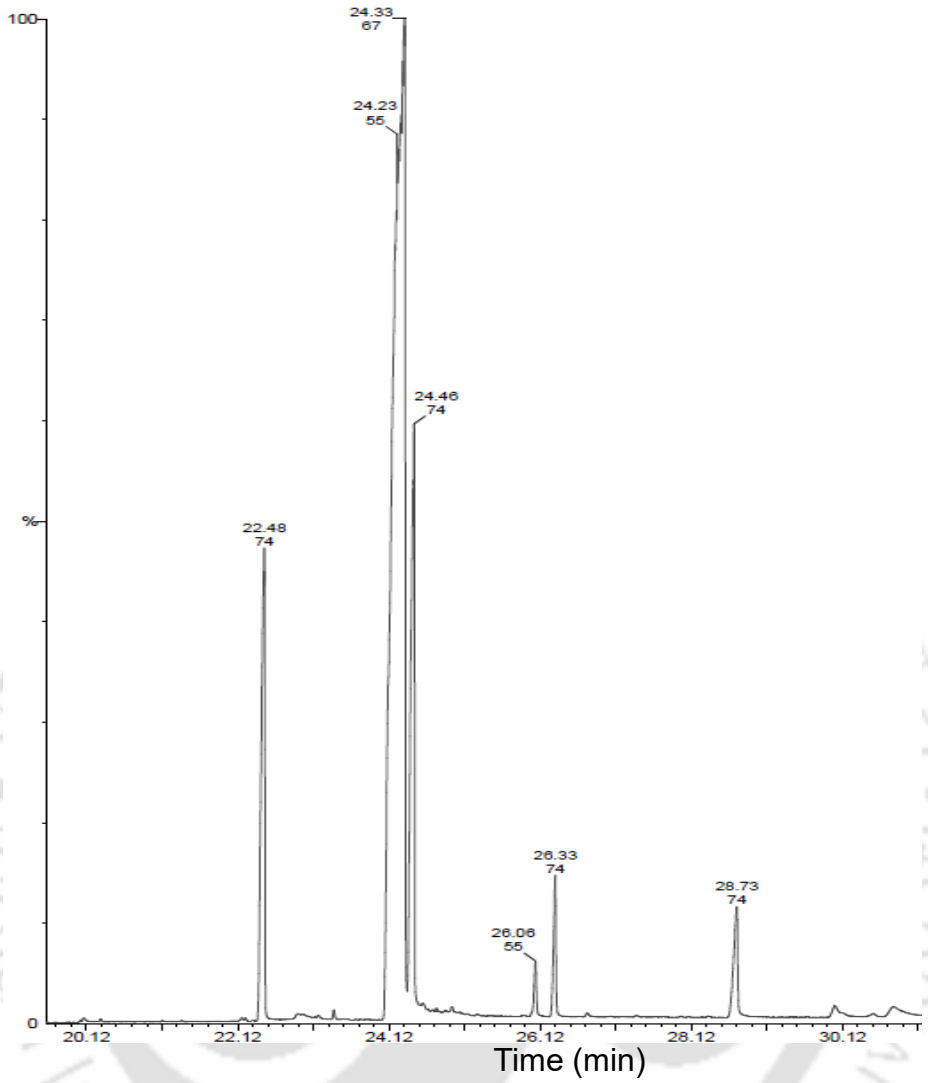

Figure 6.6: GCMS analysis of KOME.

Table 6.3: Composition of KOME

FAME	Retention time (min)	Molecular formula	Molar mass, kg/k mol
Hexadecanoic acid	22.48	$C_{17}H_{34}O_2$	270
11-Octadecenoic acid	24.33	$C_{19}H_{36}O_2$	296
Octadecenoic acid	24.46	$C_{18}H_{34}O_2$	282.47
CIS-11-Eicosanoic acid	26.06	$C_{20}H_{38}O_2$	310.51

The chemical components and presence of ester in KOME are analyzed by Gas Chromatography and Mass Spectrometry (GCMS) using Perkin Elmer, Model-Clarus 680 GC

and Clarus 600C MS (USA). Figure 6.6 shows the GCMS graph of KOME where x- and y-axis of the GCMS graph indicates the retention time in minutes and intensity in %, respectively. The major peaks of the GCMS analysis, which are methyl ester are presented in Table 6.3.

6.4. Experimental process and data analysis

The detail comparative analysis of physicochemical and electrical properties of the MO, CKO and KOME are carried out. The characteristics of the aforementioned oil are analyzed as per ASTM standard and compared with the specifications available in new natural ester oil guide IEEE C57.147 and new MO guide IEEE C57.106. However, the major physicochemical and electrical properties of the KOME are satisfying the IEEE guidelines confirming its usability in transformer as a TO presented in Table 6.4.

Table 6.4: Measured Physicochemical and electrical properties of KOME, MO and specification as per IEEE C57.147 for an insulating oil

Characteristics	ASTM	MO	CKO	KOME	IEEE C57.147	IEEE C57.106
Relative density (kg/m^3)	D1298	0.825	0.93	0.89	0.96	
Kinematic viscosity (25°C)	D445	10.5	32.0	12.00	≤50	≤12
Water content (ppm)	D1533	18	1086	364	-	≤50
Color	D1500	L0.5	L1.5	L0.5	Max. L1.0	Max. L0.5
Iodine number (wt%)	D5554	-	7.5	≤1	-	-
Flash point (°C)	D92	152	≥290	284	≥270	≥140
Pour point (°C)	D97	4	≥-25	-5	≤-10	≤-6
Acid number (mg KOH/g)	D664	-	1.3	≤0.9	-	0.03
IFT (N/m)	D971	0.041	0.02	0.03	-	0.04
Dielectric constant	D924	2.1	2.08	2.02	-	2.2
(DDF) at 90°C	D924	94×10^{-5}	8×10^{-4}	25×10^{-5}	2×10^{-3}	2×10^{-3}

6.4.1 Thermal conductivity

The measured thermal conductivity for both the MO and KOME at room and elevated temperature are presented in Figure 6.7.

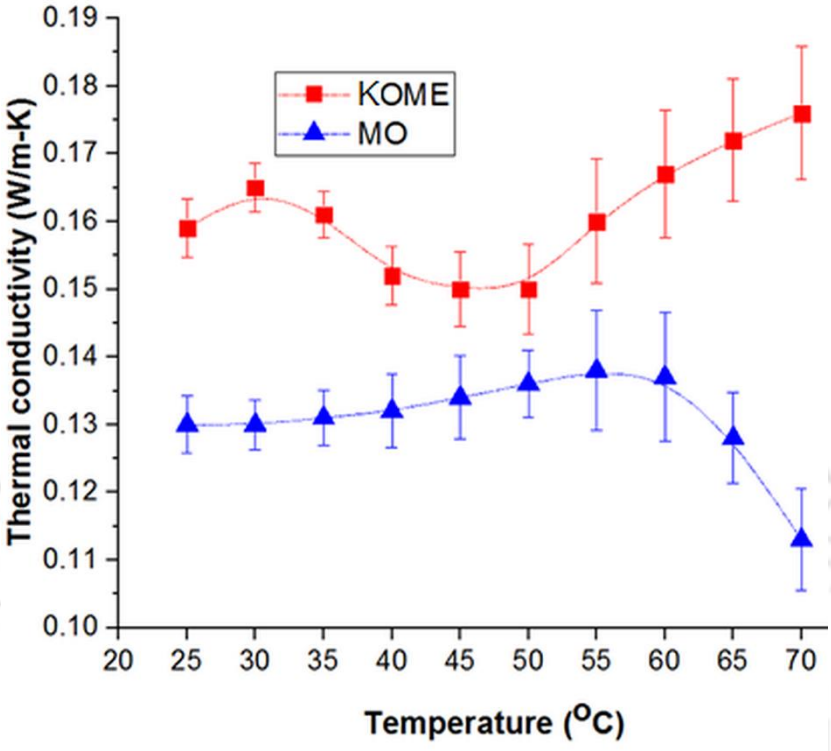

Figure 6.7: Thermal conductivity of MO and KOME at varying temperature.

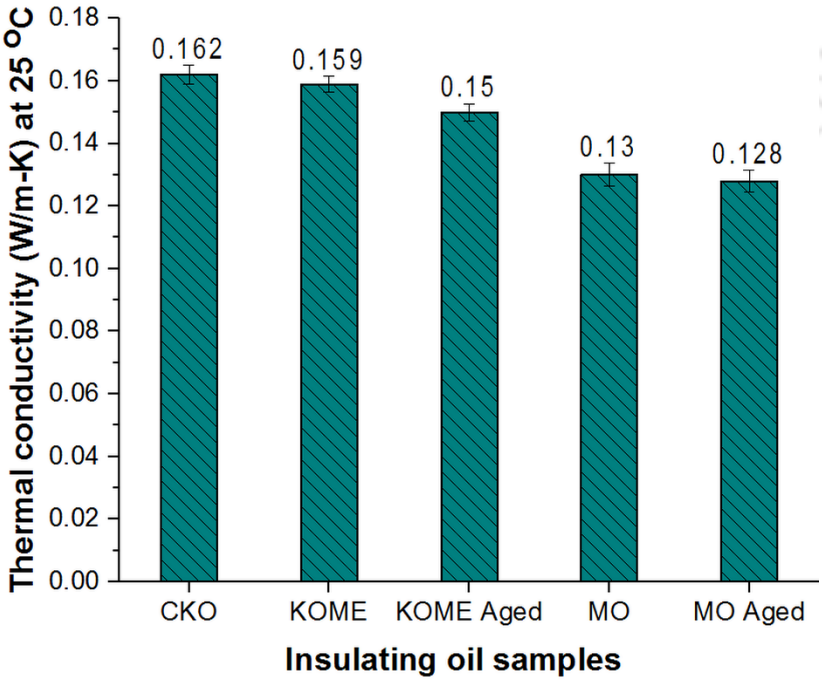

Figure 6.8: Thermal conductivity of the oil sample at room temperature.

It is observed from the Figure 6.7 that there is a significant enhancement of thermal conductivity for KOME compared to MO which is about to 23% at room temperature (25^{o}C). Since the temperature goes on increasing, the thermal conductivity of the MO is hardly increased because of the randomness of the hydrocarbon molecules. However, the thermal conductivity of the KOME is not stable with the rise in temperature. Because of the methyl ester which has higher heat transfer capability makes this oil as a potential heat transfer fluid. Between the temperature range of 30-40^{o}C, an abrupt change in thermal conductivity nature has been observed because of the molecular randomness of the methyl ester. Even though the thermal conductivity of the KOME fluctuates between the temperature range of 30-40^{o}C, the value of thermal conductivity is always higher compared to MO. It is also observed that beyond 55^{o}C, with the rise in temperature upto 70^{o}C, the thermal conductivity of MO is decreasing whereas, it is increasing in case of KOME. The molecular randomness and the alternation in the chemical chain of KOME at high temperature, allows thermal stress to be distributed uniformly and absorbs heat at faster rate. Thus, thermal conductivity of KOME rises at an elevated temperature. As the cycloalkane chain of the MO breaks at an elevated temperature; the heat transfer is interrupted due to weak heat transport properties of the broken MO molecules. Therefore, the value of thermal conductivity of MO starts to descend from 55 to 70 ^{o}C. Since the methyl ester is responsible for the high heat transfer in the KOME, it is a suitable heat transfer fluid for power and distribution transformer.

Figure 6.8 shows the comparative analysis of fresh and aged insulating liquid and its crude at room temperature. KOME is derived from the CKO, which has higher thermal conductivity because of the triglyceride molecular structure. This triple bond of the CKO is responsible of transmitting the heat efficiently. The modification of triglyceride of CKO to mono-glycerides of KOME degrades its heat transfer capabilities by 2%. The effect of oxidative aging for both MO and KOME are analyzed to ascertain the thermal degradation of the insulating oil. There is a 6% reduction in the thermal conductivity of the KOME aged compared to pure KOME. In the same way, decay of thermal conductivity of aged MO to MO is about 1.5%. But the comparative degradation of aged MO to aged KOME is 17% which is significant. Though the oxidative ageing degradation of the KOME is higher compared to MO, but beyond 50^{o}C, stable thermal conductivity is achieved for KOME.

6.4.2 Thermogravimetric analysis

The quantitative degradation of the insulating oil with respect to temperature has been analyzed using thermogravimetric analyzer (TGA) Netzsch, Model: STA449F3A00 shown in Figure 6.9 a.

(a)

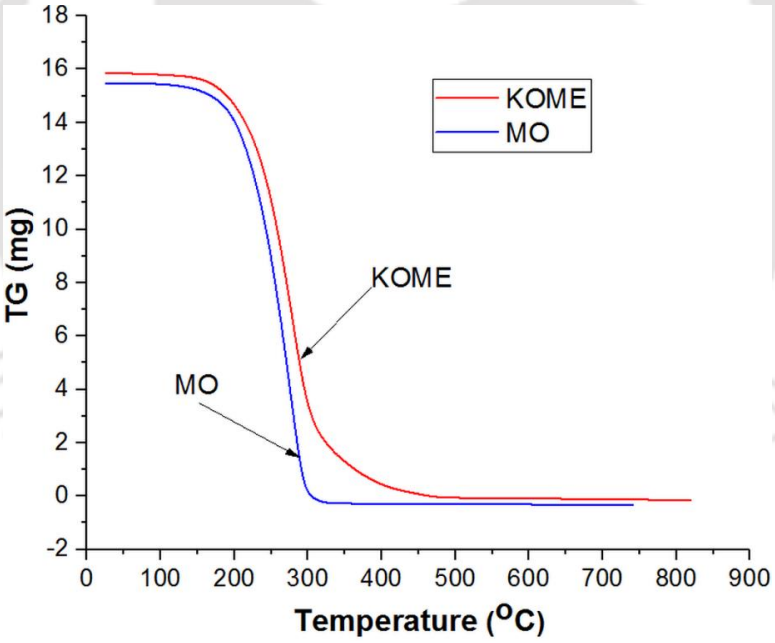

(b)

Figure 6.9: TGA (a) thermogravimetric analyzer (b) TGA analysis of MO and KOME.`

The liquid samples are heated upto 900°C in an inert environment to observe its quantitative degradation with temperature as shown in Figure 6.9 b. TGA analysis for KOME and MO are carried out and the results are compared. In both the samples at around 150°C moisture evaporates. The hydrocarbon chain of MO breaks with the rise in temperature and there is a liner degradation of the MO with the increase in temperature. At 300°C, 100% degradation is observed

for MO. However, the degradation of KOME is nonlinear. Initially dissolve moisture evaporates and then gradually the methyl ester degrades and even at 350°C the degradation is around 80%. Since VO contains long chain fatty acid which has minimum affinity towards heat, 100% degradation of KOME is observed at 400°C which is superior than MO confirming its fire resistance capability.

6.4.3 ACBDV analysis

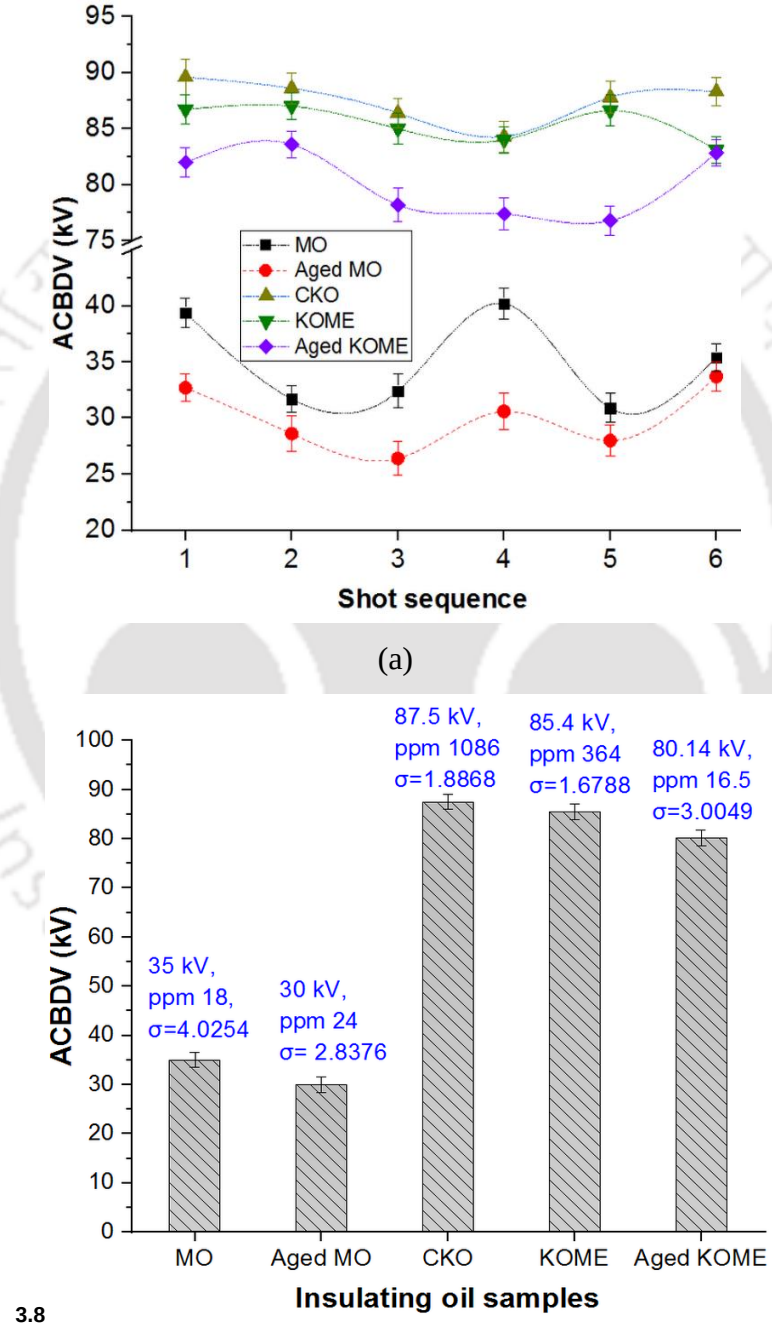

Figure 6.10: Study of ACBDV of insulating oils (a) measured for five insulating oil at 6 different shots (b) mean and standard deviation of the measured ACBDV.

The dielectric strength of the insulating oil is the measure of ACBDV. Moisture in the insulating oil plays an important role in maintaining its dielectric integrity. The ACBDV studied are also further carried out for the oxidative aged insulating oil samples of MO and KOME and a comparative analysis is carried out. The BDV of CKO, KOME, aged KOME, MO, aged MO are measured by six different shots and the results are reported in Figure 6.10 (a). The mean and standard deviation (σ) of measured ACBDV of the oil samples are evaluated at an indicated moisture level in ppm as shown in Figure 6.10 (b). Minimum moisture content is observed for the fresh MO yet, the value of BDV is lowest. The moisture content in the CKO is maximum because of the triglyceride and glycerol has huge affinity for arresting moisture in it. Upon formation of CKO to KOME, there is a decrease in the moisture level upto 70% because of the single chain ester has less position to accommodate water molecules. There is an enhancement of 150 and 135% in BDV for CKO and KOME from MO respectively. Methyl esters have high dielectric integrity which makes KOME as a suitable insulant for transformer. Comparing the BDV of aged sample of KOME and MO, it is observed that the ppm level of aged KOME are lesser than MO. Polar contamination of the aged MO increased which has strong affinity to capture moisture that affect its dielectric integrity. Whereas, ageing of the KOME resulting release of moisture and at the same time dielectric integrity affected. ACBDV of aged KOME is 165 and 129 % higher than that of aged MO and MO respectively. The ageing has less impact on the dielectric and insulating performance of KOME compared to MO.

6.4.4 Weibull Analysis

Out of the aforementioned insulating oil, ACBDV of CKO is observed to be superior. However, the crude oil is not suitable for the transformer application. But the breakdown probability of the KOME and aged KOME will provide a clear insight in terms of dielectric failure. Hence, Weibull probability analysis of ACBDV with 2-parameter model has been carried out for CKO, KOME, aged KOME and MO.

This reliability technique is used to model the strength of materials, times to failure of components of an electrical or a mechanical system [90]. Two parameter Weibull distribution of cumulative density function is given as follows:

$$F(t:\alpha,\beta)=1-\exp(-(t/\alpha))^{\beta}, \quad t>0 \tag{6.4}$$

Where t is the time (s) to breakdown, α is the scale parameter, and β is the shape parameter.

A set of 10 ACBDV test are carried continuously with a time gap of two minutes between the two consecutive measurements. Therefore, total 40 ACBDV measurement data are collected from four sets of same oil for the statistical analysis of the ACBDV using Weibull

distribution. The frequency of the measured ACBDV of the four insulating oil are shown in Figure 6.11. It is seen from the figure that the maximum observed BDV of CKO is in the range of 84-88kV and measured ACBDV for the KOME and aged KOME are in the range of 80-83 kV. Whereas, the ACBDV of MO is in the range of 32-35 kV.

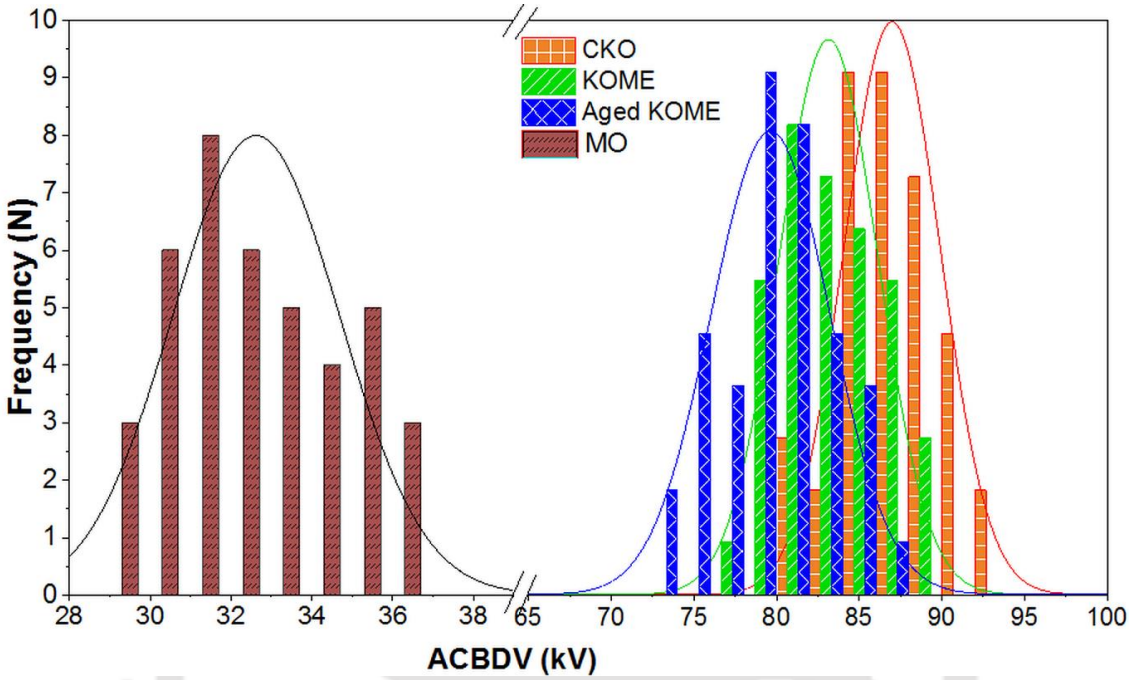

Figure 6.11: Frequency distribution of ACBDV.

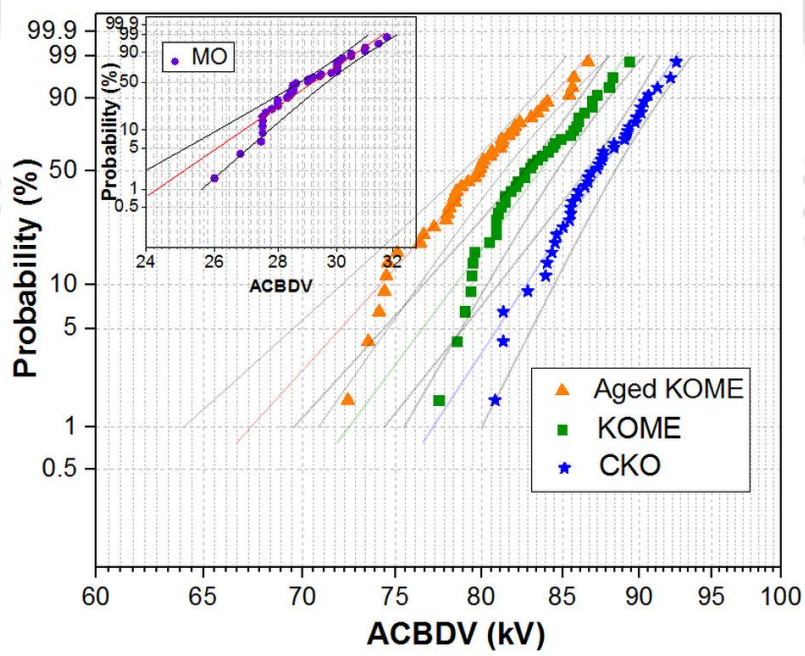

Figure 6.12: Weibull analysis of ACBDV.

Weibull distribution of ACBDV of CKO, KOME, aged KOME and MO are plotted in Figure 6.12 at a 95% confidence interval. The moisture level is measured for each sample as mentioned in the Figure 6.10. Middle line shows for the fitting results; the boundary lines

indicate the 95% confidence intervals. The breakdown voltage (kV) and cumulative probability *F(t)* are plotted along x- and y-axis respectively. Breakdown voltages analysis are carried out at the probabilities of 5, 10, 50 and 63.2%, for 2-parameter models as shown in Table 6.5. It is observed that the failure probability of KOME before and after the oxidative ageing is always lower compared to MO.

Table 6.5: Withstand voltages for each dielectric liquids

	ppm	Breakdown probability (%)			
		63.20%	50%	10%	5%
CKO	1084	88.2	87	83.3	81.3
KOME	586	84.3	82.8	79.4	78.8
Aged KOME	16.5	81	79.9	74.5	73.7
MO	18	33.2	32.17	30	26.7

6.5 Summary of the chapter

The KOME is extracted from CKO by the two step transesterification process which makes its usability in the transformer as an insulating dielectric liquid. The physicochemical, thermal and electrical properties of the KOME such as acidity, IFT, thermal conductivity, flash point, pour point, viscosity, ACBDV, dielectric constant and dissipation factor are analyzed. The thermal and electrical properties of KOME is observed to be superior then MO even after oxidative aging. The pour point and IFT of the KOME are not as per the specification provided in IEEE C57.106 guide. However, the above two parameters can be enhanced using additives. Considering the aforementioned superior properties of the proposed VO based liquid dielectric, it will be a suitable replacement for existing MO based TO in the future power and distribution transformer.

The concept of making non-edible crude VO to the KOME based TO fit for transformer application required systematic investigation of its physiochemical and electrical performance. Moreover, to observe the degradation performance of the developed KOME in the transformer for a long run, oxidative ageing study is essential. Therefore, an oxidative ageing study is performed for KOME in the next chapter.

Note: This work, "Karanji oil as a potential dielectrics liquid for transformer" has been published in IEEE Transaction of Dielectric and Electrical Insulation.

7

Ageing study of non-edible VO, NF and MO

Contents

7.1 Introduction

Transformer is the most populated, stressed and important power apparatus in the electrical power system network. The overall insulation of the transformer is maintained by a suitable arrangement of solid and liquid insulation mechanism. The liquid insulation in terms of TO is responsible for the major percentage of the overall insulation in the transformer. The primary purpose of the TO is to maintain the electrical insulation to the different energized portions and enhance the effective heat dissipation through conduction. The vital and most important aspect of the TO is to act as a protective coating layer on the winding for the prevention of oxidation on the metal surfaces [153].

TO, apart from providing the electrical insulation and thermal cooling, it also regulates the insulating health of the transformer. Periodically examining the physicochemical, thermal and dielectric insulation performance ascertains the health of the transformer [19, 82, 92]. Any fault which develops inside the transformer dissipates energy through the TO and hence the chemical degradation occurs in the liquid insulating. The oil in the transformer is tested periodically to recognize the severity of degradation and possibility of harmful contamination in it. Therefore, it is required to observe the ageing degradation behaviour of the new TO before using the same in the actual transformer.

Form the last ten decades, MO is the front runner being an insulant and coolant in power and distribution transformers [148]. However, due to limited availability of the petroleum crude and inferior physicochemical, electrical performance of the MO motivates the scientist to come up with a superior TO for an efficient power transmission and distribution network. A few research has been carried out for the improvement of the thermal performance of the MO by the dispersion of suitable nanoparticles [34, 52, 53]. However, a very few nanofillers has the potential to improve the thermal and insulation capability of the base fluid upon addition of the nanofillers [46, 47]. However, low fire resistant, biodegradability and injurious dumping effect of MO and MO-based NF is not suitable for the environment in the long run.

Therefore, an environment-friendly, fire resistant, biodegradable oil has been heavily researched. It is observed that VO based liquid dielectric is an alternative and suitable TO [154]. Studied has been found out that the oil extracted from the edible food crops such as soybean, palm kernel, rapeseed, canola, sunflower, peanut, coconut, palm, rice bran etc. are suitable for transformer application [155]. But the edible VO based TO will affect the food economy. So in this study, a suitable non-edible VO based transformer oil has been proposed.

The studied non-edible VO is of high oleic natural ester which has a high degree of monounsaturated fatty acid content. The concept of making non-edible crude VO to the non-edible ester oil (NEO) based TO fit for transformer application required systematic investigation of its physiochemical and electrical performance. Moreover, to observe the degradation performance of the developed NEO in the transformer for a long run, ageing study is essential [94, 125, 126].

Hence, the study presents an investigation of thermal, physiochemical and electrical properties of the aged oil. A comparative ageing study of the NEO with MO and NF has been carried out. Thermal conductivity, physicochemical properties such as colour, viscosity, moisture, interfacial tension (IFT), flash point, fire point, pour point, acidity, and electrical properties such as ACBDV, DC, DDF and resistivity are experimentally investigated as per IEEE C57.106-2006 [148]. Since the breakdown phenomena of the insulating oil is a critical parameter to ascertain the dielectric integrity of the aged oils, the probability of ACBDV failure are analyzed using Weibull statistical analysis. Probability of ACBDV failure of the fresh and aged TOs are analyzed for the three insulating oil at failure percentage of 1, 5, 10, 50, 63.5% and then compared. Furthermore, fluorescence based analysis has been carried out to monitor the oil degradation due to ageing. Thermal, physicochemical, and electrical characteristic of fresh and aged sample of MO, NF and NEO are studied for the suitable implementation of non-edible ester based TO.

7.2 Oxidative ageing degradation

The Figure 7.1 shows the ageing stresses involved in the transformer and the possible ageing degradation in the insulating oil. An open beaker oxidative ageing facility described in the chapter 3, section 3.3 is used to study the comparative ageing degradation of NEO, MO and NF. The preparation of Eh-BN/MO-NF is described in the chapter 2, section 2.2 and 2.3. The used VO otherwise known as NEO in this oxidative ageing study is extracted and characterizes in the chapter 6, and the MO is procured from the Apar industries, limited, India.

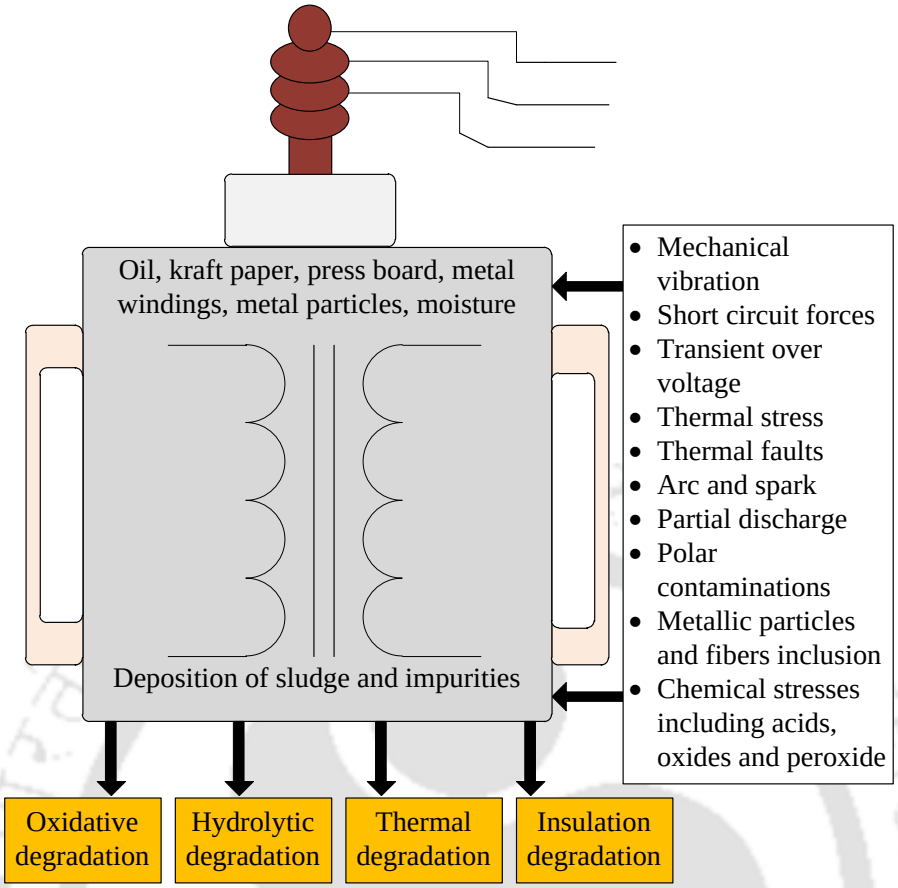

Figure 7.1: Factors affecting the ageing and types of ageing degradation in the TO.

7.2.1 Oxidative ageing reaction of NEO

The oxidative ageing study is an important technique used to test new TO for the measurement of thermal, electrical and chemical degradation before implementing into the transformer. Three different insulating oil namely MO, NF and NEO are selected for the ageing study. The oil samples of MO and NF follow the filtration and vacuum drying process before pouring into the aging container. However, NEO undergoes the process of refined, bleached, deodorized, filtration and vacuum drying (RBDFVD) before pouring to ageing. An open beaker oxidative ageing study has been performed for the insulating oil samples as per the ASTM D1934 [113]. The ageing of the insulating oil is performed in the presence of equivalent amount of metal catalyst (1 mm copper wire of electrolytic grade 99.9% purity level) in the samples. The time period and oxidative ageing is strictly maintained for 164 hours for the three insulating oil samples. To study the degradation in the insulating oil after ageing, the physicochemical and electrical properties of the aged oils are verified and compared with the fresh oil.

It is always believed that the high value of oxidation stability is a necessary criterion for an improved service life of the TO. However, the oxidation stability of the TO can be enhanced by the addition of suitable anti-oxidants such as butylated hydroxy toluene (BTH), butylated hydroxy anisole, gallic acid (GA), 2-6 ditertiary-butyl phenol (DBP) and ditertiary-butyl para-cresol (DBPC) thereby enhancing the service life of the TO and transformer [156].

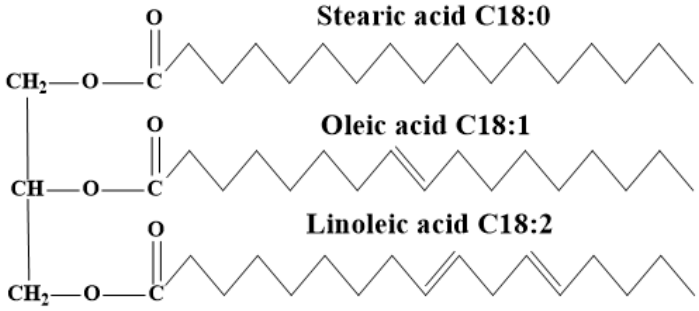

Figure 7.2: Triglyceride structure of NEO.

The thermal and electrical performances of NEO is higher compared to MO. Moreover, superior environmental, health and fire resistance characteristic of NEO is explored for oxidative ageing before using into the transformer. NEO extracted from nonedible crude karanji oil. The crude karanji oil is basically consisting of high percent of triglyceride the chemical structure is shown in Figure 7.2. Presence of saturated compound and high value of free fatty acid in the crude oil makes it incompatible for TO application. Hence, two step transesterification process has been followed to convert triglyceride of crude oil to fatty acid methyl ester of NEO as shown in equation (6.1) and 6.2.

Oxidation is the major degradation phenomena for NEO, which is a radical chain reaction comprises of three important stages namely initiation, propagation and termination. The crude VO oxidizes even at room temperature because of major percentage of polyunsaturated fatty acids. However, mono-unsaturated fatty acid content in NEO oxidizes at high temperature. Therefore, degree of unsaturation plays a crucial role in the oxidation stability of the NEO [19, 156].

The dispersion of antioxidant in NEO slows down the oxidative ageing process. Antioxidants act as a free radical as shown in equation (7.1) acts as a scavenger by hindering the formation of acid and peroxides. The chain reaction of antioxidant with the radical of alkyl (*R*·), alkoxy (*RO*·) and peroxy (*ROO*·) fatty acid leads to the formation of fatty acid *RH, ROH, ROOH* and radical of antioxidant (*A*·), which is stable in itself. The details reaction

process is given in equation (7.2 to 7.3).

$$RH \rightarrow R^{\bullet} + H \quad \textit{(Free radical initiation)} \tag{7.1}$$

$$R^{\bullet} + AH \rightarrow RH + A^{\bullet} \tag{7.2}$$

$$RO^{\bullet} + AH \rightarrow ROH + A^{\bullet} \tag{7.3}$$

$$ROO^{\bullet} + AH \rightarrow ROOH + A^{\bullet} \tag{7.4}$$

Further reaction propagation of antioxidant radical with alkyl, alkoxy and peroxy radicals give rise to a stable and non-radical products such as *RA, ROA and ROOA* as mentioned in (7.5) to (7.7) by neutralizing the free radical of the fatty acids. Furthermore, neutralization of free radical of fatty acids occurs by the oxidization of antioxidants is mentioned in (7.8).

$$R^{\bullet} + A^{\bullet} \rightarrow RA \tag{7.5}$$

$$RO^{\bullet} + A^{\bullet} \rightarrow ROA \tag{7.6}$$

$$ROO^{\bullet} + A^{\bullet} \rightarrow ROOA \tag{7.7}$$

$$Antioxidant + O_2 \rightarrow Oxidized\ Antioxidant \tag{7.8}$$

7.3 Degradation analyses of ageing

Physiochemical properties of the TO include the study of thermal conductivity, kinematic viscosity, density, colour, interfacial tension (IFT), acid number, moisture content, flash and pour point analysis. Form the study of physiochemical properties, the direct influence of ageing on the heat transfer, polar contaminations, acid and sludge formations in the insulating oil are studied. However, physiochemical properties have indirect influence in the electrical properties of the TO. Hence, a comparative study of physiochemical properties is carried out as per the standard mentioned in the Table 7.1.

During the oxidative ageing, insulating oils are exposed to the thermal and chemical stresses mutually, which in turn hamper the physicochemical, optical and electrical properties of the oil. The changes in physical appearance of the insulating oil is due to the byproducts such as acids, oxides, peroxides and suspended carbonaceous nanoparticles. A brief study has been performed to investigate any deviations and loss of fluorescence intensity and red shifting of the emission band which could be further related to degradation of the oil.

7.3.1 Colour

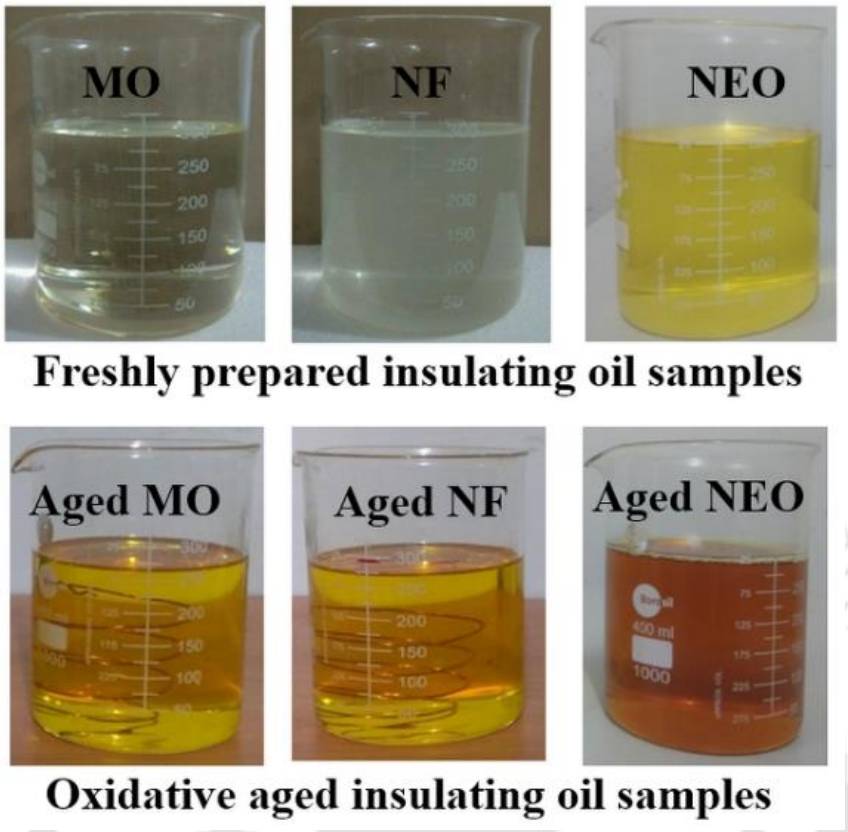

Figure 7.3: Change of color due to ageing.

The physical appearance of the oil is the indication of the possible contamination and degradation of the oil. Hence, the colour scale is measured for the fresh and aged sample of the insulating oil shown in Figure 7.3. It is observed that the colour of the oil sample changes appreciably with degradation. The changes in the colour after ageing is light yellowish for aged MO and aged NF and dark yellow is observed for aged NEO. As the NEO has maximum exposure to oxidation without an antioxidant, an antioxidant is required for the NEO to prevent early chemical degradation due to oxidative ageing. The colour scale measurement is presented in Table 7.1

7.3.2 Moisture content

With ageing, moisture absorption in the MO and NF increases because of the affinity towards polar contamination of the oil. Moreover, with ageing, moisture contamination in the aged NEO significantly reduces from fresh NEO. The presence of solid cellulosic insulation such as kraft paper and press board in the oil during ageing absorbs moisture from the NEO and hence decrement of the moisture in the aged NEO occurs.

Table 7.1: Physicochemical, thermal and electrical properties of fresh and aged insulating oil.

Properties	Insulating oil samples						ASTM Standards
	MO	Aged MO	NF	Aged NF	NEO	Aged NEO	
Moisture (ppm)	25	28	18	22	324	170	D1533
Density (Kg/m^3)	0.825	0.83	0.830	0.84	0.88	0.90	D1298
Kinematic viscosity (cSt)	11.2	11.5	11.5	11.2	14	16	D445
Colour scale	$0 \leq 0.5$	0.5-1.0	$0 \leq 0.5$	0.5-1.0	0.5	1	D1500
Acidity (mg KOH/g)	0.00	0.030	0.00	0.023	0.2	0.32	D664
IFT (dyne/cm)	38.8	34.0	42.2	39.1	31.2	28.4	D971
Flash point (°C)	146	142	170	165	286	270	D92
Fire point (°C)	165	150	182	175	330	310	D92
Pour point (°C)	-6	-5	-10	-8	-12 (Nil PPD) -35 (With PPD)	-10 (Nil PPD) -30 (With PPD)	D97

7.3.3 Density

Densities of the MO and aged MO are lowest compared to fresh and aged sample of NF and NEO. The highest density is observed for the fresh and aged NEO due to unsaturated fatty acid and high oleic composition.

7.3.4 Viscosity

From the Table 7.1, it is observed that the viscosity of the insulating oils rises with ageing which is in the support to the ageing degradation of the oil. Rise in viscosity of the oil slows down its flowability in the various parts of the transformer and hence experiences the ineffective heat transfers in the TO. In this study, the highest viscosity is obtained for aged NEO however, the superior thermal performance of the NEO maintains the uniform cooling in the transformer. The viscosity of the NEO obtained experimentally is 14 cSt which is within the range repeated in IEEE C57.106-2006 standard.

7.3.5 Acidity

Generation of acids in the TO is due to the oxidation phenomena in the aged oil. The acid level accelerates in the presence of polar contaminations, solid dirt and saturated acids. Freshly prepared MO and NF are less acidic compared to NEO, because NEO has higher saturated fatty acid content. With the course of ageing, due to high affinity of polar contamination in the MO and NF, it gets affected and acid value increases. However, high acidic value is observed for aged NEO but the level of acidity and ageing rate can be normalized with the dispersion of suitable antioxidants.

7.3.6 Interfacial tension

The oil quality is ascertained by the IFT value. Rise in value of IFT indicates lesser polar contaminants in the oil and hence validates the better performance of the oil. It is observed from the Table 7.1 that with the rise in ageing duration, IFT value decreases. Since the ageing studies of the three sample of the insulating oils are performed in the presence of oxygen, it may lead to the formation of sludge and impurities in the oil. It is observed from the table that IFT and acid number are inversely proportional to each other i.e. lower the IFT, higher the acid number. The reason of formation of sludge/impurities in the MO is due to the amalgamation of oil, moisture and copper catalyst in the presence of heat.

7.3.7 Flash, fire, and pour point

Higher value of flash and fire point in the TO avoids the accidental ignition and fire breakdown. It is observed from Table 7.1 that with ageing flash point of aged MO, NF and NEO are degraded from the corresponding fresh samples by 2.73, 2.94 and 5.59% respectively. Similarly, the observed fire point degradations are 9.09, 3.89 and 6.06% respectively for oxidative aged samples of MO, NF and NEO. Moreover, the observed flash and fire point for fresh NF are 16.43 and 10.36% higher than fresh MO. And the increment for flash and fire point of fresh NEO compared to fresh MO is observed to be 95.8 and 100% respectively.

The pour point should be minimum in order to use the TO at very low environmental temperature. Since the pour point performance of the NEO seems to be weak, the pour point depressant (PPD) is used so that the oil is suitable for the low temperature environmental application.

7.3.8 Thermal conductivity

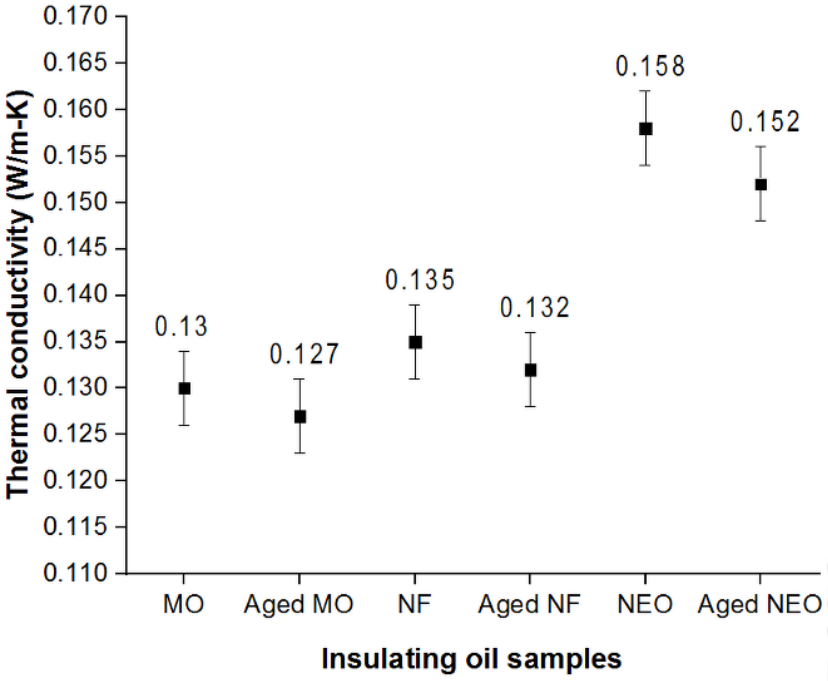

Figure 7.4: Thermal conductivity of fresh and aged oil samples.

It is observed from the Figure 7.4 that the fresh NEO has highest thermal conductivity compared to fresh and aged sample of NF and MO. With the course of ageing, formation of carbonaceous particles and sludge in the oil which act as an inhibitor for the heat transfer in the liquid. Hence, the thermal conductivity value of the aged oil is lower than that of the fresh oil. However, the thermal conductivity of the aged NEO is 19.68 and 16.92% higher than that of aged and fresh MO respectively. Similarly, the thermal conductivity of the NF and aged NF has 12.59 and 15.15% lower value compared to aged NEO. Though there is a degradation in the thermal conductivity for of age NEO from NEO around 4%, yet it has superior thermal performance compared to fresh and aged oil of MO and NF. Therefore, NEO is a required heat transfer and cooling liquid for the transformer even in the ageing environment.

7.3.9 Fluorescence analysis of aged oil

Fluorescence spectra of the insulating oil sample are analyzed at an excitation of 350 nm using HORIBA fluoroMax-4 spectrofluorometer. The observed fluorescence of the fresh and aged insulating oil is reported in the Figure 7.5. It is observed that the fluorescence maxima of the fresh and aged sample of MO and NF are in the range of 379 and 398nm with a hump. Whereas, in the case of NEO, the fluorescence maxima are observed to be 441nm. With the

ageing of 164 hours, gradual decreases in the fluorescence intensity and a progressive red shift in emission maxima of the NEO oil sample from 441 to 470 nm.

(a)

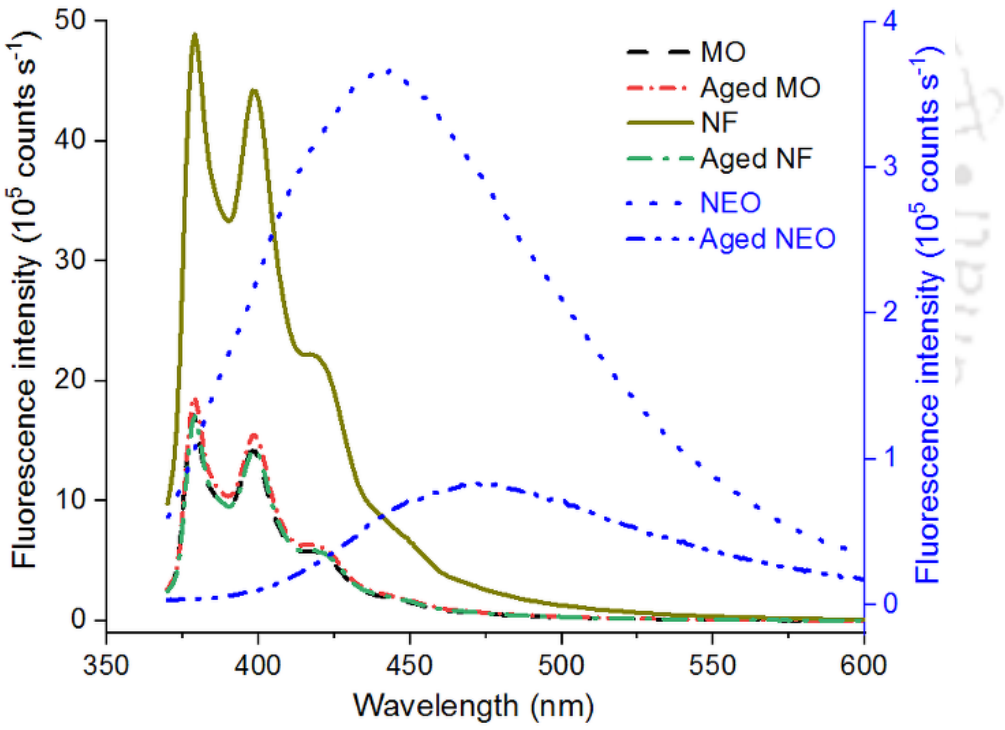

(b)

Figure 7.5: Fluorescence spectra (a) HORIBA fluoroMax-4 spectrofluorometer (b) fluorescence spectra analysis of the fresh and aged insulating oils.

7.3.10 DC, DDF and resistivity

To verify any probable influence of ageing on the dielectric constant of the insulating oil, oil permittivity is measured and the results are depicted in the Table 7.2. It is clearly seen

from the table that the dielectric constant of the three insulating oil goes on decreasing with the ageing. Out of the three oils, MO has the lowest dielectric constant compared to the NF and NEO. The decline values of dielectric constant for the MO and NF because of its ageing is not at all preferred for transformer application, as it disturbs the electric field distribution. In the course of ageing, NEO has negligible decrement and superior stability in the dielectric constant compared to aged MO and NF.

Table 7.2: Electrical properties of the insulating oil.

Oil Sample	DC	DDF	Resistivity (Ω-cm)×10^{14}
MO	2.1	0.0082	1.81
Aged MO	2.05	0.009	1.62
NF	2.2	0.0005	2.4
Aged NF	2.08	0.002	2.2
NEO	2.5	0.00025	2.8
Aged NEO	2.4	0.0012	2.6

The measure of the degradation in dielectric losses in the three insulating oil has been reported. The effect of ageing on DDF of MO, NF and NEO are evaluated at an ageing duration of 164 hours. It is observed from the Table 7.2 that with ageing, DDF increases indicating the decay in dielectric properties. It is observed that MO has higher DDF than that of NF and NEO at ageing, which shows the weak dielectric strength of MO. The DDF of a freshly prepared sample of MO is greater than that of the NFs, which informs that the NF is a better dielectric fluid to minimize the discharge and enhance the resistivity. It is also observed from the Table that even after oxidative ageing, the DDF of NEO is less affected compared to MO and NF. Since the resistivity and DDF are mutually related to each other, the rise in DDF decreases the resistivity of the oil. However, out of three insulating oil even after ageing, NEO has minimum dielectric losses and higher resistivity making it better insulating liquid for the transformer application.

7.3.11 ACBDV study

The enhancement in ACBDV of the NF compared to MO is because of the more number of electrons are scavenged by the nanoparticles which created a time lag and breakdown process slowdowns. This electron scavenging technique which is briefly explained by the multi-layer Tanaka's model and Peppas et. al. [157, 67]. In case of NEO the ACBDV is

significantly higher which is 183.33% and more than the MO and NF respectively as seen in Table 7.3.

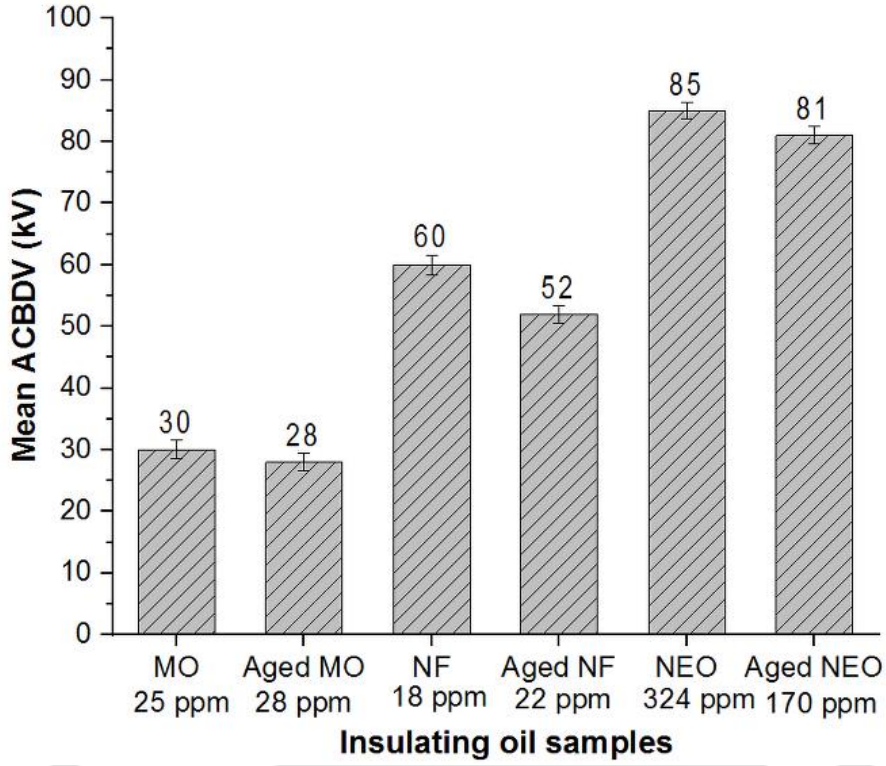

Figure 7.6: Mean ACBDV of fresh and aged oil sample.

Table 7.3: Comparative ACBDV percentage analysis.

Oil Samples	ACBDV (kV)	% decrement of ACBDV with ageing	% enhancement in ACBDV compared to MO
MO	30	0	0
Aged MO	28	6.67	--
NF	60	0	100
Aged NF	52	13.33	--
NEO	85	0	183.33
Aged NEO	81	4.7	--

The electric strength of the NEO is superior than MO and NF even at higher ppm level. It is observed that the NEO can store 18 times more water in it than the MO base TO. During ageing, the carbonaceous nanoparticles are generated in the oil which further take part in the formation of polar contaminations and sludge. The presence of sludge and impurity in the aged oil degrades its dielectric properties and hence the ACBDV. However, even after ageing

the breakdown strength of the NEO nearly unaffected compared to the MO and NF which shows the rigid dielectric integrity of the NEO. Since NEO has highest mean ACBDV among the three insulating oil, evaluation of its percentage of probability of the ACBDV failure is required to verify the consistency in the electrical breakdown strength.

7.3.12 ACBDV distribution

Primary motivation of these experiments are to determine the range of breakdown test voltages of the fixed sample of tests. The breakdown level of the insulating oil is an important aspect when TO is taken into consideration for dielectric insulation purpose. So, a closer look at the ACBDV range will provide a better idea to ascertain the lowest level at which the oil will exhibit breakdown properties. A total number of 40 ACBDV measurements are performed per batch of sample and the occurrence distribution of 40 instants are presented in Figure 7.7.

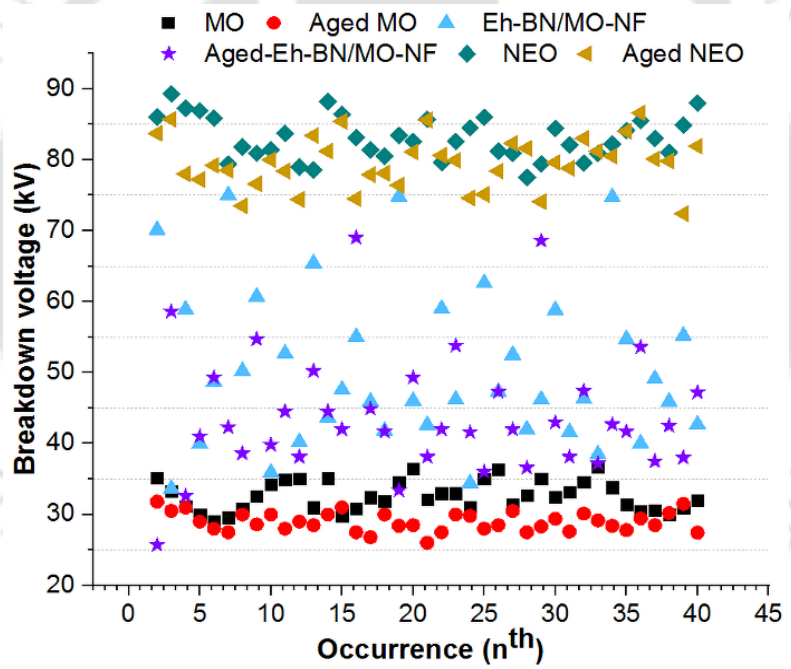

Figure 7.7: The distribution of ACBDV data for fresh and aged sample of MO, NF and NEO.

The frequency of ACBDV distribution results are presented in Figure 7.8. It is observed from the figure that the frequency of maximum breakdown occurs in the range of 30-35 kV for MO, 28-31 kV for aged MO, 40-60 kV for NF and 40-50 kV for aged NF, 78-87 kV for NEO and 73-85 kV for aged NEO for the ppm mentioned in the Figure 7.6.

7.3.13 Statistical analysis

There are many statistical methods to analyses the given set of data, out of which Weibull distribution is a preferred method for the ACBDV analysis in liquid dielectric. There are

many statistical methods to analyze the given set of data, out of which Weibull distribution is a preferred method for the ACBDV analysis in liquid dielectric. In this study, the distribution of ACBDV data for MO, NF and NEO for different ppm moisture content are plotted in Figure 7.7. The Weibull distribution of cumulative density function expressed in (4.6) is plotted with a correlation factor of 95% and the distribution parameters are presented in Table 7.4.

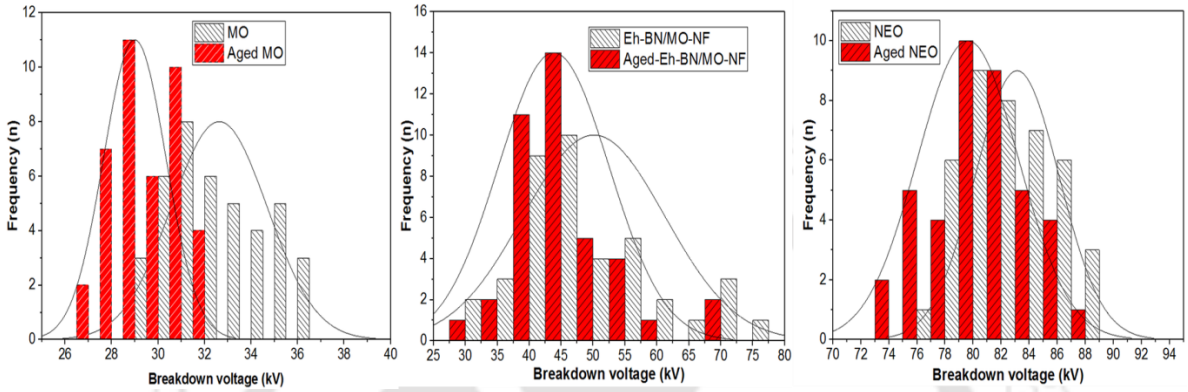

(a) (b) (c)

Figure 7.8: Frequency of distribution of fresh and aged sample of (a) MO, (b) NF and, (c) NEO.

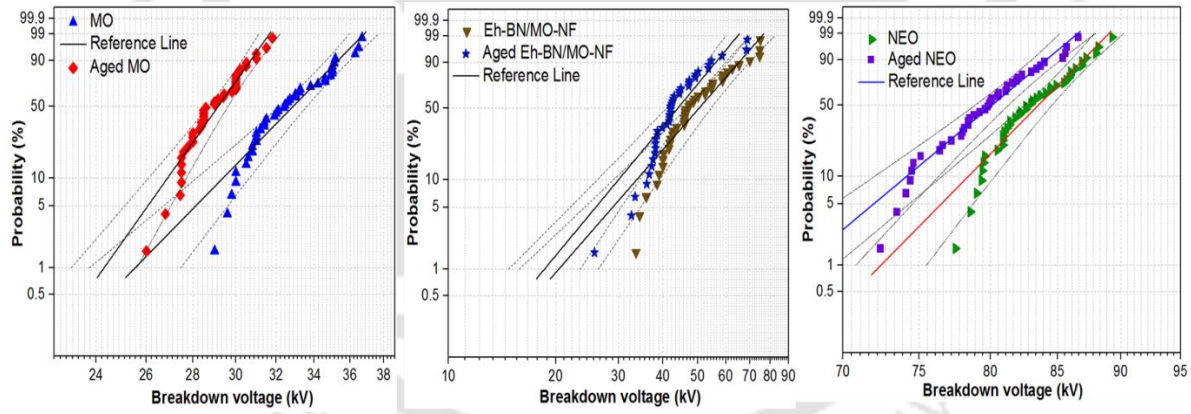

(a) (b) (c)

Figure 7.9: Weibull 2 parameter statistical analysis of fresh and aged sample of (a) MO, (b) NF and, (c) NEO.

The ACBDV and its probability of failure at different percentages are presented in Table 7.5. It is observed from the Figure 7.9 and Table 7.5 that upon comparing a sequence of probability of failure from 1 to 63.5% for fresh and aged insulating oil, the lowest probability of failure is observed for NEO. The ageing of the insulating oils affects the failure probability but the aged NEO failure probability percentage is marginally affected. Hence, the consistent in the ACBDV performance of the fresh and aged NEO supports its applicability for a dielectric fluid for power and distribution transformer.

Table 7.4: Weibull distribution parameters.

ppm	25	28	18	22	324	170
Oil	MO	Aged MO	NF	Aged NF	NEO	Aged NEO
α	33.608	29.632	54.637	47.435	84.587	81.325
β	16.751	23.1976	4.6672	4.9111	29.6774	24.3824
ρ	95%	95%	95%	95%	95%	95%

Table 7.5: Weibull failure probability percentage.

Oil	ppm	Probability				
		1 %	5 %	10 %	50 %	63.5 %
MO	25	≤28 kV	29.60 kV	30 kV	32.40 kV	33.5 kV
Aged MO	28	≤25 kV	26.75 kV	27.49 kV	28.5 kV	29.25 kV
NF	18	≤33 kV	35.11 kV	38.5 kV	47.46 kV	52 kV
Aged NF	22	≤25.5 kV	32.7 kV	36.34 kV	41.6 kV	43.5 kV
NEO	324	≤75 kV	78.4 kV	79.4 kV	82 kV	84.3 kV
Aged NEO	170	≤72 kV	74 kV	74.5 kV	79.2 kV	80.1 kV

7.4 Summary of the chapter

Application of ester-based insulating oils improves the fire safety of transformers. In addition, ester insulating oils show a protective behavior to typical cellulosic insulation material used in power transformers, increasing the life expectancy and overloading capability. In a way similar to the degradation of mineral oil, the thermo-oxidative process is mainly responsible for ageing of ester oil. In addition, ester oil can be subjected to hydrolytic degradation in the presence of moisture. However, the ageing behavior of vegetable oil-based insulating oil has not yet been studied comprehensively.

NF in dielectric application is an emerging technology by aiming at an improvement in the physicochemical and electrical characteristics. Therefore, in the next chapter, the spectroscopic analysis of the fresh and aged VO and VO-NF is performed to understand the chemical degradation of the TO.

8

Spectroscopic analyses of the aged VO and VO-NF

Contents

8.1 Introduction

Transformer and its demand of high performance is increasing day by day with the increase in population, power consumption, environment safety and reliability. MO filled transformers are the front runner from last ten decades. The source of the petroleum crude which produces MO is limited. Moreover, the nature of non-biodegradability, injurious dumping to environment and weak fire resistance properties of the MO makes the material and insulation scientist to think of an alternative insulating oil for oil filled power and distribution transformer.

Several studies have been carried out on the VO based TO having high electric strength, superior fire resistance and biodegradability compared to MO. Studies have also been reported that the thermophysical and electrical performance of the VO are improved compared to MO based TO [38, 15, 87, 91, 158-160]. Different types of nanofillers such as conductive, semi-conductive and insulating NPs are dispersed into VO to prepare the nanofluid to improve the thermophysical and dielectric properties of TO for transformer application. Dispersion of conductive NPs (Fe_2O_3, Fe_3O_4, ZnO etc.) improves the fire resistance and electric strength of the MO and VO. Dispersion of semi-conductive NP (TiO_2) shows the physicochemical stability whereas, other NP viz. SiO_2 improve the ACBDV and thermal conductivity upon dispersion to MO. Studies are also reported that with the dispersion of insulating exfoliated hexagonal boron nitride (Eh-BN) into the MO improves the dielectric and thermal properties of the NF [47, 161, 162]. Early oxidative ageing tendency of natural ester oil based VO ages faster creating hurdles in its full-fledged application [19, 163]. VO is biodegradable and extracted from renewable resources, and hence it is environment-friendly. Moreover, studies show that the VO has higher capacity to dissolve moisture [1, 164, 165] than MO, which leads to lower degradation in paper and enhancement of life of the oil-paper insulation system in a transformer. The usability and feasibility study of the NF-based TO requires to analyze the degradation behavior of VO and VO-NF. Therefore, an oxidative ageing study is performed to understand the probable effect of the polar contaminants on the ageing of liquid insulation. An open beaker oxidative ageing instrument not available commercially is developed in our research laboratory as per ASTM D1934 [113]. In this research work, VO based insulating NF is prepared and physicochemical and electrical characteristics of the oil at fresh and oxidative ageing conditions are studied.

With the rise in localized temperature beyond 200^{o}C in the transformer, temperature stresses are distributed among the solid and liquid insulations which in turn initiates the alteration in the chemical bond in cellulosic solid insulation and then formation of acidic byproducts. Therefore, oxidative ageing studied is performed to understand the

physicochemical and electrical characteristics of the TO at non-uniform thermal and chemical stress condition. Various spectroscopic tools are used to study the degradation properties of the TO, out of which UV-vis and fluorescence absorption range of wavelengths are studied for the fresh and aged oil [165, 166].

The oxidative ageing degradation is reflected in the fluorescence spectroscopy analysis at different ageing duration. The authors have used various spectroscopic tools to measure the chemical degradation of the insulating liquid such as VO and VO-NF for different ageing duration. Since the chemical degradation and the dielectric integrity of the insulating oil are interrelated, the authors have found it is important to measure the ACBDV of the VO and VO-NF at fresh and aged condition. TO experience chemical, electrical and thermal stresses during full loading condition, the spectroscopic analysis of the chemical degradation and the measurement of dielectric and electrical strength at ageing provide the handful information of effect of ageing on VO and VO-NF before using in transformer. Therefore, the relevant measurements are performed in detail to justify the VO-NF for its potential application in transformer.

8.2 Preparation of VO-NF and ageing

Table 8.1: Specifications of MO and VO as per ASTM D 6871

Characteristic	Specification of MO	Specification of VO
Density (gm/cc)	0.828	0.9
Kinematic viscosity at 27^{o}C (cSt)	13.67	16.67
Interfacial tension at 27^{o}C (mN/m)	47	21.2
Flash point (^{o}C)	146	≥275
Pour point in (^{o}C)	-18	<-10
Dielectric dissipation factor at 90 ^{o}C	0.0085	≤0.05
Water content (ppm)	25	35
AC breakdown voltage (kV)	30	82
Thermal conductivity (W/m-K)	0.128	0.160

Experiment is carried out into two broad categories: firstly, processing and preparation of VO-NF and secondly, oxidative ageing study of VO and VO-NF. FR3 VO (Envirotemp) purchased from Cargill India Pvt. Ltd., is used as the base fluid to prepare the VO-NF. The comparative properties of MO and VO are presented in the Table 8.1 used for NF preparation. High aspect ratio and two-dimensional layer structure of Eh-BN NP treated as a suitable nanofiller. Two-step dispersion

method is followed to prepare the VO-NF as shown in Figure 8.1. Experimentally confirming the dispersion of 0.01 wt% of nanofillers into VO to be stable, 0.01 wt% of NP is dispersed in to VO to prepare the VO-NF.

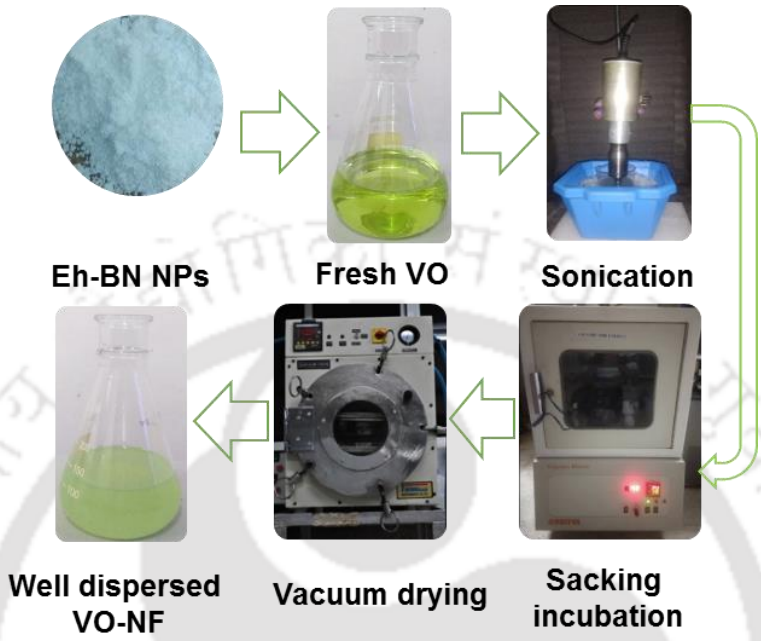

Figure 8.1: Preparation of VO-NF.

An open beaker ageing study as mentioned in the chapter 4 is followed to analyses the ageing effect on the VO and VO-NF. The operating temperature in this ageing study is mentioned at 115±1^{o}C with accelerated ageing duration of from 0 to 500 hours. A uniform ageing environment is mentioned for VO and VO-NF samples by simultaneous air blowing and continuous rotation of the oil sample base at 2±0.1 rpm in the ageing chamber. After the ageing of VO and VO-NF for the duration of 100, 300 and 500 hours, physicochemical and electrical characteristics are analyzed and compared with the fresh oil.

8.3 Results and Discussion

Since the oxidative ageing at an elevated temperature for a certain ageing period affects the physical appearance and chemical structure of the fresh insulating oil, a comparative analysis has been carried out for physicochemical and electrical characteristics for aged VO and VO-NF with fresh oil. Moreover, the investigation is also carried out to study the response of UV-vis and fluorescence spectra of the VO-NF and its response to ageing.

8.3.1 Stability of VO-NF

To verify the dispersion stability of h-BN and Eh-BN NP in the base fluid, Zeta potential analysis is carried for NFs. The observe stability by measuring Zeta potential analysis of NFs are presented in Figure 8.2. It is observed that the consistency in stability is maintained for Eh-BN dispersed NF compared to pure h-BN NF upto 500 hours. Pure h-BN NPs are large spherical agglomerates having strong Van der Waals force of attraction among the particles resulting early sedimentation and instability (Chapter 2). Whereas, weak Van der Waals force of attraction, strong electrical double layer repulsion [157] and high aspect ratio of surface modified two-dimensional Eh-BN NPs has minimum tendency for settlement. Therefore, 0.01 wt% Eh-BN NP is chosen as a suitable nanofillers to prepare a VO-NF for oxidative ageing upto 500 hours and the study of its physicochemical and electrical properties.

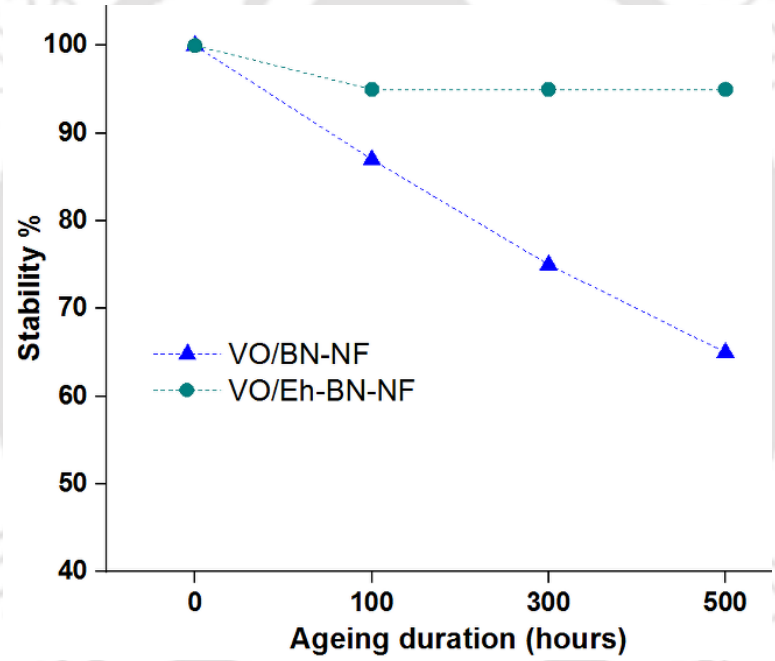

Figure 8.2: Stability of study of VO-NF by zeta potential analysis.

8.3.2 Colour characteristics

The change in the colour of the oil sample provides a firsthand information regarding the severity of degradation. The physical appearance of the aged oil sample compared to fresh oil at certain ageing time is studied. The changes in colour of the VO and VO-NF with ageing is observed in the Figure 8.3 and Figure 8.4. The measurement of the colour scale is performed as per ASTM- D 1500 [128]. It is observed from the measurement that with ageing, colour of the VO and VO-NF changes. Severity in degradation of both the sample is observed on or after

300 h of ageing. Accelerated oxidative ageing environment and temperature leads to alter the physicochemical properties of the oil which is reflected in the changes of colour.

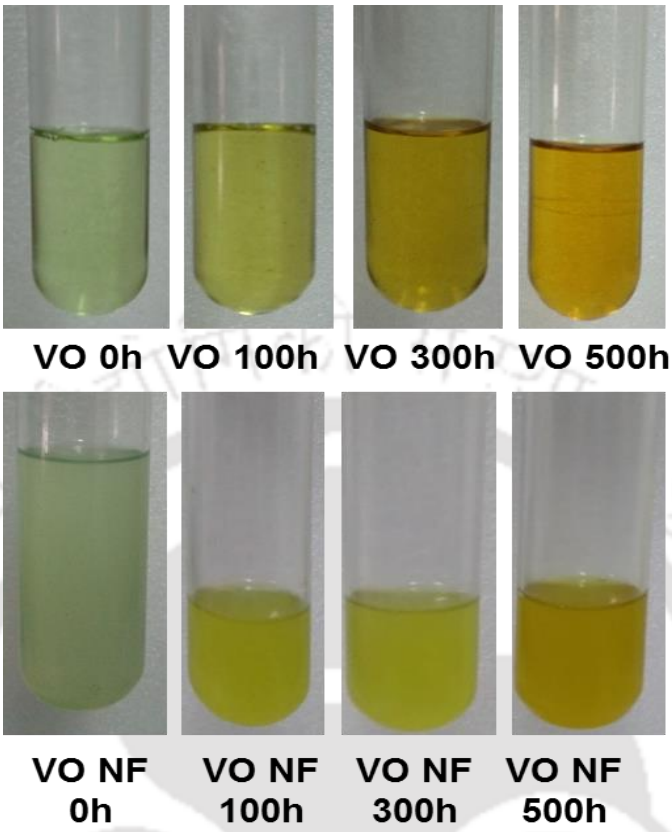

Figure 8.3: Change of colour with ageing degradation from fresh oil.

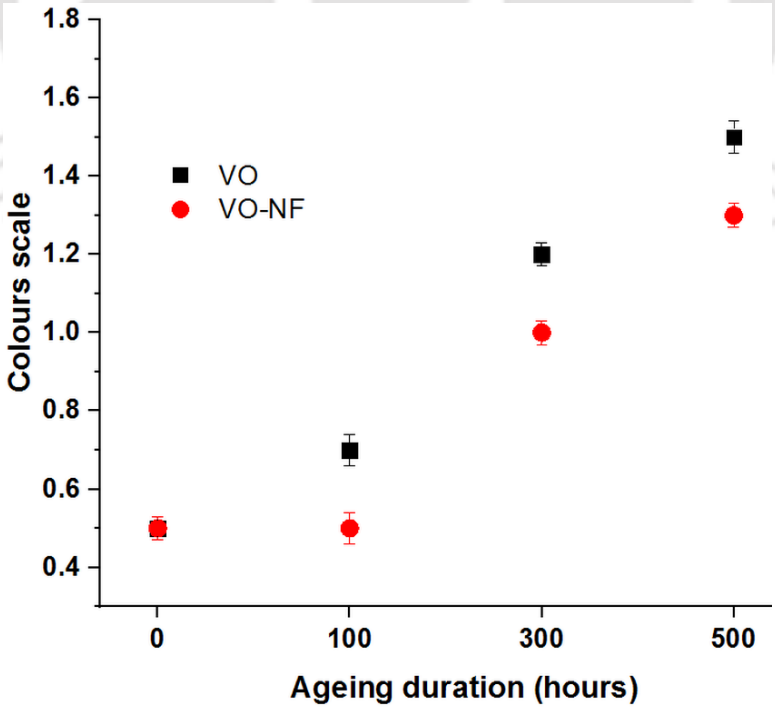

Figure 8.4: Ageing degradation measurement using colour scale.

8.3.3 NMR analysis

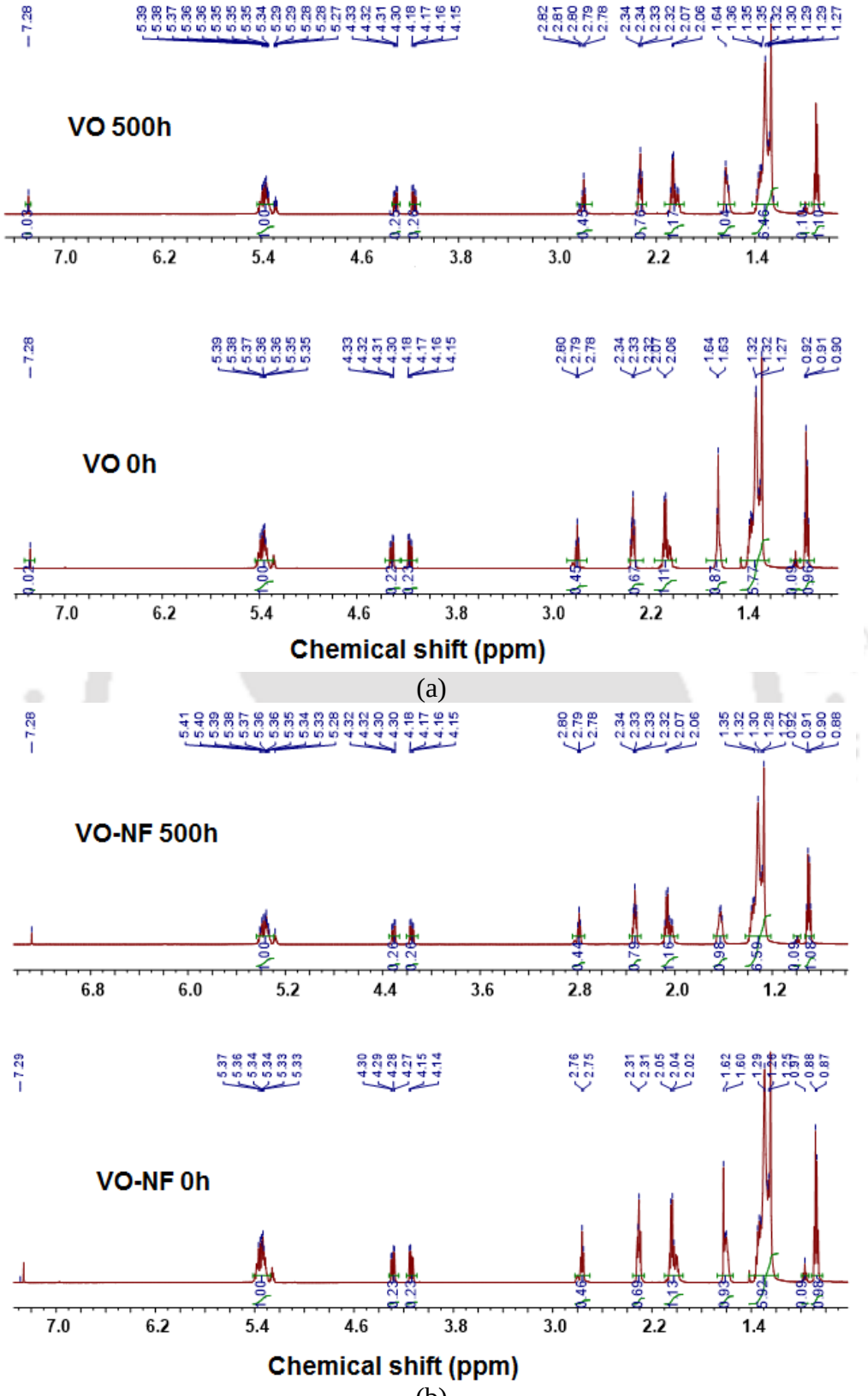

Figure 8.5: ^{1}H-NMR study of fresh and aged (a) VO, (b) VO-NF.

The effect of ageing on the chemical composition of VO and VO-NF, and its alteration is studied using the proton nuclear magnetic resonance (^{1}H-NMR) spectroscopy using BRUKER,

Switzerland, model: Advance 600 MHz. In this technique, the purity of the oil samples at fresh and oxidative ageing condition is determined. The 1H-NMR spectroscopic analysis (600 MHz) carried out using deuterated chloroform (CDCl3) as a solvent for VO and VO-NF at 0 and 500h of oxidative ageing independently are shown in Figure 7. From the observed peaks, the proton counts for respective ppm for the VO at 0 hour are δ (ppm): 5.34 (m, 1H), 4.310 (m, 0.25H), 4.16 (m, 0.26H), 2.80 (m, 0.45H), 2.3 (m, 0.76H), 2.06 (m, 1.17H), 1.6 (s, 1H), 1.3 (m, 5.46H), 0.9 (m, 1H). In 1H-NMR study, the notations 's' and 'm' stand for singlet and multiple peaks respectively. The peaks at 0 and 7.28 ppm, represent tetramethylsilane ($Si(CH3)_4$) and chloroform solvent respectively for both VO and VO-NF which are the reference peak for all spectrum. It is observed that at 2.3 ppm, the presence of α-carbonyl methylenes is observed which is a signature peak for presence of methyl ester on VO. It is observed from both Figures 8.5a and 8.5b that with ageing, the primary chemical composition of the fresh and aged sample does not alter. Since the VO-NF is a well dispersed nanocomposite mixture of NP and base fluid, upon ageing the organic compounds in the NF remain unaffected. Therefore, the number of proton counts closely match for both VO and VO-NF at fresh and ageing condition without any deviation of the proton signals. These results also confirm the high stability of the VO and VO-NF even at harsh environmental conditions.

8.3.4 FTIR analysis

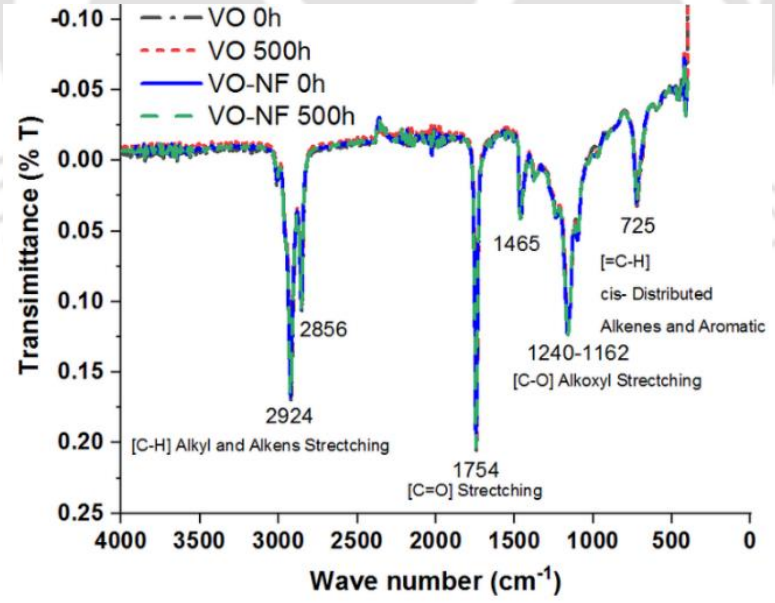

Figure 8.6: FTIR spectrum of VO and VO-NF at fresh and aged conditions.

The presence of probable functional group in the fresh and aged oil samples are verified through Fourier Transform Infrared Spectroscopy (FTIR) analysis. The functional groups and

its bands equivalent to various stretching and bending vibrations in the VO and VO-NF with ageing at 0 and 500 hours studied in the range of 4000–400 cm^{-1} and the results are shown in Figure 8.6. In the present study, with aging, the transmittance of the VO and VO-NF is nearly unaffected around the finger prints region. The signals from 2850-3000 cm^{-1} represent the C-H alkyl stretching in both VO and VO-NF. At a transmittance wave number 1754 cm^{-1}, a long sharp peak is observed for all samples which represents C=O stretching confirming the presence of ester. Again, the peak in the wave number range of 1162-1240 cm^{-1}, represents the single bond stretching of C-O confirming the chemical compound of ester is retained with ageing. With ageing, the formation of carbonaceous particle is expected to affect the VO-NF. However, the existence of functional group properties remains unaltered even after the completion of 500 hours of oxidative ageing for VO and VO-NF.

8.3.5 Analysis of UV-vis

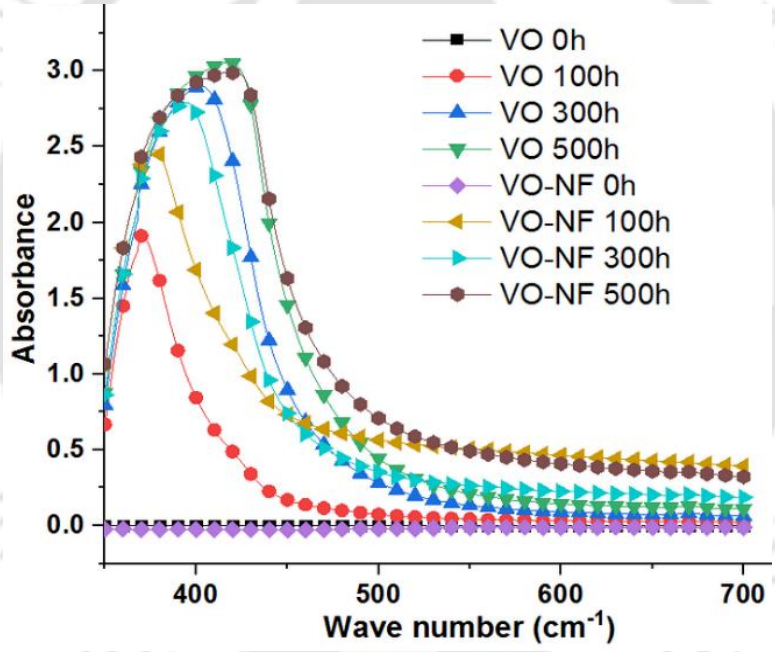

Figure 8.7: UV-vis spectrum of VO and VO-NF at various ageing conditions.

The ultra-violate visible infrared spectroscopy (UV-vis) measures the absorption spectra of VO and VO-NF obtained at different interval using PerkinElmer (Singapore) are presented in Figure 8.7. It is seen from the figure that initially; the fresh oil samples do not show any absorbance band. At 100 hours ageing, a strong absorbance appears at 375 and 385 nm for the VO and VO-NF respectively, which suffered a steady red shift in their maximum absorption with ageing. Such appearance of red shifted absorbance band is due to the increase in their density with ageing. This is alternatively correlated to the increase in the oil concentration with ageing. Besides, the grown up base line of the oil sample with ageing also confirmed their

enhanced aggregation. However, the NMR titration study assure the complete chemical stability of the oils even after 500 hours of ageing.

8.3.6 Acid number and interfacial tension with ageing

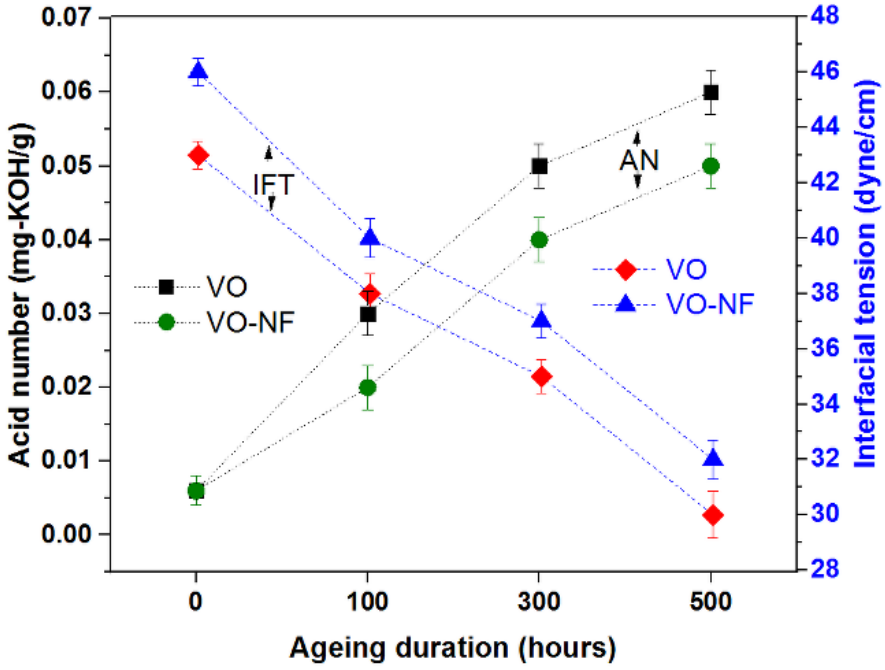

Figure 8.8: AN and IFT of VO and VO-NF at various ageing conditions.

The measurement of two important and sensitive parameters such as acid number (AN) and interfacial tension (IFT) of VO and VO-NF are performed which are used as health indicator for the TO. The AN (mg-KOH/g) and IFT (dyne/cm) of the insulating oil are interrelated to each other from the prospective of oil insulation capability. Therefore, analysis of AN and IFT for VO and VO-NF is carried out at different ageing duration which is reported in Figure 8.8. It is observed that, with progress in ageing duration, AN in VO and VO-NF rises. However, AN in NF is lesser compared to VO at all the cases of ageing. The low value of AN in NF confirms the minimum chemical degradation in the oil at certain ageing duration. As VO and NF are exposed to accelerated oxidative ageing environment, the formation of impurity and sludge in the oil dominates the properties for the rise of AN. Though the NF has gone through the similar ageing environment, but the presence of uniformly insulating NP in the base fluid dissuades the rate of ageing and hence the low AN is achieved for NF.

The presence of polar contaminants in the insulating oil is measured by IFT. Its value ascertains the presence of relative quantity of polar contamination in the oil including moisture, acid, sludge etc. IFT is measured as the interlayer molecular force of attraction between water and the insulating oil. It is observed that with the rise in ageing, AN increases and IFT value decrease. Higher the value of IFT, better the insulation capability achieved for TO. Higher

value of IFT is achieved for VO-NF compared to VO at fresh and aged condition. Highly insulating and thermally conducting Eh-BN NP, upon dispersion with VO, reduces affinity towards the polar contaminations in the VO-NF. Even though the rise in polar contaminations is observed for both VO and VO-NF with ageing, NF is less affected to oxidative ageing showing minimum affinity towards polar contamination and superior dielectric performance.

8.4 Fluorescence spectroscopy

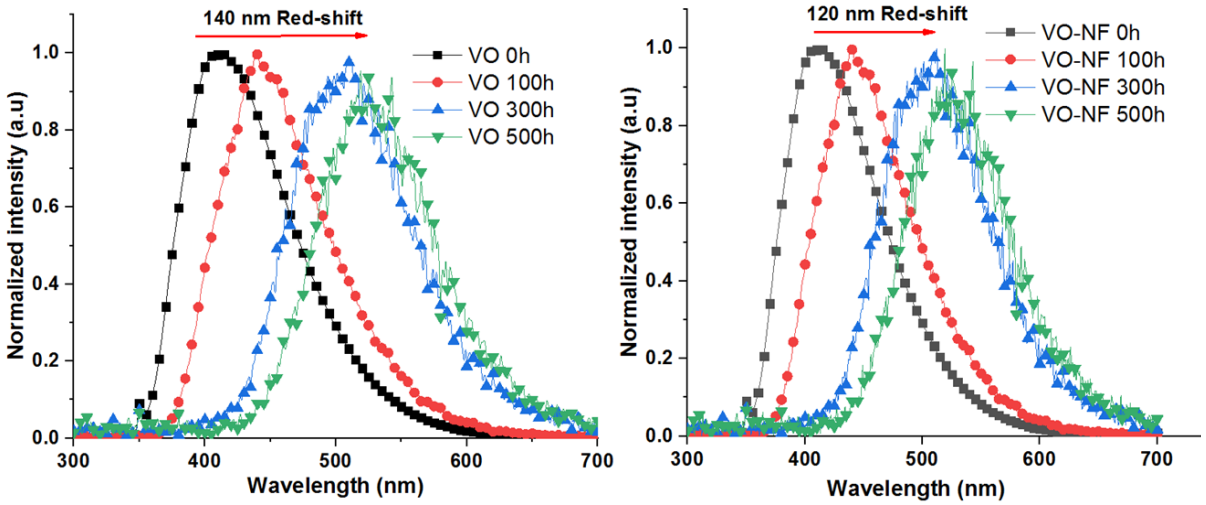

(a) (b)

Figure 8.9: Fluorescence spectra (a) VO and (b) VO-NF on 0, 100, 300 and 500 hours ageing with 350 nm excitation.

The fluorescence properties of VO and VO-NF with ageing are analyzed by exciting at 350 nm as shown in Figure 8.9 The fluorescence properties of VO and VO-NF with ageing are analyzed by exciting at 350 nm as shown in figure. It is seen from the figure that the fluorescence maxima of both VO and VO-NF centered at ~400 nm suffered a steady red shift of 140 and 120 nm in emission maxima of VO and VO-NF respectively with ageing. The red shifting of emission band is attributed to the increase in the oil concentration with ageing due to the formation of sludge and polar contamination. it was observed that the organic molecules generally undergo self-aggregation with red shift of emission band to that of their monomer unit due to the formation of distinct fluorophoric component [166, 167], and can be more prominent with ageing time at high pressure and/or temperature. However, the relatively low red-shift of the fluorescence maxima in VO-NF as compared to that of VO could be attributed to the relatively less self-aggregations in VO-NF due to the presence of surface modified insulating NP.

8.4.1 Analysis using 2D EEM spectra

The 2D excitation emission matrix (EEM) spectra of the oil samples are recorded to better understand the fluorescence properties of the multi-component oil samples with ageing. Figure 8.10 summarizes the EEM spectra of both VO and VO-NF at different ageing time.

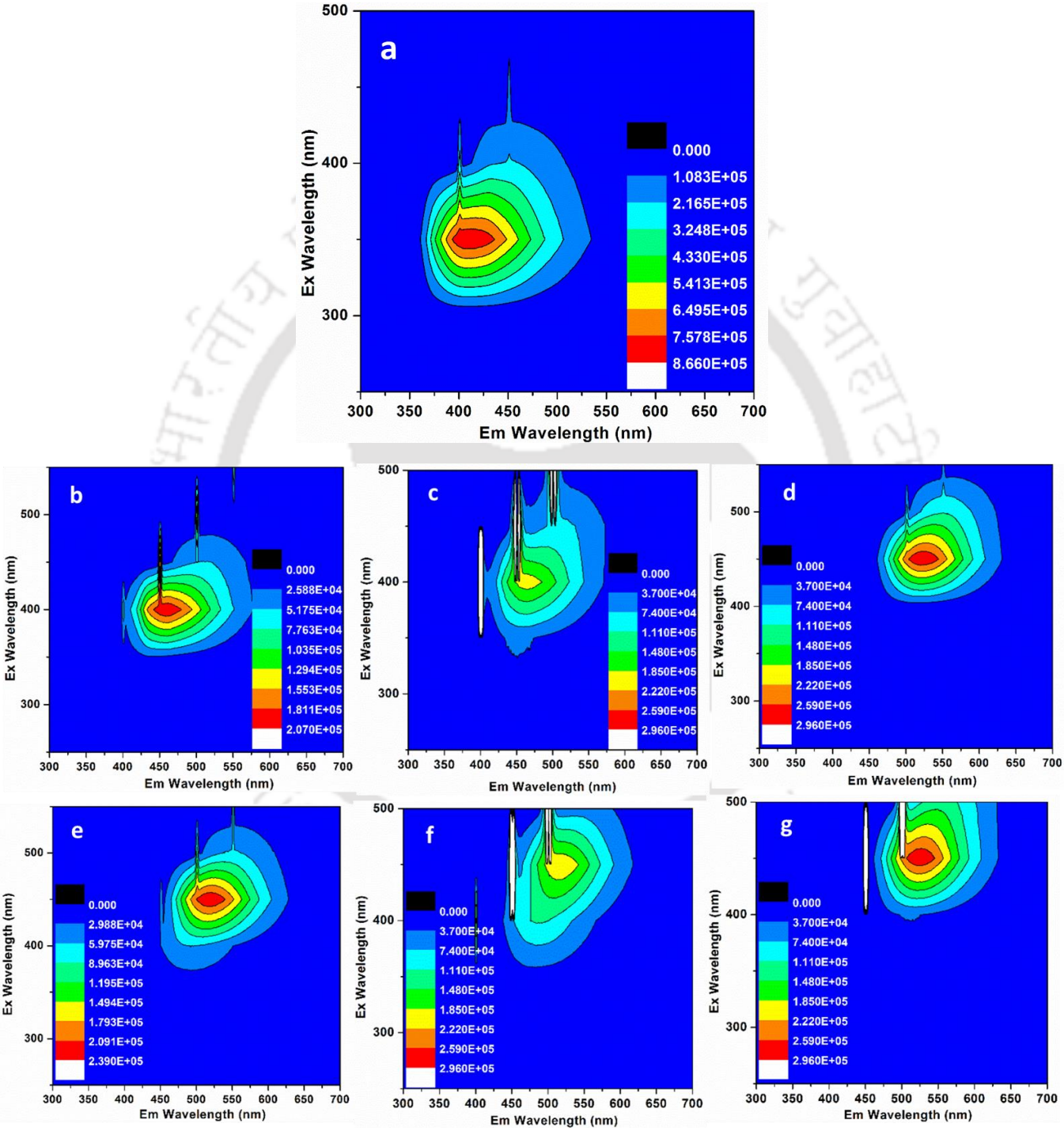

Figure 8.10: 2D EEM spectra (a) fresh VO, (b, c, d) for aged VO and (e, f, g) for aged VO-NF on 0, 100, 300 and 500 hours respectively with 350 nm excitation.

This figure shows the fluorescence emission of VO in the region from 370-580 nm with emission maximum at around 420 nm and the excitation spectra extended from 310-430 nm. As similar to Figure 8.10, with increasing ageing time, the progressive red shift of the contour profiles, are observed at higher wavelength values of both excitation (Ex) and emission (Em) as shown in Figure 8.11. Quite consistent fluorescent properties of the VO in both absence and presence of the NP suggests its inertness towards the chemical perturbation of the VO. The NMR titration study also supported the speculation where the VO is found to be chemically stable with addition of NP and with ageing as well. Besides, the oil samples become more viscous with ageing, which enhances its relative permittivity, refractive index, and thus results in high degree of scattering.

8.5 DGA study

Table 8.2: Detected gas quantities concentration in ppm

Gases	VO-NF 100 h	VO 100 h	VO-NF 300 h	VO 300 h	VO-NF 500 h	VO 500 h
Ethane	7.97	13.48	11.38	21.42	27.19	39.30
Ethylene	ND	0.68	ND	ND	6.34	1.41
Hydrogen	ND	ND	ND	ND	14.15	21.93
Oxygen	5020	9439	5540	8119	5040	5122
Nitrogen	10923	43829	11797	19404	28933	17937
Carbon Monoxide	10.55	11.05	8.19	8.97	22.24	33.71
Carbon Dioxide	287.9	525.8	327.2	369.8	522.52	741.4
Propane	1.52	1.44	1.95	1.11	2.56	3.23
Propylene	1.55	2.34	2.03	2.27	2.07	1.77

Note: ‘h’ denotes ageing duration in hours and ‘ND’ is for not detected

Due to accelerated oxidative ageing, yielding of sludge and acidity along with harmful chemical gases generation is possible in the aged oil. Therefore, dissolve gas analysis (DGA) of the aged VO and VO-NF is carried out using Gas Chromatograph (make: Agilent Technologies, model 7890B & 7697A) as per ASTM 3612 C.

The detected gasses from the aged oil at different ageing duration are reported in the Table 8.2. It is observed from the Figure 8.11 and Table 8.2 that the detected gasses are of two types: first type is from environmental inclusion (O_2, CO_2, N_2) or contamination and others (H_2, CO,

C_2H_4, C_2H_6, C_3H_6, C_3H_8) are generated due to the alteration of the chemical bond of the oil chain with ageing. The concentration of ethane (C_2H_6) with ageing gradually increases for both VO and NF, but it is a stable gas unless contaminated with hydrogen (H_2) which makes it a flammable gas as seen in Figure 8.11 a.

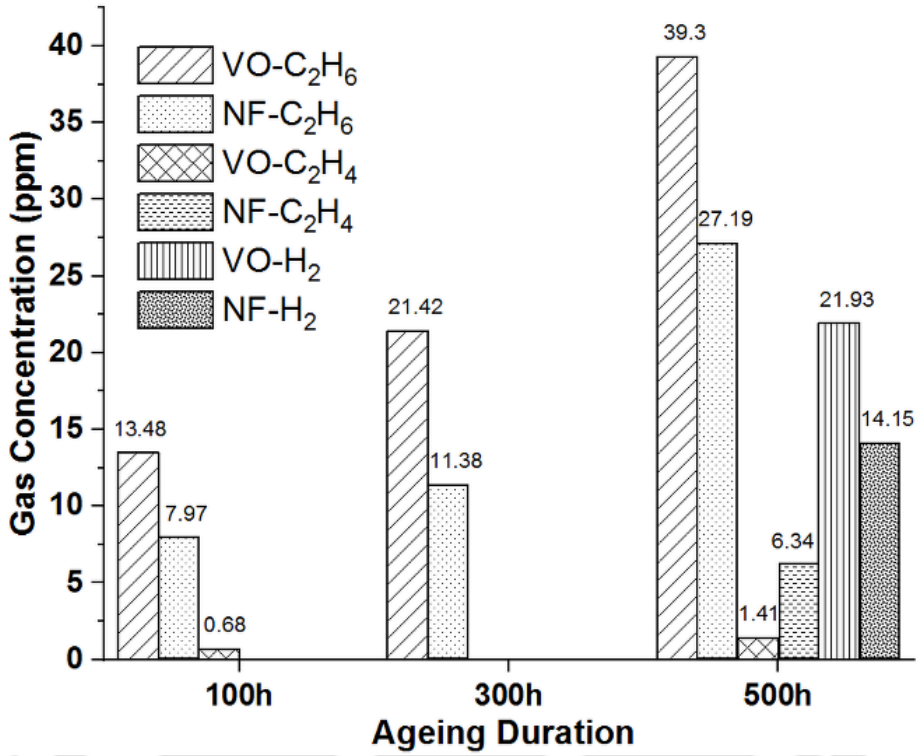

(a)

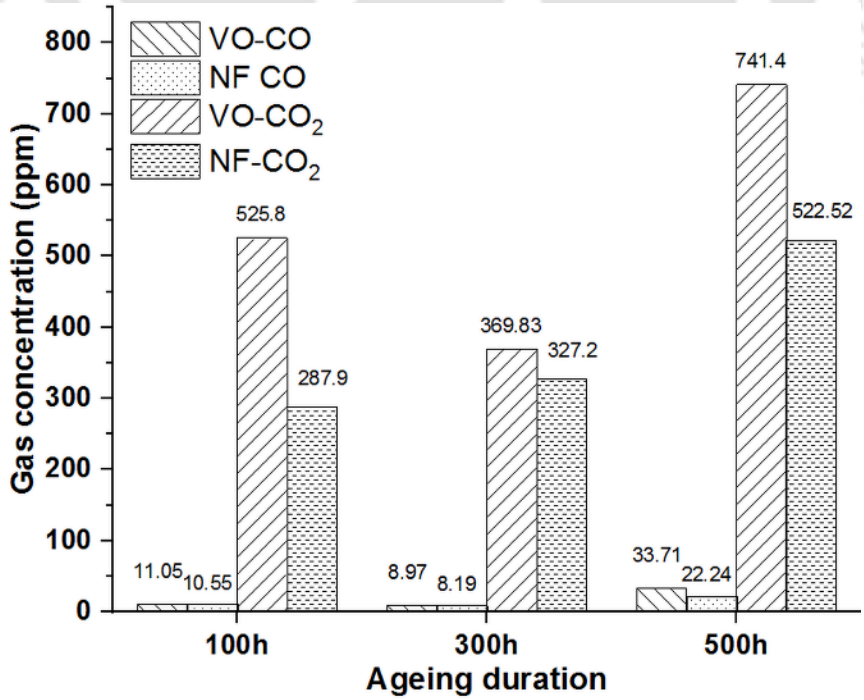

(b)

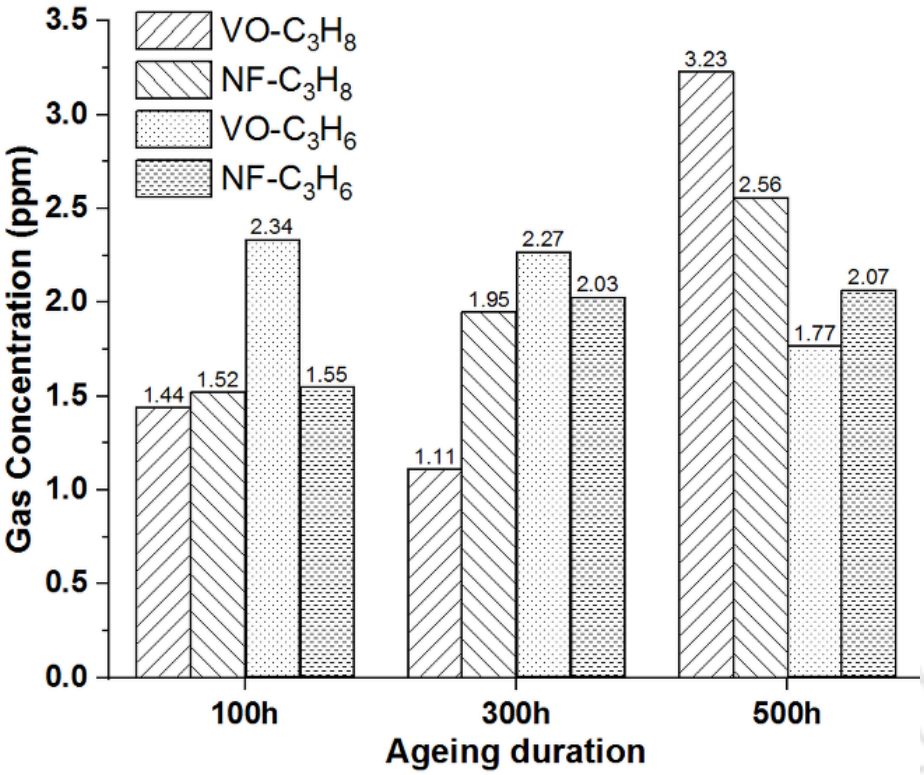

(c)

Figure 8.11: DGA analysis of aged VO and NF (a) Ethane, Ethylene and Hydrogen (b) Carbon Monoxide and Carbon dioxide (c) Propane and Propylene.

The detection of H_2 is observed at 500 hours of ageing for both the oil samples, so the flammable gases at 500 hours of ageing is expected. The lower concentration of H_2 gas at 500 hours of ageing makes the VO less flammable. The presence of carbon dioxide (CO_2) and carbon monoxide (CO), Figure 8.11 b in the aged oil are detected for different ageing durations. The formation of CO_2 in the oil may be from the ageing environment or deterioration of oil molecules in the presence of heat. CO is the degraded byproduct of aged oil impregnated cellulosic material and its detection concentration is highest at 500 hours of ageing. It supports the formation of hazardous sludge and highly flammable gases which may create local hotspot in the oil. However, the concentration of CO in the NF shows the minimal degradation of the solid insulation during the oxidative ageing environment. The detection of propane (C_3H_8), Figure 8.11 c and propylene (C_3H_6) in the oil may be due to oil processing and refining of the ester oil. The oil quality, in context with the gas formation, is marginally affected by the presence of C_3H_8 and C_3H_6. The gas concentration in the prospective VO and VO-NF based TO increases with ageing and its early detection can prevent catastrophic failures in the

transformer due to incipient faults. From the above DGA analysis, it is observed that the presence of insulating NP decelerates the gas generation tendency of NF compared to VO.

8.6 Electrical properties

8.6.1 ACBDV analysis

The dielectric reliability and electrical strength of the insulating oil are best analyzed by measuring its AC breakdown voltage (ACBDV). Superior breakdown voltage (BDV) of insulating oil aids in lengthening the life of the transformer by minimizing partial discharge and hotspot formation inside the transformer. Therefore, ACBDV analysis of VO and VO based NF is carried out in this study. The ACBDV study is performed by using Baur DTA-100C as per ASTM D1816 at room temperature (25^{o}C) with a power frequency of 50±0.5 Hz. A series of tests, each of five BDV measurements are carried out for both fresh and aged sample of VO and NF at 0, 100, 300 and 500 h of ageing. The comparative distribution of ACBDV for each sample for five measurements are reported in Figure 8.12 a. Analysis of the distributed BDV data for eight sequence is carried out, it is observed that NF has higher BDV values compared to VO for most of the measurements. Therefore, the mean ACBDV ($\bar{x}$) and the standard deviation (s) for each shot sequence is measured.

The mean ACBDV of insulating VO and VO-NF measured at fresh and aged condition presented in Figure 8.12 b. Since the moisture content in the insulating oil sample plays a dominant role in altering the ACBDV, respective moisture content in ppm for each oil sample is studied and reported. The fresh oil sample at 35ppm, percentage enhancement of ACBDV for NF to VO is nearly 4%. Since the more number of charge trapping occurs for NF [76], its breakdown process slowdowns at similar charging condition resulting high value of ACBDV in the NF. With the course of ageing, BDV follows the decline trends for both VO and NF. However, NF shows lower degradation in ACBDV when exposed to ageing conditions. The variation in the differential percentage rise in ACBDV of NF with respect to VO at distinct ageing hour are 6, 10 and 7.4% at 100, 300 and 500 h respectively. The rise in moisture content for both VO and NF is observed with the extended ageing duration. VO having methyl ester compounds has strong affinity towards polar contamination and moisture absorption resulting in higher ppm levels. The insulating and hydrophobic nature of Eh-BN NP has minimum tendency to attract polar contaminants. With the dispersion of these NPs in VO, it is expected to minimize the moisture level in VO-NF with ageing. Therefore, the ppm count drops for VO-NF and ACBDV is maintained at an upper level compared to VO at similar ageing duration.

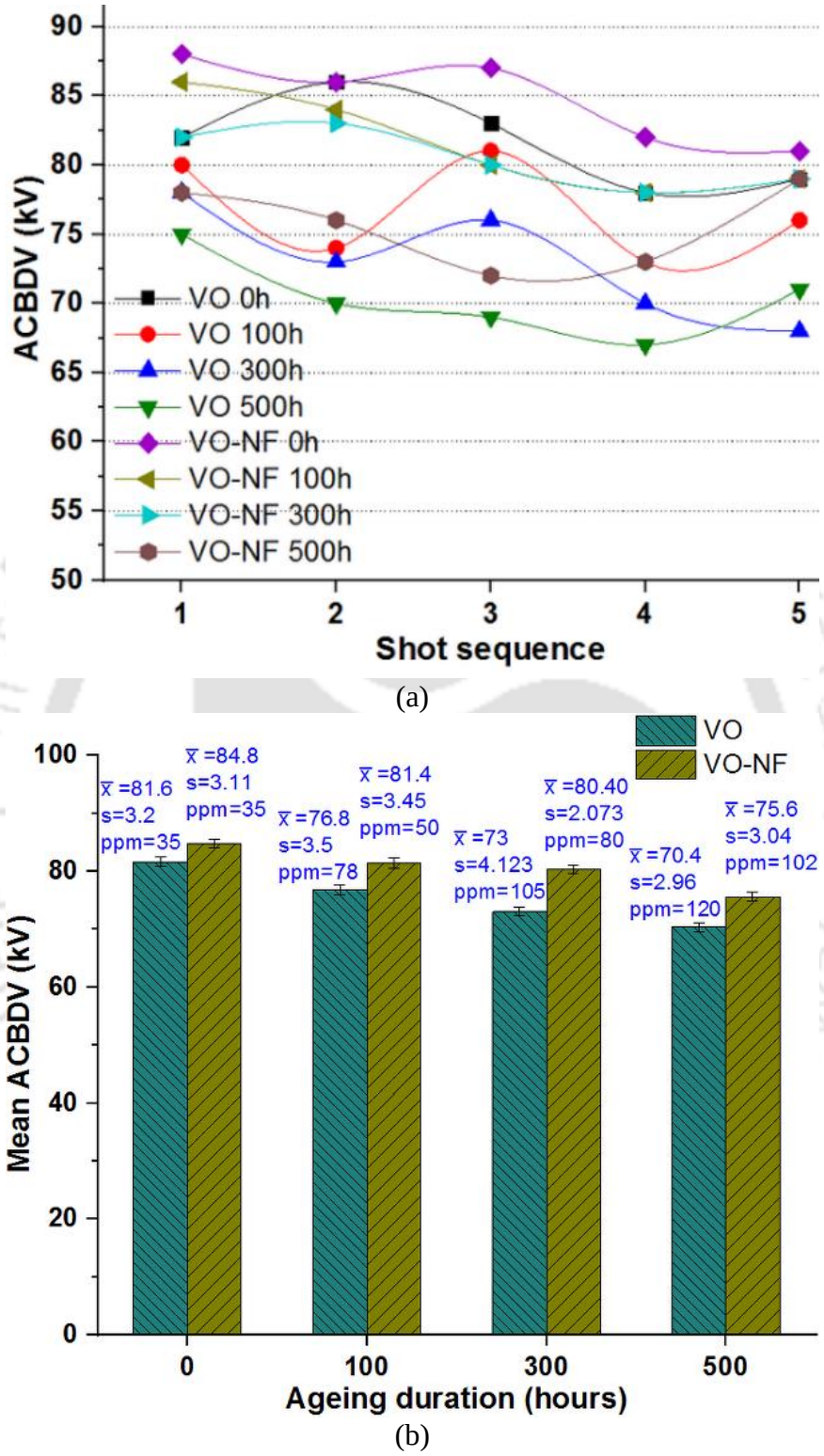

Figure 8.12: ACBDV analysis of fresh VO, VO-NF at 0, 100, 300, 500 h of ageing (a) shot sequence ACBDV (b) Mean ACBDV.

8.6.2 DDF and resistivity

The dielectric response such as DDF and resistivity are studied for VO and VO-NF at an oxidative ageing environment for distinct time frame shown in Figure 8.13. The resistivity of the insulating oil deteriorates with the increase in the sludge, polar contaminants and unwanted byproducts. During the oxidative ageing, VO is vastly affected and hence the DDF is noted higher. Whereas, insulating and Eh-BN dispersed VO-NF has minimal affinity towards ageing degradation up to 500 hours and hence, the resistivity is slightly affected producing insignificant number of ageing byproduct with low DDF.

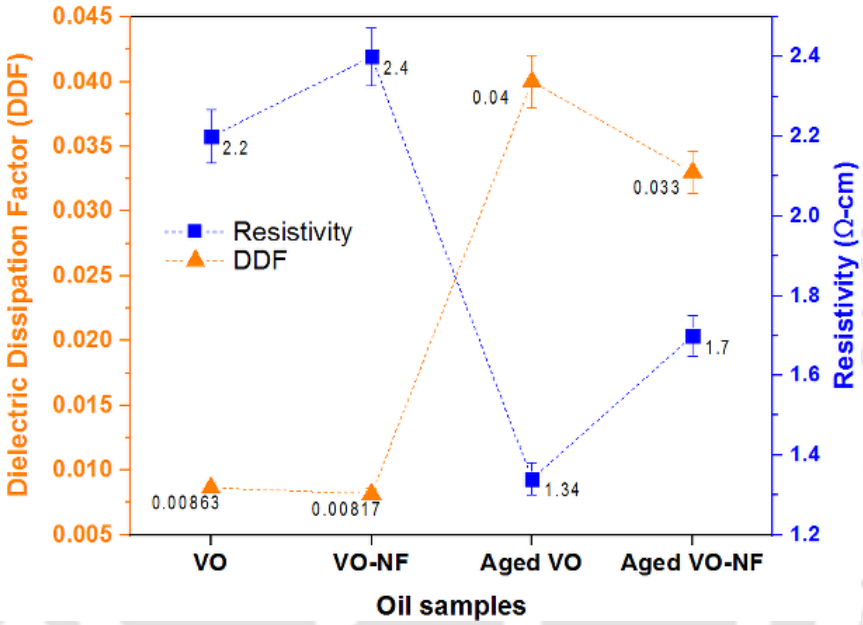

Figure 8.13: DDF and resistivity of fresh and aged (500 h) VO and VO-NF.

8.7 Summary of the chapter

The condition assessment of the VO and VO-NF is carried out by analyzing the various physicochemical and electrical characteristics by the novel open beaker oxidative ageing technique. The measurement in insulation and chemical degradation of the developed oil samples due to ageing are performed and summarizes below:

- From the colour scale measurement, the physical appearance of the VO-NF is observed to be less affected than the VO. The darker colour of the VO is because of higher exposure to chemical degradation.
- Since the high value of IFT in TO provides an information of lesser polar contaminations and AN, superior IFT value and lesser AN at 500 hours of oxidative ageing, ascertain that VO-NF has lesser affinity to polar contamination than VO.
- The progressive red shift maxima of 20 nm are observed for VO compared to VO-NF from

the spectroscopic measurement of the oil samples. The red shifting of emission band is attributed to the increase in the oil concentration with ageing due to the formation of higher sludge and polar contamination in VO than VO-NF.

- The chemical degradation of the oil due to oxidative ageing generates the flammable and harmful gases. The concentration of the observed flammable gases in VO-NF is lower than VO at 500 hours of ageing, which ascertains lesser chances of incipient faults thereby maintaining sound health of the transformer upon application of VO-NF based TO.
- The enhancement in ACBDV of VO-NF compared to VO with respect to ageing duration is 6, 10 and 7.4% at 100, 300 and 500 hours of ageing respectively. Hence, the electrical insulation properties of the VO-NF are always superior than VO.

Considering the above physicochemical properties, electrical properties and the chemical degradation by spectroscopic analysis, VO-NF base transformer can be proposed by the end user to the transformer manufacturer.

In the next chapter, conclusions and possible future works are presented.

9

Conclusion and future research

Contents

9.1 Summary of the present work

This thesis presents the development of alternative dielectric fluid such as insulating NF and nonedible VO based TO with enhanced physicochemical, thermal and electrical performance for transformer application. The ageing study of the developed oil and the oil impregnated solid insulation is performed to ascertain the degradation of oil-paper insulation system at sever ageing environment.

In Chapter 2, an insulating NF is prepared by dispersing 0.01wt % of insulating Eh-BN NP into the MO. Material characterization such as XRD, FESEM and TEM is carried out for the Eh-BN NP at bulk and exfoliated stages. The stability of the NF is verified using the Zeta potential analysis at 0.01 wt % of NP dispersion in to the MO. The thermophysical properties such as viscosity, flash point, fire point, interfacial tension, thermal conductivity, acid number and the electrical properties such as ACBDV, DDF and DC are studied for the Eh-BN/MO-NF and compared with MO. The enhancement in thermal performance of the NF compared to MO is observed. The rise in thermal conductivity of the NF is because of the uniformly dispersed high aspect ratio Eh-BN NP with large surface area which acts as a heat conducting surface. The theoretical explanation about the high thermal conductivity of the NF compared to MO is explained with the help of F-K model. The higher thermal conductivity of the developed NF makes the TO as a superior coolant in dielectric application. The dielectric integrity of the NF and MO is studied by evaluating the ACBDV at certain moisture level. The cause of enhancement in ACBDV of the NF compared to MO is analyzed with the help of charge dynamics and electron scavenging mechanism. Further, the dielectric characteristics of the MO and NF are investigated studying the DDF, DC and resistivity. It is observed that the NF based insulating fluid has superior performance in terms of thermal as well as dielectric and electrical performances. Therefore, the developed Eh-BN/MO-NF has the characteristics of being electrically insulant and thermally coolant for the transformer application.

In Chapter 3, open beaker oxidative ageing analysis is performed for two batches of NF such as TiO_2/MO, Eh-BN/MO along with MO. An open beaker oxidative ageing apparatus is developed to attain the oxidative ageing environment for the oil samples. The ageing study is performed at three different ageing duration such as 164, 328 and 492 hours at a fixed temperature of 115±1 ^{o}C. The physicochemical and electrical properties of the NFs are studied upon completion of different ageing period and compared with MO. From the physicochemical analysis of the aged oil, it is observed that the insulating Eh-BN/MO-NF has shown minimum

exposure to the oxidative ageing degradation compared to semi-conductive TiO_2/MO-NF and MO. Even after completion of 492 hours of oxidative ageing, because of the superior thermal conductivity of the Eh-BN/MO-NF, its thermal degradation is minimum. Higher affinity towards polar contaminants of the TiO_2/MO-NF and MO actively take part in the formation of sludge acidity by lowering the IFT with ageing. Since the Eh-BN/MO NF scavenges the more number of electrons compared to TiO_2/MO-NF during the process of evaluation of electric strength, Eh-BN MO-NF has superior ACBDV than MO and TiO_2 based TO.

In Chapter 4, using the sealed beaker oxidation stability measurement setup, oxidation stability test of the TO is analyzed for the different ageing duration up to 492 hours as per ASTM-D2440. During the period of ageing, MO and Eh-BN/MO NF are exposed to oxygen and heated in the presence of the copper catalyst in a sealed beaker. The evaluation of thermoelectrical properties such as interfacial tension (IFT), acid number (AN), dielectric dissipation factor (DDF), resistivity and thermal conductivity are performed. Moreover, probability of failure in the ACBDV of the aged oil samples are evaluated using the Weibull statistical analysis of the breakdown failure of the insulating oil. During the progress of the ageing period, there is a degradation of the thermophysical and electrical properties of both the oils. However, higher hydrophobicity and aspect ratio of the insulating Eh-BN NP has minimum affinity towards oxidation hindering early degradation of electrothermal properties of the NF. The breakdown probability of the MO and NF at five instances such as 5, 10, 50, 63.5% has been studied and it is observed that in each instance, the NF has lower breakdown probability than MO. As the thermophysical and electrical properties of the NF is superior than the MO, NF based transformer will increase the power transmission efficiency, reliability and reduce the cost of transmission.

The accelerated thermal ageing analysis of MO and NF impregnated solid insulation are studied in Chapter 5. Natural and force convection imposed accelerated thermal ageing apparatus is designed in the laboratory with temperature controlled and motorize stirring mechanism along with real time ageing environment for the ageing analysis. A comparative thermal ageing study on the MOIKP and NFIKP are carried out for different ageing duration such 100, 500, 1000 and 2000 hours. The ageing degradation characteristics of the impregnated paper such as colour, ACBDV, tensile strength and DP are studied and compared with fresh kraft paper. The temperature, the main cause of accelerated ageing, causes the degradation of the cellulosic kraft paper by altering and weakening the molecular structure which in turn changes the physical properties. The DP and the mechanical strength of the oil impregnated

kraft paper are proportional to each other. Superior thermal conductivity of the liquid insulating medium uniformly transfers the heat and hence, NFIKP experiences minimum ageing degradation compared to MOIKP.

In Chapter 6, for transformer application of nonedible VO based liquid dielectric, a detail comparative analysis of physicochemical and electrical properties of the MO, CKO and KOME are carried out. High percentage of FFA content and high viscosity in the CKO restricts its application for direct implementation as dielectric liquid. Therefore, the chemical processing such as two-step transesterification process is followed to make KOME as suitable TO. Various chemical characterization techniques such as FTIR, NMR and GCMS are carried out to observe the standard chemical characteristics. However, to validate the similar properties of the TO, the major physicochemical and electrical properties of the KOME are investigated and compared with the existing MO based TO. To evaluate the dielectric and electrical strength of KOME, mean ACBDV, DC and DDF are studied. To ascertain the probability of dielectric failure, comparative Weibull statistical analysis is performed for the three insulating oil. It is observed that the proposed KOME based VO liquid dielectric expected to be a potential replacement for existing MO based TO.

In Chapter 7, insulation monitoring of different potential TO is studied using the ageing diagnostic technique. The comparative analysis of physicochemical, thermal and electrical characteristics of the fresh and aged liquid dielectrics such as NEO, NF and MO are performed. By fluorescence spectroscopy analysis of the fresh and aged sample of TO, the formation of fluorophoric components are clearly identified. The presence of high volume of fluorophoric components indicates the severe chemical degradation of the oil. With an ageing degradation, NEO seems to have lesser chemical and insulation degradation compared to MO and Eh-BN/MO NF. Therefore, from the above analysis of fresh and aged sample, it is observed that NEO has less affected to the ageing leads to deliver superior performance in dielectric application.

In Chapter 8, condition monitoring and diagnosis of the aged ester based NF through physicochemical and spectroscopic measurement are performed. In this study, various spectroscopic tools are used to measure the chemical degradation of the insulating liquid such as VO and VO-NF for different ageing duration. Spectroscopic measurement methods such as NMR, FTIR, UV-vis and most importantly fluorescence based spectroscopy are performed. By analyzing the 2D EEM spectra of the aged oil samples of VO and VO-NF, the formation of

polar contaminations in terms of chromophoric moieties are detected. To regulate the formation of flammable and harmful gases in the aged oil, DGA is performed. It is observed that the presence of insulating NPs, the ester oil decelerates the gas generation tendency of NF compared to VO during ageing process. Since the chemical degradation and the dielectric integrity of the insulating oil are interrelated, the ACBDV of the fresh and aged VO and VO-NF is measured. As TO experience chemical, electrical and thermal stresses during full loading condition, the spectroscopic analysis of the chemical degradation and the measurement of dielectric and electrical strength at ageing provides the handful information of probable effect of ageing on VO and VO-NF before using in transformer. Therefore, the measurements are performed in detail to justify the VO-NF for its potential application in transformer.

9.2 Contribution of the thesis

The major contribution of the thesis for development of alternative dielectric fluid for power and distribution transformer are given as follows:

- The development of Eh-BN NP based NF has superior thermophysical and electrical performance at fresh and aged condition compared to MO.
- Superior dispersion stability is observed for 0.01 wt.% of Eh-BN NP for the preparation of MO and VO-NF.
- Thermal, insulation and chemical degradation of the prospective TO such as MO, NF and VO is studied with the help of developed open beaker oxidative ageing apparatus.
- Insulation monitoring and the prediction of insulation life of the TO paper insulation system is evaluated using the developed accelerated thermal ageing simulator.
- Development of an alternative nonedible VO i.e. KOME to replace the edible VO, synthetic ester oil and MO based TO.

9.3 Suggestions for future research

The suggestions for further research are given as follows:

- Partial discharge study of the fresh and aged insulating oil can be investigated to understand the pre-breakdown phenomena of the TO.
- A multiphysics model can be developed to study the electro-thermal response of the MO and NF based TO.

9. Conclusion and future works

- The frequency domain spectroscopy analysis of the fresh and aged NF and NF impregnated kraft paper can be performed.
- Noise attenuation properties of the NF filled transformer can be investigated to evaluate the probable effect of NF in the noise reduction.

Bibliography

[1]. T. V. Oommen, “Moisture equilibrium charts for transformer insulation drying practice,” *IEEE Trans. on Power Appar*. and Sys., vol. 103, no. 10, pp. 3063-3067, 1984.

[2]. D. M. Nail and P. H. Shoun, “"Retrofilling" - a technique to reduce polychlorinated biphenyls (pcb's),” *IEEE power engg. rev.*, vol. 4, no. 3, pp. 26-26, 1984.

[3]. I. Webber, D. B. Pilgrim and M. A. Thompson, “The safe disposal of polychlorinated biphenyls,” in *IEEE Trans. Ind. Appl.*, vol. IA-20, no. 1, pp. 159-166. 1984.

[4]. S. K. Das, S. U. S. Choi, W. Yu and T. Pradeep, “Nanofluids: Science and Technology”, *John Wiley & Sons*, Inc., 2008.

[5]. Y. Xuan and Q. Li, “Heat transfer enhancement of nanofluids”, *Int’l. J. Heat and Fluid Flow*, vol. 21, pp. 58-64, 2000.

[6]. C. Choi, H. S. Yoo and J. M. Oh, “Preparation and heat transfer properties of nanoparticle in transformer oil dispersions as advanced energy-efficient coolants”, *Curr. Appl. Phy.*, vol. 8, pp. 710-712, 2008.

[7]. Y. Du, Y. Lv, Z. Jian-quan, X. Li and C. Li, "Breakdown properties of transformer oil-based TiO_2 nanofluid," *IEEE Conf. Electr. Insul. Dielectr. Phenomena*, West Lafayette, IN, pp. 1-4, 2010.

[8]. V. A. Primo, B. Garcia and R. Albarracin, "Improvement of transformer liquid insulation using nanodielectric fluids: A review," *IEEE Electr. Insul. Mag.*, vol. 34, no. 3, pp. 13-26, 2018.

[9]. D. Wen and Y. Ding, "Natural convective heat transfer of suspensions of titanium dioxide nanoparticles (nanofluids)," *IEEE Trans. Nanotech.*, vol. 5, no. 3, pp. 220-227, 2006.

[10]. L. Yu and D. Liu, "Study of the thermal effectiveness of laminar forced convection of nanofluids for liquid cooling applications," *IEEE Trans. Compon., Packag. and Manufacturing Techno.*, vol. 3, no. 10, pp. 1693-1704, 2013.

[11]. W. Guan et al., "Finite element modeling of heat transfer in a nanofluid filled transformer," *IEEE Trans. Magnet.*, vol. 50, no. 2, pp. 253-256, 2014.

[12]. D. Liu, Y. Zhou, Y. Yang, L. Zhang and F. Jin, "Characterization of high performance AIN nanoparticle-based transformer oil nanofluids," *IEEE Trans. Dielectr. Electr. Insul.*, vol. 23, no. 5, pp. 2757-2767, 2016.

[13]. H. Jin, T. Andritsch, I. A. Tsekmes, R. Kochetov, P. H. F. Morshuis and J. J. Smit, "Properties of mineral oil based silica nanofluids," *IEEE Trans. Dielectr. Electr. Insul.*, vol. 21, no. 3, pp. 1100-1108, 2014.

[14]. M. Schaible, Electrical insulating papers – an overview. *IEEE Electr. Insul. Mag.* vol. 3, no. 1, pp. 8–12, 1987.

[15]. T. V. Oommen, “Vegetable oils for liquid-filled transformers”, *IEEE Electr. Insul. Mag.*, vol. 18 (1) pp. 6–11, 2002.

[16]. L. E. Lundgaard, W. Hansen, D. Linhjell, T. J. Painter, “Aging of oil-impregnated paper in power transformers,” *IEEE Trans. on Power Deliv,* vol. 19, no. 1, pp. 230–239. 2004.

[17]. M. M. Emara, D. A. Mansour and A. M. Azmy, "Mitigating the impact of aging byproducts in transformer oil using TiO_2 nanofillers," *IEEE Trans. Dielectr. Electr. Insul.*, vol. 24, no. 6, pp. 3471-3480, 2017.

[18]. R. Cimbala, S. Bucko, L. Kruželák and M. Kosterec, "Thermal degradation of transformer pressboard impregnated with magnetic nanofluid based on transformer oil," *18th Int'l. Scientific Confer. on Electr. Power Engg. (EPE)*, Kouty nad Desnou, pp. 1-5, 2017.

[19]. T. K. Saha, P. Purkait, Transformer ageing: monitoring and estimation techniques, *John Wiley & Sons Singapore Pte. Ltd.*, pp. 312-314, 2017.

[20]. J. Gao, L. Yang, Y. Wang, X. Liu, Y. Lv and H. Zheng, "Condition diagnosis of transformer oil-paper insulation using dielectric response fingerprint characteristics," *IEEE Trans. Dielectr. Electr. Insul.*, vol. 23, no. 2, pp. 1207-1218, 2016.

[21]. R. Liao, S. Liang, L. Yang, J. Hao and J. Li, "Comparison of ageing results for transformer oil-paper insulation subjected to thermal ageing in mineral oil and ageing in retardant oil," *IEEE Trans. Dielectr. Electr. Insul.*, vol. 19, no. 1, pp. 225-232, 2012.

[22]. A. Mikulecky and Z. Stih, "Influence of temperature, moisture content and ageing on oil impregnated paper bushings insulation," *IEEE Trans. Dielectr. Electr. Insul.*, vol. 20, no. 4, pp. 1421-1427, 2013.

[23]. M. Mandlik and T. S. Ramu, "Moisture aided degradation of oil impregnated paper insulation in power transformers," *IEEE Trans. Dielectr. Electr. Insul.*, vol. 21, no. 1, pp. 186-193, 2014.

[24]. P. Sun, W. Sima, M. Yang and J. Wu, "Influence of thermal aging on the breakdown characteristics of transformer oil impregnated paper," *IEEE Trans. Dielectr. Electr. Insul.*, vol. 23, no. 6, pp. 3373-3381, 2016.

[25]. R. Liao, J. Hao, G. Chen and L. Yang, "Quantitative analysis of ageing condition of oil-paper insulation by frequency domain spectroscopy," *IEEE Trans. Dielectr. Electr. Insul.*, vol. 19, no. 3, pp. 821-830, 2012.

[26]. R. Liao, Y. Lin, P. Guo, H. Liu and H. Xia, "Thermal aging effects on the moisture equilibrium curves of mineral and mixed oil-paper insulation systems," *IEEE Trans. Dielectr. Electr. Insul.*, vol. 22, no. 2, pp. 842-850, 2015.

[27]. T. V. Oommen, C. C. Claiborne, E. J. Walsh and J. P. Baker, "A new vegetable oil based transformer fluid: development and verification," *IEEE Conf. Electr. Insul. Dielectr. Phenomena*, Victoria, BC, Canada, vol.1, pp. 308-312, 2000.

[28]. C. P. McShane, "Relative properties of the new combustion-resist vegetable-oil-based dielectric coolants for distribution and power transformers," *IEEE Trans. Dielectr. Electr. Insul.*, vol. 37, no. 4, pp. 1132-1139, 2001.

[29]. C. P. McShane, "Vegetable-oil-based dielectric coolants," in *IEEE Ind. Appl. Mag.*, vol. 8, no. 3, pp. 34-41, 2002.

[30]. M. Hrkac, P. Papageorgiou, I. Kosmoglou and G. Miatto, "BIOTEMP® transformer technology for innovative compact substation," *7th Mediterranean Conference and Exhibition on Power Generation, Transmission, Distribution and Energy Conversion (MedPower 2010)*, Agia Napa, pp. 1-6, 2010.

[31]. H. B. H. Sitorus, R. Setiabudy, S. Bismo and A. Beroual, "Jatropha curcas methyl ester oil obtaining as vegetable insulating oil," *IEEE Trans. Dielectr. Electr. Insul.*, vol. 23, no. 4, pp. 2021-2028, 2016.

[32]. S. Choi, D. A. Siginer, H. P. Wang, "Enhancing thermal conductivity of fluids with nanoparticles," *Dev. Appl. Non-Newton. Flows, ASME, FED*, vol. 231, no. 66, pp. 99–105,1995.

[33]. C. Choi, S. H. Yoo, J. M. Oh, "Preparation and heat transfer properties of nanoparticle-in-transformer oil dispersions as advanced energy efficient coolants," *J. Curr. Appl. Phys.*, vol. 8, pp. 710–712, 2008.

[34]. X. Q.Wang, A. S. Mujumdar, "Heat transfer characteristics of nanofluids: A review," *Int. J. Therm. Sci.*, vol. 46, no. 1, pp. 1–19, 2007.

[35]. J. A. Eastman, S. U. S. Choi, S. Li, "Anomalously increased effective thermal conductivities of ethylene glycol-based nanofluids containing copper nanoparticles," *Appl. Phys. Lett.*, 78, (6), pp. 718–720, 2001.

[36]. R. Prasher, P. Bhattacharya, P. E. Phelan, "Thermal conductivity of nanoscale colloidal solutions," *Phys. Rev. Lett.*, vol. 94, no. 2, p. 025901, 2005.

[37]. S. Lee, S.U.S. Choi, S. Li, J. A. Eastman, "Measuring thermal conductivity of fluids containing oxide nanoparticles," *Trans. ASME J. Heat Transfer*, vol. 121, no. 2, pp. 280–289, 1999.

[38]. R. Saidur, K. Y. Leong, H. A. Mohammad, "A review on applications and challenges of nanofluids," *Renewable and Sustain. Energy Rev.*, vol. 15, pp. 1646–1668, 2011.

[39]. T. Tanaka and T. Imai, "Advances in nanodielectric materials over the past 50 years," *IEEE Electr. Insul. Mag.*, vol. 29, no. 1, pp. 10–23, 2013.

[40]. T. J. Lewis, "Nanometric dielectrics," *IEEE Trans. Dielectr. Electr. Insul.*, vol. 1, no. 5, pp. 812–825, 1994.

[41]. T. Andritsch, Epoxy Based Nanodielectrics for High Voltage DC-Applications: Synthesis, Dielectric Properties and Space Charge Dynamics. *Delft Univ. of Technol.*, Doctoral Thesis, 228 pp, 2010.

[42]. M. F. Frechette, M. L. Trudeau, H. D. Alamdari, and S. Boily, "Introductory remarks on nanodielectrics," *IEEE Trans. Dielectr. Electr. Insul.*, vol. 11, no. 5, pp. 808–818, 2004.

[43]. Y. Li, J. Zhou, S. Tung, E. Schneider, and S. Xi, "A review on development of NF preparation and characterization," *Powder Technol.*, vol. 196, no. 2, pp. 89–101, 2009.

[44]. G. D. P. Mahidhar, R. Sarathi, N. Taylor and H. Edin, "Study on performance of silica nanoparticle dispersed synthetic ester oil under AC and DC voltages," *IEEE Trans. Dielectr. Electr. Insul.*, vol. 25, no. 5, pp. 1958-1966, 2018.

[45]. H. Jin, "Dielectric strength and thermal conductivity of mineral oil based nanofluids," PhD thesis, *Delft Univ. of Technol.*, 2015.

[46]. C. Zhi, Y. Xu, Y. Bando, D. Golberg, "Highly thermo conductive fluid with boron nitride nanofillers", *Amer. Chem. Soc. (ACS) Nano*, vol. 5, no. 8, pp. 6571–6577, 2011.

[47]. J. Taha-Tijerina, T. N. Narayanan, G. Gao, M. Rohde, D. A. Tsentalovich, M. Pasquali, and P. M. Ajaya, "Electrically insulating thermal nano-oils using 2d fillers", *Amer. Chem. Soc. (ACS) Nano*, vol. 6, no. 2, pp. 1214-1220, 2012.

[48]. H. Masuda, A. Ebata, K. Teramae, N. Hishinuma, "Alteration of thermal conductivity and viscosity of liquid by dispersing ultrafine particle," *Netsu Bussei*, vol. 7, no. 4, pp. 227-233, 1993.

[49]. J. A. Eastman, S. U. S. Choi, S. Li, L. J. Thompson, and S. Lee. "Enhanced thermal conductivity through the development of nanofluids" *Fall Meeting of the Materials Research Society (MRS)*, Boston, USA (1996).

[50]. H. Xie, J. Wang, T. Xi, and Y. Liu."Thermal Conductivity of Suspensions Containing Nanosized SiC Particles" *Int. Journal of Thermophys.*, vol. 23 no. 2, pp. 571-580, 2002.

[51]. W. Yu, H. Xie, X. Wang, and X. Wang, "Highly efficient method for preparing homogeneous and stable colloids containing graphene oxide," *Nanoscale Res. Lett.*, vol. 6, p. 47, 2011.

[52]. G. Shukla and H. Aiyer, "Thermal conductivity enhancement of transformer oil using functionalized nanodiamonds," *IEEE Trans. Dielectr. Electr. Insul.*, vol. 22, no. 4, pp. 2185-2190, 2015.

[53]. Nnanna, A., "Experimental model of temperature-driven nanofluid," *ASME J. Heat Transfer*, vol. 129, no. 6, pp. 697–704, 2007

[54]. M. Liu, M. Lin, I. Huang and C. Wang, "Enhancement of thermal conductivity with CuO for nanofluids", *Chemical Engg. & Technol.*, vol. 29, pp. 72-77, 2006.

[55]. S. M. S. Murshed, K. C. Leong, and C. Yang, "Enhanced thermal conductivity of TiO_2-water based nanofluids" *Int. Journal of Therm. Sci*, vol. 44, no. 4, pp. 367-373, 2005.

[56]. J. H. Lee, K. S. Hwang, S. P. Jang, B. H. Lee, J. H. Kim, S. U. S. Choi, "Effective viscosities and thermal conductivities of aqueous nanofluids containing low volume concentrations of Al_2O_3 nanoparticles," *Int'l. J. Heat Mass Transfer*, vol. 51 no. (11–12), 2651–2656, 2008.

[57]. V. Segal and K. Rajb, "An investigation of power transformer cooling with magnetic fluids," *Indian J. Eng. Mater. Sci.*, vol. 5, pp. 416–422, 1998.

[58]. W. Sima, J. Shi, Q. Yang, S. Huang, and X. Cao, "Effects of conductivity and permittivity of nanoparticle on transformer oil insulation performance: Experiment and theory," *IEEE Trans. Dielectr. Electr. Insul.*, vol. 22, no. 1, pp. 380–390, 2015.

[59]. Y. Lv, Y. Zhou, C. Li, Q. Wang, and B. Qi, "Recent progress in nanofluids based on transformer oil: Preparation and electrical insulation properties," *IEEE Electr. Insul. Mag.*, vol. 30, no. 5, pp. 23–32, 2014.

[60]. F. M. O'Sullivan, "A model for the initiation and propagation of electrical streamers in transformer oil and transformer oil based nanofluids," PhD thesis, *Massachusetts Inst. Technol.*, 2007.

[61]. M. E. Ibrahim, A. M. Abd-Elhady, and M. A. Izzularab, "Effect of nanoparticles on transformer oil breakdown strength: Experiment and theory," *IET Sci. Meas. Technol.*, vol. 10, no. 8, pp. 839–845, 2016.

[62]. J. Li, R. Liao, and L. Yang, "Investigation of natural ester based liquid dielectrics and nanofluids," in *2012 Int. Conf. High Volt. Eng. Appl.*, pp. 16–21, 2012.

[63]. Y. Zhong, Y. Lv, C. Li, Y. Du, M. Chen, S. Zhang, Y. Zhou, and L. Chen, "Insulating properties and charge characteristics of natural ester fluid modified by TiO_2 semiconductive nanoparticles," *IEEE Trans. Dielectr. Electr.Insul.*, vol. 20, no. 1, pp. 135–140, 2013.

[64]. G. Dombek, Z. Nadolny, and P. Przybylek, "The study of thermal properties of mineral oil and synthetic ester modified by nanoparticles TiO_2 and C60," presented at the 2014 *Int. Conf. High Volt. Eng. Appl. (ICHVE),* Poznan, Poland, 2014.

[65]. B. Wang, J. Li, B. Du, and Z. Zhang, "Study on the stability and viscosity of Fe_3O_4 nano-particles vegetable insulating oils," *Int'l. Conf. High Volt. Eng. Appl.*, pp. 307–310, 2012.

[66]. A. Raymon, S. Sakthibalan, C. Cinthal, R. Subramaniaraja, and M. Yuvaraj, "Enhancement and comparison of nano-ester insulating fluids," *IEEE Trans. Dielectr. Electr. Insul.*, vol. 23, no. 2, pp. 892–900, 2016.

[67]. M. G. Danikas, A. Bakandritsos, G. D. Peppas, V. P. Charalampakos, E. C. Pyrgioti, and I. F. Gonos, "Statistical investigation of AC breakdown voltage of nanofluids compared with mineral and natural ester oil," *IET Sci. Meas. Technol.*, vol. 10, no. 6, pp. 644–652, 2016.

[68]. B. Du, J. Li, B. M. Wang, and Z. T. Zhang, "Preparation and breakdown strength of Fe3O4 nanofluid based on transformer oil," *Int'l. Conf. High Volt. Eng. Appl.*, pp. 311–313, 2012.

[69]. L. Pislaru-Danescu, A. M. Morega, G. Telipan, M. Morega, J. B. Dumitru, and V. Marinescu, "Magnetic nanofluid applications in electrical engineering," *IEEE Trans. Magn.*, vol. 49, no. 11, pp. 5489–5497, 2013.

[70]. J. Li, B. Du, F. Wang, W. Yao, and S. Yao, "The effect of nanoparticle surfactant polarization on trapping depth of vegetable insulating oil-based nanofluids," *Phys. Lett.*, vol. 380, no. 4, pp. 604–608, 2016.

[71]. Y. Du, Y. Lv, C. Li, M. Chen, Y. Zhong, J. Zhou, X. Li, and Y. Zhou, "Effect of semiconductive nanoparticles on insulating performances of transformer oil," *IEEE Trans. Dielectr. Electr. Insul.*, vol. 19, no. 3, pp. 770–776, 2012.

[72]. Y. Li, J. Zhou, S. Tung, E. Schneider, and S. Xi, "A review on development of nanofluid preparation and characterization," *Powder Technol.*, vol. 196, no. 2, pp. 89–101, 2009.

[73]. G. Jeong, S. P. Jang, H. Lee, J. Lee, S. Choi and S. Lee, "Magnetic-thermal-fluidic analysis for cooling performance of magnetic nanofluids comparing with transformer oil and air by using fully coupled finite element method," in *IEEE Trans. on Magnetics*, vol. 49, no. 5, pp. 1865-1868, 2013.

[74]. J. L. Davidson, "Nanofluid for cooling enhancement of electrical power equipment," Vanderbilt faculty. *Department of Electrical Engineering*, 2009.

[75]. W. H. Lee, W. S. Lee and J. C. Lee, "Influence of magnetic nanoparticles on the breakdown voltage of transformer oil", *17th Int'l. Sympos. on High Volt. Eng. (ISH)*, Germany, E-080, 2011.

[76]. J. G. Hwang, M. Zahn, F. M. O'Sullivan, L. A. A. Pettersson, O. Hjortstam and R. Liu, "Effects of nanoparticle charging on streamer development in transformer oil-based nanofluids", *Journal of Appl. Phy.*, vol. 107, p. 014310, 2010.

[77]. M. Zahn, N. Lavesson, O. Widlund, and Borg, "Effects of impulse voltage polarity, peak amplitude, and rise time on streamers initiated from a needle electrode in transformer oil," *IEEE trans. on plasma sci.*, vol. 40, no 3, 2012.

[78]. Y. Z. Lv, X. Li, Y. F. Du, F. C. Wang, R. Li, "Preparation and breakdown strength of TiO_2 fluids based on transformer oil," *IEEE Conf. Electr. Insul. Dielectr. Phenomena*, West Lafayette, IN, pp. 1-3, 2010.

[79]. D. E. Mansour, E. G. Atiya, R. M. Khattab, A. M. A. Azmy, "Effect of titania nanoparticles on the dielectric properties of transformer oil-based nanofluids *IEEE Conf. Electr. Insul. Dielectr. Phenomena*, Montreal, QC, pp. 295-298. 2012.

[80]. Y. F. Du, Y. Z. Lv, F. C. Wang, and C. R. Li, "Effect of TiO_2 nanoparticles on the breakdown strength of transformer oil," *IEEE Int'l. Sympos. on Electr. Insul*., pp.1-3, 2010.

[81]. H. Jin, T. Andritsch, P.H.F. Morshuis, J.J. Smit, "AC breakdown voltage and viscosity of mineral oil based SiO_2 nanofluids," *Trans. Dielectr. Electr. Insul* vol. 978, pp. 1252-1255, 2012.

[82]. B. X. Du, X. L. Li, "High thermal conductivity transformer oil filled with BN nanoparticles," *IEEE Int'l. Conference on Liquid Dielectr.s*, vol. 978 no. 1-4799-2063, 2014.

[83]. Y. Lv, W. Wang, K. Ma, S. Zhang, Y. Zhou, C. Li, Q. Wang, "Nanoparticle effect on dielectric breakdown strength of transformer oil-based nanofluids," *IEEE Conf. Electr. Insul. Dielectr. Phenomena*, pp. 680-682, 2013.

[84]. S. Ponmania, J. K. M. Williama, R. Samuelb, R. Nagarajanc, J. S. Sangwaia, "Formation and characterization of thermal and electrical properties of CuO and ZnO nanofluids in xanthan gum," *Colloids and Surfaces A: Physicochemical and Engineering Aspects*, vol. 443, no. 20 pp. 37–43, 2014.

[85]. T. V. Oommen, C. C. Claiborne, and J. T. Mullen, "Biodegradable electrical insulation fluids," *IEEE Electr. Insul., Electr. Manufacturing and Coil Winding Conf.*, pp. 465-468, 1997.

[86]. C. P. McShane, "New dielectric coolant concepts for distribution and power transformers," *IEEE Pulp and Paper, Ind. Technical Conf.*, pp. 55 –62, 1999.

[87]. M. Mazzaro, D. De Bartolomeo, L. Calcara, M. Pompili, F. Scatiggio, A. Vailant, M. Rebolini, E. Bemporad, S. Berardi, A. Ledda, M. Falconi, A. Vecchio, A. Sturchio, M. Salvadori, F. Mauri, "Power Transformer Fire and Environmental Risk Reduction by Using Natural Esters," *Int'l. Conf. Dielectr. Liquids (ICDL)*, 2017.

[88]. L. Pompili, A. Calcara, C. F. Sturchio, "Natural esters distribution transformers: a solution for environmental and fire risk prevention," *Int.l' Annu. Conf. Sustainable Development in the Mediterranean Area, Energy and ICT Networks of the Future*, 2017.

[89]. T. A. Prevost and T. V. Oommen, "Cellulose insulation in oil-filled power transformers: Part I - history and development", *IEEE Electr. Insul. Mag.*, vol. 22, no. 1, pp. 28-35, 2006.

[90]. D. Martin and Z. D. Wang, "Statistical analysis of the AC breakdown voltages of ester based transformer oils," *IEEE Trans. Dielectr. Electr. Insul.*, vol.15, pp. 1044-1050, 2008.

[91]. C. Perrier and A. Beroual, ''Experimental investigations on insulating liquids for power transformers: mineral, ester, and silicone oils," *IEEE Electr. Insul. Mag.*, vol. 25, no. 6, pp. 6–13, 2009.

[92]. D. Martin, N. Lelekakis, and W. Guo, "Further studies of a vegetable-oil-filled power transformer," *IEEE Electr. Insul. Mag.*, vol. 27, pp. 6-13, 2011.

[93]. Y. Lijun, L. Ruijin, C. Sun, and Z. Mengzhao, "Influence of vegetable oil on the thermal aging of transformer paper and its mechanism," *IEEE Trans. Dielectr. Electr. Insul.*, vol.18, pp. 692-700, 2011.

[94]. L. Ruijin, H. Jian, G. Chen, M. Zhiqin, and Y. Lijun, "A comparative study of physicochemical, dielectric and thermal properties of pressboard insulation impregnated with natural ester and mineral oil," *IEEE Trans. Dielectr. Electr. Insul.*, vol.18, pp. 1626-1637, 2011.

[95]. P. K. Sahoo, S. N. Naik, M. K. G. Babu and L. M. Das, "Biodiesel development from high acid value polanga seed oil and performance in a CI engine," *Fuel*, vol. 86, pp. 448–54, 2007.

[96]. P.K. Sahoo and L.M. Das, "Combustion analysis of jatropha, karanja and polanga based biodiesel as fuel in a diesel engine," *Fuel*, vol. 88, pp. 994–999, 2009.

[97]. M. S. Rao and R. B. Anand, "Production characterization and working characteristics in DICI engine of Pongamia biodiesel," *Ecotox. Environ. Safe.*, vol. 121, pp. 16–21, 2015.

[98]. B. Baiju, M.K. Naik, and L.M. Das, "A comparative evaluation of compression ignition engine characteristics using methyl and ethyl esters of Karanja oil," *Rene. Ene.*, vol. 34, pp. 1616–1621, 2009.

[99]. E. C. Nsofor, "Recent patents on NFs (nanoparticles in liquids) heat transfer," *Recent Pat. on Mech. Eng.*, vol. 1, no. 3, pp. 190-197, 2008.

[100]. B. C. Pak and Y. I. Cho, "Hydrodynamic and Heat transfer study of dispersed fluids with submicron metallicoxide particles," *Exp. Heat Transfer*, vol.11, pp.151–170, 1998.

[101]. S. K. Das, N. Putra, P. Thiesen and W. J. Roetzel, "Temperature dependence of thermal conductivity enhancement for nanofluids," *J. Heat Transfer*, vol. 125, no. 4, pp. 567–574, 2003.

[102]. C. T. Nguyen, G. Roy, C. Gauthier, and N. Galanis, "Heat transfer enhancement using Al_2O_3–water nanofluid for an electronic liquid cooling system," *Appl. Therm. Eng.*, vol. 27, no. 8–9, pp. 1501–1506, 2007.

[103]. G. A. Risha, Boyer, B. J. Evans, K. K.Kuo, and R.Malek, "Characterization of nano sized particles for propulsion applications," *J. Mater. Res.Soc. Proc.*, vol. 800, pp. 243–54, 2004.

[104]. Y. Ding, H. Alias, D. Wen and R. A. Williams, "Heat transfer of aqueous suspensions of carbon nanotubes (CNT nanofluids)", *Int'l. J. of Heat Mass Transfer*, vol. 49, pp. 240-250, 2006.

[105]. A. T. Utomo, H. Poth, P. T. Robbins and A. W. Pacek, "Experimental and theoretical studies of thermal conductivity, viscosity and heat transfer coefficient of titania and alumina nanofluids", *Int'l. J. of Heat and Mass Transfer*, vol. 55, pp. 7772-7781, 2012.

[106]. W. Duangthongsuk, and S.Wongwises, "An experimental study on the heat transfer performance and pressure drop of TiO2–water nanofluids flowing under a turbulent flow regime," *Int'l. J. Heat Mass Transfer*, vol. 53, pp. pp. 334–344, 2010.

[107]. K-Q. Ma and J. Liu, "Nano liquid–metal fluid as ultimate coolant," *Phys Lett A*, vol. 361, pp. 252–6, 2007.

[108]. E. G. Atiya, D. E. A. Mansour, R. M. Khattab, and A. M. Azmy "Dispersion behavior and breakdown strength of transformer oil filled with TiO_2 nanoparticles," *IEEE Trans. Dielectr. Electr. Insul.*, vol. 22, No. 5, pp. 2463-2471, 2015.

[109]. W. Yu and H. Xie, J. Nanomater., "A Review on Nanofluids: Preparation, Stability Mechanisms, and Applications," *Journal of Nanomaterials*, vol. 2012, Article ID 435873435873, pp.1-17, 2012.

[110]. S. Ozerinc, S. Kakac and A. Yazlcloglu, "Enhanced thermal conductivity of nanofluids: a state-of-the-art review," *Microfluid. Nanofluid.*, vol. 8, no. 2, pp. 145–170, 2010.

[111]. S. A. Putnam, D. G. Cahill, P. V. Braun, Z. B. Ge, and R. G.Shimmin, "Thermal conductivity of nanoparticle suspensions," *J. Appl. Phys.*, vol. 99, no. 8, pp. 084308/1-084308/6, 2006.

[112]. S. Khrisnamurthy, P. Bhattacharya, and P. E. Phelan, "Enhanced mass transport in nanofluids," *Nano Lett.*, vol. 6., pp. 419–23, 2006.

[113]. ASTM D1934-12, Standard test method for oxidative aging of electrical insulating petroleum oils by open-beaker method.

[114]. ASTM D1533, Standard test method for water in insulating liquids by coulometric karl fischer titration.

[115]. ASTM D93, Standard test methods for flash point by pensky-martens closed cup tester.

[116]. ASTM D971, Standard test method for interfacial tension of oil against water by the ring method.

[117]. ASTM D1816, Standard test method for dielectric breakdown voltage of insulating liquids using VDE electrodes.

[118]. ASTM D924, Standard test method for dissipation factor (or power factor) and relative permittivity (dielectric constant) of electrical insulating liquids.

[119]. ASTM D2440, Standard test method for oxidation stability of mineral insulating oil.

[120]. Y. Xuan, and Q. Li, "Heat transfer enhancement of nanofluids," *Int'l. Journal of Heat and Fluid Flow*, vol. 21, no. 1, pp. 58-64. 2000

[121]. A. S. Abdullah, Z. S. Ahmet, S. Y. Bekir, "Measurement of thermal and electrical properties of multiwalled carbon nanotubes–water nanofluid," *ASME J. Heat Transfer*, 2016, vol. 138, no. 7, pp. 072401.

[122]. J. Viertel, K. Ohlsson, and S. Singha, "Thermal aging and degradation of thin films of natural ester dielectric liquids," *IEEE Int'l. Conf. Dielectr. Liquids (ICDL),* Trondheim, Norway, 2011.

[123]. G. K. Frimpong., T. V. Oommen, R. Asano, "A survey of aging characteristics of cellulose insulation in natural ester and mineral oil," *IEEE Electr. Insul. Mag.*, 27, (5) pp. 36-48, 2011.

[124]. L. R. Lewand, C. Claiborne, D. B. Cherry, "Oxidation and oxidation stability of natural ester dielectric liquids," *Section IM, 77th Annual Int'l. Doble Client Conf.*, 2010.

[125]. M. Kohtoh, G. Ueta., S. Okabe., "Transformer insulating oil characteristic changes observed using accelerated degradation in consideration of field transformer conditions," *IEEE Trans. Dielectr. Electr. Insul.*, vol. 17, no. 3, pp. 808-818. 2010.

[126]. J. Jeong., J. S. An, C. S. Huh, "Accelerated aging effects of mineral and vegetable transformer oils on medium voltage power transformers," *IEEE Trans. Dielectr. Electr. Insul.*, vol. 19, no. 1, pp.156-161, 2012.

[127]. Y. Nagasaka, A. Nagashima, "Absolute measurement of the thermal conductivity of electrically conducting liquids by the transient hot-wire method", *J. Phys. E Sci*., vol. 14, pp. 1435–1440, 1981.

[128]. ASTM D1500, Standard test method for ASTM color of petroleum products.

[129]. ASTM D445, 'Standard test method for kinematic viscosity of transparent and opaque liquids.

[130]. J. A. Eastman, U. S. Choi, S. Li, Thomson, S. Lee "Enhanced thermal conductivity through the development of nanofluids," *MRS Proceedings*, vol. 457, pp. 3–11, 1997.

[131]. O. Navid, F. H. Ghaziani, "Convective heat transfer of Al_2O_3 nanofluids in porous media," *ASME J. Heat Transfer*, vol. 139, pp. 032601, 2016.

[132]. W. Evans, R. Prasher., J. Fish, P. Meakin, P. Phelan, P. Keblinski "Effect of aggregation and interfacial thermal resistance on thermal conductivity of nanocomposites and colloidal nanofluids," *Int'l. J. Heat Mass Transfer*, vol. 51 no. (5–6), pp. 1431–14. 2008.

[133]. C. Perrier, A. Beroual, J. L Bessede, "Improvement of power transformers by using mixtures of mineral oil with synthetic esters", *IEEE Trans. Dielectr. Electr. Insul*, vol. 13, no. 3, pp. 1070-1078, 2006.

[134]. T. Takada, Y. Hayase, Y. Takada, "Space charge trapping in electrical potential well caused by permanent and induced dipoles for LDPE/MgO nanocomposite", *IEEE Trans. Dielectr. Electr. Insul.*, vol. 15, no. 1 pp. 152-160, 2008.

[135]. R. C. Smith, C. Liang, M. Landry, J. K. Nelson and L. S. Schadler "The mechanisms leading to the useful electrical properties of polymer nanodielectrics", *IEEE Trans. Dielectr. Electr. Insul.*, vol. 15, no. 1, pp.187-196, 2008.

[136]. T. J. Lewis, and B. W. Ward, "A statistical interpretation of the electrical breakdown of liquid dielectrics," *Proc. R. Soc.*, vol. 269 pp. 109-124. 1962.

[137]. Y. Hadjadj, I. Fofana, "Assessing insulating oil degradation by means of turbidity and uv/vis spectrophotometry measurements," *IEEE Trans. Dielectr. Electr. Insul.*vol. 22, no. 5, pp. 2653-2660, 2015.

[138]. H. M. Wilhelm, L. Tulio, R. Jasinski and G. Almeida "Aging markers for in-service natural ester-based insulating fluids," *IEEE Trans. Dielectr. Electr. Insul.*, vol. 18, no. 3, pp. 714-719, 2011

[139]. J. Carcedo, I. Fernández, A. Ortiz, F. Delgado, C. J. Renedo and C. Pesquera "Aging assessment of dielectric vegetable oils," *IEEE Electr. Insul. Magaz.*, vol. 31, no. 6, pp. 13-21, 2015.

[140]. ASTM D974, Standard test method for acid and base number by color-indicator titration'

[141]. ASTM D5334, Standard test method for determination of thermal conductivity

[142]. ASTM D117-10, Standard guide for sampling, test methods, and specifications for electrical insulating oils of petroleum origin.

[143]. L. E. Lundgaard, W. Hansen, and S. Ingebrigtsen, "Ageing of mineral oil impregnated cellulose by acid catalysis", *IEEE Trans. Dielectr. Electr. Insul.* vol. 15, no. 2, pp. 540-546, 2008.

[144]. ASTM D828, Standard test method for tensile properties of paper and paperboard using constant-rate-of-elongation apparatus.

[145]. ASTM D4243, Standard test method for measurement of average viscometric degree of polymerization of new and aged electrical papers and boards.

[146]. B. K. Barnwal and M. P. Sharma, "Prospects of biodiesel production from vegetable oils in India," *Renew. and Sust. Ene. Rev.*, vol. 9, pp. 363–378, 2005.

[147]. V. K. Gore and P. Satyamoorthy, "Determination of pongamol and karanjin in karanji oil by reverse phase HPLC," *Anal. Lett.*, vol. 33, pp. 337-346, 2000.

[148]. IEEE Std. C.57.147, Guide for acceptance and maintenance of natural ester fluids in transformers.

[149]. ASTM D6871, Standard specification for natural (vegetable oil) ester fluids used in electrical apparatus.

[150]. L. C. Meher, Vidya S. S. B. Dharmagadda and S. N. Naik, "Optimization of alkali-catalyzed transesterification of pongamia pinnata oil for production of biodiesel," *Biores. Technol.*, vol. 97, pp. 1392–1397, 2006.

[151]. ASTM D3487, 'Standard specification for mineral insulating oil used in electrical apparatus.

[152]. G. Gelbard, O. Bres, R. M. Vargas, F. Vielfaure and U.E Schuchardt, "^{1}H Nuclear magnetic resonance determination of the yield of the transesterification of rapeseed oil with methanol," *JAOCS*, vol. 72, 1239-1241, 1995.

[153]. T. V. Oommen and T. Prevost, "Cellulose insulation in oil-filled power transformers: Part II Maintaining insulation integrity and life," *IEEE Elect. Insul. Mag.*, vol. 22, no. 2, pp. 5–14, 2006.

[154]. C. P. McShane, G. A. Gauger and J. Luksich, "Fire Resistant Natural Ester Dielectric Fluid and Novel Insulation System for Its Use", *IEEE/PES Transmission & Distribution Conf.*, New Orleans, USA, vol. 2, pp. 890-894, 1999.

[155]. S. M. Ilyas, "Study on the characteristics of jatropha and ricinnus seed oils as liquid insulating materials", *IEEE Conf. Electr. Insul. Dielectr. Phenomena*, pp.162-166, 2006.

[156]. A. Raymon, S. Pakianathan, M.P.E. Rajamani and R. Karthik, "Enhancing the critical characteristics of natural esters with antioxidants for power transformer applications", *IEEE, Trans. Dielectr. Electr. Insul.*, vol. 20, no.3, pp. 899-911, 2013.

[157]. T. Tanaka, "Dielectric nanocomposites with insulating properties," *IEEE Trans. Dielectr. Electr. Insul.*, vol. 12, pp. 914–928. 2005.

[158]. K. Folgero, "Broad-band dielectric spectroscopy of low-permittivity fluids using one measurement cell," *IEEE Trans. Instrum. Meas.*, vol. 47, no. 4, pp. 881-885, 1998.

[159]. A. R. P. Ramaian Thirugnanam, W. I. Maria Siluvairaj and R. Karthik, "Performance studies on dielectric and physical properties of eco-friendly based natural ester oils using semi-conductive nanocomposites for power transformer application," *IET Sci. Measure. & Technol.*, vol. 12, no. 3, pp. 323-327, 2018.

[160]. J. Li, Z. Zhang, P. Zou, S. Grzybowski, and M. Zahn, "Preparation of a vegetable oil based nanofluid and investigation of its breakdown and dielectric properties," *IEEE Electr. Insul. Mag.*, vol. 28, no. 5, pp. 43–50, 2012.

[161]. B. X. Du, and X. L. Li, "Dielectric and thermal characteristics of vegetable oil filled with BN nanoparticles," *IEEE Trans. Dielectr. Electr. Insul.*, vol. 24, no. 2, pp. 956-963, 2017.

[162]. D. Liu, B. Du, F. Liu, S. Wang, "Effects of multiple parameters on static electrification and breakdown strength of transformer oil," *IET Sci. Measure. & Technol.*, vol. 10, no. 6, pp. 597-601, 2016.

[163]. A. Reffas, O. Idir, A. Ziani, H. Moulai, A. Nacer, I. Khelfane, M. Ouagueni, A. Beroual, "Influence of thermal ageing and electrical discharges on uninhibited olive oil properties," *IET Sci. Measure. & Technol.*, vol. 10, no. 7, pp. 711-718, 2016.

[164]. V. Vasovic, J. Lukic, C. Perrier and M. L. Coulibaly, "Equilibrium charts for moisture in paper and pressboard insulations in mineral and natural ester transformer oils," *IEEE Electr. Insul. Mag.*, vol. 30, no. 2, pp. 10-16, 2014.

[165]. J. Li, "Support vector Regression for the determination of the nutritional components of edible oil by Terahertz Spectroscopy," *IEEE Trans. Instrum. Meas.*, vol. 59, no. 8, pp. 2094-2098, 2010.

[166]. X. Wu, Z. Pan, Y. Zhao, H. Liu, and L. Zheng, "Application of fluorescence spectra and parallel factor analysis in the classification of edible vegetable oils," *Spectroscopy and Spectral Analysis*, vol. 34, no. 8, pp. 2137-42, 2014.

[167]. N. Meher and P. K. Iyer, "Pendant chain engineering to fine-tune the nanomorphologies and solid state luminescence of naphthalimide AIEEgens: application to phenolic nitro-explosive detection in water," *Nanoscale*, vol. 9, pp. 7674-7685, 2017.

[168]. N. Meher, S. R. Chowdhury and P. K. Iyer, "Aggregation induced emission enhancement and growth of naphthalimide nanoribbons via J-aggregation: Insight into disaggregation induced unfolding and detection of ferritin at nanomolar level," *J. Mater. Chem. B*, vol. 4, pp. 6023-6031, 2016.

List of Publications

Patent publications

1. **Maharana M**, Nayak S K, Sahoo N, "Nonedible vegetable oil based dielectric liquid and use thereof in power and distribution transformer" Indian patent office – (Application No. 201831013006 A. 2018 (Online).

2. **Maharana M**, Nanda A, Nayak S K, Sahoo N, "Natural and force convection imposed accelerated thermal ageing simulator to predict the life of the insulating oil before using in transformer", Indian patent –Application No.201731045816 A, 2017. (Online).

3. Bordeori M M, **Maharana M**, Baruah N, Nayak S K, Sahoo N "Design and development of an automated open beaker oxidative ageing assessment apparatus", Indian patent – Application No. 201731047043 A, 2017. (Online).

Journals publication

1. **Maharana M**, Nayak S K, Sahoo N, Karanji oil as a potential dielectrics liquid for transformer, *IEEE Transaction of Dielectric and Electrical Insulation*, vol. 25, no. 5, pp. 1871-1879, Oct. 2018.

2. **Maharana M**, Bordeori M M, Nayak S K, Sahoo N, Nanofluid based transformer oil: effect of aging on thermal, electrical and physio-chemical properties, *IET Science, Measurement & Technology*, vol. 12, no. 7, pp. 878-885, 10 2018.

3. **Maharana M**, Baruah N, Nayak S K, Sahoo N, "Effect of oxidative ageing on the thermophysical and electrical properties of the nanofluid with statistical analysis of AC breakdown voltage", *IET Science, Measurement & Technology*, vol. 12, no. 8, pp. 1074-1081, 11 2018.

Conferences publications

1. **Maharana M**, Baruah N, Nayak S K, Sahoo N, (2018) "Electro-mechanical and chemical strength analysis of thermally aged nanofluid impregnated kraft paper", *IEEE Conference on Electrical Insulation and Dielectric Phenomenon (CEIDP)*, 21-24 October, Cancun, Mexico 2018, pp. 121-124, DOI: *10.1109/CEIDP.2018.8544795*

2. **Maharana M**, Baruah N, Nayak S K, Sahoo N, (2018) "Nanofluid and transformer oil impregnated aged kraft paper: analysis of its mechanical strength" *10th IEEE PES Asia-Pacific Power and Energy Engineering Conference 2018 (APPEEC)*, 7-10 October, Sabah, Malaysia. DOI: *10.1109/APPEEC.2018.8566647*

3. **Maharana M**, Baruah N, Nayak S K, Sahoo N, (2018) "Thermoelectrically enhanced nanofluid is a suitable replacement for transformer oil", 36th *IEEE Electrical Insulation Conference (EIC)*, 11-14 June, San Antonio, TX, 2018, pp. 204-207. DOI: *10.1109/EIC.2018.8481034*

4. **Maharana M**, Baruah N, Nayak S K, Sahoo N, (2017) "Comparative study of mechanical and electrical strength of kraft paper in nanofluid based transformer oil and mineral oil", 8th *IEEE International Symposium on Electrical Insulating Materials (ISEIM)*, 12-15 September, Toyohashi, Japan, 2017, pp. 646-649. DOI: *10.23919/ISEIM.2017.8166573*, **(won best paper award)**.

5. **Maharana M**, Nayak S K, Sahoo N, Chakraborty M, (2017) "Comparative statistical analysis on AC breakdown voltage of thermally aged nanofluid with mineral oil, *35th IEEE* international *Electrical Insulation Conference (EIC)*, 11-14 June, Baltimore, MD, USA, DOI: *10.1109/EIC.2017.8004601*

6. Baruah N, **Maharana M**, Nayak S K, (2018) "An electrode model to ascertain the effects of voltage and tip radius with gap distance on electric field of transformer oil", *2nd International Conference on Energy, Power and Environment 2018 (ICEPE 2018)*, 1-2 June, Shillong, Meghalaya India. DOI: *10.1109/EPETSG.2018.8658753*

7. Baruah N, **Maharana M**, Nayak S K, (2018) "Investigation of the Electric field variation on surface of nanoparticle added to transformer oil", *10th IEEE PES Asia-Pacific Power and Energy Engineering Conference 2018 (APPEEC)*, 7-10 October, Sabah, Malaysia. DOI: *10.1109/APPEEC.2018.8566656*

8. Baruah N, **Maharana M**, Dey S S, Nayak S K, (2018) "Enhancement of heat transfer property in insulating fluids using Nanoparticles", *8th IEEE Power India International Conference (PIICON)*, 10-12 December, Kurukshetra, India.